Institut Camille Jordan
UMR 5208 du CNRS

Triangulations colorées aléatoires

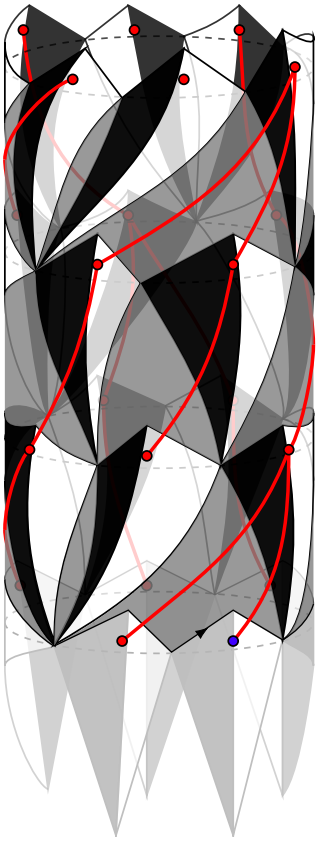

Ariane Carrance

Thèse de doctorat

Université Claude Bernard Lyon 1

Université Claude Bernard Lyon 1
École doctorale InfoMaths (ED 512)
Spécialité : Mathématiques
n°. d'ordre : 2019LYSE1150

Triangulations colorées aléatoires

Thèse présentée en vue d'obtenir le diplôme de
Doctorat de l'Université de Lyon

soutenue publiquement le 20 septembre 2019 par
Ariane Carrance

devant le jury composé de :

Marie Albenque	École Polytechnique	Examinatrice
Jérémie Bouttier	CEA Saclay	Invité
Nicolas Curien	Université Paris Sud	Rapporteur
Christophe Garban	Université Lyon 1	Examinateur
Christina Goldschmidt	University of Oxford	Rapporteuse
Alice Guionnet	ENS Lyon	Examinatrice
Razvan Gurău	École Polytechnique	Examinateur
Grégory Miermont	ENS Lyon	Co-directeur
Fabien Vignes-Tourneret	Université Lyon 1	Directeur

suite aux rapports de :

Nicolas Curien	Université Paris Sud
Christina Goldschmidt	University of Oxford

Remerciements

Je commence tout naturellement ces remerciements par mes directeurs.

Fabien, merci pour ta disponibilité, ta franchise, ta bienveillance, ton enthousiasme. Merci pour le courage et la curiosité nécessaires pour l'encadrement d'une thèse qui touchait à plusieurs sujets hors de ta zone de confort. Merci pour ta patience pour mes questions de physique, souvent naïves et répétitives. Merci aussi pour les longues digressions sur TeX et tikz, qui ont beaucoup contribué à l'aspect de ce manuscrit !

Grégory, j'admire ta patience et ta pédagogie depuis le cours de L3 où tu m'as appris les bases des probabilités. Depuis cette lointaine époque, j'ai eu aussi l'occasion d'apprécier la beauté de ton domaine de recherche, ainsi que ta grande culture scientifique, ton ingéniosité et ta confiance. Merci aussi de m'avoir montré qu'en recherche, même les difficultés peuvent être source d'enthousiasme, voire de fous rires !

Merci à vous deux de m'avoir laissé le temps d'apprendre et d'essayer par moi-même, tout en étant là pour me repêcher quand j'étais vraiment sous l'eau, et pour me pousser à perfectionner ce que j'avais déjà.

Je tiens aussi à remercier Jérémie Bouttier, qui a été un interlocuteur indispensable pour la partie la plus combinatoire de mon travail de thèse. Jérémie, merci pour ta patience et ton aide, qui ont donné lieu à une collaboration que j'espère féconde !

Merci à Nicolas Curien et Christina Goldschmidt d'avoir accepté de rapporter ce manuscrit. L'un comme l'autre l'ont relu avec une attention particulière que j'apprécie grandement. Merci à Christina pour ses commentaires très détaillés et profitables, et merci à Nicolas pour les nombreuses pistes que j'ai hâte d'explorer avec lui. Je remercie également Marie Albenque, Christophe Garban, Alice Guionnet et Razvan Gurău d'avoir accepté de faire partie de mon jury.

Je voudrais aussi remercier toutes les autres personnes avec qui j'ai eu des conversations scientifiques enrichissantes au cours de ma thèse, et en particulier : Bruno Salvy, pour son aide précieuse avec Maple, Jean-François Le Gall, avec qui j'ai hâte de travailler, Mireille Bousquet-Mélou, Gilles Schaeffer, Thomas Budzinski, Linxiao Chen, Mickaël Maazoun, Guillaume Chapuy, Fay Dowker, Luis Fredes, et enfin l'ensemble de la « tensor family », notamment Valentin Bonzom, Nicolas Delporte, Luca Lionni, Dine Ousmane-Samary, Romain Pascalie, Vincent Rivasseau et Reiko Toriumi.

Pour leur apport moins scientifique mais non moins déterminant, un grand merci à Simon A. et Caterina, avec qui j'ai partagé les fameux mois de rédaction. Je le répète

encore, je ne sais pas comment j'aurais fait sans vous ! Simon, merci pour les BD, les expérimentations culinaires, et pour les ondes positives que tu diffuses autour de toi l'air de rien. Caterina, dear comrade in struggles and joys, I'm so glad that we passed this hurdle together ! Thank you for the fancy brioches, and for all the rest.

Merci aussi à mes autres co-bureaux : Benjamin C, Cécilia, Colin, François D, Godfred, Ivan, Romain P, Seidon, Théo. Merci pour les lundis pâtisserie, les blagues de qualité douteuse, la BD-thèque, l'entraide administrative, et les nombreux prétextes à la procrastination.

Je remercie aussi les autres doctorants, doctorantes, postdocs et autres ATER avec qui j'ai partagé un bout des mes années à l'ICJ : Anatole, Andrea, Antoine, Avelio, Benjamin D., Chih-Kang, Christian (dont j'admire la double identité de logicien et de poète vagabond), Clément, Coline, Corentin, Daniel, Félix B. (merci pour toutes les conversations de jdr au milieu des Moldus !), François V. (merci pour tes belles histoires !), Garry, Gwladys (merci pour ton courage et ta bonne humeur !), Hugo, Isabel, Jiao (avec qui j'ai le plaisir de partager ma date de soutenance et ma commande de vin), Jorge, Kévin, Liugia, Lola (merci pour ta bienveillance et ta ténacité !), Marina, Martin (merci pour les traquenards au 109E !), Marion (merci pour l'énergie que tu consacres aux autres, pour les gâteaux impromptus, et pour tout le reste !), Mathias[1], Maxime H., Maxime P., Mélanie, Michele, Nadja, Niccolo, Nils, Octave (et son rire machiavélique), Olga (спасибо за разговоры на разных языках !), Pan, Quentin, Rémy, Samuel, Shmuel, Simon B. (merci, entre autres, pour les discussions métaphysiques et les bubble teas !), Simon C., Simon Z. (merci de me faire profiter de tes talents en cuisine, bricolage, escalade et autres), Sylvain, Tanessi (ça a été un plaisir de partager des TD avec toi !), Tania, Thomas G., Tingxiang[2], Vincent, Xiaolin, Yannick (merci pour ta joie de vivre et ta motivation !).

Merci aussi aux Vieilles et aux Vieux, qui, sans avoir forcément été au labo à la même époque que moi, m'ont appris tout ce que je devais savoir pour réussir une thèse[3] : Adriane, Agathe, Benoît La., Blanche, Cécile C., Cécile F., Corentin, François D., François L.M., François V., Fred, Mathias, Romain P., Thomas L. Merci pour les randos, les soirées jeux ou escalade, et pour l'affection que vous cachez derrière vos petites piques.

Merci aux équipes administratives et techniques de l'ICJ, et en particulier à Aurélie, Betty, Céline, Laurent et Vincent F, pour leur indispensable travail, et pour leur contribution à l'atmosphère conviviale du labo.

Pour leur accueil chaleureux, merci aux membres de mes deux affiliations plus ou moins officielles, l'équipe de probabilités et l'équipe de physique mathématique.

Merci aussi à toutes les autres chercheuses et chercheurs avec qui j'ai eu plaisir à discuter de la vie du labo et du reste : Anne, Anne-Laure, Élise, François L., Frédéric, Maria, Morgane, Thibault, Thomas B., Véronique, et toutes les personnes que j'oublie sans doute.

Outre ma fluctuation entre les équipes de l'ICJ, une partie non négligeable de ma thèse s'est déroulée dans les locaux de l'UMPA, qui habritent de nombreuses personnes dont j'ai beaucoup apprécié la présence.

Merci tout d'abord à l'équipe de probabilités de l'UMPA, pour son accueil tout aussi agréable que celui de sa sœur villeurbannaise.

Un merci tout particulier à Mickaël, mon grand petit frère de thèse, pour son écoute attentive et ses conseils pertinents, tant quand je peinais dans une preuve, que pour mes répétitions d'exposés. Merci aussi pour les discussions de comptoir, et pour tous les cafés

[1] 90 ♠ !

[2] "Fired rice ! !"

[3] coincher et cultiver l'art du mauvais esprit

que je t'ai taxés !

Merci à mes deux autres co-bureaux, Benoît Lo. et Félix P., pour avoir rendu mes séjours lyonnais très conviviaux.

Merci aux autres membres non-permanents avec qui j'ai eu le plaisir de passer du temps : Alexandre (qui est aussi un super proprio !), Arthur, Auguste, Ignacio, Jonathan, Léo, Loïc de R., Loïc R., Sam, Thomas L. (notre papy à toustes !), Valentine (merci pour tous les goûters/dîners à l'improviste !).

Je voudrais aussi remercier toutes les personnes ont rendu ces années de thèse plus belles hors de mon quotidien professionnel.

Pour nos intenses aventures de papier, merci en particulier à Félix B., Florine, Marine, Romain D., Camille, Lambert, Martin, Mickaël Mo., Ophélie, Arnaud, Cara, Guillaume, Julie, Simon B. (et notre boss de fin Elisha). Pour les histoires plus incarnées, un grand merci (et un très gros câlin) à l'ensemble du très chatoyant Club du 4^{e} étage.

Et pour les plus belles aventures que j'aie vécues ces dernières années, merci à toutes les personnes formidables que j'ai pu rencontrer grâce à ATD, et notamment à l'équipe de choc de Gerland : Jean, Laurence, Pascale, Patrick, Peggy, Roseline, Sidonie, et au très dynamique groupe jeunes : Aimée, Déborah, Émie, Éric, Franck, Martial, Nathalie, Steve.

Hugo, merci pour tout ce qu'on partage.

Alejandro, Alexys, Fanny, Gabrielle (et ses questions indiscrètes), Joëlle (dont j'admire la bienveillance et la générosité !), Manon, Mathieu (et le petit Arthur), Sandrine, merci pour votre compagnie toujours appréciée.

Paul, merci pour les balades, pour les Discussions Sérieuses et les autres, et pour ton Envie De Faire communicative.

Je pense aussi aux précieuses amitiés qui ont subsisté depuis les bancs de l'école : Anne-Laure, Judith, Léopold, Sophie, merci pour les moments de détente et de joie qu'on partage toujours.

Je voudrais enfin remercier deux personnes qui ont toujours été très importantes pour moi. Merci à ma grand-mère, Dolly, pour sa tendresse, sa curiosité, son amour des débats et du beau langage, et bien sûr pour les gâteaux aux noix.

Et merci à Nathalie, la toute première mathématicienne que j'aie connue. Merci pour ta présence constante et ton soutien inconditionnel, et pour tous les enthousiasmes que tu m'as transmis.

Table des matières

Première partie

Introduction

CHAPITRE 1

Une introduction succinte

Les lois fondamentales de la physique ne sont jamais exactes. Elles gagnent cependant en précision quand on parvient à les étendre à un cadre plus général. Ainsi, au début du XX^{e} siècle, la mécanique newtonienne a été doublement bouleversée.

D'une part, dans le domaine des petites distances, la mécanique quantique décrit des systèmes au comportement aléatoire, qui ne semblent déterministes qu'à notre échelle. D'autre part, dans le domaine des hautes énergies, la relativité générale remplace l'idée classique d'un espace et d'un temps immuables par un espace-temps qui se déforme au gré de ses interactions avec la matière qui le peuple, selon les règles de la gravitation d'Einstein. Ces deux révolutions ont non seulement profondément modifié les intuitions qu'on pouvait se faire du monde physique, mais ont aussi été accompagnées par le développement de nouveaux outils et objets mathématiques, et motivent encore aujourd'hui des recherches tant mathématiques que physiques.

Une question reste notamment ouverte : comment unifier ces deux théories, les décrire comme différentes approximations de lois plus générales ?

Comment définir un espace-temps à la fois relativiste donc géométrique, et quantique donc aléatoire ?

Avec les moyens techniques actuels, et pour encore bien longtemps sans doute, on ne peut espérer que des expériences ou des observations nous guident vers la réponse.

Un peu comme les philosophes de l'antiquité grecque qui souhaitaient décrire les composants élementaires de la matière, nous ne pouvons donc nous fier qu'à des critères presque esthétiques : une théorie est-elle cohérente mathématiquement ? La mécanique quantique et la relativité générale en découlent-elles clairement, facilement ? Est-elle simple, astucieuse, belle ?

Plutôt que d'obtenir la bonne réponse, le but est d'explorer des pistes, de contribuer à la tâche collective d'étoffer la culture mathématique afin qu'il y existe, le jour où l'on saura sonder les trous noirs, l'équivalent de l'atome pour la gravité quantique.

Cette thèse aborde ainsi des aspects mathématiques d'une approche récente à la gravité quantique, les **modèles de tenseurs colorés**. Nous résumons ici brièvement le contenu de ce manuscrit.

1.1 Graphes $(D+1)$-colorés

Pour $D \in \mathbb{N}$, les **graphes $(D+1)$-colorés** sont des graphes $(D+1)$-réguliers, munis d'une coloration propre de leurs arêtes avec $D+1$ couleurs, usuellement $\{0, 1, \ldots, D\}$. Pezzana [Pez74 ; Pez75] a montré dans les années 1970 que les graphes $(D+1)$-colorés encodent des structures topologiques *linéaires par morceaux* (PL dans la suite), qu'on appellera dans la suite de cette introduction des **complexes colorés**, et qu'on peut voir comme des ensembles de simplexes de dimension D collés les uns aux autres. Les variétés PL sont de telles structures, et peuvent donc être décrites avec un vocabulaire venant de la combinatoire et de la théorie des graphes. Cette description a été plus amplement développée par Gagliardi et son groupe (cf. [FGG86]), menant notamment à des résultats de classification pour les variétés PL de dimensions 3 et 4 de faible complexité [CM15 ; CC15]. Outre ces succès en topologie PL, les graphes $(D+1)$-colorés ont suscité l'intérêt de physiciens théoriciens, à commencer par Gurau à partir de 2010. En effet, ces graphes sont au cœur d'une nouvelle approche de la gravité quantique, les **modèles de tenseurs colorés** [GR12], qui généralisent des **modèles de matrices** en dimensions supérieures. Notamment, les modèles de tenseurs colorés, comme les modèles de matrices, présentent un « développement en $1/N$ » des fonctions de corrélation en amplitudes de graphes, où la puissance de N dans l'amplitude d'un graphe G dépend d'une quantité, le **degré** de G, $\omega(G)$, qui généralise le genre en dimensions supérieures. Plus précisément, le degré d'un graphe G est la somme des genres de ses *plongements réguliers* :

Définition 1.1.1. Soit G un graphe $(D+1)$-coloré. Un **plongement régulier** de G dans une surface S est une fonction injective et continue $G \to S$ telle que :

- les composantes connexes de $S \backslash G$, appelées **faces**, soient homéomorphes à des disques
- il existe un $(D+1)$-cycle τ tel que toute face soit bordée par un cycle d'arêtes bicolores, de couleurs $\{i, \tau(i)\}$ pour un $i \in \{0, 1, \ldots, D\}$.

On se restreint aux graphes bipartis ; en effet, c'est une condition équivalente à l'orientabilité du complexe coloré associé. On définit alors :

Définition 1.1.2. Le **degré** d'un graphe biparti $(D+1)$-coloré G est : $\omega(G) = 1/2 \sum_\tau g_\tau$ où g_τ est le genre du plongement régulier associé au cycle τ.

Au cours de ma thèse, j'ai étudié des distributions de probabilité sur les graphes bipartis $(D+1)$-colorés et les quantités associées telles que le degré, dans le but de définir des espaces PL aléatoires, et aussi de permettre une meilleure compréhension de l'espace-temps quantifié décrit par les modèles de tenseurs colorés. Ceci a donné lieu à deux projets distincts : la construction de modèles aléatoires en dimension quelconque (Section 1.2), et l'étude d'un cas particulier en dimension 2 (Section 1.3).

1.2 Modèles aléatoires uniformes de graphes colorés

Une des motivations de cette thèse était de trouver des modèles aléatoires de graphes $(D+1)$-colorés présentant une limite intéressante quand on fait tendre la taille du graphe vers l'infini : notamment, on cherche à obtenir un espace-temps continu comme limite d'échelle de complexes colorés aléatoires, vus comme des espaces métriques (en ne retenant d'un complexe coloré que ses sommets et la distance de graphe entre ceux-ci). Un tel résultat serait une généralisation en dimension $D > 2$ de la construction de la **carte brownienne** comme limite d'échelle de nombreuses familles de cartes planaires (cf. [LG13 ; Mie13] par exemple). Notons toutefois qu'en dimensions supérieures, la topologie de l'espace aléatoire

n'est pas fixée. Comme première étape dans cette direction, j'ai étudié plusieurs modèles sur les graphes $(D+1)$-colorés, bipartis, étiquetés de taille p : un **modèle uniforme** sur ces graphes, U_p^D, et une classe de **modèles décolorés-uniformes** G_p où la structure des arêtes de couleur $1, 2, \ldots, D$ est fixée par un graphe D-coloré G, tandis que les arêtes de couleur 0 sont formées par des appariements uniformes. Parmi les modèles décolorés-uniformes, j'ai étudié plus finement le **modèle quartique** Q_p^D, où le graphe G est quartique, D-coloré. Les techniques utilisées reposent sur des encadrements de caractères du groupe symétrique [LS08] notamment utilisés pour des modèles aléatoires de recollement de polygones [PS06 ; CP16], ainsi que sur des résultats concernant le modèle de configuration [CF04 ; FH17]. Ce travail a donné lieu à un article ([Car19]), reproduit dans le chapitre 6, et dont voici les principaux résultats :

J'ai tout d'abord montré que U_p^D et G_p sont asymptotiquement presque sûrement (a.p.s.) connexes :

Théorème 1.2.1. *Pour tout $D \geq 2$, U_p^D est connexe a.p.s., et*

$$\mathbb{E}\big[\#\textit{composantes connexes de } U_p^D\big] = 1 + O\bigg(\frac{1}{p^{D-1}}\bigg).$$

De même, pour tout $D \geq 2$, pour tout graphe biparti D-coloré G, G_p est connexe a.p.s., et

$$\mathbb{E}[\#\textit{composantes connexes de } G_p] = 1 + O\bigg(\frac{1}{p^{t-1}}\bigg),$$

où $t = 1/2 \cdot \#\textit{sommets}(G)$.

J'ai aussi étudié le comportement du degré des graphes, pour les modèles uniforme et quartique. J'ai obtenu les premiers et seconds moments de ces lois, ainsi qu'un théorème central limite pour le genre d'un plongement régulier. Les techniques utilisées m'ont permis d'établir également un théorème central limite pour le genre d'une carte étiquetée uniforme.

L'étude des sous-parties d'un graphe $(D+1)$-coloré G contenant des arêtes de couleurs appartenant à un sous-ensemble de $\{0, 1, \ldots, D\}$ permet d'obtenir des informations sur la structure du complexe coloré associé $\Delta(G)$. J'ai ainsi démontré les théorèmes suivants sur les sommets des complexes colorés associés à mes modèles :

Théorème 1.2.2. *Pour $D \geq 3$,*

$$\mathbb{E}\big[\#\textit{sommets de } \Delta(U_p^D)\big] = D + 1 + O\bigg(\frac{1}{p^{D-2}}\bigg).$$

Théorème 1.2.3. *Pour tout $D \geq 3$, pour tout graphe biparti D-coloré G, on a*

$$\mathbb{E}[\#\textit{sommets de } \Delta(G_p)] = p + \alpha_G + o(1),$$

où α_G est une constante qui dépend de G.

De plus, si u, v sont deux sommets de $\Delta(G_p)$ choisis indépendamment et uniformément, alors $d(u, v) = 2$ a.p.s.

Dans les deux cas, ces résultats impliquent que ces modèles ne peuvent pas avoir une limite d'échelle comme les cartes planaires uniformes. Pour se rapprocher du but, il faut donc construire de nouveaux modèles aléatoires de graphes colorés, en donnant sans doute un rôle plus important au degré, qui est une quantité centrale dans les modèles de tenseurs colorés développés en physique théorique.

1.3 Triangulations eulériennes

Parmi les modèles de tenseurs colorés, le modèle dit **i.i.d.** est particulièrement fondamental, et les graphes dominants de ce modèle sont ceux de degré nul. Pour $D \geq 3$, un graphe de degré nul converge vers l'**arbre Brownien** ([GR14]).

Dans le cas de la dimension 2, les graphes (2+1)-colorés bipartis de degré nul sont les graphes duaux des **triangulations planaires eulériennes** (c'est-à-dire dont les sommets sont tous de valence paire). Un autre projet de cette thèse, présenté en partie III, a donc été de prouver qu'une triangulation planaire eulérienne de taille n uniforme converge vers la carte brownienne quand $n \to \infty$:

Théorème 1.3.1. *Soit $\mathcal{T}_n$ une triangulation eulérienne planaire enracinée à n faces noires, choisie uniformément au hasard, munie de sa distance de graphe usuelle d_n. Soit $(\mathbf{m}_\infty, D^*)$ la carte brownienne. Il existe une constante $\mathbf{c}_0 \in [2/3, 1]$, telle qu'on ait la convergence suivante*

$$n^{-1/4} \cdot (V(\mathcal{T}_n), d_n) \xrightarrow[n\to\infty]{(d)} \mathbf{c}_0 \cdot (\mathbf{m}_\infty, D^*),$$

pour la distance de Gromov-Hausdorff sur l'espace des classes d'isométrie des espaces métriques compacts.

Habituellement, pour montrer qu'une famille de cartes planaires converge vers la carte brownienne, on utilise l'existence d'une **bijection** entre ces cartes et des arbres aux sommets étiquetés par des entiers, qui conservent des informations sur les distances entre les sommets de la carte correspondante. De telles bijections ont été établies pour de nombreuses familles de cartes, notamment par Cori-Vauquelin [CV81], Schaeffer [Sch98] et Bouttier-Di Francesco-Guitter [BDFG04]. Du côté des arbres étiquetés, on peut facilement passer à la limite continue qui est un **arbre Brownien** muni d'un **serpent Brownien** (qui correspond à la limite des étiquettes). Pour conclure pour la convergence des cartes, il faut ensuite définir la distance continue correspondant au serpent Brownien.

Pour les triangulations eulériennes, cette procédure est beaucoup plus compliquée car la bijection naturelle est liée à une **distance orientée** [BDFG03], ce qui empêche une définition directe de la distance continue. J'ai donc contourné cette difficulté en prouvant que cette distance orientée est asymptotiquement proportionnelle à la distance de graphe :

Théorème 1.3.2. *Soit $\mathcal{T}_n$ une triangulation eulérienne planaire enracinée à n faces noires, choisie uniformément au hasard, et soit $V(\mathcal{T}_n)$ l'ensemble de ses sommets. On note $\vec{d}_n$ la distance orientée de $\mathcal{T}_n$. Pour tout $\varepsilon > 0$, on a*

$$\mathbb{P}\left(\sup_{x,y \in V(\mathcal{T}_n)} |d_n(x,y) - \mathbf{c}_0 \vec{d}_n(x,y)| > \varepsilon n^{1/4} \right) \xrightarrow[n\to\infty]{} 0.$$

Pour montrer ce résultat, j'ai procédé de manière similaire à ce que Curien-Le Gall ont fait pour étudier des modifications de distance dans les triangulations quelconques [CLG19] : construire des modèles de triangulations (eulériennes dans mon cas) infinies du demi-plan, reliés aux cartes finies grâce à une **décomposition en couches** de ces dernières, puis utiliser le théorème de sous-additivité ergodique de Liggett [Lig85] pour en déduire que les distances orientée et non-orientée sont asymptotiquement proportionnelles. Ce travail est l'objet du chapitre 7. Cette décomposition en couches a nécessité des résultats inédits d'énumération, ce qui a donné lieu à une collaboration encore en cours avec Jérémie Bouttier. Une version préliminaire des résultats de cette collaboration est donnée dans le chapitre 9. Il contient aussi des résultats d'énumération utilisés dans le chapitre 8 pour étudier plus en détail la structure d'un modèle de triangulation eulérienne infinie du demi-plan.

CHAPITRE 2

The problem of quantum gravity

This chapter does not have the pretention of being a complete introduction to neither quantum mechanics nor general relativity, nor even to models of random geometry related to quantum gravity. It is also not necessary to read it to understand the other parts of this thesis, nor most of the rest of the introduction. Moreover, it mostly states formal facts without giving proofs or references to more substantiated sources. Before you decide that such trash is unworthy of being in a PhD thesis in mathematics, and tear its pages to shreds, let me explain why it might have a legitimate place here.

During my PhD, there were numerous instances where I felt lost regarding some notions or objects that are fundamental to my topic (I dare believe that it is not uncommon for a PhD student). As my research area stands at an interface between several disciplines, this problem touched questions in mathematics and theoretical physics alike. For mathematical questions, it always seemed that spending enough time reading a relevant article or textbook would most probably replace my ignorance with basic understanding, or at least give me some clear-cut definitions and results to go back to if needed. However, for physical questions, which dealt with quantum field theory (hereafter QFT) and its interactions with the problem of quantum gravity, it seemed that there was always a gap between my incomplete, pre-existing knowledge, and what was explained in whichever source I found. I felt that there was some sort of circular law, that stipulated that one had to already belong to the Arcane Society of People who Understand Quantum Field Theory, to be able to understand even the introduction of an article about a specific model or framework. The only way to be allowed into that Society seemed to be doing a PhD in QFT, that is, get one's hand dirty and try and solve complicated QFT questions oneself. This was a perhaps too ambitious plan on top of the mathematical facet of my PhD, which entailed learning, practically from scratch, about the combinatorial and probabilistic aspects of random graphs and higher-dimensional objects. So I made do with what I could, and read a good number of more or less mathematically-oriented papers, listened stubbornly to talks that I only half-understood, and, most importantly, asked a lot of questions to my advisor Fabien, who very graciously and patiently answered them as best as he could.

I still do not feel that I have as good a grasp on physical questions related to quantum gravity and random geometry, as do members of this Society. However, I think I am now able to somewhat understand the physical motivations of studying models of random maps or complexes, beyond the cookie-cutter assertion that some very intelligent physicists found this to be a good way to deal with the problem of unifying quantum mechanics and general

relativity. I thus wanted to record what I had gathered, in a way that is hopefully less impenetrable and imbued with mystery to a (mathematically-inclined) neophyte, than the usual productions of the Society. The introduction of my PhD thesis seemed like a good place to take on this task. Indeed, trying to understand these motivations was, to me, an important part of my PhD. Furthermore, people often turn to PhD theses to get palatable overviews of a research topic. As I hope the next chapters belong to that category, it only made sense to add this one as a preamble, putting them into a slightly broader perspective.

A few last remarks and disclaimers before you can dive into the heart of the matter. First, what follows assumes that the reader has a basic understanding of core notions of Newtonian mechanics, such as a trajectory or equations of motion, and is not averse to building up on it with quite mathematical and abstract concepts. Moreover, it is in no way a historical review of quantum field theory or general relativity, and as such does not cite a lot of names, and even fewer references, as most of it became part of the basis of modern physics, after being refined during several decades in the alembics of a lot of very prominent physicists.

2.1 A primer on quantum mechanics

An informal way to describe how the quantum world differs from the classical (Newtonian) one, is to say: "Deterministic behavior becomes random". To make this statement more precise, let us start from the Lagrangian description of classical physics. The behavior of a given physical system is described by a **trajectory** φ in the configuration space E. For instance, if we are considering a point particle moving in $\mathbb{R}^3$ under the action of some force, φ is going to be a (smooth) function $\mathbb{R} \to E = \mathbb{R}^3$. In the Lagrangian formulation, the laws for the evolution of the system are encoded into, as one could expect, the **Lagrangian**, which is a function

$$\begin{aligned} \mathcal{L} : \mathbb{R} \times E^2 &\to \mathbb{R} \\ (t, x, v) &\mapsto \mathcal{L}(t, x, v). \end{aligned}$$

Related to the Lagrangian is the **action** functional

$$S[\varphi] = \int \mathcal{L}(t, \varphi(t), \mathring{\varphi}(t))\mathrm{d}t$$

that associates a value to each possible trajectory φ. Here, $\mathring{\varphi}$ denotes the time derivative $\frac{\mathrm{d}}{\mathrm{d}t}\varphi$.

We then get the equations of motion as the **Euler-Lagrange equation**:

$$0 = \frac{\delta S}{\delta \varphi} := \mathcal{L}_\varphi - \frac{\mathrm{d}}{\mathrm{d}t}\mathcal{L}_{\mathring{\varphi}},$$

where

$$\mathcal{L}_\varphi = \vec{\nabla}_\varphi \mathcal{L}, \text{ and } \mathcal{L}_{\mathring{\varphi}} = \vec{\nabla}_{\mathring{\varphi}} \mathcal{L},$$

so that

$$\frac{\mathrm{d}}{\mathrm{d}t}\mathcal{L}_{\mathring{\varphi}} = \frac{\partial}{\partial t}\mathcal{L}_{\mathring{\varphi}} + \mathring{\varphi}\vec{\nabla}_\varphi \mathcal{L}_{\mathring{\varphi}} + \mathring{\mathring{\varphi}}\vec{\nabla}_{\mathring{\varphi}} \mathcal{L}_{\mathring{\varphi}}.$$

Therefore, a classical system will follow a trajectory that is a critical point of the functional S, which, in reasonable cases, will also be an extremal point.

Now, for the same Lagrangian (and thus the same underlying interactions), the trajectory ψ of a quantum system will not be as clearly determined, but will rather be a random

variable, following a probability distribution that should give to a possible trajectory φ a weight proportional to $\exp(-\lambda S[\varphi])$, for a fixed real parameter λ [1]. Thus, informally, ψ follows a probability distribution that may be written as, up to a multiplicative constant,

$$\hat{\mu}_S(D\varphi) := e^{\frac{i}{\hbar}S[\varphi]}D\varphi,$$

where $\hbar$ is the **Planck constant**, and $D\varphi$ is a "canonical" measure on the functions taking value in the phase space E. This is the **path integral** formulation of quantum mechanics, whose conceptualization is due to Feynman.

The meticulous reader might rightfully object that a putative "Lebesgue measure" on a space of functions defined on $\mathbb{R}$ makes no sense, so that the above measure is ill-defined. Furthermore, assiging a complex weight to each function φ cannot possibly yield a positive measure!

We ask you to hold back these objections for a moment, to let us sketch how this formulation relates to more familiar or large-spread pictures of quantum mechanics.

Indeed, in this new framework, one can for instance define the **wavefunction** of a quantum particle e, a complex-valued function Ψ, defined on space and time, that will quantify the probability of observing the particle in an elementary region of space $\mathrm{d}x$ around position x at time t, with the equation

$$\mathbb{P}(e \text{ in } \mathrm{d}x \text{ at time } t) = |\Psi(x,t)|^2 \mathrm{d}x.$$

(In more formal words, we can say that $|\Psi(x,t)|^2$ is the density with respect to the Lebesgue measure, for the random variable describing the location of the particle.)

To define Ψ, we first set the initial input $\{\Psi(x,0)\}$, then use the action functional to describe the time evolution of Ψ:

$$\Psi(y,t) \equiv \int \left(\int \mathbb{1}_{\{x(0)=x,\, x(t)=y\}} e^{\frac{i}{\hbar}S[\varphi]} D\varphi \right) \Psi(x,0)\mathrm{d}x,$$

where the integral in the action S is taken from 0 to t.

It can then be proven, under reasonable assumptions on the action S, that Ψ satisfies the famous **Schrödinger equation**:

$$i\hbar \frac{\partial}{\partial t}\Psi(t,x) = H\Psi(t,x),$$

where the Hamiltonian H is the Legendre transform of the Lagrangian.

Let us now go back to the question of the precise definition of the measure $\hat{\mu}_S$.

As we have just explained, the measure $\hat{\mu}_S$ contains the information of the quantum system driven by the Lagragian $\mathcal{L}$. However, what can actually be seen as a probability measure, and what we will focus on in the sequel, is a slightly different measure:

$$\mu_S(D\varphi) := e^{-S[\varphi]}D\varphi,$$

which you can already envision to be positive, provided it is properly defined.

Obviously, a positive measure is still not always a probability measure, so that one quantity to consider is the **partition function** of the theory, which is the total weight of the measure:

$$Z = \int \mu_S(D\varphi).$$

[1] In the sequel, we will write ψ for the quantity describing a quantum trajectory, and φ for the variable that we integrate to define ψ, to distinguish between the two.

In the rest of this chapter, we will not use this notion, but it will appear again in other chapters of the introduction.

For reasons that will hopefully be clearer later, μ_S is called the **Euclidean** QFT associated to S, and $\hat{\mu}_S$, the **Lorentzian** one. For now, we can say that, if the formulation of μ_S can recall concepts of statistical mechanics, it really is $\hat{\mu}_S$ that describes a quantum system. For relatively well-behaved actions S, one can prove (though, as for many other statements, we will not attempt to do so here) that if we can make sense of an Euclidean QFT, then there exists a corresponding Lorentzian one.

Let us make a distinction that has little consequence on the mathematical formulation we are describing, but is very important conceptually. Up until now, we have considered the example of one particle characterized by a Lagrangian, so that, with the path integral formulation, we have described **quantum mechanics**. If we now consider fields ψ that contains information on a undetermined number of particles (this information can be, for instance, the density of photons in elementary regions of space), we enter the realm of **Quantum Field Theory**.

Let us now give a more precise meaning to the measure μ_S. In most cases arising in quantum field theory, the Lagrangian $\mathcal{L}$ has a very specific form: it is a polynomial in the second variable, together with a quadratic term in the third variable:

$$\mathcal{L}(t, \varphi, \mathring{\varphi}) = \frac{1}{2}\mathring{\varphi}^2 + \sum_k a_k \varphi^k.$$

This quadratic term is the *kinetic* term, and the rest corresponds to an *interaction potential*. (To simplify notation, we assume in the remainder of this subsection that φ has real values.)

In this special case, the corresponding action functional can be defined for functions φ defined on any non-empty space X, up to replacing $\mathring{\varphi}^2$ by a discrete equivalent if X is ... discrete:

$$S_{kin}[\varphi] = \int_X \frac{1}{2}\mathring{\varphi}^2(t)\mathrm{d}t \to S_{kin}[\varphi] = \frac{1}{2}\sum_{i,j\in X} h_{i,j}\varphi(i)\varphi(j),$$

for some set of coefficients $\{h_{i,j}\}$.

In particular, X can be a finite set, as will be the case for the explicit examples that will be treated in detail in the sequel. Finite X's can appear when studying instrinsically discrete structures such as lattices. We can also have a discrete space X when the actual underlying space X' is continuous and compact, but we take a cutoff of the Fourier transform to obtain functions φ on a finite set.

Let us consider for a moment the case where we only have a quadratic term, so that the measure μ_S is

$$\mu_s(D\varphi) = e^{-S_{kin}[\varphi]}D\varphi.$$

In the case where X is finite, we simply have:

$$\mu_s(D\varphi) = e^{-\sum_{i,j\in X}\frac{1}{2}h_{i,j}\varphi(i)\varphi(j)}\prod_{i\in X}\mathrm{d}\varphi_i,$$

which is (up to a multiplicative constant) a **Gaussian measure** on $\mathbb{R}^X$ with covariance matrix h^{-1}.

In the case where $X = \mathbb{R}^n$, we can circumvent the thorny question of defining a hypothetical canonical measure $D\varphi$, and define directly ψ as the **Gaussian Free Field** on X. This is a random variable on distributions living in the Sobolev space $H^1(\mathbb{R}^n)$, characterized by its covariance, which is the Green function of the Laplace operator in $\mathbb{R}^n$. Indeed, assuming that our path integral is on paths φ with zero boundary conditions, we have:

$$S[\varphi] = \int_X \frac{1}{2} \overset{\circ}{\varphi}{}^2(t) \mathrm{d}t = \int_X \frac{1}{2} \varphi \Delta \varphi(t) \mathrm{d}t,$$

where Δ is the Laplace operator on X.

Thus, by analogy with the finite case, here ψ should be a Gaussian process on X, with covariance

$$K(x, y) = \Delta^{-1}(x, y).$$

This is precisely the Green function associated to the Laplace operator on X, and we can perfectly make sense of this Gaussian process, being careful that it is not a random function, but a random distribution.

We can thus properly define the random field ψ when the Lagrangian is purely kinetic, and note the corresponding Gaussian measure $\mu_G(D\varphi)$. Let us now explain how to make sense, in a **pertubative** (non-rigorous) way, of a field governed by a more complicated action functional S. To simplify notation, we will focus on the case of the simplest pertubation of a Gaussian field theory, the so-called $\boldsymbol{\varphi^4}$ **theory**, for which the action is, unsurprisingly:

$$S[\varphi] = S_{kin}[\varphi] + \int_X \varphi(x)^4 \mathrm{d}x.$$

First note that what is actually meaningful in physics, is what can be *measured* or *observed* experimentally. In the case of a quantum field theory, this is essentially the **correlation functions**:

$$\mathbb{E}[\psi(z_1) \cdots \psi(z_p)]_S = \int \varphi(z_1) \cdots \varphi(z_p) \mu_S(D\varphi).$$

For our theory of interest, this can also be written as

$$\int \varphi(z_1) \cdots \varphi(z_p) e^{-\lambda \int_X \varphi(x)^4 \mathrm{d}x} \mu_G(D\varphi).$$

We first take the major liberty of swapping the integral on φ and the infinite series of the exponential in the previous equation. This yields the formal series:

$$\sum_{n \geq 0} \frac{(-\lambda)^n}{n!} \int \varphi(z_1) \cdots \varphi(z_p) \left(\int_x \varphi(x)^4 \mathrm{d}x \right)^n \mu_G(D\varphi).$$

We can already see why the calculations we have undertaken are said to be perturbative. Indeed, we have brought out a Taylor expansion around zero in the parameter λ: we thus want to think of the non-kinetic part of the action as a small perturbation from a Gaussian free field, with its smallness being controlled by λ. As we will mention again further below, this picture is unfortunately incorrect, as this formal series in λ has quite often a zero radius of convergence. (This entails that we cannot write an equality between the two previous quantities, but we will get back to this later.)

Switching the Gaussian expectation and the integral, we recognize correlation functions for our Gaussian measure μ_G:

$$\sum_{n\geq 0}\frac{(-\lambda)^n}{n!}\int\left(\int\varphi(z_1)\cdots\varphi(z_p)\varphi(x_1)^4\cdots\varphi(x_n)^4\mu_G(D\varphi)\right)\mathrm{d}x_1\cdots\mathrm{d}x_n.$$

For the quantity between parentheses to be non-zero, p must be even. Moreover, by **Wick's theorem**, we then have:

$$\int\varphi(z_1)\cdots\varphi(z_p)\varphi(x_1)^4\cdots\varphi(x_n)^4\mu_G(D\varphi)=\sum_{\text{pairing }\sigma}\prod_{\{i,j\}\in\sigma}\mathbb{E}[\varphi(y_i)\varphi(y_j)]_G,$$

where $y_1, y_2, \ldots$ is some arbitrary ordering of the z_i and the x_i, and by pairing we mean a fixed-point-free involution σ on $\{1, 2, \ldots, 4n+p\}$.

Thus, for a given pairing σ, if we represent each factor $\varphi(x_i)^4$ by a 4-valent vertex, and each pair $\{y_i, y_j\}$ by an edge, we get a graph with n 4-valent vertices and p **external legs**, or external lines, that is, edges that have one end which is unattached to any vertex. Each of these external lines carries one of the external positions z_i. (We postpone to Chapter 3 a more precise definition of graphs and related objects.)

This gives the representation of our correlation function by **(open) Feynman diagrams**:

$$\mathbb{E}[\psi(z_1)\cdots\psi(z_p)]_S=\sum_{n\geq 0}\frac{(-\lambda)^n}{n!}\sum_{\Gamma\text{ with }n\text{ vertices}}\frac{1}{\mathrm{Aut}(\Gamma)}\mathcal{A}(\Gamma),$$

where the second sum is on graphs of the aforementioned type, and, for such a graph Γ, $\mathcal{A}(\Gamma)$ is its **amplitude**:

$$\mathcal{A}(\Gamma)=\int\prod_{\{i,j\}\in\sigma}\mathbb{E}[\varphi(y_i)\varphi(y_j)]_G\mathrm{d}x_1\cdots\mathrm{d}x_n,$$

and $\mathrm{Aut}(\Gamma)$ is its symmetry factor, that is, the number of different pairings that produce Γ.

We will call **closed Feynman diagrams**, the graphs obtained from open diagrams by pairing together external lines to get a genuine graph as defined in Chapter 3.

Note that this perturbative expansion works for any polynomial potentials, and yields of course different classes of graphs according to the potential.

For finite underlying spaces X, the integral in the amplitude is actually a finite sum, and, up to our perturbative approximation, we have obtained a purely combinatorial handbook to compute the correlation functions of our theory.

For infinite spaces, it remains to handle the integrals in the x_i's. This is in no way straightforward, as this brings out divergence problems already at each order n. To treat these divergences, **renormalization** techniques are needed. We will not go into the detail of those techniques, which are very involved, and will not appear in the other sections of this introduction.

Even with the caveat of renormalization, the perturbative expansion is both very convenient, since it makes it possible to use combinatorial tools to study QFT, and quite intuitive, as its vertices can be interpreted as particles of sorts, interacting through the

edges or *propagators*. Moreover, as we will mention again later, it has proven to be very efficient to give precise predictions in domains such as particle physics.

This is why several approaches, grouped together under the umbrella term of **constructive QFT**, try to give it a more rigorous meaning. A common factor in these approaches is the use of analytical tools such as the **BKAR forest formula**. Let us cite two important such approaches: the cluster expansion [MM41], that focuses on *local* theories, and the multi-loop vertex expansion [GR15], that focuses on matrix- and tensor-valued field theories (that we will come upon later in this introduction).

Let us also mention that other formulations of QFT do not even involve a functional integral, such as the axiomatic approach (see for instance [Rib]), or recent algebraic approaches (see [Rej16]).

2.2 A primer on general relativity

As we have touched on in the previous subsection, going from Newtonian mechanics to quantum mechanics entails a paradigm shift, from the fundamental notion of a deterministic trajectory, to one of a diffuse density of states. Going from classical mechanics to general relativity causes a paradigm shift of similar magnitude, that can be seen as twofold.

The first part of this shift can already be seen in **special relativity**, which is, technically as well as conceptually, an intermediate step between Newtonian physics and general relativity.

Before explaining this step, let us first briefly recall how the physical world is described in Newtonian mechanics. We are considering matter, living in the Euclidean space $\mathbb{R}^3$. The quintessential object in that formulation is a point-particle, for which one will want to establish equations of motion, that express the rules governing the time evolution of the position of the particle. If one successfully solves these equations, one gets the trajectory of the particle, that is, a function of time (represented by $\mathbb{R}$ or an interval of it) with values in $\mathbb{R}^3$.

One can take a sidestep from this canonical picture, and consider space and time together in the Euclidean space $\mathbb{R}^4$. Then, instead of trajectories in $\mathbb{R}^3$, one looks at **events** on $\mathbb{R}^4$, which would for instance be: "both particles A and B are at position (x, y, z) at time t". Note that, even if we have grouped time and space together, time is still a special coordinate that is naturally separated from the others.

We also recall a fundamental principle in Newtonian mechanics: **Newton's first law of motion** states that, in **inertial reference frames**, an object on which no force acts moves at constant velocity. This implies that all equations of motion have the same form in all inertial reference frames.

This principle also implies that these inertial reference frames are themselves moving at constant velocity from one another. More precisely, the transformations of $\mathbb{R}^4$ that send an inertial frame to another are generated by the time and space translations, the space rotations, and the **shear mappings**, which are of the form

$$(\vec{x}, t) \mapsto (\vec{x} - \vec{v}t, t),$$

where $\vec{v}$ is a fixed vector of $\mathbb{R}^3$.

This is indeed how the coordinates of a system change, when adding constant velocity $\vec{v}$ to the reference frame.

The set of transformations sending an inertial frame to another is called the **Galilean group**, and it is the subset of isometries of the Euclidean space $\mathbb{R}^4$ that preserve the direction of time.

Note that those transformations allow any constant velocity between inertial frames, and thus any velocity for an observed particle. The resulting lack of upper bound on the speed of particles, and therefore on the exchange of information of some type, can be quite disconcerting from a physical point of view.

Moreover, for some very important areas of physics, such as electromagnetic fields, the equations inferred from experimental observations are not invariant under Galilean changes of coordinates.

This is why Einstein postulated that, in addition to the fact that equations of motion are the same in all inertial reference frames (which will still be frames moving at constant velocity from one another), there should be a maximal value c for the speed of any object, which should be the same in all inertial frames. To resolve the problem of the equations of the electromagnetic fields, c should be the **speed of light**.

The only possibility to have this speed to be constant in all inertial frames, is to accept that time is no longer absolute, but rather **relative** to the chosen reference frame.

To grasp more precisely the consequences of Einstein's second postulate, let us look at what is the new fundamental example in the context of relativity: the emission and reception of a light signal. In a given inertial frame, let us denote by (t_1, x_1, y_1, z_1) the spacetime coordinates of the emission of the signal, and (t_2, x_2, y_2, z_2), the coordinates of its reception. The distance d travelled by the signal from the emitter to the receiver can be written in two ways:

$$d = \sqrt{(x_2 - x_1)^2 + (y_2 - y_1)^2 + (z_2 - z_1)^2}$$

and

$$d = c(t_1 - t_2).$$

Thus, in every inertial frame, we must have the equality:

$$c^2(t_1 - t_2)^2 - \big((x_2 - x_1)^2 + (y_2 - y_1)^2 + (z_2 - z_1)^2\big) = 0.$$

We want to show that the quantity

$$s^2 = \Delta(ct)^2 - (\Delta x^2 + \Delta y^2 + \Delta z^2)$$

between two events is always invariant in all inertial frames, even if the events are not separated by the travel of some light signal. We derive this slightly heuristically. Consider two infinitesimally separated events, for which the putative invariant may be written, in some inertial frame $\mathcal{O}$:

$$\mathrm{d}s^2 = c^2\mathrm{d}t^2 - (\mathrm{d}x^2 + \mathrm{d}y^2 + \mathrm{d}z^2).$$

Denote by $\mathrm{d}s'^2$ the equivalent quantity for another inertial frame $\mathcal{O}'$. Then, $\mathrm{d}s^2 = 0$ if and only if $\mathrm{d}s'^2 = 0$, as explained just above, and they are of the same infinitesimal order. (Here we assume the (still undetermined) change of coordinates from $\mathcal{O}$ to $\mathcal{O}'$ is linear, which can be seen as a consequence of the more fundamental assumption that spacetime must be homogeneous in all inertial frames.) Therefore, there exists some scalar a depending only on the relative velocity between $\mathcal{O}$ and $\mathcal{O}'$, such that

$$\mathrm{d}s'^2 = a\mathrm{d}s^2.$$

Now, as we want spacetime to be homogeneous and space to be isotropic in all inertial frames, this a can only depend on the relative *speed* between $\mathcal{O}$ and $\mathcal{O}'$, so that $a = a^{-1} = 1$.

We have thus obtained that $\mathrm{d}s^2$ is invariant in all inertial frames. This implies that the associated pseudo-metric[2] s is also invariant. The vector space $\mathbb{R}^4$, endowed with s, is called the **Minkowski space**.

Hence, in special relativity, the coordinates between two inertial frames are related by an isometry of the Minkowski space, that preserves the direction of time. Theses isometries are generated by spacetime translations, space rotations, and **Lorentz boosts**, which are the relativistic equivalents of shear mappings, as they express the change of coordinates induced by adding a constant velocity $\vec{v}$ to a reference frame. The Lorentz boost for a velocity of speed v along the x axis corresponds to the following change of coordinates:

$$\begin{cases} t & \mapsto \gamma\left(t - \frac{vx}{c^2}\right) \\ x & \mapsto \gamma(x - vt) \\ y & \mapsto y \\ z & \mapsto z, \end{cases}$$

where γ is the **Lorentz factor**

$$\gamma = \frac{1}{\sqrt{1 - \frac{v^2}{c^2}}}.$$

Note that one recovers the shear mapping associated to $\vec{v}$ by taking the limit $v/c \to 0$.

As the above expressions show, in special relativity time and space are deeply intertwined, so that one really has to describe physical systems in terms of events in $\mathbb{R}^4$, rather that trajectories in $\mathbb{R}^3$.

This can be first combined with the Lagrangian formulation of (non-quantum) mechanics. We now denote by $(x_\mu)_{0\leq\mu\leq 3}$ the coordinates of spacetime, with $x_0 = ct$, and write ∂_μ for $\frac{\partial}{\partial x_\mu}$. The relativistic version of the Euler-Lagrange equation, for a Lagrangian $\mathcal{L}(\{x_\mu\}, \varphi, \{\partial_\mu\varphi\})$, may be written as:

$$0 = \frac{\partial \mathcal{L}}{\partial \varphi} - \sum_\mu \partial_\mu \left(\frac{\partial \mathcal{L}}{\partial_\mu \varphi}\right).$$

This can then be further refined into **relativistic QFT**, with the formalism of path integrals. Relativistic QFT is in particular the framework of the **Standard Model**, which is to this day the most precise description of matter at subatomic scale.

While this shift from separated time and space to an entangled spacetime might seem puzzling, it gives to *causality* the central role that it was lacking in Newtonian mechanics. Indeed, in Minkowski space, pairs of events $\{A, B\}$ can be classified into three types:

- **timelike** separated events, for which the spacetime interval

  $$s^2 = (t_A - t_B)^2 - \left((x_A - x_B)^2 + (y_A - y_B)^2 + (z_A - z_B)^2\right)$$

  is positive: this means that a physical system that is slower than light can go from A to B

- **lightlike** separated events, whose spacetime interval s^2 is null: this means that only light can go from A to B

[2]In other chapters of this thesis, we use the term pseudo-metric for functions $f : X^2 \to \mathbb{R}_+$ that are symmetric and satisfy the triangle inequality, but are not positive-definite. Here, we use it for non-degenerate quadratic forms that do not have signature $(1, \ldots, 1)$. However, this should not cause confusion, as we will not talk about the latter in any other chapter.

- **spacelike** separated events, whose spacetime interval s^2 is negative: this means no physical system can go from A to B.

Thus, the events that can be causally related to an event A are either timelike or lightlike separated from it. The set of those events is called the **lightcone** from A, as its boundary, consisting of the lightlike separated events, forms a cone in $\mathbb{R}^4$.

Note that Minkowski space and $\mathbb{R}^4$ endowed with its usual Euclidean metric can be formally related by the operation $t \mapsto it$. This is called a **Wick rotation**, as it corresponds to a rotation in the complex t-plane (that has only a formal meaning). We can see that this rotation is also what relates a Lorentzian QFT with the corresponding Euclidean one, which explains this choice of terminology.

Let us now describe the second step, from special to general relativity. Special relativity gives an adequate formalism to describe both mechnics and electromagnetism, and has the additional perk of having a more intrinsic notion of causality. However, it still relies on making a (seemingly artificial) distinction between inertial frames and all other possible reference frames. This can be conceptually very problematic: if for instance Earth does not happen to be an inertial frame, then we cannot relate any experimental observation with theoretical predictions obtained from equations of motion.

This is why Einstein, adding on to his previous and already revolutionary refinement of the description of spacetime, set out to determine how should the coordinates of a physical system should change, when one adds a non-zero acceleration to the reference frame.

Consider two physical systems, one having constant acceleration $\vec{a}$, and another being at rest but subjected to a constant gravitational field $-\vec{a}$. The fundamental observation of Einstein was that these two systems should have the same equations of motion. This lead him to assume that more generally, a gravitational field is physically equivalent to an acceleration of the reference frame.

Thus, one assumes that in general, the differential 2-form of $\mathbb{R}^4$ that is invariant under change of frame is not necessarily

$$c^2\mathrm{d}t^2 - (\mathrm{d}x^2 + \mathrm{d}y^2 + \mathrm{d}z^2),$$

but

$$\mathrm{d}s^2 = \sum_{0\leq\mu,\nu\leq 3} g_{\mu\nu}\mathrm{d}x_\mu\mathrm{d}x_\nu,$$

where the coefficients $g_{\mu\nu}$, which are smooth functions on $\mathbb{R}^4$, characterize the gravitational field in the considered reference frame, or equivalently its acceleration[3].

In modern mathematical terms, each reference frame equips the spacetime $\mathbb{R}^4$ with the structure of a **Lorentzian manifold**, with metric tensor $\{g_{\mu\nu}\}$. This tensor quantifies how spacetime deforms under the gravitational field. Thus, for the inertial frames of special relativity, where the gravitational field is considered null, the metric is the flat one of

[3]Note that, for general changes of reference frames, the speed of light c is actually no longer constant: however, the form of the induced change of coordinates ensure that laws such as the Maxwell equations for the electromagnetic field (which were what guided Einstein to postulate the invariance of the speed of light under change of inertial frames), are still invariant.

Minkowski space, given by the diagonal tensor

$$\begin{pmatrix} 1 & 0 & 0 & 0 \\ 0 & -1 & 0 & 0 \\ 0 & 0 & -1 & 0 \\ 0 & 0 & 0 & -1 \end{pmatrix}.$$

When considering some physical system in spacetime, the evolution of the tensor $g_{\mu\nu}$ must be part of the description of the system. Using only formal considerations on the behavior of quantities related to the metric tensor, Einstein derived the law of its evolution, called the **Einstein field equation**. In a modern language, it may be written as

$$R_{\mu\nu} - \frac{1}{2} g_{\mu\nu} R + \Lambda g_{\mu\nu} = \frac{8\pi G}{c^4} T_{\mu\nu}$$

where $R_{\mu\nu}$ is the **Riemann curvature** associated to the (pseudo-)metric, R is the **Ricci scalar**, Λ is the **cosmological constant** (accounting for dark matter), and $T_{\mu\nu}$ is the **stress-energy tensor** (which describes the density and flux of energy and momentum in spacetime). We take the liberty not to define these quantities precisely, as we will not discuss this equation in detail in the sequel.

It can be expressed as the Euler-Lagrange equation for the **Einstein-Hilbert action**

$$S_{EH}(\Lambda, G) = \int_M \mathrm{d}\xi \sqrt{-g(\xi)} \left(\frac{1}{16\pi G} (R(\xi) - 2\Lambda) + \mathcal{L}_{mat} \right),$$

where M is spacetime with its Lorentzian structure, g is the determinant of the Lorentzian pseudo-metric on M (so that $\mathrm{d}\xi \sqrt{-g(\xi)}$ is the canonical volume form), and $\mathcal{L}_{mat}$ is the part of the Langrangian accounting for matter.

As the QFT formalism of the Standard Model seems to describe very accurately all the fundamental interactions of matter except for gravity, it is natural to want to also refine Einstein's theory of gravity, by applying to it the procedure we saw in the previous subsection, to go from classical to quantum mechanics. However, this procedure fails in the case of the gravitational field. Indeed, the perturbative expansion yields terms that diverge order by order, and cannot be transformed into convergent ones by renormalization techniques (see eg. [Des00]).

In fact, this technical failure can be predicted by a conceptual objection: in classical physics, as well as special relativity, spacetime is a background on which physical matter lives. This combines well with the path integral formalism, where physical systems are described by measures on functions (or distributions) on spacetime. In general relativity, however, spacetime is itself an actor of the physical world, that dynamically interacts with the rest of it. Trying to express the geometry of spacetime as a function of itself is bound to create an unescapable loop.

One must therefore find some other way(s) to combine general relativity and quantum mechanics, to create a theory of **quantum gravity**.

2.3 The random geometry approach

As we have seen in Section 2.1, a quantum theory can be related to a genuine random measure, by a Wick rotation. This motivates the idea of approaching the problem of quantum gravity by studying relevantly chosen *random* geometric spaces.

We use the expression "geometric spaces" in a purposefully loose way, as the precise type of spaces will heavily depend on the specific approach. The only common denominator is

that the chosen structure should yield, in the classical (non-quantum) limit, the Lorentzian manifolds of general relativity.

And some approaches do not even have this goal, but the alternative one of having *Riemannian* manifolds as classical limits. This is motivated by what can be seen as an additional Wick rotation: if one can recover a Riemannian spacetime as the classical limit of a quantum theory, then performing a "Wick rotation" on the quantum spacetime should yield an actual Lorentzian spacetime as the limit. While Wick rotations between QFTs are relatively well understood, the notion of Wick rotation in the context of general relativity is very hazy, so that this motivation is quite heuristic. This is, however, the framework of the **colored tensor models** that are central to this thesis, and that we will define later.

Suppose now that one wants to keep the formalism of QFT to obtain some sort of Euclidean quantum spacetime. To circumvent the failure of the canonical quantization of Einstein's theory, a possible strategy is to get rid of the background spacetime by having a purely combinatorial theory, with a discrete underlying space. This implies that the structure of the spacetime built on top of it will necessarily be discretized. A continuum spacetime can then only recovered by taking a **scaling limit**, with the number of points in the underlying space going to infinity, and the size of the cells of the discretized structure going to zero.

In this context, one thus wants to have an action on discrete structures that somehow yields the Einstein-Hilbert action in a continuum limit. Regge [Reg61] derived such an action for simplicial spaces, that is, made of gluings of D-dimensional simplices along their $(D-1)$-dimensional faces. Note that even though the ultimate goal is to define a 4-dimensional spacetime, this formalism can be used in any dimension.

Let us start with the Einstein-Hilbert action without any matter field:

$$S_{EH}(\Lambda, G) = \frac{1}{16\pi G}\int_M \mathrm{d}\xi \sqrt{-g(\xi)}(R(\xi) - 2\Lambda).$$

This has two terms, one proportional to the total volume, and the other equal to the integral of the Ricci scalar. We replace the volume term by the sum of the volumes of the D-simplices, and the curvature one by the sum of the **deficit angles** ε around the $(D-2)$-simplices :

$$\varepsilon(\sigma) = 2\pi - \sum_{\substack{\sigma_D,\\ \sigma\in\sigma_D}} \theta(\sigma, \sigma_D) \tag{2.3.1}$$

where $\theta(\sigma,\tau)$ is the dihedral angle of the $(D-2)$-simplex σ in the D-simplex τ. If we only consider regular simplices, this angle is:

$$\varepsilon(\sigma) = 2\pi - \sum_{\substack{\sigma_D,\\ \sigma\in\sigma_D}} \arccos\frac{1}{D}. \tag{2.3.2}$$

We thus get the **Regge action**:

$$S_R(\Lambda, G) = \frac{1}{16\pi G}\Big(2\Lambda\sum_{\sigma_D} v(\sigma_D) - \sum_{\sigma_{D-2}} v(\sigma_{D-2})\varepsilon(\sigma_{D-2})\Big) \tag{2.3.3}$$

where $v(\sigma)$ is the volume of the simplex σ, and where the sum $\sum_{\sigma_k}$ is over the k-simplices of the considered simplicial space.

Later in this introduction, we will present the theory of colored tensor models, where we will see this action appear again in a slightly different form. For now, let us mention a few other approaches to quantum gravity.

There are two very prominent approaches to quantum gravity. The first one is **string theory**, which builds up on the Standard Model by replacing point-particles by extended, one-dimensional objects called strings (see [BBS07]). This makes it possible to add to the Standar Model a new particle, the graviton, that carries the gravitational force, like the photon carries the electromagnetic force. While this approach is conceptually very different from the random geometrical theories, it describes trajectories as 2-dimensional objects, on which one may want to define a "natural" probability measure: this goal meets the one of the random geometry approach for 2-dimensional spacetime. We will get into more details on this in the next section.

The other very prominent approach to quantum gravity is **Loop Quantum Gravity**. It is, rather than a random geometrical approach, an intrinsically *quantum* geometrical approach, as it describes spacetime as a set of quanta of spacetime with volume and boundary area given by the quantum numbers of a spin system (see for instance [Rov11]).

Closer to colored tensor models, the models of **dynamical triangulations** are also random models of simplicial spaces using the Regge action, but that were investigated with numerical tools rather than pertubative QFT (for $D = 3$ or 4). **Euclidean Dynamical Triangulations** are models of Euclidean simplicial spaces: they were found to yield singular scaling limits [Tho99], including a **crumpled phase** similar to the one I have established with mathematical techniques for colored tensors (see Chapters 4 and 6). **Causal Dynamical Triangulations** have a Lorentzian structure, which yields more encouraging numerical results (see for instance [AGJL14]). For $D = 2$, dynamical triangulations, like colored tensor models, are closely related to **random maps**, which will be discussed in detail in Chapter 3.

2.4 Matrix models

We finish this "physical" part of the introduction, by presenting an approach to quantum gravity that is motivated by string theory, but can be seen as a $2D$ version of the random geometry approach. As we will see, it is related to random models of maps that will be presented in Chapter 3.

Liouville Quantum Gravity

As was briefly mentioned in the previous subsection, string theory replaces point-particles with one-dimensional objects, so that trajectories are replaced by two-dimensional objects, still embedded in spacetime.

Thus, one would like to make sense of the "string of a free particle", if possible in the formalism of QFT dear to physicists. Suppose a string Σ is parametrized as $x(z), z \in \mathbb{C}$, in spacetime X. In a seminal article [Pol81], Polyakov made the conceptual inversion of considering Σ as a background two-dimensional spacetime equipped with "matter fields" $x(z)$, describing the physical spacetime. This makes it possible to endow Σ with any kind of field, starting with the 0-dimensional toy model with a trivial field.

The idea is that we want to have a global action on strings Σ that may be written as

$$S_{tot}[\Sigma] = S_{self}[\Sigma] + S_{int}[\Sigma]$$

where S_{int} encodes the interaction of the string and the physical spacetime X, and S_{self} corresponds to its "self-interaction". The latter depends on the volume and curvature of the string, like the Einstein-Hilbert action: thus, we can also interpret this theory as genuinely describing a two-dimensional quantum spacetime, although this point of view is less directly thrilling for the purpose of describing our actual, four-dimensional Universe.

For a parametrization of the string $x(z) \in X$, this self-interaction term would write, as argued by Polyakov:

$$S_{self} = \int \sqrt{g} \left(\sum_{\substack{1 \leq a,b \leq 2 \\ 1 \leq \mu,\nu \leq D}} g^{ab} \partial_a x^\mu \partial_b x^\nu G_{\mu\nu}(x) \right) \mathrm{d}z,$$

where g_{ab} is the metric of the string, D is the dimension of the spacetime X, and $G_{\mu\nu}$ is its metric.

Such an action is difficult to tackle, so that Polyakov took the route of considering string metrics g in one fixed conformal class. This leads to the theory of **Liouville Quantum Gravity**. We will not explain Polyakov's original derivation, but rather sketch the content of this theory, in a modern mathematical formulation that greatly borrows from [DKRV] and [GRV].

Let g be the metric of a smooth Riemann surface M. The uniformization theorem states that in the class of metrics that are conformally equivalent to g:

$$[g] = \{e^\varphi g | \varphi \in C^\infty(M)\},$$

there exists a unique metric $g_0 = e^{\varphi_0}$ of constant scalar curvature -2. This metric is found by minimizing the functional

$$F[\varphi] = \int_M \left(\frac{1}{2} |\nabla \varphi_g|^2 + R_g \varphi + 2e^\varphi \right) \mathrm{d}v_g.$$

Making the change of variables $\varphi \to \varphi/\gamma$, we get a new functional, called the **classical Liouville functional**:

$$S_{L,c}[\varphi] = \frac{1}{4\pi} \int_M \left(|\nabla \varphi_g|^2 + Q_c R_g \varphi + 4\pi\mu e^{\gamma\varphi} \right) \mathrm{d}v_g,$$

where the parameters Q_c, μ, γ satisfy $Q_c = 2/\gamma$ and $\pi\mu\gamma^2 = 1$. Indeed, we have

$$S_{L,c}[\varphi] = F[\gamma\varphi]/(2\gamma^2\pi).$$

Note that minimizing $S_{L,c}[\varphi]$ is equivalent to satisfying the **Liouville equation**

$$\Delta_g \varphi - R_g = 2e^\varphi,$$

hence its name.

The classical Liouville functional is **conformally invariant**, in the sense that, if we apply a conformal transformation f to M, and change the field by $\varphi \to \varphi \circ f + 2/\gamma \log |f'|$, this leaves the action unchanged.

We now want to quantize this theory, which should give quantum fluctuations of the string metric around the representative g_0.

It turns out [DKRV; GRV] that, due to renormalization, to have conformal invariance for the associated QFT, one must use the slightly different action:

$$S_L[\varphi] = \frac{1}{4\pi} \int_M \left(|\nabla \varphi_g|^2 + Q R_g \varphi + 4\pi\mu e^{\gamma\varphi} \right) \mathrm{d}v_g,$$

with $Q = 2/\gamma + \gamma/2$. This conformal invariance is quite important, as it puts Liouville Quantum Gravity in the class of **Conformal Field Theories**, for which a lot of specific techniques have been developed.

Note that the value of γ, which tunes the correction that we must apply on the field when doing a conformal transformation, can be interpreted as tuning the coupling of "matter field" with the $2D$ string "spacetime". Physical arguments imply that the dimension of the matter field (that is, the physical spacetime) is

$$D = 25 - 6Q^2 = 25 - 6\left(\frac{2}{\gamma} + \frac{\gamma}{2}\right)^2.$$

Mathematically rigorous approaches of this QFT, using the framework of **Gaussian multiplicative chaos**, were first achieved for the range $\gamma \in (0, 2]$ [DS; DKRV]. These values of γ correspond to $D \in (-\infty, 1]$, a quite frustrating range for the dimension of a physical spacetime. However, there has been recent progress for complex values of γ [GHPR], which corresponds to $D \in (1, 25)$.

Recall that in the $2D$-spacetime interpretation, the underlying spacetime is seen as a "matter field" on the string. For particular values of γ, corresponding to

$$D = 1 - 6/(m(m+1))$$

for some integer $m \geq 2$, this matter field corresponds to well-known models of statistical physics. We will touch on this again in Chapter 3.

We will not get into more details on the techniques of Liouville Quantum Gravity, as we will now present a different strategy for tackling these quantum/random surfaces: *discretizing* them into maps.

Matrix models and maps

Let us focus on the case of $D = 0$, that is, a pure theory of strings, without a physical spacetime. We want to make sense of a theory of surfaces Σ, with an action of the form

$$S(\Sigma) = \alpha A(\Sigma) - \beta R(\Sigma), \tag{2.4.1}$$

where α, β are some parameters, A is the area of the surface, and R a measure of its curvature.

If we consider, instead of smooth surfaces, **triangulations**, *i.e.* PL surfaces made of equilateral triangles glued along their edges, we found ourselves in the $2D$ case of the Regge action of (2.3.3). Thus, for a triangulation T with V vertices, E edges and F faces, its area is just its number of faces F, and its curvature is its **Euler characteristic**

$$\chi(T) := V - E + F.$$

Note that this can be done with more general polygons, which yields general **maps** instead of triangulations. We postpone to Chapter 3 a more thorough definition of maps and related objects.

We have thus replaced a functional integral over smooth surfaces, with a sum over maps, with a weight that depends on their number of faces and their Euler characteristic:

$$\sum_m a^{F(m)} b^{\chi(m)}. \tag{2.4.2}$$

We will now briefly explain how we can recover a QFT formalism for this discretized model.

As we have explained in Chapter 2, the correlation functions of a scalar QFT can be perturbatively encoded into Feynmann graphs. Let us consider now a QFT on complex hermitian $N \times N$ matrices:

$$\mu_S(\mathrm{d}M) = e^{-S[M]}\mathrm{d}M,$$

with an action S such as

$$S[M] = N\frac{\mathrm{tr}(M^2)}{2} - \sum_{p\in I} \lambda N \frac{\mathrm{tr}(M^p)}{p},$$

and as the canonical measure $\mathrm{d}M$, the Haar measure on H_N, normalized so that

$$\int_{H_N} e^{-N\frac{\mathrm{tr}(M^2)}{2}}\mathrm{d}M = 1.$$

If we perturbatively expand the correlation functions or the partition function of the theory, we get coefficients of the form:

$$\frac{(-1)^n}{n!}\int_{H_N}\left(\prod_{1\leq k\leq n}\lambda N\frac{\mathrm{tr}(M^{p_k})}{p_k}\right)e^{-N\frac{\mathrm{tr}(M^2)}{2}}\mathrm{d}M.$$

As before, the measure $e^{-N\frac{\mathrm{tr}(M^2)}{2}}\mathrm{d}M$ is Gaussian, with covariances between matrix coefficients:

$$\mathbb{E}[M_{ij}M_{kl}] = \frac{\delta_{il}\delta_{jk}}{N},$$

so that, under this measure, we have the following form of Wick's theorem:

$$\mathbb{E}\left[\prod_{1\leq k\leq n} N\frac{\mathrm{tr}(M^{p_k})}{p_k}\right] = (\lambda N)^n \prod_{1\leq k\leq n}\sum_{1\leq i_1^{(p_k)},\ldots,i_{p_k}^{(p_k)}\leq N}\sum_{\text{pairing }\sigma}\prod_{(i_j^{(p)},i_l^{(p')})\in\sigma}\frac{\delta_{i_j^{(p)}i_{l+1}^{(p')}}\delta_{i_l^{(p')}i_{j+1}^{(p)}}}{N}, \tag{2.4.3}$$

where the pairing σ is over all the indices belonging to the tuples $i_1^{(p)},\ldots,i_p^{(p)}$, and, by convention, $i_{p+1}^{(p)} = i_1^{(p)}$.

To get, as before, a graphical representation of this expression, we associate to each p-tuple $i_1,\ldots,i_p$ a p-valent vertex, whose incident edges are indexed by the pairs $(i_j^{(p)}, i_{j+1}^{(p)})$: we can imagine these edges as being strands with two boundaries, each one bearing an index, rather than just a line. Then, σ describes the pairing of these half-strands into edges, with the condition that the upper index of a half-strand is equal to the lower one of the other, and vice versa.

There are several ways to see that this construction yields maps rather than abstract graphs. One is to observe that the indices around a vertex give a cyclic ordering of the incident edges, which does yield the structure of a map, as will be explained in Chapter 3. Another would be to recognize that the fattening of the edges into strands induces a **ribbon graph**, which is also equivalent to a map. In any case, we do get maps for the Feynmann graphs of our theory, and (2.4.3) can be rewritten as

$$\mathbb{E}\left[\prod_{1\leq k\leq n}\lambda N\frac{\mathrm{tr}(M^{p_k})}{p_k}\right] = \sum_m \frac{\lambda^n N^{\chi(m)}}{\#\mathrm{Aut}(m)}, \tag{2.4.4}$$

where the sum is over maps m with n vertices, of respective valences $p_1,\ldots,p_n$, and $\#\mathrm{Aut}(m)$ is their number of automorphisms.

Thus, we have obtained a weighting of maps of the form of (2.4.2), as the perturbative expansion of a QFT on hermitian matrices. We will not go into much more detail for this family of QFTs, but we will refer to it in Chapter 4 when we get to the setting of *tensor*-valued QFTs. For a detailed account on matrix models in the context of $2D$ quantum gravity, see for instance [FGZJ95].

While we got to matrix models by trying to emulate a Regge-like action on families of maps, another way to get to them from continuum theories is to see the matrix-valued field as the cutoff of the Fourier transform of a field parametrizing a smooth surface (see for instance [Ori09], for an explanation in the framework of Group Field Theory).

With that point of view, it is natural to consider the size N of the matrices as a parameter that is meant to be sent to infinity in the continuum limit. In particular, (2.4.4) is called a **$1/N$ expansion**, since maps of increasing genus are increasingly suppressed when N is large.

The "naive" way of taking a large-N limit is to just keep the dominant maps, which are the planar ones, and then search for a scaling limit for these (by taking their number of vertices to infinity, and rescaling appropriately their mesh size). This is a route that we will explore in Chapter 3, and also for the higher-dimensional tensor models of Chapter 4.

A less naive method would be to fine-tune the limit $N \to \infty$ and the scaling limit: this is called a **double scaling limit**. This has the advantage of mixing different topologies, but it is trickier to get non-trivial limit objects this way, as we will see in the case of tensors in Chapter 4.

Note that this $1/N$ expansion, that depends on the genus of the considered maps, induces a recursion on the genus for calculating quantities related to these maps. This recursion can be seen as a particular case of **topological recursion**, which is a general framework for enumerating various topological structures with respect to their natural notion of topological complexity [Eyn16].

CHAPITRE 3

Geometry of random maps

We will now do a quick tour of the thriving domain of random maps, with a particular attention to their geometric properties.

We start by recalling in Section 3.1 basic definitions that we will need in the sequel, as well as presenting a few fundamental techniques and results.

We will then present complementary points of view for investigating geometric properties of random maps: the bijective approach in Section 3.2, peeling processes, in Section 3.3 and layer decompositions, in Section 3.4.

Finally, in Section 3.5, we will focus on the family of maps that we are more specifically interested in, Eulerian triangulations.

3.1 Basic definitions and results

We begin by giving precise definitions of a few graph-theoretic and combinatorial notions that will be used in the sequel.

Graphs

Definition 3.1.1. A (finite) **graph** is a pair $G = (V, E)$, where V is a finite set, and E is a set of unordered pairs of elements of V.

The elements of V are called the **vertices** of G, and the elements of E, its **edges**. For an edge $e = \{u, v\}$, u and v are called the **extremities** of e, and e is said to be **incident** to u and to v, and reciprocally. If two edges are incident to the same vertex, we say they are **adjacent**.

In the sequel, we will sometimes consider the set $\vec{\boldsymbol{E}}$ of **oriented edges** of G, which are edges of G together with one of their extremities, called their **initial vertex**. We usually indicate that an edge is oriented by drawing an arrow from its initial vertex to its other extremity (see for instance Figure 3.1.2). To simplify notation, we will denote both oriented and non-oriented edges by e, e' and so on, precising when we are dealing with oriented edges to avoid confusion. For an oriented edge e, we will denote by $e-$ its initial vertex.

A priori, we allow our graphs to have **loops**, *i.e.* edges whose both extremities are the same vertex, and **multiple edges**, *i.e.* different edges with the same extremities.

By convention, we consider that a loop still has two choices of orientation (this will be more natural when we get to maps), so that we always have $\#\vec{E} = 2\#E$.

In the sequel, we will come upon more specific classes of graphs:

Definition 3.1.2. A graph $G = (V, E)$ is **bipartite** if V can be partitioned into black and white vertices, in such a way that a black vertex only shares edges with white vertices, and *vice versa*.

The **valence** of a vertex is the number of edges incident to it (a loop counting for 2). A graph G is ***d*-regular**, if all its vertices have valence d.

Cell complexes and maps

To define maps, and include them in the more general notion of **cell complexes** that we will use in the next chapter, we now recall a bit of combinatorial topology.

Definition 3.1.3. An **open *n*-cell** is a topological space homeomorphic to the open unit ball of $\mathbb{R}^n$, denoted by $\mathbb{B}^n$. Likewise, a **closed *n*-cell** is a topological space homeomorphic to the closed unit ball of $\mathbb{R}^n$, denoted by $\overline{\mathbb{B}}^n$.

Definition 3.1.4. Let X be a topological space. A **cellular decomposition** of X is a partition $\mathcal{E}$ of X into open cells of different dimensions, satisfying the following conditions: for every cell $e \in \mathcal{E}$ of dimension $n \geq 1$, there exists a continuous function Φ of some closed n-cell D into X (called **characteristic function of *e***), that induces a homeomorphism from $\mathring{D}$ into e, and that sends ∂D into the union of cells of $\mathcal{E}$ of dimension less than n.
A **cell complex** is a Hausdorff space X, together with some cellular decomposition $\mathcal{E}$. We then denote the complex by $(X, \mathcal{E})$, or only X if there is no ambiguity.

In the sequel, we will mostly consider **finite** cell complexes, *i.e.* complexes $(X, \mathcal{E})$ where $\mathcal{E}$ is finite. We then call **dimension of the complex** the maximal dimension of the cells of $\mathcal{E}$. Let us note that any finite cell complex is necessarily compact.

A cell complex comes naturally with the notion of subcomplexes:

Definition 3.1.5. Let $(X, \mathcal{E})$ be a cell complex. A **subcomplex** of X is a subspace $Y \subseteq X$, that is a union of cells, such that, if Y contains a cell, then it also contains its closure.
For any $n \in \mathbb{N}$, we define the ***n*-skeleton X_n** of X as the union of cells of X of dimension smaller than or equal to n. It is clear it is a subcomplex of X.
The 0-skeleton of X is also called the **set of vertices** of X.

A graph G can thus be naturally seen as a cell complex of dimension 1, whose 0-cells are the vertices of G, and whose 1-cells are the edges of G. In particular, we can consider the embeddings of the induced topological space into other topological spaces.

Definition 3.1.6. An embedding f of a connected graph G into a surface S is called **2-cellular**, if all the connected components of $S \setminus f(G)$, called its **regions**, are all homeomorphic to the open disk.

Such an embedding defines a 2-cell complex whose 1-skeleton is $f(G)$: we call it a **map** with underlying graph G. The 2-cells of a map $\mathfrak{m}$ are naturally called its **faces**, and we denote the set of faces of $\mathfrak{m}$ by $F(\mathfrak{m})$.

A **rooted** map is a map together with a distinguished oriented edge. We call **root vertex** the initial vertex of the root edge, and **root face**, the face incident to the left of the root edge.

In the sequel, we only consider maps on **orientable** surfaces. In particular, a map that is embedded into the sphere is called a **planar** map. When representing a planar map, we often draw it in the plane, by blowing up one of its faces into an unbounded face (see for instance Figure 3.1.2).

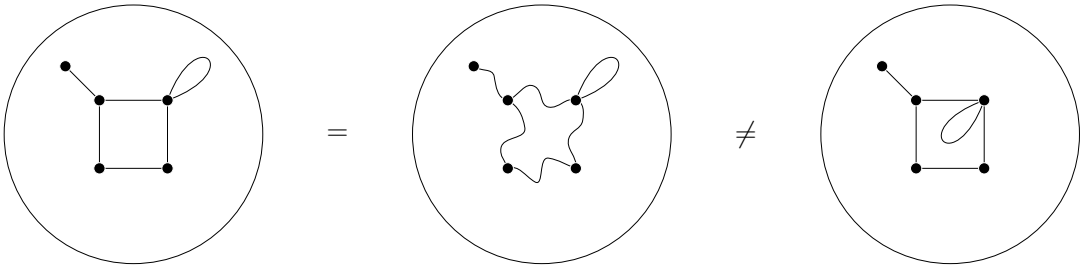

Figure 3.1.1 – Maps are defined up to orientation-preserving homeomorphisms of the surface they are embedded into.

We usually consider maps up to isomorphisms, that is, up to orientation-preserving homeomorphisms of the surface S (see Figure 3.1.1), as this yields a finite number of maps with, say a given number of edges and faces. We naturally define map automorphisms as isomorphisms from a map onto itself. It is quite convenient to consider rooted maps, because they have no non-trivial automorphisms:

Proposition 3.1.7. *An automorphism of a map that fixes one oriented edge fixes all the edges of the map.*

We will denote by $\mathcal{M}$ the set of rooted maps considered up to isomorphisms.

Considering topological objects up to isomorphism can be a bit awkward. It turns out that maps considered up to isomorphisms admit a more direct and combinatorial definition, that we give now.

Consider a map $\mathfrak{m}$, on a surface S. If we cut S along the edges of $\mathfrak{m}$, we obtain a finite number of polygons, so that, rather than seeing $\mathfrak{m}$ as the 2-cellular embedding of graph, we can see it as a gluing of polygons (see Figure 3.1.2).

Let us orient the boundaries of these polygons counterclockwise, so that each polygon lies to the left of its oriented edges, and each oriented edge in $\vec{E}(\mathfrak{m})$ appears on the boundary of exactly one polygon. Thus, we can define a permutation φ on $\vec{E}$, that sends an oriented edge belonging to the boundary of some polygon, to the next oriented edge on this boundary: the cycles of φ are naturally identified with the faces of $\mathfrak{m}$.

Since, for an edge e of $\mathfrak{m}$, the two oriented versions of e (seen as oriented edges on the boundary of some polygon) are glued together in $\mathfrak{m}$, we can also define a fixed-point free involution α on $\vec{E}(\mathfrak{m})$, whose cycles are naturally identified with the edges of $\mathfrak{m}$.

Finally, it is straightforward to check that the permutation $\sigma = \alpha\varphi^{-1}$ sends the oriented edge e to the oriented edge e', where e' is the next edge clockwise around $e-$ in $\mathfrak{m}$. Thus, the cycles of σ are naturally identified with the vertices of $\mathfrak{m}$.

Moreover, as we consider connected maps, for any two oriented edges e, e' in $\vec{E}(\mathfrak{m})$, there exists a word on the alphabet $\{\sigma, \alpha, \varphi\}$, that sends e to e', so that the group of permutations $\langle \alpha, \sigma, \varphi \rangle$ generated by σ, α, φ acts transitively on $\vec{E}(\mathfrak{m})$.

This motivates the following definition:

Definition 3.1.8. Let X be a finite set of even cardinality. A **fatgraph structure** on X is a triple $(\sigma, \alpha, \varphi)$ of permutations of X, such that $\varphi\alpha\sigma = 1$, α is a fixed-point free involution, and the group $\langle \alpha, \sigma, \varphi \rangle$ acts transitively on X.

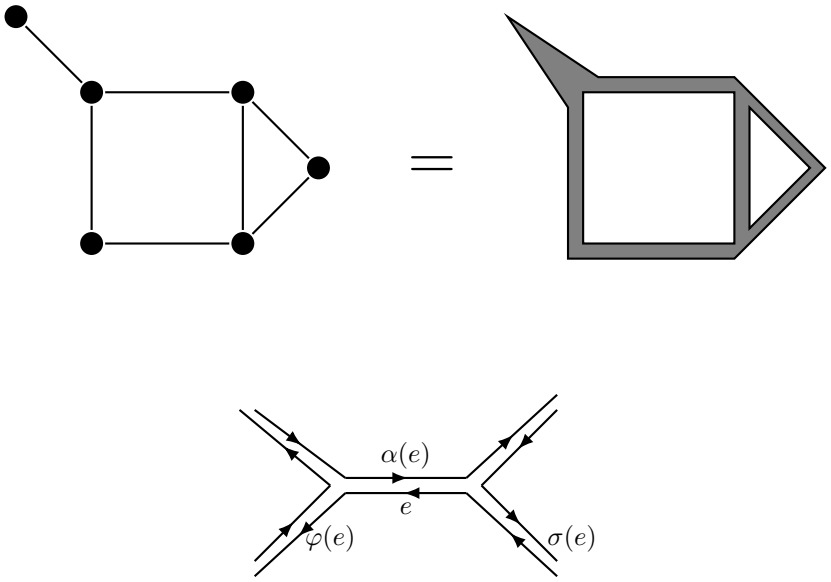

Figure 3.1.2 – Maps can be defined as gluings of polygons (top), which can be described by a triplet of permutations (bottom).

Two fatgraph structures $(\sigma, \alpha, \varphi)$ on X and $(\sigma', \alpha', \varphi')$ on X' are **isomorphic** if they are the same up to relabeling, *i.e.* if there exists a bijection $\pi : X \to X'$ such that

$$\pi\sigma\pi^{-1} = \sigma', \quad \pi\alpha\pi^{-1} = \alpha', \quad \pi\varphi\pi^{-1} = \varphi'.$$

Theorem 3.1.9. [MT01] *The set of maps considered up to isomorphisms is naturally identified with the set of fatgraph structures considered up to isomorphisms.*

Note that a fatgraph structure is also equivalent to an abstract graph, together with a cyclic ordering of the edges around each of its vertices (as given by σ): this description of a map is sometimes called a **rotation system**.

Viewing a map as a gluing of oriented polygons, not only yields this convenient combinatorial characterization, but makes it also more straightforward to define some basic notions that we have not mentioned yet.

Thus, the **degree** of a face f of a map is the perimeter of the corresponding polygon: it might not be the number of distinct edges incident to f, as some may be visited twice along the boundary of f. We call such an edge, an **isthmus** in the face f.

Let p be an integer greater than 2. A map $\mathfrak{m}$ is called a ***p*-angulation**, if all faces of $\mathfrak{m}$ have degree p. For the $p = 3$, we use the term **triangulation** instead of 3-angulation, and for $p = 4$, **quadrangulation**.

The orientation of edges around the faces of a map also allows us to define the notion of corners:

Definition 3.1.10. Let $\mathfrak{m}$ be a map, and let f be a face in $\mathfrak{m}$, and $e_1, \ldots, e_d$ the oriented edges around f ordered counterclockwise. To every $i \in \{1, \ldots, d\}$, we associate a **corner**, namely, an angular sector included in f and bounded by the edges e_{i-1} and e_i , where by convention $e_0 = e_d$.

We can associate to each corner the vertex that is incident to it: if a vertex v is incident to several corners of a given face f, we say v is a **separating vertex** of f. A face with no separating vertex is said to be **simple**.

A **map with boundaries** is a map with a certain number of distinguished faces, that are called its **external faces**. The other faces of the map are naturally called its **internal faces**. We allow two external faces to share vertices, but not edges. If all the internal faces of a map $\mathfrak{m}$ with boundaries have degree p, we call $\mathfrak{m}$ a ***p*-angulation with boundaries**. We call **map of the p-gon**, a planar map with one external face of degree p. We will usually denote by $\partial\mathfrak{m}$ the boundary cycle of a map with one boundary.

A very important object associated to a map is its dual map:

Definition 3.1.11. Let $\mathfrak{m}$ be a map given as the fatgraph structure $(\alpha, \sigma, \varphi)$. We define the **dual** of $\mathfrak{m}$ as the map induced by $(\varphi, \alpha, \alpha\sigma\alpha)$, and denote it by $\mathfrak{m}^*$.

Graphically, $\mathfrak{m}^*$ can be constructed by putting a dual vertex v_f at the center of each face f of $\mathfrak{m}$, and, for two faces f, f' of $\mathfrak{m}$ sharing an edge e, drawing a dual edge e^* between v_f and $v_{f'}$, that crosses e and does not intersect any other edge of $\mathfrak{m}$ (see Figure 3.1.3). This construction does yield a graph embedded into the same surface as $\mathfrak{m}$, and it is straightforward to check that its structure is the one given in the above definition.

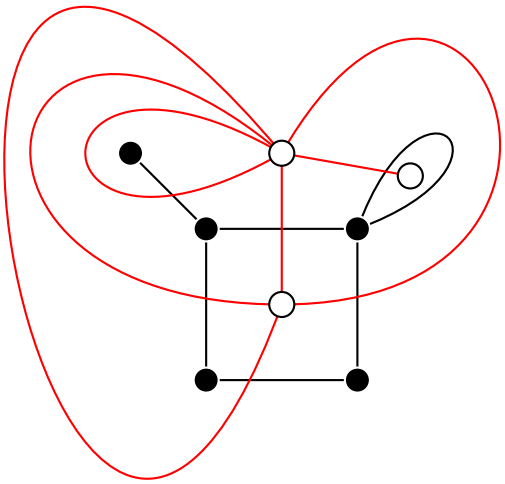

Figure 3.1.3 – A map (black vertices and edges) and its dual (white vertices and red edges).

Theorem 3.1.12 (Euler's formula)**.** *Let $\mathfrak{m}$ be a map on an orientable surface S of genus g. Then*

$$\#V(\mathfrak{m}) - \#E(\mathfrak{m}) + \#F(\mathfrak{m}) = 2 - 2g.$$

*The number $\chi = 2 - 2g$ is called the **Euler characteristic** of S.*

Note that Euler's formula the dual of a map may be written exactly the same way, since the number of vertices and faces are exchanged, while the number of edges remains the same.

Abstract and plane trees

Definition 3.1.13. An **abstract tree** is a connected graph with no cycle. Equivalently, it is a connected graph $G = (V, E)$ such that $\#V = \#E + 1$.

A **forest** is a set of abstract trees.

A **plane tree** is a map $\mathfrak{t}$ which, as a graph, is a tree. Since $\mathfrak{t}$ has no cycle, any embedding of $\mathfrak{t}$ is necessarily on the sphere. Moreover, the absence of cycles is equivalent to the fact that, as a map, $\mathfrak{t}$ has a unique face.

Let $\mathfrak{t}$ be a tree with n edges. Let $e_0, e_1, \cdots, e_{2n-1}$ be the sequence of oriented edges bounding the unique face of $\mathfrak{t}$, starting with the root edge, and ordered counterclockwise around this face. Then let $u_i = e_i^-$ be the i-th visited vertex in this contour exploration, and set the **contour process** of $\mathfrak{t}$ at time i to be:

$$C_{\mathfrak{t}}(i) := d_{\mathfrak{t}}(u_0, u_i),\ 0 \leq i \leq 2n-1,$$

where $d_{\mathfrak{t}}$ is the graph distance on $\mathfrak{t}$, and with the convention that $u_{2n} = u_0$ and $C_{\mathfrak{t}}(2n) = 0$. We also extend $C_{\mathfrak{t}}$ by linear interpolation between integer times: for $0 \leq s \leq 2n$

$$C_{\mathfrak{t}}(s) = (1 - \{s\})C_{\mathfrak{t}}(\lfloor s \rfloor) + \{s\}C_{\mathfrak{t}}(\lfloor s \rfloor + 1),$$

where $\{s\} = s - \lfloor s \rfloor$ is the fractional part of s. Thus, the contour process $C_{\mathfrak{t}}$ is a non-negative path of length $2n$, starting and ending at 0, with increments of 1 between integer times. We call such paths, **discrete excursions of length $2n$**, and denote their set by $\mathcal{E}_n$. It is straightforward to show that the mapping that associates with every tree its contour process is a bijection.

Generating functions and analytic combinatorics

Now that we have defined maps as combinatorial objects, we may want to *enumerate* certain types of maps. For instance, we might want to count the number of rooted plane trees with n edges, denoted by t_n. For this purpose, a very important object is the associated **generating function**:

$$T(x) := \sum_{n \geq 0} t_n x^n,$$

which is a formal series in x, with integer coefficients.

A way to obtain an explicit expression for this series is to use Tutte's recursion, which decomposes the tree into smaller ones by removing the root edge (see Figure 3.1.4). This yields

$$T(x) = 1 + xT(x) + x^2T(x)^2 + \cdots = \frac{1}{1 - xT(x)}.$$

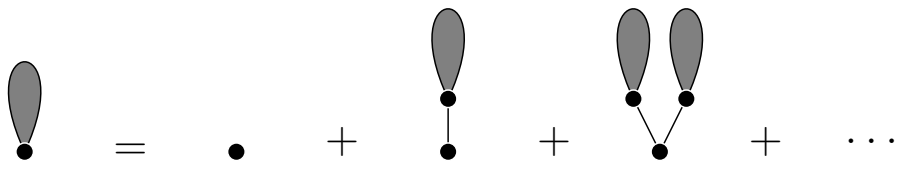

Figure 3.1.4 – Tutte's recursion for rooted plane trees.

Considering that the coefficients of T must be non-negative, we deduce that

$$T(x) = \frac{1 - \sqrt{1 - 4x}}{2x},$$

which gives

$$t_n = \frac{1}{n+1}\binom{2n}{n} \equiv C_n,$$

which are the well-known **Catalan numbers**.

We might be interested in enumerating a broader class of maps, such as the set $\mathcal{M}$ of rooted planar maps. The natural variable with respect to which we want to enumerate the maps of $\mathcal{M}$ is their number of edges. However, it is more convenient to use a bivariate generating function:

$$M(x,y) = \sum_{\mathfrak{m}\in\mathcal{M}} x^{\#E(\mathfrak{m})} y^{\deg(f_{e_*})},$$

where e_* is the root of the considered map. The additional variable y will allow us to determine the function $M(x,1) \equiv M(x)$ that we are actually insterested in. Hence, y is called a **catalytic variable**.

Applying the same decomposition as before (see Figure 3.1.5), we obtain for M the follwoing equation

$$M(x,y) = 1 + xy^2 M(x,y)^2 + xy\frac{M(x) - yM(x,y)}{1-y}.$$

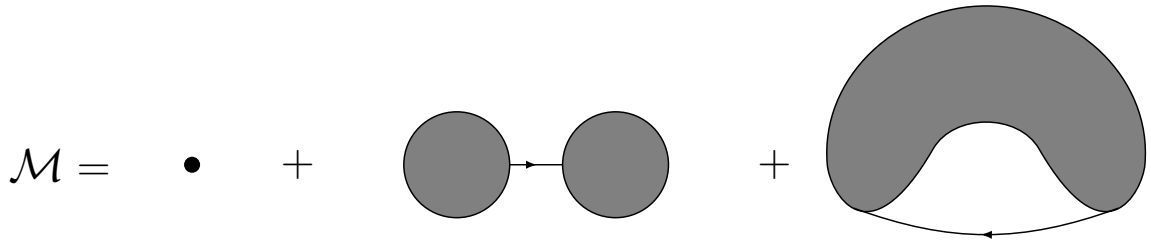

Figure 3.1.5 – Tutte's recursion for general rooted planar maps.

Tutte [Tut63] devised a method called the **quadratic method** to determine $M(x)$ from the previous equation. As this equation is quadratic in $M(x,y)$, we can write it in the form

$$(a_1 M + a_2)^2 = a_3,$$

where the a_i are formal power series in x, y. The idea of the quadratic method is to introduce a parametrization of the catalytic variable y in terms of x, $y = \alpha(x)$ where α is a formal power series, along which $a_3(x, \alpha(x)) = 0$. In that case, since a_3 may be written as a square, we will have not only $a_3 = 0$, but also

$$\frac{\partial a_3}{\partial x} = 0,$$

which gives two equations for the two unknowns $\alpha(x)$ and $M(x)$. After calculations that we do not detail, this yields

$$M(x) = \frac{1 - 4\theta(x)}{(1-3\theta(x))^2},$$

where $\theta(x)$ is the formal power series such that

$$\theta(x) = \frac{x}{1-3\theta(x)}.$$

We can then use the **Lagrange inversion formula** to express the coefficients of $M(x)$ in terms of x, namely

$$m_n = [x^n]M(x) = \frac{2\cdot 3^n}{n+2} C_n. \tag{3.1.1}$$

The fact that this expression is very simple, and incorporates the number of trees with n edges, begs for an explanation of this formula that relates general maps and trees. We will get to such an explanation in Section 3.2.

Some generating functions, such as the ones we will come upon in Chapter 9, are more unwieldy, and we cannot extract explicit expressions for their coefficients. However, what mostly interests us is the *asymptotic* behavior of these coefficients. For that purpose, one very important result is the **transfer theorem**. For a formal power series f that is regular enough when considered as a function on $\mathbb{C}$, it relates the asymptotic behavior of f near its dominant singularity, and the asymptotic behavior of its coefficients. The fundamental statement of the transfer theorem is the following [FS09]:

Theorem 3.1.14. *Let f be a function that is Δ-analytic,* i.e. *analytic in a domain of the form*

$$\Delta(\phi, R) = \{z \in \mathbb{C} \,|\, |z| < R,\, z \neq 1,\, |arg(z-1)| > \phi\}$$

for some $R > 1$ and $0 < \phi < \pi/2$ (see Figure 3.1.6 for an illustration). Assume that, for some $\alpha, \beta \in \mathbb{R}$, f satisfies, in the intersection of a neighbourhood of 1 with its Δ-domain $\Delta(\phi, R)$,

$$f(z) = o\left((1-z)^{-\alpha}\left(\log\frac{1}{1-z}\right)^{\beta}\right).$$

Then,

$$[z^n]f(z) = o\Big(n^{\alpha-1}\log n^{\beta}\Big).$$

Thus, if a function g can be written near its dominant singularity as the sum of another function h and a correction f of the above type, and if we have explicit expressions for the coefficients of h, we will know the asymptotic behavior of the coefficients of f.

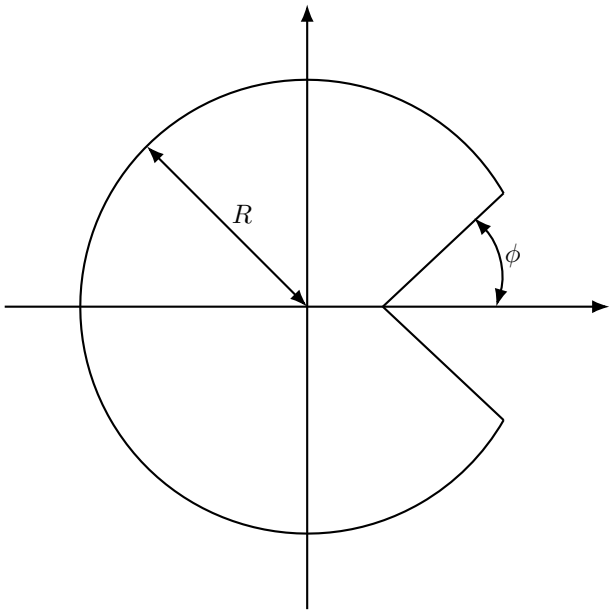

Figure 3.1.6 – A Δ-domain.

Note that, while the above theorem ony treats singularities at $z_0 = 1$, if $f(z) = g(\gamma z)$ for some $\gamma \in \mathbb{C}$, then

$$[z^n]f(z) = \gamma^n [z^n]g(z),$$

so that the theorem actually applies to any functions that are Δ-analytic around their singularity z_0, no matter what the value of z_0 is.

Limits of graphs and maps

So far, we have only presented tools to describe the asymptotic *enumerative* properties of families of (rooted) maps. We now define two notions of limit, or topology, that will help us describe their asymptotic *geometric* properties. As we will see in the next sections and in Part III, these two notions are complementary.

The first one is the notion of *local* topology.

Definition 3.1.15. Let $\mathfrak{m}$ be a finite rooted map. The **ball of radius** r $\mathcal{B}_r(\mathfrak{m})$ of $\mathfrak{m}$ is obtained from $\mathfrak{m}$ by keeping only the edges and faces incident to at least a vertex at distance at most $r-1$ from the root, and cutting along the boundary edges (*i.e.*, the ones incident in $\mathfrak{m}$ to a face containing a vertex at distance at most $r-1$ from the origin, but that do not contain themselves a vertex at distance at most $r-1$).

By gluing open disks to the boundaries created by this cutting, we can consider $\mathcal{B}_r(\mathfrak{m})$ as a map itself (see Figure 3.1.7).

Note that, with this gluing operation, $\mathcal{B}_r(\mathfrak{m})$ is a 2-cell complex, but that it is not a subcomplex of $\mathfrak{m}$, as some edges and vertices of $\mathfrak{m}$ are duplicated in $\mathcal{B}_r(\mathfrak{m})$ (see Figure 3.1.7). However, it is a particular case of the notion of submaps:

Definition 3.1.16. Let $\mathfrak{m}$ be a rooted map, and let $\mathfrak{e}$ be a rooted map with simple boundaries. We say that $\mathfrak{e}$ is a **submap** of $\mathfrak{m}$, and write $\mathfrak{e} \subset \mathfrak{m}$, if $\mathfrak{m}$ can be obtained from $\mathfrak{e}$, by gluing to each boundary f_i of $\mathfrak{e}$ some finite map $\mathfrak{u}_i$.

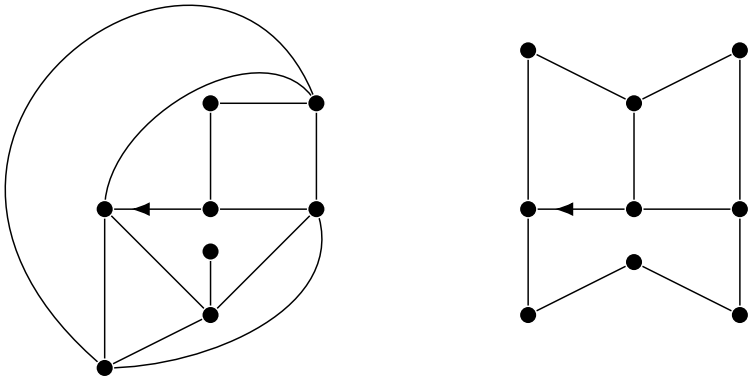

Figure 3.1.7 – A map (left) and its ball of radius 1 (right).

For $m, m' \in \mathcal{M}$, we define the **local distance** between m and m' as

$$d_{loc}(m,m') = \frac{1}{1+\sup\{R \geq 1 | \mathcal{B}_R(m) = \mathcal{B}_R(m')\}}.$$

It is clearly a distance on $\mathcal{M}$, and the completion $(\overline{\mathcal{M}}, d_{loc})$ of the space $(\mathcal{M}, d_{loc})$ is a Polish space. The notion of convergence in this space will be called **local limit**. The elements of $\overline{\mathcal{M}} \backslash \mathcal{M}$ are thus **infinite** maps that can be defined as the local limit of finite rooted maps.

The second notion of topology that we will use, is the *Gromov-Hausdorff* topology.

As this is a topology that makes it possible to compare compact metric spaces, we first have to explain how to get a metric space out of a map $\mathfrak{m}$ (or even a graph). It is really straightforward: we just consider the space whose elements are the vertices of $\mathfrak{m}$, with the distance given by the graph distance on $\mathfrak{m}$: in other words, if $u, v \in V(\mathfrak{m})$, then the distance between them is the number of edges in a shortest path from u to v in $\mathfrak{m}$.

We start by defining a notion of distance between two subsets of the same metric space:

Definition 3.1.17. If (Z, δ) is a metric space and $A, B \subset Z$, the **Hausdorff distance** between A and B is given by

$$\delta_H(A, B) = \max\{\delta(x, B) \,|\, x \in A\} \vee \max\{\delta(y, A) | y \in B\},$$

where by definition $\delta(x, C) = \inf\{\delta(x, y) | y \in C\}$ for $C \subset Z$. The function δ_H defines a distance function on the set of non-empty, closed subsets of Z.

We can then compare two metric spaces by embedding them into a third one:

Definition 3.1.18. Let (X, d) and (X', d') be two compact metric spaces. The **Gromov-Hausdorff distance** between these spaces is defined by

$$d_{GH}((X, d), (X', d')) = \inf \delta_H(\varphi(X), \psi(X')),$$

where the infimum is taken over all metric spaces (Z, δ) and all isometric embeddings φ, ψ from X, X' respectively into Z.

Clearly, if (X, d) and (X', d') are isometric metric spaces, then their Gromov-Hausdorff distance is 0, so d_{GH} defines at best a pseudo-metric[1] between metric spaces. This is actually a good thing, because the class of all compact metric spaces is too big to be a set in the set-theoretic sense, while the family of compact metric spaces seen up to isometries is indeed a set, in the sense that there exists a set $\mathbb{M}$ such that any compact metric space is isometric to exactly one element of $\mathbb{M}$.

Theorem 3.1.19. *The function d_{GH} induces a distance function on the set $\mathbb{M}$ of isometry classes of compact metric spaces. Furthermore, the space $(\mathbb{M}, d_{GH})$ is Polish.*

The definition of d_{GH} through a huge infimum makes it quite daunting. However, there is a very useful alternative description via *correspondences*:

Definition 3.1.20. If X and X' are two sets, a **correspondence** between X and X' is a subset $R \subset X \times X'$ such that, for every $x \in X$, there exists $x' \in X'$ such that $(x, x') \in R$, and for every $x' \in X'$, there exists $x \in X$ such that $(x, x') \in R$. We let $\mathrm{Cor}(X, X')$ be the set of all correspondences between X and X' .

If now (X, d) and (X', d') are metric spaces, and $R \in \mathrm{Cor}(X, X')$, the **distortion** of R with respect to d, d' is defined by

$$\mathrm{dis}(R) = \sup\{|d(x, y) - d'(x', y')| \,;\, (x, x'), (y, y') \in R\}.$$

Proposition 3.1.21. *Let (X, d) and (X', d') be compact metric spaces. Then*

$$d_{GH}((X, d), (X', d')) = \inf_{R \in \mathrm{Cor}(X, X')} \mathrm{dis}(R).$$

[1] In the sequel, we will use the term pseudo-*distance* for functions $f : X^2 \to \mathbb{R}_+$ that satisfy the triangle inequality and are positive-definite, but are not necessarily symmetric. To avoid confusion, we therefore only use the term pseudo-metric, when refering to functions $f : X^2 \to \mathbb{R}_+$ that are symmetric and satisfy the triangle inequality, but are not definite-positive.

3.2 Bijective techniques

Scaling limit of trees

We start by considering T_n, a uniform random element in the set $\mathbf{T}_n$ of rooted plane trees with n edges. We denote by $e_0^n, e_1^n, \dots, e_{2n-1}^n$ the corners encountered in the contour exploration of T_n, starting with the root corner, and by C_n the associated contour process. As the mapping that associates to a tree its contour process is a bijection, C_n is itself a uniform random element of $\mathcal{E}_n$.

Note that, if $(S_k, k \geq 0)$ is the simple random walk in $\mathbb{Z}$, C_n has the same distribution as $(S_t, 0 \leq t \leq 2n)$, conditioned on $A_n = \{S_k \geq 0, 0 \leq k \leq 2n\} \cap \{S_{2n} = 0\}$. Thus, having in mind the convergence of the rescaled random walk $(S_{nt}/\sqrt{n})_{0 \leq t \leq 1}$ to the standard Brownian motion B_t, we want to state that a rescaled version of C_n converges to a sort of continuum excursion. The correct notion is that of the **normalized Brownian excursion** $\mathfrak{e}$. One way to define it is the following: let B be a standard Brownian motion, and let

$$g = \sup\{t \leq 1 \,|\, B_t = 0\}, \quad d = \inf\{t \geq 1 \,|\, B_t = 0\}.$$

Since $B_1 \neq 0$ a.s., we have that $g < 1 < d$ with probability 1, and that the portion of the path B on $[g, d]$ is the excursion of B away from 0 that straddles 1. We normalize it by setting

$$\mathfrak{e}_t = \frac{|B_{g+t(d-g)}|}{\sqrt{d-g}}, \; 0 \leq t \leq 1.$$

Let us denote by $C_{(n)}$ the normalized contour process of T_n, defined by

$$C_{(n)}(t) = \frac{C_n(2nt)}{\sqrt{2n}}, \; 0 \leq t \leq 1.$$

Theorem 3.2.1. *The following convergence in distribution holds in $\mathcal{C}([0,1], \mathbb{R})$:*

$$C_{(n)} \xrightarrow[n \to \infty]{(d)} \mathfrak{e}.$$

We might want to translate this convergence into one for the uniform tree T_n, and the induced metric space. For that purpose, we must use a framework in which the Brownian excursion can encode a metric space, similarly to how C_n encodes T_n.

Let $f : [0,1] \to \mathbb{R}_+$ be a non-negative, continuous function, with $f(0) = f(1) = 0$. We call such a function an **excursion function**, and denote by $\mathcal{E}$ the set of excursion functions, that we endow with the uniform norm. For every $s, t \in [0,1]$, let

$$\check{f}(s,t) = \inf\{f(u) \,|, s \wedge t \leq u \leq s \vee t\},$$

and set

$$d_f(s,t) = f(s) + f(t) - 2\check{f}(s,t).$$

Proposition 3.2.2. *The function d_f on $[0,1]^2$ is a pseudo-metric: it is non-negative, symmetric, and satisfies the triangle inequality.*

Definition 3.2.3. Let (X, d) be a metric space. We say that X is a **geodesic metric space** if, for every $x, y \in X$, there exists an isometric embedding $\phi : [0, d(x,y)] \to X$ such that $\phi(0) = x$ and $\phi(d(x,y)) = y$. This isometric embedding is called a **geodesic path**, and its image a **geodesic segment**, between x and y.

We say that (X, d) is an **$\mathbb{R}$-tree** if it is a geodesic metric space, and if there is no embedding (continuous injective mapping) of S^1 into X. In other words, the geodesic segments are the unique injective continuous paths between their endpoints.

Let f be an excursion function. Since d_f is a pseudo-metric on $[0,1]$, the set $\{d_f = 0\} = \{s,t \in [0,1] \,|\, d_f(s,t) = 0\}$ is an equivalence relation on $[0,1]$.

Let $\mathcal{T}_f = [0,1]/\{d_f = 0\}$ be the quotient set, and $p_f : [0,1] \to \mathcal{T}_f$ the canonical projection. The function d_f naturally induces a (true) distance function on the set T_f, and we still denote this distance by d_f.

Proposition 3.2.4. *The space $(\mathcal{T}_f, d_f)$ is a compact $\mathbb{R}$-tree. It is naturally "rooted" at $\rho_f = p_f(0) = p_f(1)$.*

We let $[\![a,b]\!]$ be the unique geodesic segment from a to b in the tree $\mathcal{T}_f$. Note that $\mathcal{T}_f$ carries a genealogical structure, namely, for every $a, b \in T_f$, there is a unique point $a \wedge b$ (the most recent common ancestor) such that $[\![\rho_f, a]\!] \cap [\![\rho_f, b]\!] = [\![\rho_f, a \wedge b]\!]$. The geodesic segment $[\![a,b]\!]$ is then the concatenation of $[\![a, a \wedge b]\!]$ with $[\![b, a \wedge b]\!]$. We can thus see T_f as a continuum equivalent of a rooted plane tree, and so we call f its **contour function**.

Definition 3.2.5. The **Continuum Random Tree** (hereafter CRT) is the $\mathbb{R}$-tree $(\mathcal{T}_{\mathbb{e}}, d_{\mathbb{e}})$ encoded by the normalized Brownian excursion $\mathbb{e}$.

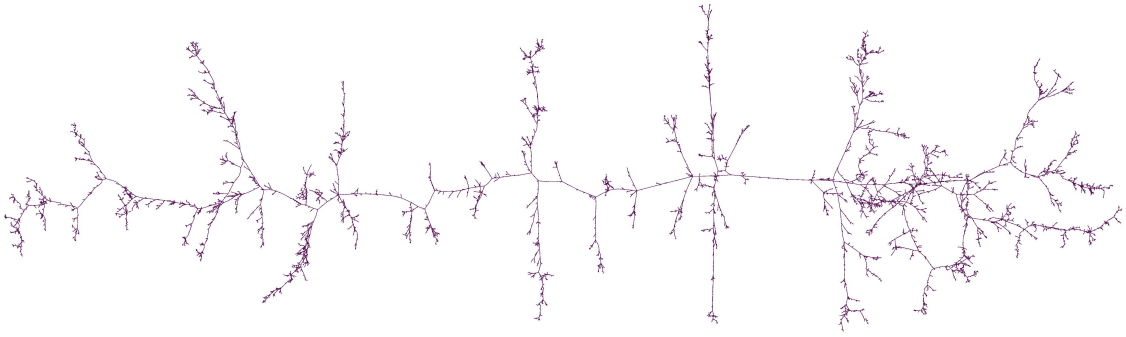

Figure 3.2.1 – A simulation of the CRT, courtesy of Jérémie Bettinelli.

A consequence of Theorem 3.2.1 is thus:

Theorem 3.2.6. *We have the following convergence in distribution*

$$(V(T_n), \frac{1}{\sqrt{2n}} d_{T_n}) \xrightarrow[n\to\infty]{(d)} (\mathcal{T}_{\mathbb{e}}, d_{\mathbb{e}})$$

for the Gromov-Hausdorff topology.

As we have seen in Section 3.1, the explicit enumeration of general planar maps hints at a link between them and plane trees. With the previous result, we can expect that, using such a link, we may able to obtain a scaling limit for general planar maps as well. Let us thus explain the link between general planar maps and trees, in terms of an explicit and very useful bijection.

The CVS bijection

We will actually first present a bijection between general maps and quandrangulations, called **Tutte's bijection**, then describe a bijection between planar quadrangulations and some specific family of trees.

The first bijection is very simple: consider a map $\mathfrak{m}$ with n edges. We start by adding to $\mathfrak{m}$ its dual vertices. For each face f of $\mathfrak{m}$, join its dual vertex v_f to each of the corners of f, by non-intersecting edges staying inside f. Erase then the original edges of $\mathfrak{m}$. The

resulting map $\mathfrak{q}$ is a quadrangulation with n faces (see Figure 3.2.2). If $\mathfrak{m}$ is rooted at (e, v), we root $\mathfrak{q}$ at the first edge of $\mathfrak{q}$ coming after e counterclockwise around v.

Let us describe the inverse transformation. Start from a rooted, planar quadrangulation $\mathfrak{q}$, and color in white the vertices at odd distance from the root, and in black the vertices at even distance from the root. In each face, draw the diagonal between the two black vertices, and erase the original edges of $\mathfrak{q}$ as well as its white vertices. If $\mathfrak{q}$ is rooted at (e, v), the resulting map $\mathfrak{m}$ can be rooted at the first outgoing edge of $\mathfrak{m}$ coming after e clockwise around v.

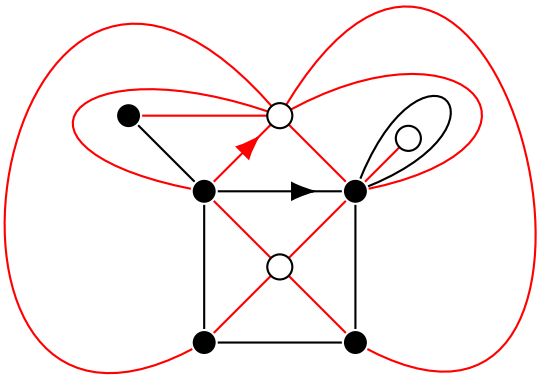

Figure 3.2.2 – A rooted planar map (vertices and edges in black), and the corresponding quadrangulation (black and white vertices and red edges).

Let us now get to the bijection between rooted planar quadrangulations with n faces, and a family of decorated trees with n edges. Let $\mathfrak{t}$ be a rooted plane tree, with root edge e_0 and root vertex u_0. An **admissible label function** on $\mathfrak{t}$ is a function $l : V(\mathfrak{t}) \to \mathbb{Z}$ such that $l(u_0) = 0$, and, for every adjacent $u, v \in V(\mathfrak{t})$

$$|l(u) - l(v)| \leq 1.$$

We denote by $\mathbb{T}_n$ the set of all pairs $(\mathfrak{t}, l)$, where $\mathfrak{t}$ is a rooted plane tree with n edges, and l is an admissible label function on $\mathfrak{t}$. We also denote by $\mathbf{T}_n$ the set rooted plane trees with n edges.

Consider a labeled tree $\mathfrak{t} \in \mathbb{T}_n$. Let $e_0, e_1, \cdots, e_{2n}$ be, as before, the contour exploration of the oriented edges of $\mathfrak{t}$, and let u_i be the initial vertex of e_i. We extend the sequences (e_i) and (u_i) to $\mathbb{N}$ by periodicity. We will often identify the oriented edge e_i with the associated corner, and thus use the notation $l(e_i)$ for $l(u_i)$ when it is more convenient.

For every $i \geq 0$, we define the **successor** of i by

$$s(i) = \inf\{j > i \,|\, l(e_j) = l(e_i) - 1\},$$

with the convention that $\inf \varnothing = \infty$. Note that $s(i) = \infty$ if and only if $l(e_i) = \min l$, as the values of l decreases only by unit steps.

Consider a point v_* in $\mathbb{S}^2$ that does not belong to the support of $\mathfrak{t}$, and denote by e_∞ a corner around v_*. We set

$$l(v_*) = l(e_\infty) = \min l - 1.$$

We can then define, for every $i \geq 0$, the successor of the corner e_i as $s(e_i) = e_{s(i)}$.

The CVS construction consists in drawing, for every $i \in \{0, 1, \ldots, 2n-1\}$, an edge, that we will call an **arc**, from the corner e_i to the corner $s(e_i)$, without crossing $\mathfrak{t}$, v_*, or

another arc (see Figure 3.2.3). Let us denote by $\mathfrak{q}$ the embedded graph with vertex set $V(\mathfrak{t}) \cup \{v_*\}$, and edge set formed by the arcs. We can then prove that, as its name suggests, $\mathfrak{q}$ is a quadrangulation with n faces.

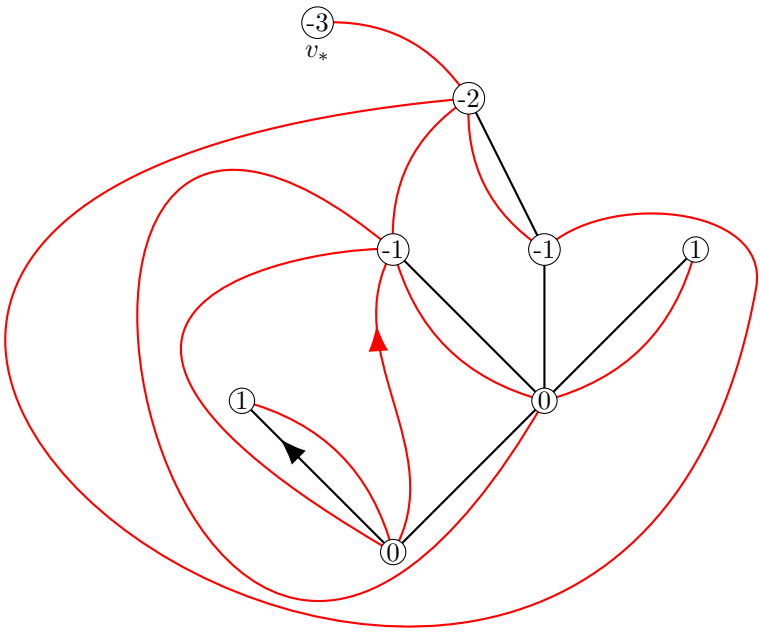

Figure 3.2.3 – A rooted labeled plane tree (edges in black, excluding the vertex v_*), and the corresponding quadrangulation (edges in red), making the choice $\varepsilon = -1$ for the rooting convention.

Note that the quadrangulation $\mathfrak{q}$ has a distinguished vertex v_* , but for now it is not a rooted quadrangulation. To fix this root, we will need an extra parameter $\varepsilon \in \{-1, 1\}$. If $\varepsilon = 1$ we let the root edge of $\mathfrak{q}$ be the arc linking e_0 with $s(e_0)$, and oriented from $s(e_0)$ to e_0. If $\varepsilon = -1$, the root edge is this same arc, but oriented from e_0 to $s(e_0)$.

We have thus defined a mapping Φ from $\mathbb{T}_n \times \{-1, 1\}$ to the set $\mathcal{Q}_n^\bullet$ of pointed planar quadrangulations $(\mathfrak{q}, v_*)$.

Theorem 3.2.7 ([CS04]). *For every $n \geq 1$, Φ is a bijection from $\mathbb{T}_n \times \{-1, 1\}$ onto $\mathcal{Q}_n^\bullet$.*

Note that we do recover from this theorem the expression of (3.1.1) for the number of rooted planar quadrangulations with n faces, as, by Euler's formula, such maps all have $n + 2$ vertices.

A very convenient aspect of the CVS bijection is that the labels of the tree keep track, in some way, of the distances in the quadrangulation. A first evidence of this fact is that, if $(\mathfrak{q}, v_*) = \Phi((\mathfrak{t}, l), \varepsilon)$, then, for every $v \in V(\mathfrak{q})$,

$$d_{\mathfrak{q}}(v, v_*) = l(v) - \min l + 1,$$

where by convention $l(v_*) = \min l - 1$.

Let u, v be two vertices in $V(\mathfrak{q}) \setminus \{v_*\}$, and let e, e' be two corners of $\mathfrak{t}$ such that u is adjacent to e, and v to e'. We denote by $[e, e']$ the set of all corners of $\mathfrak{t}$ encountered when going counterclockwise around $\mathfrak{t}$, starting from e and ending at e'. Another very important

relation between distances in $\mathfrak{q}$ and the labeling function l, that we do not prove here, is the following:

$$d_{\mathfrak{q}}(u,v) \leq l(u) + l(v) - 2 \min_{e'' \in [e,e']} l(e'') + 2. \tag{3.2.1}$$

Another useful aspect of the CVS bijection is that it can be formulated in terms of uniform random variables: indeed, if $(\mathfrak{q}, v_*)$ is a uniform random element of $\mathcal{Q}_n^\bullet$, and $(\mathfrak{t}, l)$ is a uniform random element of $\mathbb{T}_n$, then $(\mathfrak{q}, v_*)$ has the same law as $\Phi((\mathfrak{t}, l), \varepsilon)$, where ε is chosen uniformly at random in $\{-1, 1\}$.

The Brownian map

We now extend the convergence of Theorem 3.2.1, to labeled trees. Let $(\mathfrak{t}_n, l_n)$ be a uniform random element in $\mathbb{T}_n$. Let ε be uniform in $\{-1, 1\}$ and independent of $(\mathfrak{t}_n, l_n)$, and let $\mathfrak{q}_n$ be the random uniform quandrangulation with n faces and a uniformly chosen vertex v_*, obtained from $((\mathfrak{t}_n, l_n), \varepsilon)$ via the CVS bijection.

Then, the tree $\mathfrak{t}_n$ is uniform in $\mathbf{T}_n$, and, given $\mathfrak{t}_n$, l_n is uniform on the 3^n possible admissible labelings. Let us give another description of l_n. Assign independently to every edge e of $\mathfrak{t}_n$ a random variable Y_e, uniform on $\{-1, 0, 1\}$. Then, for each vertex $u \in V(\mathfrak{t}_n)$, let $S_u = \sum_e Y_e$, where the sum is over the edges of the unique path from the root to u (if u is the root vertex, we have the convention that this empty sum gives 0). Then, given $\mathfrak{t}_n$, $(S_u)_{u \in V(\mathfrak{t}_n)}$ has the same law as l_n. Thus, the label function l_n can be seen as a random walk along the paths in $\mathfrak{t}_n$, so we might expect that it has a scaling limit as well.

Consider the rescaled label function defined for $t \in [0, 1]$ by

$$L_{(n)}(t) = \left(\frac{9}{8n}\right)^{1/4} L_n(2nt),$$

where, similarly as for the contour function $C_{(n)}$, we define $L_n(i)$ as the label of $u_i^{(n)}$ for $i \in \{0, 1, \ldots, 2n-1\}$, then interpolate between integer times.

We have the following result:

Theorem 3.2.8 ([JM05])**.** *It holds that*

$$\left(C_{(n)}, L_{(n)}\right) \xrightarrow[n\to\infty]{(d)} (\mathbb{e}, Z), \tag{3.2.2}$$

in distribution in $\mathcal{C}([0,1], \mathbb{R})^2$, where $\mathbb{e}$ is a standard Brownian excursion, and, conditionally on $\mathbb{e}$, Z is a continuous, centered Gaussian process with covariance

$$Cov(Z_s, Z_t) = \check{\mathbb{e}}_{s,t},\ s, t \in [0, 1].$$

The process Z is called the **head of the Brownian snake**, but in the sequel we will sometimes abuse notation and refer to it as the Brownian snake, as the actual snake will not appear in these pages.

Let us denote by d_n the graph distance on $\mathfrak{q}_n$. We also define a rescaled distance $D_{(n)}$ on $[0, 1]^2$, by first setting, for $i, j \in \{0, 1, \ldots, 2n\}$:

$$D_{(n)}\left(\frac{i}{n}, \frac{j}{n}\right) = \left(\frac{9}{8n}\right)^{1/4} d_n(u_i^{(n)}, u_j^{(n)}),$$

then linearly interpolating to extend $D_{(n)}$ to $[0, 1]^2$.

The convergence of Theorem 3.2.8, together with (3.2.1), implies that the family $(D_n)_n$ is relatively compact for the weak topology on probability measures on $\mathcal{C}([0, 1]^2, \mathbb{R})$, so that,

along some subsequence n_k, D_n converges to some random function D. It is straightforward to prove that D must satisfy the triangle inequality, so that, the quotient space $S = [0,1]/\{D=0\}$ is a metric space, when equipped with the projection of D, still denoted by D. We then have the following convergence, along the subsequence n_k

$$(V(\mathfrak{q}_n), \left(\frac{9}{8n}\right)^{1/4} d_n) \xrightarrow[n\to\infty]{(d)} (S, D),$$

for the Gromov-Hausdorff topology.

What remains to prove is that D is necessarily equal to a pseudo-metric D^* that is naturally defined in terms of Z, so that the previous convergence holds without taking a subsequential limit, and involves a universal object that we will call the Brownian map. Let us first define this object.

Like the Brownian excursion $\mathbb{e}$ encoded a continuum equivalent of a tree, we want to see Z as encoding a continuum equivalent of a map. For this, let us construct from Z a pseudo-metric on $[0,1]$, that will induce a quotient metric space, much like $\mathbb{e}$ induces the CRT $\mathscr{T}_{\mathbb{e}}$.

We want to have a function that relates to Z, similarly to the way the distances in the quadrangulation relate to the label function. Taking inspiration from the bound (3.2.1), let us first define, for $s \le t \in [0,1]$,

$$D^\circ(s,t) = D^\circ(t,s) := Z_s + Z_t - 2\max(\min_{r\in[s,t]} Z_r, \min_{r\in[t,1]\cup[0,s]} Z_r).$$

This function does not satisfy the triangle inequality, which brings us to

$$D^*(s,t) := \inf\left\{ \sum_{i=1}^{k} D^\circ(s_i,t_i) \,\middle|\, k\ge 1,\ s_1 = s, t_k = t,\ d_{\mathbb{e}}(t_i, s_{i+1}) = 0 \ \ \forall\, i \in \{1,2,\dots,k\} \right\}.$$

We can now define the **Brownian map** $\mathbf{m}_\infty$, by setting $\mathbf{m}_\infty = [0,1]/\{D^* = 0\}$, and equipping this space with the distance induced by D^*, which is still denoted by D^*. We will not say much about the fascinating properties of this metric space, but note at least that we can prove (see [LGP08]) that the Brownian map is homeomorphic to the sphere a.s., which is welcome for a putative scaling limit of planar maps.

As advertized, we do have that the Brownian map is the scaling limit of planar quadrangulations:

Theorem 3.2.9. *The following convergence holds*

$$(V(\mathfrak{q}_n), \left(\frac{9}{8n}\right)^{1/4} d_n) \xrightarrow[n\to\infty]{(d)} (\mathbf{m}_\infty, D^*),$$

for the Gromov-Hausdorff topology.

This result was proven independently by Le Gall [LG13] and Miermont [Mie13] In [LG13], the proof of Le Gall also applies to $2p$-angulations for any $p \ge 3$, and to triangulations: this relies on bijections similar to the CVS bijection, that were derived by Bouttier, Di Francesco and Guitter [BDFG03].

Other families of planar maps, such as general maps [BJM14], bipartite maps [Abr16], and recently p-angulations for odd $p \ge 5$ [ABA], were proven to converge to the Brownian map with the same method. Notably, in a paper [ABA17] where this method is adapted to simple triangulations and quadrangulations, Addario-Berry and Albenque also establish a "black box", that systemizes its application to families of planar maps in bijection with

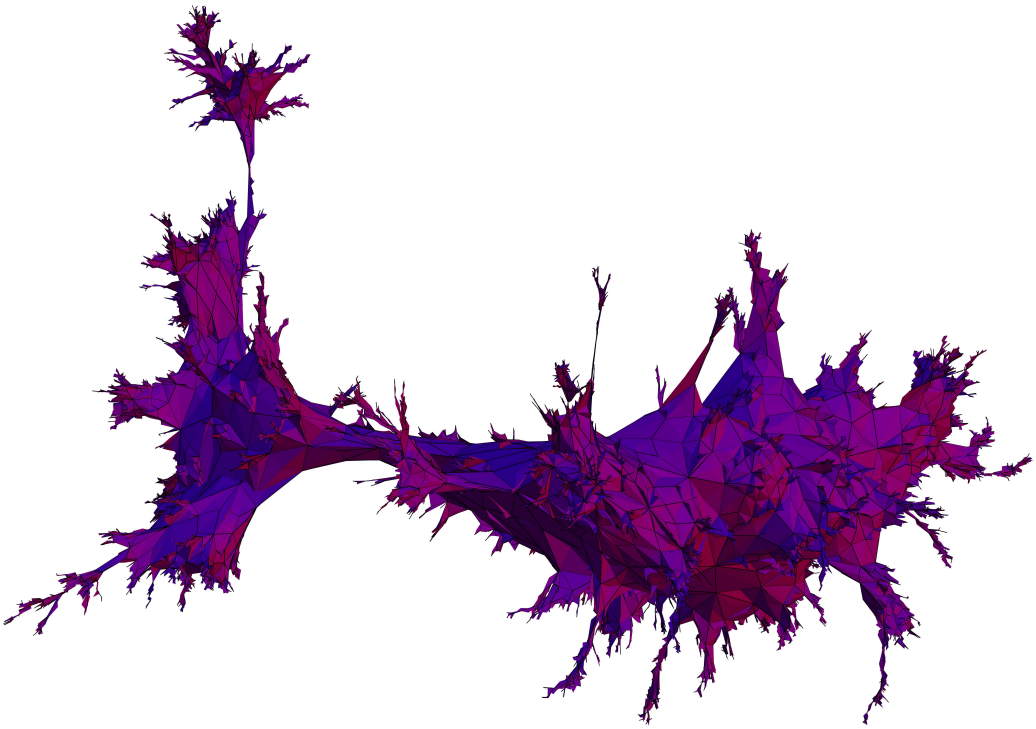

Figure 3.2.4 – A simulation of the Brownian map, courtesy of Jérémie Bettinelli.

various types of decorated trees. It is also this method that we adapt to the case of Eulerian triangulations in Chapter 7, as we will explain in more detail in Section 3.5.

Let us note that all these families have similar singularities in their generating functions, or equivalently by the transfer theorem, their enumeration has the same asymptotic behavior, of the form

$$m_n \sim C\rho^n n^{-5/2}. \tag{3.2.3}$$

While this is not enough to deduce that they have similar scaling limits, it is a strong hint that they have the same asymptotic behavior for many other quantities, or, in other words, that they are in the same universality class[2].

Let us also mention that there has been a lot of recent work to relate the Brownian map to Liouville Quantum Gravity (defined in Section 2.4) with the parameter $\gamma = \sqrt{8/3}$ (see for instance [MS]).

It is undoubtedly interesting to further investigate an already known universality class, but it is also stimulating to look for new scaling limits. Thus, other scaling limits of planar maps have been derived: the Brownian plane [CLG14], that can be constructed by "zooming in" on the Brownian map, the related hyperbolic Brownian plane [Bud18], the Brownian disk [BM17], that is the scaling limit of maps with a boundary whose perimeter is fine-tuned with their size.

Another thriving topic is the one of *decorated* random maps, in which we consider random planar maps biased by a statistical physics model, such as the Ising model, Bernoulli percolation, or spanning trees. In particular, there has been recent work on bijective approaches for some of these models, see for instance [GKMW18; BHS; GHS]. However, we are still far from the twofold goal of constructing scaling limits for these objects, and

[2]It is very tricky to properly define the multi-faceted notion of universality class, and we will not attempt to do so here.

showing that these scaling limits can be identified with Liouville Quantum Gravity for particular values of γ.

Bijections for maps with boundaries

While we saw that bijections between families of planar maps and classes of decorated trees were very useful to derive scaling limits, they can also help in deriving *local* limits. Indeed, these bijections yield explicit enumerations of the maps in question, that, as we will see in the next sections, are central in the construction of some particular infinite random maps as local limits of finite random maps.

3.3 Peeling processes

In this section, we will briefly explain how random models of infinite maps can be defined *via* a Markovian exploration process, called the **peeling process**. While this method will not be used in Part III, it is of great importance for the investigation of random models of maps, and in particular random maps decorated with statistical physics models.

A notion that is central to the peeling method, as well as to the layer decomposition that we will see in the next section, is that of Boltzmann maps.

Definition 3.3.1. Let $\mathbf{q} = (q_k)_{k\geq 1}$ be a non-zero sequence of non-negative real numbers, that we call the **weight sequence**. We then define a measure on the set of all finite bipartite planar maps, by setting

$$w_{\mathbf{q}}(\mathfrak{m}) = \prod_{f\in F(\mathfrak{m})\setminus\{f_*\}} q_{\deg(f)/2},$$

where f_* is the root face of $\mathfrak{m}$. For any $l \geq 1$, we denote by $\mathcal{W}^{(l)}(\mathbf{q})$ the **Boltzmann partition function** on bipartite maps of the $2l$-gon:

$$\mathcal{W}^{(l)}(\mathbf{q}) = \sum_{\mathfrak{m}\in\mathcal{M},\deg(f_*)=2l} w_{\mathbf{q}}(\mathfrak{m}).$$

We say a weight sequence is **admissible**, if, for any $l \geq 1$, $\mathcal{W}^{(l)}(\mathbf{q})$ is finite. We can then define the $\mathbf{q}$-Boltzmann map of the $2l$-gon, as the random bipartite map with measure

$$\mathbb{P}^{(l)}_{\mathbf{q}}(\mathfrak{m}) = \frac{w_{\mathbf{q}}(\mathfrak{m})}{\mathcal{W}^{(l)}(\mathbf{q})}.$$

An admissible weight sequence $\mathbf{q}$ is **critical** if the variance of the volume of a $\mathbf{q}$-Boltzmann map is infinite.

Thus, Boltzmann maps are random planar maps with a fixed perimeter, but not a fixed size. A particular case is to take $q_k = 0$ for any $k \neq 2$ and $q_2 = 1/\rho$ (for ρ like in (3.2.3)), which yields (critical) Boltzmann quadrangulations, whose measure may be written, for any quadrangulation of the $2l$-gon with $n+1$ faces $\mathfrak{q}$:

$$\mathbb{P}^{(l)}(\mathfrak{q}) = \frac{\rho^{-n}}{\sum_m Q_{m,l}\rho^{-m}},$$

where $Q_{m,l}$ is the number of quadrangulation of the $2l$-gon with $m+1$ faces.

We can also extend the definition of Boltzmann maps to include Boltzmann triangulations, which are defined similarly to Boltzmann quadrangulations (without a parity

condition on the length of the boundary).

A peeling exploration is a way to explore a map $\mathfrak{m}$ edge by edge[3]. If $\mathfrak{e} \subset \mathfrak{m}$ is a planar map with simple boundaries, we denote by $\mathrm{Active}(\mathfrak{e})$ the set of edges adjacent to the boundaries of $\mathfrak{e}$. We suppose we have some **peeling algorithm** $\mathcal{A}$, which is a function that associates to any planar map with boundaries $\mathfrak{e}$ an element of $\mathrm{Active}(\mathfrak{e}) \cup \{\dagger\}$, where $\dagger$ is a cemetery point that we interpret as the end of the exploration.

Thus, given the algorithm $\mathcal{A}$, we will iteratively explore $\mathfrak{m}$, by "peeling the edge" determined by $\mathcal{A}$. Let $\mathfrak{e} \subset \mathfrak{m}$ be a planar map with boundaries, and $e \in \mathrm{Active}(\mathfrak{e}) \cup \{\dagger\}$. If $e \neq \dagger$, and f is the corresponding boundary face of $\mathfrak{e}$, let $f_{\mathfrak{e}}$ be the face of $\mathfrak{m}$ that is incident to e on the same side as f. The next step of the exploration, that we denote by $\mathrm{Peel}(\mathfrak{e}, e, \mathfrak{m})$, is given by one of the three following possibilities:

- if $e = \dagger$, then $\mathrm{Peel}(\mathfrak{e}, e, \mathfrak{m}) = \mathfrak{e}$
- if f_e is not a face of $\mathfrak{e}$, then $\mathrm{Peel}(\mathfrak{e}, e, \mathfrak{m})$ is obtained by gluing f_e on e (and not performing any other identifications of its edges)
- if f_e is a face of $\mathfrak{e}$, e is identified in $\mathfrak{m}$ with another edge e' that is incident to the same boundary of $\mathfrak{e}$, and $\mathrm{Peel}(\mathfrak{e}, e, \mathfrak{m})$ is obtained by performing this identifiction in $\mathfrak{e}$. Note that this splits the boundary face incident to e into two smaller boundary faces, except if e and e' are adjacent.

Definition 3.3.2. Let $\mathfrak{m}$ be an element of $\overline{M}$. The **peeling exploration** of $\mathfrak{m}$ with algorithm $\mathcal{A}$ is the sequence of planar maps with simple boundaries

$$\mathfrak{e}_0 \subset \mathfrak{e}_1 \subset \cdots \subset \mathfrak{e}_n \subset \cdots\cdots \mathfrak{m},$$

where $\mathfrak{e}_0$ is the root face f_* seen as a map with a boundary, and, for every $i \geq 0$,

$$\mathfrak{e}_{i+1} = \mathrm{Peel}(\mathfrak{e}_i, \mathcal{A}(\mathfrak{e}_i), \mathfrak{m}).$$

With the same notation as above, we denote by L_i the degree of the boundary face of $\mathfrak{e}_i$ on which e_i sits. The crucial result that makes peeling processes so powerful is that, for any peeling algorithm, the peeling exploration of a $\mathbf{q}$-Boltzmann map is a Markov chain whose transition probabilities are explicit functions of the partition functions associated to the weight sequence $\mathbf{q}$ and L_i. This an example of **spatial Markov property**: the parallel with the usual Markov property is that what is left to explore in the map only depends on the information of the perimeter of the boundary obtained by the previous step. We stay purposefully vague in the statement of this very important result, but we refer the reader to [Wat95; Ang03; AB16; Bud16; CLG17] for more detailed accounts on peeling processes.

This property makes it possible to define the infinite $\mathbf{q}$-Boltzmann map of the $2l$-gon (or the l-gon if we consider Boltzmann triangulations), by "conditioning the exploration to never stop". In particular, this is a way to define the Uniform Infinite Planar Quadrangulation, by canonically closing up the hole of the infinite Boltzmann quadrangulation of the 2-gon, and similarly for the Uniform Infinite Planar Triangulation, by canonically closing up the hole of the infinite Boltzmann triangulation of the 1-gon.

Considering the infinite Boltzmann quadrangulation of the $2l$-gon, and then letting $l \to \infty$, also gives a construction of the Uniform Half-Planar Quadrangulation. The same

[3]Note that this idea is already present in the seminal papers of Tutte.

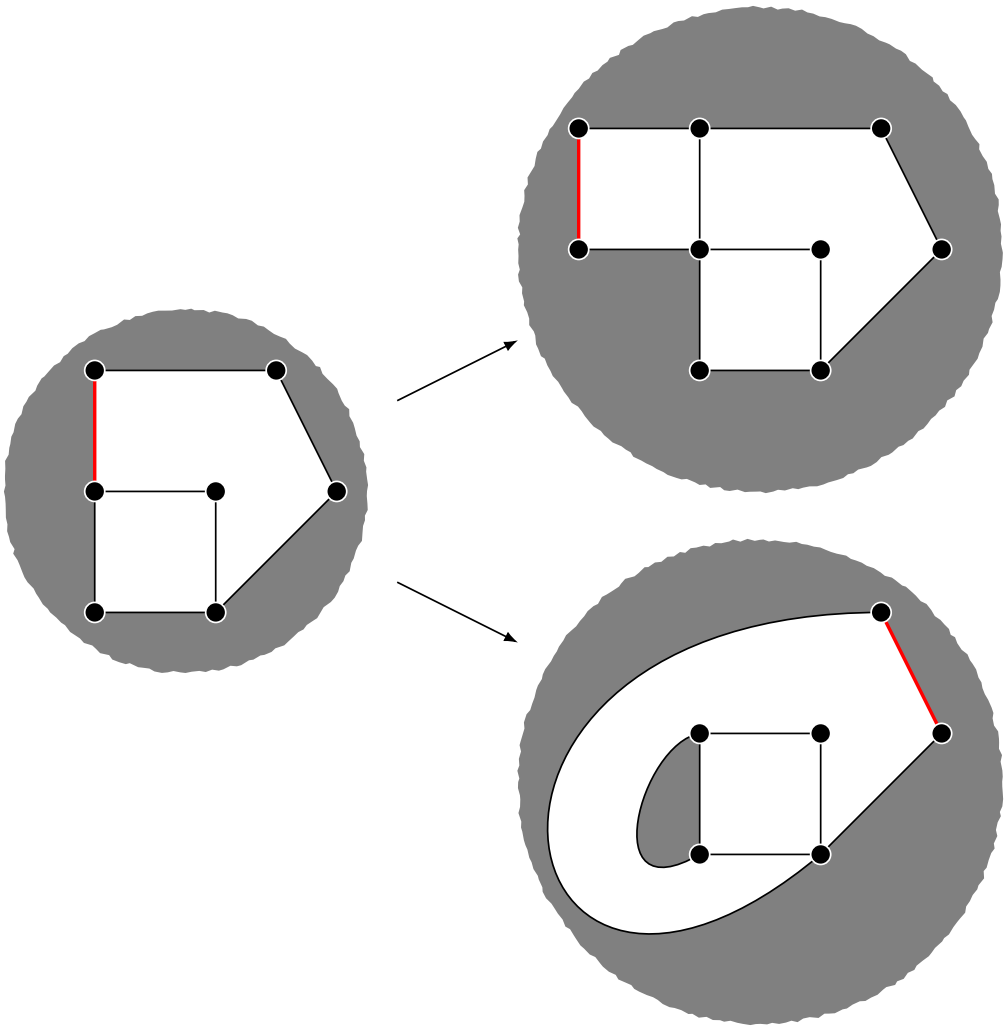

Figure 3.3.1 – The possible non-trivial steps in a peeling exploration: we start from a map with simple boundaries (in gray), with a distinguished boundary edge (in red). Either we discover a new face (top right), or we identify the distinguished edge with another boundarye edge (bottom right). In either case, the peeling algorithm selects a new boundary edge for the next step.

can be done for triangulations[4]. We will see in the next section that these infinite models can also be constructed with a layer decomposition.

A very useful application of peeling processes is the study of random models of maps endowed with statistical physics models, such as Bernoulli percolation or the Ising model. Indeed, peeling infinite maps endowed with a statistical physics model makes it possible to find their critical exponents, which is of great interest to compare these discrete models, to the special cases of continuum Liouville Quantum Gravity that are conjectured to be their scaling limit.

Let us note that, as the transition probabilities of the peeling process on **q**-Boltzmann maps depend on the associated partition functions, it is crucial to have explicit expressions for these partition functions, or at least precise information on their asymptotic behavior: this is where bijective enumeration can come into play for the construction of local limits. As we will see in the sequel, it is also possible to use more analytical methods to obtain these asymptotics, that are also central in the layer decomposition method that we present in the next section.

3.4 Layer decompositions

Like peeling explorations, the layer decomposition of a planar map builds it iteratively, which makes it possible to extract infinite maps as local limits of finite random maps. However, it is a very different process, that (for the moment) only applies to very specific families of maps, namely triangulations [Kri05; CLG19], quadrangulations (and the general maps they are in correspondence with) [LGL; Leh], and Eulerian triangulations, that we will present in the next section, and are the subject of study in the chapters of Part III. As we will go into great details about it in Chapter 7, here we just sketch the general idea of this method.

To simplify notation, let us focus in this section on (usual) triangulations. The layer decomposition of planar triangulations with a boundary relies on the notion of *vertical* balls.

Definition 3.4.1. Let A be a (finite) triangulation of the p-gon, and let r be a positive integer. The **vertical ball $B_r(A)$** of radius r in A is the submap of A obtained by keeping only the edges and faces of A that are incident to at least a vertex of distance at most $r-1$ from ∂A: it is defined, similarly to the usual ball of radius r, by cutting along the edges of A both of whose extremities are at distance r from ∂A, then filling in each hole with one simple face. Suppose A is equipped with a distinguished vertex v, then the hull $B_r^\bullet(A)$ of the ball $B_r(A)$, is the map obtained from $B_r(A)$ by gluing to it all the connected components of its complement in A that do not contain v. (If v is at distance less than $r+1$ from the boundary of A, we can fix the convention that $B_r^\bullet(A) = A$.)

Consider a pointed triangulation of the p-gon (A, v), and its successive hulls $\{B_r^\bullet(A)\}$. These hulls have two boundaries: one is ∂A, that is called the bottom boundary, and the other one, the top boundary, is incident to triangles that all have two vertices at distance r from ∂A, and one at distance $r-1$ from ∂A. We call these triangles, **downward triangles** at level r. Then, by associating to each downward triangle f at level r, a downward triangle at level $r+1$ (say, the first one encountered after f, going clockwise in $B_r^\bullet(A)$ around its top boundary). This gives a **genealogical structure** on the downward triangles of the

[4]The same construction also works for any critical weight sequence, but we will not consider more general half-planar Boltzmann maps in the sequel.

successive hulls. To describe completely A, it remains to fill in the "slots" that are between these downard triangles (see Figure 3.4.1). We call the submap of A given by the downward triangles at level r, and the slots that lie between them and the downward triangles at level $r-1$, the **r-th layer of** (A, v).

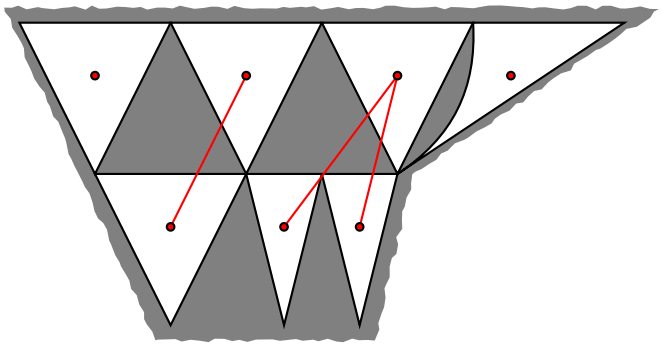

Figure 3.4.1 – A portion of a layer in a usual triangulation: the downward triangles are in white, the slots that compose the rest of the triangulation are in gray, and the genealogical structure of the downward triangles is in red.

It turns out that, if we take as our triangulation $\mathcal{T}_n^{(p)}$, a uniform random element in the set $\mathbb{T}_n^{(p)}$ of triangulations of the p-gon with n faces (together with a distinguished vertex uniform on $V(A)$), the configuration of downward triangles is given by a branching process of critical offspring distribution θ, that lies in the domain of attraction of a 3/2-stable law. Moreover, conditionally to this configuration, the slots are independent Boltzmann triangulations, whose perimeters are given by the branching process. Thus, the r-th layer of A is given by the r-th step of the branching process, together with a sequence of independent Boltzmann triangulations.

As was the case for peeling processes, this structure straigthforwardly induces random infinite maps as local limits of the random finite triangulation $\mathcal{T}_n^{(p)}$. The first step is to have an infinite number of layers (or, equivalently, an infinite number of total triangles), which gives the infinite triangulation of the p-gon, $\mathcal{T}_\infty^{(p)}$ (as mentioned in the previous section, we can once again obtain the UIPT from $\mathcal{T}_\infty^{(1)}$, by "zipping up" its boundary). Then, letting $p \to \infty$, we recover the UHPT. We can also "look down" at $\mathcal{T}_\infty^{(p)}$ from a very high layer: this yields the Lower Half-Planar Triangulation, which is closely related to the UHPQ.

Note that the Boltzmann triangulations filling in the slots have exactly the same law in all these models: what changes is the branching process. In the LHPT it is simply a doubly infinite sequence of independent Galton-Watson trees, while in the UHPT, it is an infinite tree consisting of an infinite spine and independent Galton-Watson trees connected to it: in these two cases, the layers extend infinitely horizontally. However, in $\mathcal{T}_\infty^{(p)}$ and in finite triangulations, the branching process consists in a finite sequence of trees that are not independent, due to "edge effects", as each layer is finite. However, a **comparison principle** makes it possible to compare events for the branching structure associated $\mathcal{T}_n^{(p)}$, and the independent Galton-Watson trees we find in the LHPT.

Thus, it proves quite straightforward to obtain results on the LHPT and the UHPT, as they are described by quite simple branching processes. Then, their being local limits of finite triangulations, together with the comparison principle, allows us to transfer these results to these finite triangulations.

Before the work detailed in Part III, this decomposition has mostly been used to show that uniform planar triangulations (or quadrangulations), equipped with some distance d' that is a local modification of their usual graph distance d, also converge to the Brownian

map. A central argument is that, as the layers of the LHPT are completely i.i.d., one can use an ergodic subadditivity theorem, to prove that, in the LHPT, the distance d' is proportional to d. The comparison principle then makes it possible to carry this proportionality to large finite triangulations: this necessitates a few additional technical arguments, some of them related to the enumeration of triangulations with a boundary, others relying on the already known convergence of triangulations, equipped with the usual graph distance, to the Brownian map.

As we will briefly explain in Chapter 5, and see in thorough detail in Part III, the case of Eulerian triangulations is quite different, since we prove the convergence to the Brownian map for the two distances simultaneously.

It is also worth noting that, in all these uses of the layer decomposition, results on the scaling limit of a family of random maps are proven using local limits of these maps, which is not a common occurence.

Before getting to Eulerian triangulations, let us mention the model of **causal maps** defined by Curien, Hutchcroft and Nachmias [CHN], that are naturally constructed by their layer decomposition: starting from a plane tree $\mathfrak{t}$, we construct a planar map Causal($\mathfrak{t}$), by adding the "horizontal" edges linking successive vertices in the cyclical ordering of each level of the tree. By putting additional "vertical" edges in Causal($\mathfrak{t}$), we obtain a planar triangulation, CauTri($\mathfrak{t}$).

To obtain information on geometric properties of these causal maps, Curien, Hutchcroft and Nachmias use a **block decomposition**. A block of height r in the causal map Causal($\mathfrak{t}$) or CauTri($\mathfrak{t}$), is the submap delimited by two successive subtrees of $\mathfrak{t}$ of height at least r. Using a renormalization scheme for these blocks makes it possible to estimate the global width of the causal map: we use similar arguments in Chapter 7, to estimate distances along the layers of the Eulerian equivalent of the LHPT.

Note that causal maps are a mathematical formulation of the $2D$ case of causal dynamical triangulations, that were mentioned in Chapter 2, and are thus the first non-numerical investigation of the properties of these models.

3.5 Eulerian triangulations

We will now focus on Eulerian triangulations, to explain their different characterizations, and give an outline of the works presented Part III.

Definition 3.5.1. An **Eulerian triangulation** is a triangulation in which all vertices have even degree. Equivalently, it is a triangulation A, such that the faces of A can be partitioned into black and white faces, each black face being only adjacent to white faces, and *vice versa* (see Figure 3.5.1).

Another characterization of Eulerian triangulations uses their **canonical orientation**. Given an Eulerian triangulation A, consider a proper bicoloration of its faces, as above. Then, we can orient the edges of A so that they go clockwise around black faces, and anticlockwise around white faces[5]. In the sequel, when we consider rooted Eulerian triangulations, their root edge will be oriented according to their canonical orientation. Furthermore, for a rooted Eulerian triangulation, any mention of orientation in the sequel refers to the canonical orientation that matches the orientation of the root edge.

[5]Note that, for a given Eulerian triangulation, we have two choices for the bicoloration of its faces, as well as for a canonical orientation. Obviously, with our convention for orienting the faces, making the choice for the colors is equivalent to making the choice for the orientation.

Yet another characterization, is that Eulerian triangulations are triangulations whose vertices can be properly tricolored. Indeed, considering a canonical orientation of an Eulerian triangulation A: we can assign the colors, say, red, blue, green, to the vertices of some black face of A, and then propagate these colors to all vertices of A, by respecting the condition that the cyclic order of the colors must be the same in all black faces (see Figure 3.5.1).

This last characterization will allow us to identify Eulerian triangulations with *3-colored graphs* in Chapter 4, and we can use it now to construct bijections between Eulerian triangulations and other combinatorial objects.

Consider first a bipartite map $\mathfrak{m}$, with a proper bicoloration of its vertices in black and white. For each face f of $\mathfrak{m}$, add a vertex v_f inside f, that we will call a $*$-vertex, then draw an edge between v_f and each vertex incident to f in $\mathfrak{m}$, so that the edges stay inside f and do not cross. This yields a triangulation A, where each triangle contains one black vertex, one white vertex, and one $*$-vertex, and where, if f, f' are two adjacent triangles, the cyclic ordering of the vertex types around f and f' are opposite (see Figure 3.5.2): thus, A is an Eulerian triangulation. Conversely, starting from an Eulerian triangulation A, consider one of its three possible proper vertex-colorings: by removing the red vertices and the incident edges, we do obtain a bipartite map. Now, if we start from a rooted bipartite map, taking is root edge as the root of the induced Eulerian triangulation fixes the choice of the vertex-coloring. Thus, rooted bipartite maps with n edges are in bijection with rooted Eulerian triangulations with n black faces.

Bipartite maps with n edges are naturally in correspondence with **3-constellations** of size n, that can be defined as triples of permutations $(\alpha_1, \alpha_2, \alpha_3) \in \mathfrak{S}_n^3$, such that

- $\langle \alpha_1, \alpha_2, \alpha_3 \rangle$ acts transitively on $\{1, 2, \ldots, n\}$
- $\alpha_1\alpha_2\alpha_3 = \mathrm{id}$.

The observant reader might notice that this is a generalization of the notion of maps defined as fatgraphs, in which we have lifted the condition that one permutation msut be a fixed-point free involution. Thus, 3-constellations are also called **hypermaps**. Note also that, to have a proper bijection, we must once again consider the triple of permutations up to isomorphisms.

Let us also mention that 3-constellations can also be understood as **Belyi surfaces**, that is, coverings of the Riemann sphere that are unramified outside $\{0, 1, \infty\}$. We refer to [LZ04] for a detailed account on this topic.

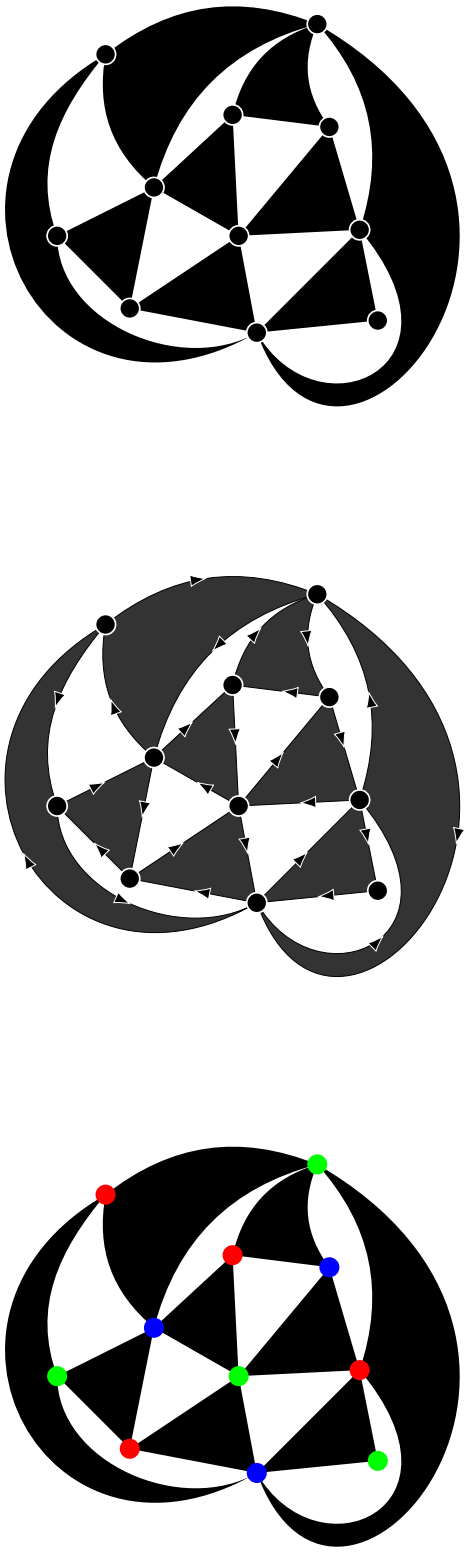

Figure 3.5.1 – The different characterizations of Eulerian triangulations: with the bicoloring of their faces, with the orientation of their edges, with the tricoloring of their vertices.

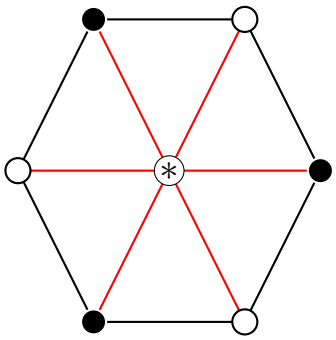

Figure 3.5.2 – The operation that maps a bipartite map (black and white vertices, black edges) to an Eulerian triangulation (with the additional $*$ vertices and red edges).

CHAPITRE 4

Colored tensor models

In what follows, D will be a positive integer, that corresponds to the dimension of some topological spaces.

4.1 Elements of combinatorial topology

In the sequel, we will present piecewise linear (hereafter PL) spaces of dimension D with a very specific combinatorial structure. To properly define these structures, we will use the slightly more general framework of **triangulated spaces** or **trisps**, following the conventions of Kozlov [Koz08].

Definition 4.1.1. A **geometric n-simplex** σ is the convex hull of a set A of $n+1$ linearly independent points of $\mathbb{R}^N$, for some $N > n$. The convex hulls of subsets of A are called the **subsimplices** or **faces** of σ, and the points defining σ are called its **vertices**. We will write $\sigma \subseteq \tau$ to say that σ is a face of τ.

We denote by $< x_1, \dots, x_n >$ the simplex whose vertices are $x_1, \dots x_n$.

The **standard n-simplex** is the simplex $< (1, 0, \dots, 0), (0, 1, 0, \dots, 0), (0, \dots, 0, 1) >$, where the points form the canonical basis of $\mathbb{R}^{n+1}$.

Let us start with a set of geometric simplices $(S_i)_{i\in\mathbb{N}}$, where S_i contains i-simplices, seen as copies of the standard i-simplex. Then, for $m \leq n$, for every order-preserving injection $f\colon \{1, \dots, m+1\} \to \{1, \dots, n+1\}$, let us have a map $B_f\colon S_n \to S_m$ such that:

(i) if f, g are two such maps that can be composed: $\{1, \dots, l+1\} \xrightarrow{g} \{1, \dots, m+1\} \xrightarrow{f} \{1, \dots, n+1\}$, then: $B_{f\circ g} = B_g \circ B_f$

(ii) $B_{id_{\{1,\dots,n+1\}}} = id_{S_n}$

This abstract structure allows us to construct a topological space. Indeed, an order-preserving injection $f\colon \{1, \dots, m+1\} \to \{1, \dots, n+1\}$ induces a linear map $M_f\colon \mathbb{R}^{m+1} \to \mathbb{R}^{n+1}$, that sends the k-th vector of the canonical basis of $\mathbb{R}^{m+1}$ to the $f(k)$-th vector of the canonical basis of $\mathbb{R}^{n+1}$. This map can be restricted to a homeomorphism from the standard m-simplex to some m-subsimplex of the standard n-simplex. For $\sigma \in S_n$, this homeomorphism thus glues a m-subsimplex of σ to the m-simplex of $B_f(\sigma) \in S_m$. The condition $B_{f\circ g} = B_g \circ B_f$ ensures that this gluing is consistent.

Definition 4.1.2. A complex $\mathcal{K} = \Big(\{S_i(\mathcal{K})\}_i, \{B_f\}_f\Big)$ constructed in the way described above is called a **triangulated space**, or **trisp**.

In a general trisp, two faces of the same simplex could be identified. In the sequel, we will focus on trisps without such identifications.

Definition 4.1.3. Let $\mathcal{K} = \Big(\{S_i(\mathcal{K})\}_i, \{B_f\}_f\Big)$ be a trisp. We say that $\mathcal{K}$ is a **regular trisp** if, for any $\sigma \in S_k(\mathcal{K})$, all its vertices are distinct, *i.e.*, the values $B_{f_i}(\sigma)$ are distinct for $i = 1, \ldots, k+1$. (The function $f_i \colon \{1\} \to \{1, \ldots, k+1\}$ begin defined by: $f_i(1) = i$.)

We present now a specific type of trisps, whose additional properties allow us to consider finer geometrical notions.

Definition 4.1.4. A **simplicial pseudo-manifold of dimension D** [Sti93] is a trisp $\mathcal{K}$ with the following properties:

(i) $\mathcal{K}$ is **pure**, *i.e.* every simplex is the face of a D-simplex

(ii) $\mathcal{K}$ is **strongly connected**, *i.e.* two D-simplices can be linked by a chain of D-simplices in which each pair of neighboring D-simplices shares a $(D-1)$-face

(iii) $\mathcal{K}$ is **unramified**, *i.e.* every $(D-1)$-simplex belongs to at most 2 D-simplices

We then call **boundary** of $\mathcal{K}$ the subcomplex $\partial\mathcal{K}$ generated by the $(D-1)$-simplices belonging to only one D-simplex.

Note that any topological manifold is a simplicial pseudomanifold:

Theorem 4.1.5. [Pez74] *Let M be a topological manifold of dimension D. Then there exists a trisp $\mathcal{K}$ of dimension D such that the space induced by $\mathcal{K}$ is homeomorphic to M.*

Like genuine manifolds, simplicial pseudo-manifolds admit a notion of orientability:

Definition 4.1.6. Let $\mathcal{K}$ be a simplicial pseudo-manifold of dimension D. An **orientation** on $\mathcal{K}$ consists in orientations on its D-simplices (as parts of $\mathbb{R}^D$), such that, if σ and π are two D-simplices sharing a $(D-1)$-face φ, then their respective orientation are opposite on φ. $\mathcal{K}$ is **orientable** if it admits an orientation.

4.2 Colored graphs and colored trisps

Colored graphs

Definition 4.2.1. A (proper, edge-) **coloring** of a n-regular graph G is a function $c \colon E_G \to \mathcal{C}$, where $\mathcal{C}$ is a set with n elements, such that, for every pair of adjacent edges e, f, $c(e) \neq c(f)$. We then call the pair (G, c) an ***n*-colored graph**, and we will simply denote it by G if there is no ambiguity. Unless specified, the set $\mathcal{C}$ will be $\{0, 1, \ldots, n-1\}$.

Remark. An n-colored graph cannot have any loops.

Remark. A very special example of a $(D+1)$-colored graph is the one with only two vertices, and all edges joining the two vertices (see Figure 4.2.1). We call this graph the **$(D+1)$-colored supermelon**, and denote it by $\boldsymbol{\mathcal{M}_D}$.

In the sequel, we will consider connected colored graphs.

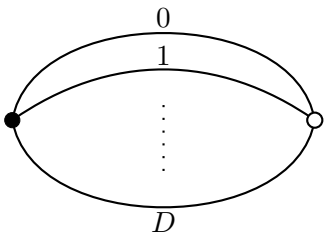

Figure 4.2.1 – Supermelons are the simplest example of colored graphs.

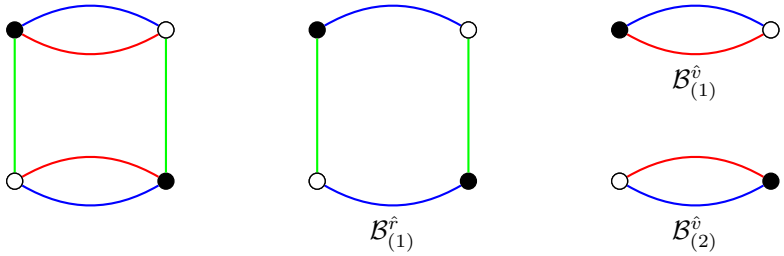

Figure 4.2.2 – A 3-colored graph (left) and some of its 2-bubbles (center and right): the unique one without the color red is denoted with a superscript $\hat{r}$, and the ones without the color green are denoted with a superscript $\hat{v}$.

Definition 4.2.2. Let $0 \leq d \leq n$ be integers. The ***d*-bubbles** of an n-colored graph (G, c) are its maximal connected subgraphs containing edges of exactly d different colors (see Figure 4.2.2). We denote them by $\mathcal{B}^{i_1,\dots,i_d}_{(\rho)}$, where $i_1 < \cdots < i_d$ are the colors of the bubble, and ρ is some index running over the different bubbles with fixed colors.

A colored graph G is equipped with the structure of a cell complex of dimension 2: the 0-bubbles of G, that are its vertices, are the 0-cells, the 1-bubbles, that are its edges, are the 1-cells, and the 2-bubbles are the 2-cells. We thus call the 2-bubbles of G its **faces**, and we denote their set by $F(G)$. We will now explain how we can construct another cell complex, this time of dimension D, with the bubbles of G.

To simplify notation, we will write $\hat{\imath}_1 \dots \hat{\imath}_d$ for $\{0, \dots, D\} \backslash \{i_1, \dots, i_d\}$, and $(\hat{\imath}_1 \dots \hat{\imath}_d)$-bubbles, for the bubbles containing exactly the colors $\hat{\imath}_1 \dots \hat{\imath}_d$.

Let (G, c) be a $(D+1)$-colored graph. To each $(D+1-k)$-bubble $\mathcal{B}^{\hat{\imath}_1 \dots \hat{\imath}_k}_{(\rho)}$, we associate a $(k-1)$-simplex whose vertices are indexed by the missing colors $i_1, \dots, i_k$. This gives us a set of simplices S_k, with an order on the vertices of each simplex. The gluing functions can be constructed in the following way: if $f \colon \{1, \dots, m+1\} \to \{1, \dots, n+1\}$ is an order-preserving injection, and if $\sigma \in S_n$ corresponds to the bubble $\mathcal{B}^{\hat{\imath}_1 \dots \hat{\imath}_{n+1}}_{(\rho)}$, B_f sends it on the m-simplex corresponding to the $(D-m)$-bubble obtained by adding to $\mathcal{B}^{\hat{\imath}_1 \dots \hat{\imath}_{n+1}}_{(\rho)}$ the colors $i_{f(1)}, \dots i_{f(m+1)}$ (see Figure 4.2.3 for a simple example). By construction, the maps B_f do satisfy the conditions (i) and (ii) given before Definition 4.1.2.

We can check that the resulting complex $\Delta(G)$ is regular, and that it is a simplicial pseudo-manifold without boundary [Gur10]. Moreover, it comes with a coloring of its vertices, so that we call it a **colored trisp**.

Note that there is a sort of duality between G and $\Delta(G)$, as $((D+1)-k)$-bubbles

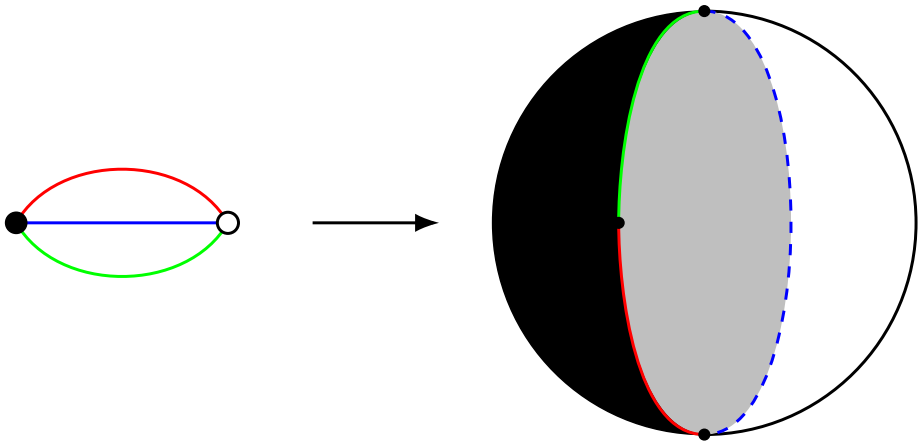

Figure 4.2.3 – The colored trisp associated to the supermelon $\mathcal{M}_2$.

of G correspond to k-simplices of $\Delta(G)$. In particular, the vertices of G correspond to D-simplices, and the edges incident to a vertex of G correspond to the $(D-1)$-simplices of the corresponding D-simplex.

Some geometric properties of $\Delta(G)$ may be read directly on the associated graph, like its orientability:

Theorem 4.2.3. [CGP80] *Δ is orientable if and only if G is bipartite.*

As we will be interested in orientable spaces, in the sequel we will restrict ourselves to bipartite graphs.

Let us note that a regular and bipartite graph G necessarily has the same number of black and of white vertices. Moreover, the faces of a bipartite colored graph are necessarily bicolored cycles.

Let us also note that the set of bipartite $(D+1)$-colored graphs with $2p$ labeled vertices (the positive and negative vertices being labelled independently from 1 to p each), is in bijection with the $(D+1)$-tuples of permutations $(\alpha_0, \dots, \alpha_D) \in (\mathfrak{S}_p)^{D+1}$.

Indeed, given such a labeled graph, for each $i \in C$, define a permutation α_i by: $\alpha_i(k) = l$ if there is an i-colored edge linking the k-th black vertex and the l-th white one. Reciprocally, given such a tuple $(\alpha_0, \dots, \alpha_D)$, we can consider p numbered black vertices and p numbered white ones, and link them according to the permutations.

In Chapter 6, we will use the permutation formulation to define random bipartite vertex-labeled $(D+1)$-colored graphs.

Note that, if we left-multiply all the permutations of a tuple $(\alpha_0, \dots, \alpha_D)$ by the same permutation α, this will not change the underlying (unlabeled) colored graph, as it only changes the labeling of the white vertices. In particular, we can multiply them by α_0^{-1}, and get the tuple $(id, \alpha_1, \dots, \alpha_D)$. Thus, a $(D+1)$-colored graph can be encoded by a D-tuple of permutations, up to global conjugacy (as this changes in a coordinated way the labelings of the black and white vertices), which is equivalent to a $(D+1)$-constellation (defined like 3-constellations were in Chapter 3).

For $D = 2$, we can already deduce that 3-colored graphs are in correspondence with Eulerian triangulations: we will get into more detail about this later in this section.

Jackets and degree of a colored graph

We present now the notion of jackets of a bipartite colored graph, that makes it possible to formalize the underlying geometric structures of the graph.

Definition 4.2.4. Let G be a $(D+1)$-colored graph. A 2-cellular embedding of G is said to be **regular** if there exists a $(D+1)$-cycle τ, such that each region is bounded by a bicolored cycle, of colors $\{i, \tau(i)\}$, for some $i \in \{0, 1, \ldots, D\}$.

Definition 4.2.5. Let G be a bipartite $(D+1)$-colored graph, a **jacket** of G is a subcomplex $\mathcal{J}$ of G (in the sense of cell complexes) of dimension 2, characterized by a $(D+1)$-cycle τ, defined in the following way:

- $\mathcal{J}$ has the same vertex set as G: $V(\mathcal{J}) = V(G)$
- $\mathcal{J}$ has the same edge set as G: $E(\mathcal{J}) = E(G)$
- the faces of $\mathcal{J}$ are: $F(\mathcal{J}) = \Big\{ f \in F(G) \,\Big|\, f = (i, \tau(i)), i \in \{0, ..., D\} \Big\}$.

If a jacket corresponds to a cycle τ, then it also corresponds to τ^{-1}. A $(D+1)$-colored graph therefore has $\frac{D!}{2}$ distinct jackets, and a given face belongs to $(D-1)!$ jackets.

A jacket $\mathcal{J}$ can be seen as a regular embedding G into some Riemann surface, since $\mathcal{J}$, like G, is bipartite. In particular, $\mathcal{J}$ has an Euler characteristic:

$$\chi(\mathcal{J}) = |F(\mathcal{J})| - |E(\mathcal{J})| + |V(\mathcal{J})| = 2 - 2g(\mathcal{J}),$$

where $g(\mathcal{J})$ is the genus of $\mathcal{J}$.

Remark. As a bubble $\mathcal{B}$ of a bipartite colored graph G is also a bipartite colored graph, it also has jackets, that can be directly obtained from the jackets of G by selecting the edges of $\mathcal{B}$.

Jackets will be useful in Section 4.3 to describe colored tensor models, but we can already note that they give us information about the space $|\Delta(G)|$, in particular when it is a topological manifold.

Definition 4.2.6. Let G be a colored graph. We define the **regular genus** of G as the minimum of the genera of its jackets, and we denote it by $\boldsymbol{\rho(G)}$.

Definition 4.2.7. Let M be an orientable, closed manifold. We denote by $\Gamma(M)$ the set of colored graphs G such that $|\Delta(G)| = M$. We define the **regular genus** of M as:

$$\mathcal{G}(M) = \min\{\rho(G) \,|\, G \in \Gamma(M)\}.$$

Definition 4.2.8. Let M be a closed manifold of dimension 3. A **Heegard decomposition of genus g** of M consists of two handle-bodies $\mathcal{A}, \mathcal{A}'$ of genus g, such that $\mathcal{A} \cap \mathcal{A}' = \partial\mathcal{A} = \partial\mathcal{A}'$, and $\mathcal{A} \cup \mathcal{A}' = M$. The surface $\partial\mathcal{A} = \partial\mathcal{A}'$ is called the **Heegard surface** of the decomposition.

We call **Heegard genus of M**, and we denote by $\boldsymbol{\mathcal{H}(M)}$, the smallest integer h such that M admits a Heegard decomposition of genus h.

The regular genus of a manifold corresponds to its genus in dimension 2, and to its Heegard genus in dimension 3:

Theorem 4.2.9. [Gag79] *Let M be a closed, orientable manifold.*

(i) If M is of dimension 2, then: $\mathcal{G}(M) = g(M)$ where $g(M)$ is the genus of M.

(ii) If M is of dimension 3, then: $\mathcal{G}(M) = \mathcal{H}(M)$.

In higher dimensions, the regular genus generalizes the genus, in the sense that it characterizes spheres among closed, orientable manifolds:

Theorem 4.2.10. [FG82] *Let M be a closed, orientable manifold of dimension $n \geq 2$. Then: $\mathcal{G}(M) = 0$ if and only if M is homeomorphic to S^n.*

We now define the degree of a bipartite colored graph, that will be a central quantity in colored tensor models.

Definition 4.2.11. Let G be a bipartite $(D+1)$-colored graph. The **degree** of G is

$$\omega(G) = \sum_{\mathcal{J}} g(\mathcal{J}),$$

where the sum runs over the set of jackets of G.

Lemma 4.2.12. [GR11] *The degree of a bipartite $(D+1)$-colored graph G is related to its number of faces, as well as the degrees of its D-bubbles $\mathcal{B}^{\hat{\imath}}_{(\rho)}$:*

(i) $|F(G)| = \frac{D(D-1)}{2}p + D - \frac{2}{(D-1)!}\omega(G)$

(ii) $\omega(G) = \frac{(D-1)!}{2}(p + D - \mathcal{B}^{[D]}) + \sum_{i,(\rho)} \omega(\mathcal{B}^{\hat{\imath}}_{(\rho)})$,

where $\mathcal{B}^{[D]}$ is the number of D-bubbles of G.

The two-dimensional case

Let us now focus for a moment on colored graphs in the case $D = 2$.

In that case, we are dealing with bipartite trivalent graphs, corresponding to colored trisps made of gluings of black and white triangles. It is thus straightforward to see that such trisps are not only maps, but more specifically Eulerian triangulations.

Note that we can also recover the colors of the vertices of a colored trisp just from the structure of an Eulerian triangulation A. Indeed, we saw in Section 3.5 that this structure induces a cyclic ordering of the vertices of each triangle of A, in a way that is consistent on the whole triangulation. This is equivalent to assigning colors in $\{0, 1, 2\}$ to the vertices of A, in a way that defines a trisp structure on A.

Moreover, as there is a unique (up to inversion) cyclic ordering of $\{0, 1, 2\}$, a bipartite 3-colored graph G has a unique regular embedding. From the definition of $\Delta(G)$, it is clear that this regular embedding embeds G into the same surface as $\Delta(G)$, and makes it its dual, in the sense of maps. In particular, the degree of G is equal to the genus of $\Delta(G)$.

Thus, considering bipartite 3-colored graphs, together with their degree, is equivalent to considering Eulerian triangulations, together with their genus.

4.3 The models

We will now define some specific QFTs that involve colored graphs, and explain how these theories can be understood as models of quantum gravity.

Definition 4.3.1. A **$(D+1)$-colored (tensor) model** is an Euclidean quantum field theory with a measure of the form:

$$d\nu = \prod_{i=0}^{D} d\mu_{C^i}(\phi^i, \bar{\phi}^i) e^{-S} \quad S = \lambda \sum_{n_i \in X^i} K_{n_1 \dots n_D} \prod_{i=0}^{D} \phi^i_{n_i} + \bar{\lambda} \sum_{\bar{n}_i \in X^i} \bar{K}_{\bar{n}_1 \dots \bar{n}_D} \prod_{i=0}^{D} \bar{\phi}^i_{\bar{n}_i}$$

where:

- like for matrix models, we consider discrete underlying spaces X^i, each having a finite number N of points, that can be thought of as the indices of the tensor fields
- the $\phi^i \colon X^i \to \mathbb{C}$ are $D+1$ complex fields: we call the index i, a **color** index
- the $C^i \in \mathbb{M}_{|X^i|}(\mathbb{C})$ are $D+1$ covariance matrices
- $K, \bar{K} \colon X^0 \times \cdots \times X^D \to \mathbb{C}$ are some sets of coefficients, hereafter called **vertex kernels**.

As the fields carry a color index, the closed Feynman diagrams of these models are $(D+1)$-colored graphs. Moreover, as the fields are complex, these graphs are bipartite.

The i.i.d. model

In the particular model that interests us, the weight of a Feynman graph only depends on its number of faces. The fields will actually be rank D tensors, that we denote by $\phi^i_{\vec{n}_i}$, where $\vec{n}_i = (n^{ii-1}, ..., n^{i0}, n^{iD} ..., n^{ii+1})$. We choose as covariance matrices and vertex kernels:

$$C^i_{\vec{n}_i, \vec{\bar{n}}_i} = \prod_{j \neq i} \delta_{n^{ij}, \bar{n}^{ij}} \quad , \quad K_{\vec{n}_0, \dots, \vec{n}_D} = \bar{K}_{\vec{n}_0, \dots, \vec{n}_D} = \frac{1}{N^{D(D-1)/4}} \prod_{i<j} \delta_{n^{ij}, n^{ji}} \tag{4.3.1}$$

We thus have the measure:

$$d\nu = \prod_{i, \vec{n}_i, \vec{\bar{n}}_i} \frac{d\phi^i_{\vec{n}_i} d\bar{\phi}^i_{\vec{\bar{n}}_i}}{2\pi} e^{-S} \tag{4.3.2}$$

with

$$S(\phi, \bar{\phi}) = \sum_{i=0}^{D} \sum_{\vec{n}_i, \vec{\bar{n}}_i} \bar{\phi}^i_{\vec{\bar{n}}_i} \delta_{\vec{n}_i, \vec{\bar{n}}_i} \phi^i_{\vec{n}_i} + \frac{\lambda}{N^{D(D-1)/4}} \sum_{\{\vec{n}\}} \prod_{i=0}^{D} \phi^i_{\vec{n}_i} + \frac{\bar{\lambda}}{N^{D(D-1)/4}} \sum_{\{\vec{\bar{n}}\}} \prod_{i=0}^{D} \bar{\phi}^i_{\vec{\bar{n}}_i}. \tag{4.3.3}$$

We call this model, the **independently and identically distributed (i.i.d.) colored tensor model**.

Proposition 4.3.2. *For this model, the amplitude of a bipartite $(D+1)$-colored graph G, with $2p$ vertices, is*

$$A(G) = (\lambda\bar{\lambda})^p N^{|F(G)| - p\frac{D(D-1)}{2}} = (\lambda\bar{\lambda})^p N^{D - \frac{2}{(D-1)!}\omega(G)}. \tag{4.3.4}$$

The i.i.d. colored tensor model can therefore be seen as a random geometry approach to quantum gravity. Indeed, the amplitude (4.3.4) for a bipartite $(D+1)$-colored graph G is equal to the Regge action (2.3.3) for its associated trisp $\Delta(G)$, when setting (see [GR12]):

$$\begin{cases} \ln(N) = & \frac{v(\sigma_{D-2})}{8G} \\ \ln(\lambda\bar{\lambda}) = & \frac{D}{16\pi G} v(\sigma_{D-2})\Big(\pi(D-1) - (D+1)\arccos\frac{1}{D}\Big) - \frac{1}{4\pi G}\Lambda v(\sigma_D). \end{cases} \tag{4.3.5}$$

Note that, in the $2D$ case, the amplitude (4.3.4) just weights 3-colored graphs, or the dual Eulerian triangulations, according to their genus. Thus, it is a particular case of the $1/N$ expansion we have seen for the matrix models of Section 2.4.

This means that the i.i.d. colored tensor model can really be considered as a generalization to higher dimensions of the model of $2D$ quantum gravity described by such matrix models.

Note that it was expected that *some sort* of tensor models properly generalized the matrix models of $2D$ quantum gravity. However, physicists did not find tensor models inducing the desired $1/N$ expansion over D-dimensional discretized spaces, until the introduction of *colored* tensors, spearheaded by Gurău [Gur11a; Gur11b; Gur12].

Indeed, the colors give to colored trisps a very straightforward combinatorial structure, which is not the case of more general simplicial spaces.

Uncolored models

Even though coloring tensors was the successful trick to generalize matrix models to higher dimension, we can still use the formalism of colored graphs and trisps, to define QFTs with a single tensor field ϕ, instead of $D+1$ tensors $\phi^0, \dots, \phi^D$ carrying a color index: such QFTs are naturally called **uncolored models**.

The motivations for studying uncolored models are twofold: on the purely QFT side, they retain $1/N$ expansions while being related to pre-existing models of D-dimensional quantum gravity that are more amenable to renormalization techniques; on the more geometrical side, as we will see in the sequel, uncolored models allow to reach other dominant graphs, and therefore other geometries, than the i.i.d. model.

To build an uncolored model, the idea is to have a theory whose Feynman graphs are still bipartite $(D+1)$-colored graphs, but to fix a finite set of possible configurations for, say, the $\hat{0}$-bubbles of our graphs, so that the only actual field corresponds to the 0-colored edges, while all the others belong to the actual vertices of the theory.

We will not write the corresponding action functionals, that can be found for instance in [BGR12]. For our purposes, it suffices to state that, on the level of graphs, this gives amplitudes similar to (4.3.4), but restricted to $(D+1)$-colored graphs with only specific $\hat{0}$-bubbles.

Let us consider the colored trisp $\Delta(G)$ corresponding to a Feynman graph G of an uncolored model. The absence of constraints on the 0-colored edges of G means that the $(D-1)$-simplices of $\Delta(G)$ that do not contain vertices of color 0 can be glued together in any way that respects the coloring of the vertices; on the contrary, the constraints on the $\hat{0}$-bubbles of G fix the possible ways the $(D-1)$-simplices missing another color i can be glued together.

Thus, instead of gluing colored D-simplices along their $(D-1)$-faces with the only constraint of matching the colors of vertices, we are actually gluing together some new

elementary building blocks, that are themselves made of colored D-simplices, and whose boundary $(D-1)$-faces are all of type $\hat{0}$.

4.4 Notable results for random geometry

Melonic graphs

From the preceding results, the dominant graphs in the i.i.d. colored model are those of degree zero, *i.e.* those that only have planar jackets.

Similarly to matrix models, this gives a model for a discretized D-dimensional quantum spacetime, by taking a colored trisp uniform on those that are dual to graphs of degree zero (and with a given number of D-simplices). Therefore, with the motivation of quantum gravity, it is important to understand the structure of colored graphs of degree zero.

Note that, for $D = 2$, the dominant graphs are dual to planar Eulerian triangulations: thus, the main result of Chapter 7 shows that the two-dimensional case of the i.i.d. colored tensor model does behave like other well-known matrix models, with dominant maps converging to the Brownian map.

Let us now focus on dimensions $D \geq 3$. Let us first note that the supermelon $\mathcal{M}_D$ has degree zero. As we will see in the sequel, it plays a very important role in the structure of graphs of degree zero, that are also called **melonic graphs**.

One of the properties of melonic graphs is that their dual trisp is spherical. However, this is not enough to characterize them.

Proposition 4.4.1. [GR11] *The dual complex of a $(D+1)$-colored graph of degree zero is homeomorphic to the D-sphere.*

Remark. The converse is not true: there exist colored graphs dual to a spherical complex, but that have non-planar jackets.

Melonic graphs were characterized in [BGRR11]: for $D \geq 3$, they exhibit a recursive structure, that yields a bijection between these graphs and a class of colored trees.

We begin with the following observation:

Proposition 4.4.2. [BGRR11] *For $D \geq 3$, any melonic graph has a D-bubble with exactly two vertices.*

For a melonic graph G, this D-bubble of G with 2 vertices can be seen as a 2-point version of the supermelon. We therefore call this bubble a **melon**. It is crucial to note that, if a melonic graph has a melon $\mathcal{B}^{\hat{\imath}}_{(\rho)}$ (and at least four vertices), if we eliminate this bubble by merging the two incident edges of color i (like in Figure 4.4.1), we obtain a colored graph that is also of degree zero from Lemma 4.2.12, since we deleted one D-bubble and two vertices.

The supermelon is thus central in the structure of melonic graphs. Indeed, consider a meloinc graph G. If G is not the supermelon, it has a D-bubble with two vertices, and has at least four vertices, so that, by eliminating this bubble, we obtain a melonic graph with two less vertices. By repeating this process, every melonic graph can thus be reduced to the supermelon, by eliminating melons. Going in the reverse order, we can recursively build melonic graphs from the supermelon, by successive insertions of melons.

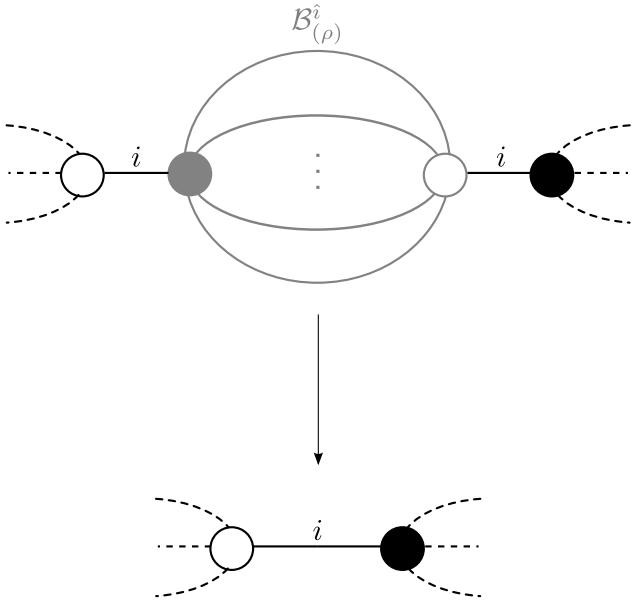

Figure 4.4.1 – Eliminating a melon.

To get a bijection with a family of trees from this recursive structure, let us rather consider melonic *2-point* graphs, which are equivalent to rooted closed melonic graphs. Without loss of generality, we can fix D as the color for the external lines.

Like for closed graphs, the only possible melonic 2-point graph with two vertices is the melon with two external lines of color D. We represent it by a tree consisting of one $D+2$-valent vertex and all its univalent neighboring vertices. One of the $D+2$ edges will be chosen as the root, and the other ones will be called leaves, as one of their extremities is a leaf. We give the color D to the root and to one leaf, and we distribute the remaining colors $i = 0, \dots, D-1$ among the D other leaves. On G, we call **active** the lines of color $i \neq D$, and the external line of color D incident to the black vertex (see Figure 4.4.2). These lines correspond to the active leaves of the tree, of colors $0, 1, \dots, D$, the root being **inactive**. This will allow us to avoid redundancies when we get to larger graphs.

We have $D+1$ graphs with four vertices: they correspond to the insertion of a melon on either of the $D+1$ active lines of the graph with two vertices. We consider the internal lines of the inserted melon, as well as the external line that touches its black vertex, as active. If the melon is inserted on the active line of color i, we associate to the graph the tree obtained from the preceding tree by connecting a new $(D+2)$-valent vertex to the leaf of color i (see Figure 4.4.3). The leaves of this new vertex are also colored from 0 to D. It is clear that we do obtain $D+1$ trees in this manner.

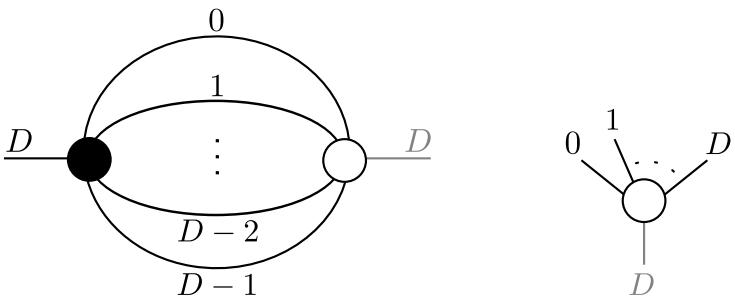

Figure 4.4.2 – A melonic graph with two vertices and two external lines of color D, and the corresponding tree. The active lines are depicted in black, and the inactive ones in gray.

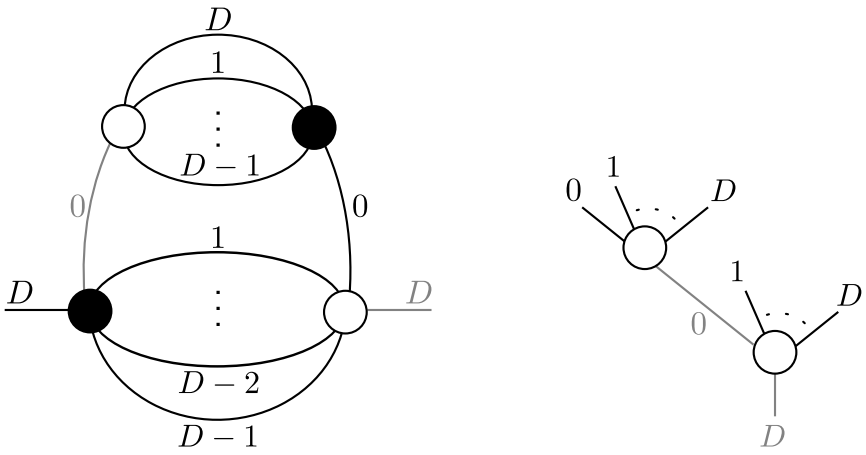

Figure 4.4.3 – A melonic graph with four vertices, and the corresponding tree.

To obtain the graphs with $2(p+1)$ vertices, we similarly insert a melon on the active line of a graph with $2p$ vertices. The internal lines of the inserted melon, as well as the external line that touches its black vertex, are active. Once again, we represent this operation on the side of trees by the connection of a $(D+2)$-valent vertex on one of the active leaves of a tree with p inner (*i.e*, $(D+2)$-valent) vertices.

Thus, 2-point $(D+1)$-colored melonic graphs with $2p$ vertices are in correspondance with rooted, edge-colored trees with p $(D+2)$-valent vertices, and $Dp+2$ leaves. Such trees are called **colored $(D+1)$-ary trees**. This allows us to count the number M_p^D of 2-point melonic graphs with $2p$ vertices:

$$M_p^D = \frac{\Big((D+1)!\Big)^p}{p!(Dp+1)!} T_p = C_p^{(D+1)}, \tag{4.4.1}$$

where

$$C_p^{(D+1)} = \frac{1}{(D+1)p+1} \binom{(D+1)p+1}{p}.$$

From Proposition 4.4.1, we have that 2-point $(D+1)$-colored melonic graphs correspond to particular colored trisps of the D-ball. Let us thus call these particular trisps **melonic D-balls**. Considering the recursive structure of melonic graphs, we might expect that melonic D-balls with a large number of maximal simplices have a tree-like scaling limit: this was proved by Gurău and Ryan in [GR14].

Note that, like we did for maps in Chapter 3, to consider a colored trisp Δ as a metric space, we use the structure given by its 1-skeleton: the elements of this metric space are the vertices of Δ, *i.e.* its 0-simplices, and the distance between two points is their graph distance on the 1-skeleton of Δ, or in other words, the number of edges of the smallest path from one to the other in the 1-skeleton.

Before stating the convergence result for the metric spaces induced by melonic D-balls, let us thus give a bit of additional notation. Let Δ_n be picked uniformly at random in the set of melonic D-balls with n D-simplices. We denote by V_n the set of inner vertices of Δ_n, and $d_n(\cdot,\cdot)$ the graph distance in the 1-skeleton of Δ_n, defined on V_n. Recall that $\mathbb{e}$ is the standard Brownian excursion, and that $(\mathscr{T}_\mathbb{e}, d_\mathbb{e})$ is the Continuum Random Tree.

Theorem 4.4.3. [GR14] *There exists some constant $c_D > 0$, such that the following convergence in distribution*

$$\left(V_n, \frac{d_n}{c_D\sqrt{n}}\right) \xrightarrow[n\to\infty]{(d)} (\mathscr{T}_{\mathbb{e}}, d_{\mathbb{e}})$$

holds for the Gromov-Hausdorff distance on compact metric spaces.

This result is drastically different from the $2D$ case, and, while mathematically interesting, is quite underwhelming from the point of view of quantum gravity, as our putative D-dimensional quantum spacetime turns out to be the CRT.

Beyond melons

To get more promising scaling limits of random colored trisps, we must get away from melonic graphs. There are several ways to do this, and we present here notable results that have been obtained in these different approaches.

A first strategy is to investigate the enumeration of general bipartite $(D+1)$-colored graphs, with respect to their size and degree.

This task was undertaken by Gurău and Schaeffer in [GS16], where they achieved a classification of colored graphs of positive degree in terms of reduced graphs called schemes. This gave in particular asymptotic results for the number of large colored graphs of a given degree:

Theorem 4.4.4. [GS16] *For any fixed $D \geq 3$ and $\delta \geq 1$, the generating function of bipartite $(D+1)$-colored graphs of degree δ has a dominant singularity at $z_0 = D^D/(D+1)^{D+1}$, and a singular expansion in a slit domain around z_0 of the form:*

$$H^0_\delta(z) = K_\delta(1 - z/z_0)^{-\mathbf{B}_{\max}} \left[1 + O\left(\sqrt{1 - \frac{z}{z_0}}\right)\right],$$

where

$$\mathbf{B}_{\max} = \max\left(2c + 3q - 1 \,|\, (D-2)c + Dq \leq \delta,\, c, q \in \mathbb{N}\right).$$

As these asymptotics lie in the same universality class as trees, this hinted that large colored trisps of fixed, positive degree also converge to a continuum "tree-like" limit.

This intuition is refined in an upcoming work by Lionni [Lio], where he proves that the enumeration results of [GS16] imply that the only possible scaling limits for large colored trisps of fixed, positive degree, are continuum random maps of fixed excess, as defined in [ABACFG].

Thus, this route, while mathematically interesting, is not very satisfactory for the purpose of quantum gravity.

Another possibility is to turn to uncolored models and their more complex building blocks, as they might lead to other geometries.

For instance, one can choose only non-melonic building blocks, to enhance non-melonic Feynman graphs, as was done in [BDR15].

Once again, the information that is relevant to the search for continuum scaling limits lies in the singularity behavior of the generating functions of the dominant graphs. In this work, the singularity can be of three different types: one corresponds to the universality class of trees, another corresponds to the universality class of maps. In-between, there is an intermediate regime, which is described in the physical literature as a "proliferation

of baby universes", as we expect it to correspond to a continuum object with a tree-like structure, but decorated by macroscopic maps.

Note that no actual scaling limit has been derived for these models, but that the singularities indicate which type of scaling limit is *possible*.

Uncolored models can also yield new geometries at the discrete level if one chooses simple, spherical building blocks, so that the associated colored trisps can be seen as higher-dimensional equivalents to specific classes of maps, such as p-angulations. This has been investigated for $D = 3$, see [BL17; Bon]. All the different choices of building blocks in these works yield generating functions for the dominant graphs that are still in the universality class of trees.

All these approaches stay relatively close to melons, by still selecting the dominant colored graphs in a $1/N$ expansion that depends on the degree, or in other words, by selecting the colored graphs with minimal degree in some specific class. Another possible approach is to start "from the other side", by taking a uniform measure on some class of colored graphs, without selecting the ones with minimal degree.

The first step in that strategy was made in the paper [Car19], reproduced in Chapter 6, in which I studied random models of colored graphs, uniformly distributed on all the possible Feynman graphs (of fixed size), of both the i.i.d. model, and uncolored models.

For the i.i.d. model, this yields a random graph chosen uniformly among all (vertex-labeled) bipartite $(D+1)$-colored graphs with $2p$ vertices, denoted U_p^D. For an uncolored model given by a D-colored graph G as an interaction vertex, this yields a random bipartite colored graph G_p containing p copies of G, with colors symmetrized on $\{1, \dots, D\}$, and 0-colored edges given by uniform pairings of the black and white vertices.

The main results that I obtained, concerning the search for continuum scaling limits, are the following:

Theorem 4.4.5. *For $D \geq 3$,*

$$\mathbb{E}\big[\#\textit{vertices of } \Delta(U_p^D)\big] = D + 1 + O\Big(\frac{1}{p^{D-2}}\Big).$$

Theorem 4.4.6. *For any $D \geq 3$, for any bipartite D-colored graph G,*

$$\mathbb{E}[\#\textit{vertices of } \Delta(G_p)] = p + \alpha_G + o(1),$$

where α_G is a constant that depends only on G. Moreover, if u, v are two vertices of $\Delta(G_p)$ chosen uniformly at random, then $d(u, v) = 2$ asymptotically almost surely.

In either case, as the distances in the random trisp stay typically bounded, there is no hope of obtaining a continuum space as a scaling limit. This is a particular instance of a more general phenomenon observed in other models of quantum gravity in higher dimensions, called the **crumpled phase**. For instance, in Euclidean Dynamical Triangulations, Monte Carlo simulations show evidence of a singularity behavior for the putative scaling limit in dimension 3 and 4, as long as the sampling of the triangulation does not depend too strongly on its curvature (see for instance [Tho99]).

The outline of the proof of these results, as well as the other results I derived on these models, are given in Chapter 5. The paper [Car19] is reproduced in Chapter 6.

While they are interesting in themselves, the enumerative or geometric results presented above are obviously not directly promising for the search for a D-dimensional continuum scaling limit of colored trisps. However, they are reassuring, in the sense that, between

the close-to-melonic models that behave like trees or maps, with large exponents for the scaling of the distances, and the uniform models, which have a singular limit, with bounded distances, one should be able to find intermediate regimes, that hopefully contain random continuum D-dimensional structures.

4.5 Other aspects

Let us finish by briefly mentioning two other current topics of research on colored tensor models, that are also of interest for the broad motivation of quantum gravity.

The SYK model

In 2016, Witten [Wit] observed that colored tensors could be used to define a QFT model whose correlation functions behave similarly to the ones of the **SYK model**, which is a QFT model with disorder notably related, via the famous AdS/CFT correspondence, to the thermodynamics of a quantum black hole in $2D$ spacetime, as described in the Bekenstein-Hawking theory. It is obviously interesting, when motivated by quantum gravity, to further the knowledge about a prominent theory describing such a central object in quantum gravity.

Since this first paper, there has been a lot of further work on SYK-like tensor models: see for instance [GKT17; DR; BGH].

Advances in constructive techniques

As mentioned in Chapter 2, some constructive techniques such as the loop vertex expansion apply to tensor-valued QFTs. This is of general interest for any application of colored tensor models, as it gives a better understanding of these models.

On that front, the most advanced achievements concern models with quartic interaction terms for tensors of rank 3 and 4 [DR16; RVT19]. A great difficulty, compared to matrix models, for which constructive techniques have been successfully applied to large N limits [KRS], is that there is no notion of "tensor analysis", contrary to the very developed field of matrix analysis, involving, among other tools, spectral analysis, orthogonal polynomial techniques, functional calculus.

CHAPITRE 5

Outline and perspectives

We now sketch the main ideas and arguments of the works that are presented in this manuscript. We proceed chronologically, starting with a first project on random models of colored trisps (defined in Chapter 4) for any dimension $D \geq 3$, before presenting a multi-faceted project on Eulerian triangulations, that are, as explained in Chapter 4, dual to the two-dimensional colored trisps.

5.1 Work in $D \geq 3$

As explained in Chapter 4, the gol of [Car19] was to start the study of random models of colored trisps, away from the melonic regime. I thus studied asymptotic properties of colored trisps chosen uniformly at random in some classes of colored trisps (or, equivalently, colored graphs) without degree constraints. To describe these random models, I used the formalism of $(D+1)$-tuples of permutations $(\alpha_0, \dots, \alpha_D)$, where, as explained in Chapter 4, the permutation α_i gives the edges of color i in the colored graph.

The first model I studied is the **uniform model**, denoted by $\boldsymbol{U_p^D}$. In this model, the permutations $(\alpha_i)_{0\leq i\leq D}$ are chosen uniformly at random and independently in $\mathfrak{S}_p$.

The second model is the **uniform-uncolored model $\boldsymbol{G_p}$**. Starting from a D-colored graph G (of colors $\{1, \dots, D\}$, we take p copies of G in which the colors are permuted by i.i.d. uniform permutations $(\gamma_k)_{1\leq k\leq p} \in (\mathfrak{S}_D)^p$, and we add α_0 uniform and independent from the rest, for the 0-edges (see Figure 5.1.1). A special case that I investigated more precisely is the **quartic model**, denoted by $\boldsymbol{Q_p^D}$, in which the base D-colored graph $G = Q^D$ is quartice (see Figure 5.1.2).

The first step was to study the connectivity and geometry of these models. Let us denote by $k(H)$ the number of connected components of the graph H. Starting with the uniform model, we have:

Theorem 5.1.1. *For $D \geq 2$, one has:*

$$\mathbb{E}\big[k(U_p^D)\big] = 1 + O\bigg(\frac{1}{p^{D-1}}\bigg).$$

For a colored graph H, let us denote by H_i the subgraph of H where we have removed the edges of color i. For a given color $i \in [\![0, D]\!]$, the graph $(U_p^D)_i$, has the same law as U_p^{D-1} (up to a color renaming). This means that Theorem 5.1.1 can also be used for the number

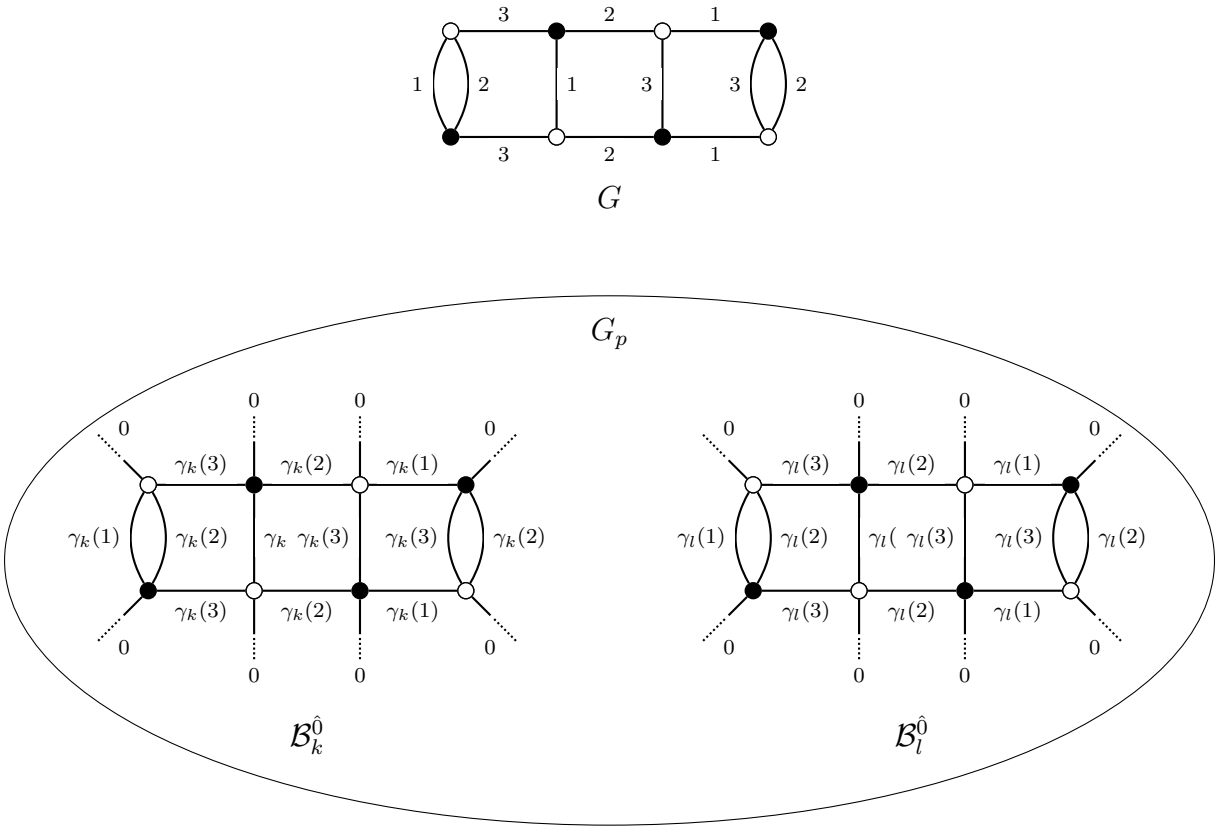

Figure 5.1.1 – Starting from a D-colored graph G (here $D = 3$), we construct a $(D+1)$-colored graph G_p, whose p $\hat{0}$-bubbles are copies of G in which the colors have been permuted.

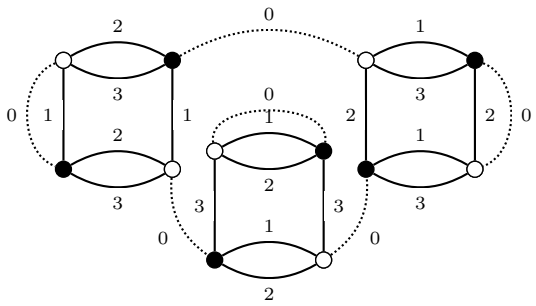

Figure 5.1.2 – The special case of the quartic model.

$b_D(U_p^D)$ of D-bubbles of U_p^{D+1}, simply by summing over all colors. It is straightforward to derive the following result:

Corollary 5.1.2. *For $D \geq 3$, one has:*

$$\mathbb{E}\big[b_D(U_p^D)\big] = D + 1 + O\bigg(\frac{1}{p^{D-2}}\bigg).$$

This means that for $D \geq 3$, there is typically only one point of each color in the dual complex, so that the associated metric space is asymptotically very singular.

Similarly to Theorem 5.1.1, we obtain for the uncolored models:

Theorem 5.1.3. *Let G be a bipartite D-colored graph with $2t \geq 4$ vertices, and let G_p be the associated uniform-uncolored model. One has:*

$$\mathbb{P}(G_p \text{ connected}) = 1 - \frac{p}{\binom{tp}{t}} + O\bigg(\frac{1}{p^{2(t-1)}}\bigg),$$

$$\mathbb{E}[k(G_p)] = 1 + O\bigg(\frac{1}{p^{t-1}}\bigg).$$

It is less straightforward to obtain geometric properties for the uniform-uncolored model. However, we can first observe that the number of points of color 0 in the trisp, which is the same as the number of $\hat{0}$-bubbles in the graph G_p, is always p. For any color i other than 0, we can relate the connectivity of the graph $(G_p)_{\hat{i}}$, to the one of an oriented *configuration model*. This yields:

Theorem 5.1.4. *For $D \geq 3$, for any bipartite D-colored graph G with $2t \geq 4$ vertices, and for any $i \in \{1, 2, \ldots, D\}$, G_p has a giant $\hat{\imath}$-bubble containing $2tp - O\big(\sqrt{p \ln p}\big)$ vertices. Moreover, the expectation value of the number of $\hat{\imath}$-bubbles of G_p is:*

$$\mathbb{E}[k((G_p)_{\hat{\imath}})] = c_G + 1 + o(1)$$

where c_G is a constant that depends only on G.

Hence, for the total number of D-bubbles of G_p:

Corollary 5.1.5. *For $D \geq 3$, $\mathbb{E}[b_D(G_p)] = p + D\,(c_G + 1) + o(1)$.*

This study of the D-bubbles of G_p gives us insight on the typical geometry of the associated complex $\Delta(G_p)$. Indeed, there are p 0-points in $\Delta(G_p)$, while for any $i \in \{1, 2, \ldots, D\}$ there are at most $O\big(\sqrt{p \ln p}\big)$ i-points, one of which is the "hub" i-point, that corresponds to the giant $\hat{\imath}$-bubble, and therefore has most 0-points as neighbors. Thus:

Theorem 5.1.6. *Let u, v be two vertices of $\Delta(G_p)$ chosen uniformly at random and independently. Then, if $D \geq 3$, $d(u, v) = 2$ a.a.s..*

This means that although the metric space associated to $\Delta(G_p)$ does have a number of points that goes to infinity as $p \to \infty$, it is very singular. The singular asymptotic behavior of the spaces associated to the uniform and uniform-uncolored models can be seen, as stated before, as instances of the crumpled phase that has also been observed in Euclidean Dynamical Triangulations.

There are several possible ways to construct new random models of trisps, in the search for a D-dimensional continuum scaling limit. One possibility is to try and fine-tune a random distribution parametrized by the degree or a related quantity, although at the moment

it seems ambitious to obtain rigorous results for this type of models. Another possibility is to look for one "miraculous" model with a nice behavior: some specific subclasses of the trisps related to the quartic model could be promising. The hope would be to generalize the findings for the first miraculous model to a broader class of models, as was done for random maps.

Another interesting perspective would be to prove that slight perturbations of the uniform models still belong to the crumpled phase. This would require new techniques, as our results deeply rely on the uniformity and the independence of the different permutations describing the trisps.

While these two models do not yield any continuum sclaing limit, they still give us insight on the typical behavior of large colored graphs. In particular, I investigated some properties related to their degree.

Starting with the uniform model, I obtained estimates for the first and second moments of its degree, using classical results on uniform random permutations:

Proposition 5.1.7.

$$\mathbb{E}\big[b_2(U_p^D)\big] = \frac{D(D+1)}{2}(\ln p + \gamma) + o(1) \tag{5.1.1}$$

$$\mathrm{Var}\big(b_2(U_p^D)\big) = \frac{D(D+1)}{2}\ln p + o(\ln p). \tag{5.1.2}$$

In terms of the Gurau degree, this means that:

$$\mathbb{E}\big[\omega(U_p^D)\big] = \frac{(D-1)!}{2}\Big(\frac{D(D-1)}{2}p + D - \frac{D(D+1)}{2}(\ln p + \gamma)\Big) + o(1)$$

$$\mathrm{Var}\big(\omega(U_p^D)\big) = \frac{(D-1)!}{2}\frac{D(D+1)}{2}\ln p + o(\ln p).$$

To obtain more precise information, I focused on the number of faces of a single regular embedding of U_p^D, rather than the total number of faces. For this, I generalized arguments that had already been used for random Belyi surfaces [Gam06] and random gluings of polygons [PS06; CP16], and that rely on techniques of representation theory. These arguments yield a Central Limit Theorem for the genus of a regular embedding of U_p^D:

Theorem 5.1.8. *Let $\mathcal{J}_p$ be a regular embedding of U_p^D, and $F_{\mathcal{J}_p}$ be the number of faces (*i.e. *regions) of $\mathcal{J}_p$. Then the quantity $\frac{F_{\mathcal{J}_p} - \mathbb{E}[F_{\mathcal{J}_p}]}{\sqrt{\mathrm{Var}(F_{\mathcal{J}_p})}}$ converges weakly to the standard normal distribution.*

As for the uniform-uncolored models, it is difficult to obtain any result in the general case. This is why I focused on the quartic model, which is a very important type of uncolored model in the physics literature on colored tensor models (see for instance [DGR13; OSVT13; DGR14; RVT19]). With techniques similar to the ones of the uniform case, we obtain:

Theorem 5.1.9.

$$\mathbb{E}\big[[b_2(Q_p^D)\big] = (D-1)^2 p + D(\ln(2p) + \gamma) + o(1) \tag{5.1.3}$$

$$\mathrm{Var}\big(b_2(Q_p^D)\big) = O\big((\ln p)^3\big). \tag{5.1.4}$$

We also get a normal limit for the number of faces of one jacket:

Theorem 5.1.10. *Let $\mathcal{J}_p$ be a regular embedding of Q_p^D, and $F_{\mathcal{J}_p}$ be the number of faces of $\mathcal{J}_p$. Then the quantity $\frac{F_{\mathcal{J}_p}-\mathbb{E}[F_{\mathcal{J}_p}]}{\sqrt{\mathrm{Var}(F_{\mathcal{J}_p})}}$ converges weakly to the standard normal distribution.*

Note that the proof of Theorem 5.1.10 also yields a Central Limit Theorem for the genus of the map M_p chosen uniformly at random in all (half-edge-labeled-)maps with p edges:

Theorem 5.1.11. *Let g_p be the genus of M_p. Then the quantity $\frac{g_p-\mathbb{E}[g_p]}{\sqrt{\mathrm{Var}(g_p)}}$ converges weakly to the standard normal distribution. Moreover, we have the following estimations:*

$$\begin{aligned}\mathbb{E}[g_p] &= \frac{p}{2} - (\ln 2p + \gamma) + 1 + o(1),\\ \mathrm{Var}(g_p) &= O\big((\ln p)^3\big).\end{aligned}$$

This result was proven independently by Budzinski, Curien and Petri [BCP], using peeling techniques. They also considered a broad class of maps described as uniform gluings of polygons, that encompasses the cases considered in the works of Pippenger and Schleich [PS06] and Chmutov and Pittel [CP16]. Let us introduce a bit of notation to state their results and a possible extension.

Consider a set of polygons $\mathcal{P} = (p^{(1)}, p^{(2)}, \dots)$, where $p^{(i)}$ is the number of polygons of perimeter i. Let us denote by $M_{\mathcal{P}}$ the map obtained by a uniform random gluing of the polygons in $\mathcal{P}$, and by $G_{\mathcal{P}}$ the underlying graph. For a sequence $\mathcal{P}_n$, it is straightforward to show that $M_{\mathcal{P}_n}$ is connected asymptotically almost surely if and only if

$$\frac{p_n^{(1)}}{\sqrt{n}} \xrightarrow[n\to\infty]{} 0 \text{ and } \frac{p_n^{(2)}}{n} \xrightarrow[n\to\infty]{} 0.$$

We call a sequence of sets of polygons **good** if it satisfies the above condition.

For a graph G, consider its vertices ordered by decreasing degree $u_1, u_2, \dots$. We denote by $[i:j]_G$ the mutual degree of u_i and u_j, that is, the number of edges shared by u_i and u_j (where loops count for 2 in $[i:i]_G$).

Budzinski, Curien and Petri obtain a universality result for the limit of the joint distribution $([i:j]_{G_{\mathcal{P}_n}})_{i,j\geq 1}$, for any good sequence $\mathcal{P}_n$. The next step would be to show that $G_{\mathcal{P}_n}$ itself admits a universal limit for good sequences $\mathcal{P}_n$.

It would be interesting to try to obtain this using representation-theoretic techniques. Another possible application of these techniques would be *non-orientable* gluings of polygons, in which we allow twistings of the edges of the polygons before gluing them.

5.2 Work in $D = 2$

Let us now give the outline of Part III. As we saw in Section 3.2, the canonical way to prove the convergence of a family of rooted planar maps to the Brownian map, is to use a bijection between these maps, and some class of trees labeled by integers that keep track of the distances in the map.

For Eulerian triangulations, such a bijection exists and was derived by Bouttier, Di Francesco and Guitter in [BDFG04]. However, it involves, rather than the usual graph distance d, the **oriented pseudo-distance** $\vec{d}$, where $\vec{d}(u,v)$ is the length of a shortest oriented path from u to v (see Figure 5.2.1). As the function $\vec{d}$ is not symmetric, it is much more difficult to go from the convergence of the labeled trees, to the convergence of the metric spaces induced by the maps. In particular, we cannot prove a bound equivalent to (3.2.1).

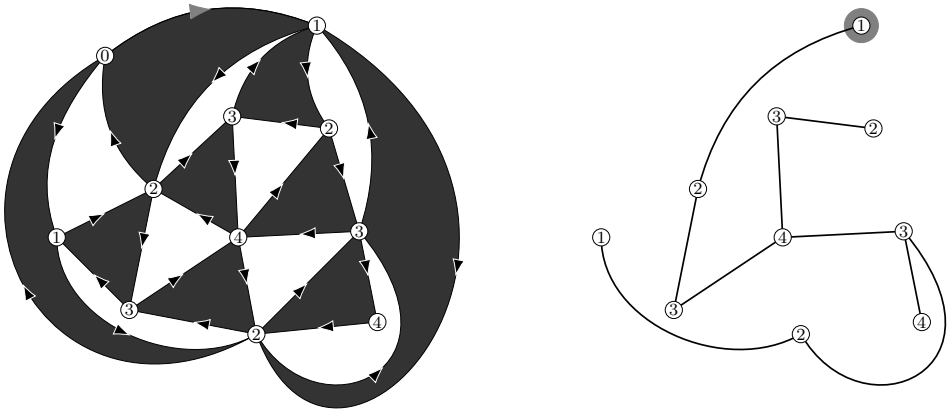

Figure 5.2.1 – A rooted planar Eulerian triangulation A equipped with its oriented pseudo-distance (left), and the corresponding rooted labeled tree T (right). The construction of T from A consists in keeping only the edge of type $n+1 \to n+2$ in each black face adjacent to vertices with oriented pseudo-distance from the root, respectively n, $n+1$, and $n+2$.

To circumvent this, a solution is to prove that the oriented pseudo-distance $\vec{d}$, and the usual graph distance d, are asymptotically proportional in large Eulerian triangulations, so that $\vec{d}$ is asymptotically symmetric. One thing to note is that $\vec{d}$ is a local modification of d, as the difference between the two is that a geodesic for $\vec{d}$ sometimes has to take a detour of two edges where a geodesic for d will only take one. Hence, we can try and adapt the layer decomposition method to Eulerian triangulations equipped with the two distances $\vec{d}$, d.

This is the object of Chapter 7, where we define the relevant notion of hulls with respect to $\vec{d}$, and then derive a layer decomposition for finite planar Eulerian triangulations. Using the procedure described in the previous section, we use this layer decomposition to define the Uniform Infinite Eulerian Triangulation, the Upper Half-Plane Eulerian Triangulation, and the Lower Half-Plane Eulerian Triangulation, that had not been constructed before.

Then, using, as explained before, an ergodic subadditivity argument, we obtain:

Theorem 5.2.1. *Let $\mathcal{T}_n$ be a uniform random rooted Eulerian planar triangulation with n black faces, and let $V(\mathcal{T}_n)$ be its vertex set. There exists a constant $\mathbf{c}_0 \in [2/3, 1]$ such that, for every $\varepsilon > 0$, we have*

$$\mathbb{P}\left(\sup_{x,y \in V(\mathcal{T}_n)} |d(x,y) - \mathbf{c}_0 \vec{d}(x,y)| > \varepsilon n^{1/4} \right) \xrightarrow[n\to\infty]{} 0.$$

Let $\mathbf{c}_0$ be the constant in Theorem 5.2.1, and let $\overleftrightarrow{d}$ be the symmetrization of $\vec{d}$, defined for any two vertices u, v of some Eulerian triangulation:

$$\overleftrightarrow{d}(u,v) = \frac{\vec{d}(u,v) + \vec{d}(v,u)}{2}.$$

Then, the asymptotic proportionality derived in Theorem 5.2.1 allows us to treat $\vec{d}$ (asymptotically) similarly to a genuine, symmetric distance, which yields:

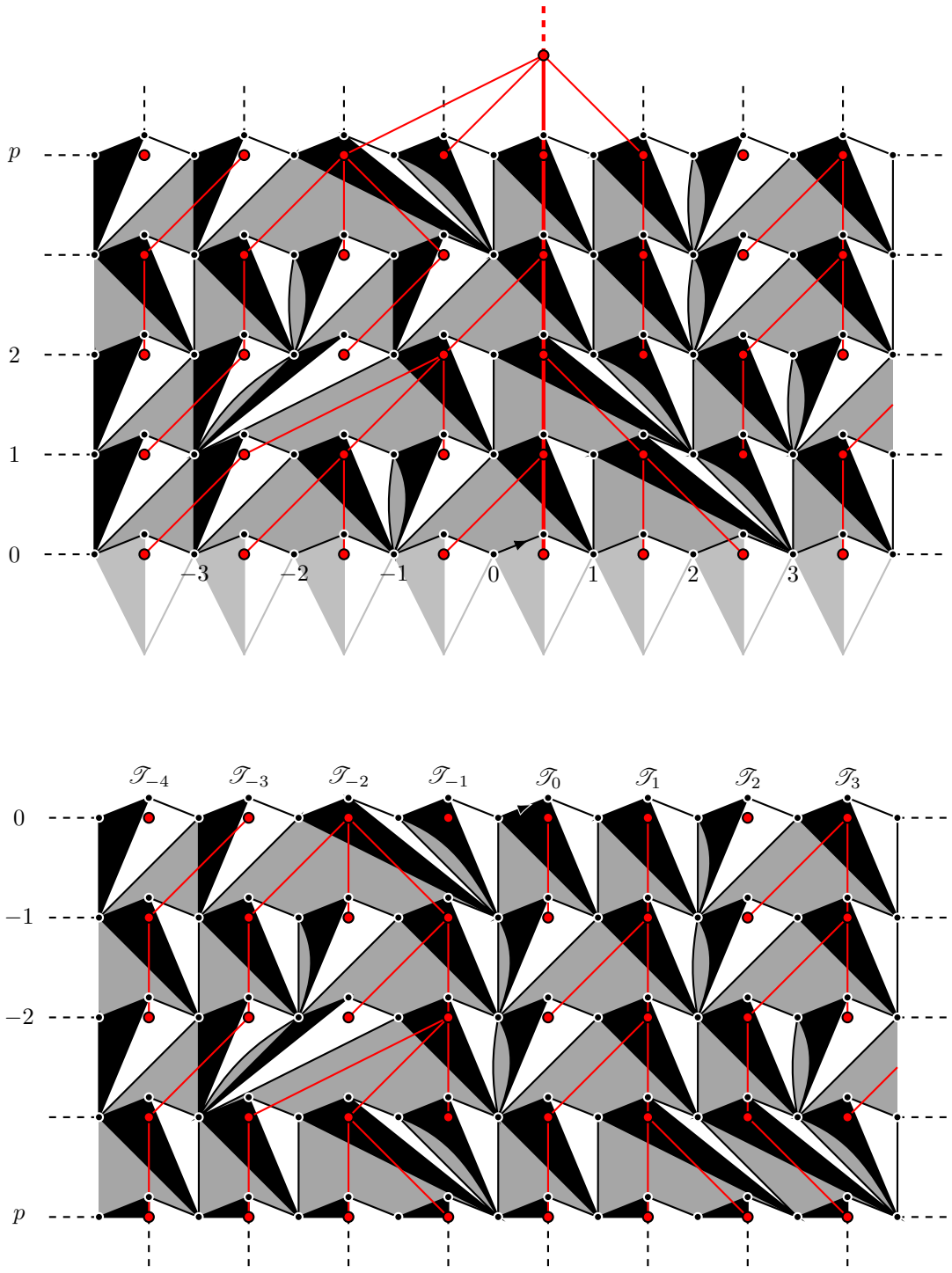

Figure 5.2.2 – A sketch of the UHPET (top) and LHPET (bottom), with their layer decompositions. The different elements of the drawings are explained in detail in Chapters 7 and 8.

Theorem 5.2.2. *Let $\mathcal{T}_n$ be a uniform random rooted Eulerian planar triangulation with n black faces, equipped with its usual graph distance d_n, and the symmetrization of its oriented pseudo-distance, $\overleftrightarrow{d}_n$. The following convergences hold jointly*

$$n^{-1/4} \cdot (V(\mathcal{T}_n), \overleftrightarrow{d}_n) \xrightarrow[n\to\infty]{(d)} (\mathbf{m}_\infty, D^*)$$
$$n^{-1/4} \cdot (V(\mathcal{T}_n), d_n) \xrightarrow[n\to\infty]{(d)} \mathbf{c}_0 \cdot (\mathbf{m}_\infty, D^*),$$

for the Gromov-Hausdorff distance on the space of isometry classes of compact metric spaces.

Note that, contrary to the case of usual triangulations and quadrangulations, our proof does not rely on any known convergence of Eulerian triangulations to the Brownian map: we only use the convergence of the associated labeled trees. Thus, this is the first case of a genuinely "hybrid" method, where we use both a bijection with labeled trees, and the layer decomposition, to prove the convergence of a family of maps to the Brownian map.

A technical ingredient of the proof of Theorem 5.2.2, like for the equivalent result for usual triangulations or quadrangulations, are estimates for the distances along a layer of the lower half-plane model, denoted $\mathcal{L}$ in either case. In the case of usual triangulations and quadrangulations, this was done by studying the (spherical) balls in the upper half-plane model $\mathcal{U}$. In Chapter 7, we use an alternative argument, that uses a block decomposition similar to the one of causal maps. This argument is much shorter than the one using $\mathcal{U}$, and should be more easily adaptable to other models admitting a layer decomposition.

However, studying the balls of $\mathcal{U}$ is of interest in itself, and this is the object of Chapter 8, in which we obtain the estimates on the distances along the layers of $\mathcal{L}$, similarly to what has been done in the case of usual triangulations or quadrangulations.

The layer decomposition, as well as the study of the balls of $\mathcal{U}$, deeply involve results on the asymptotic behavior of the enumeration of Eulerian triangulations with specific boundary conditions. This enumeration work had not been done before, and was the starting point of a joint work with Jérémie Bouttier, which is still in progress. A preliminary version of this work, that details all the results that are necessary to Chapters 7 and 8, is presented in Chapter 9. What is still in progress is to establish similar results for more general boundary conditions.

Note that, due to their bicoloring, Eulerian triangulations have a richness in boundary conditions that does not exist for usual triangulations or quadrangulations, so that even *determining* the relevant boundary conditions is an important part of Chapters 7 and 8.

Moreover, for the moment, there exists no bijection between these families of Eulerian triangulations with boundaries, and classes of decorated trees: in Chapter 9, we use analytic combinatorial techniques, such as Tutte's recursion and the *kernel method*, that sadly do not yield explicit expressions, but do give an explicit rational parametrization of the generating functions in question.

Note that one could want to prove the convergence of planar Eulerian triangulations to the Brownian map using their bijection with bipartite maps, as the convergence for these has already been proven. However, this would necessitate to treat the distances on an Eulerian triangulation as a local modification of the distances on the corresponding bipartite map, and thus use a layer decomposition of bipartite maps. As this has not been achieved yet, this route is a priori not easier than the one undertaken in Chapter 7, which has the advantage of uncovering a lot of properties of Eulerian triangulations. However, achieving a layer decomposition of bipartite maps would be interesting in itself.

It would also be interesting to apply our new "hybrid" technique, to other families of planar maps that are not amenable to the classic bijective approach. One such family is the one of Eulerian *quadrangulations*, which would present an additional level of difficulty on the enumerative side, as the boundary conditions for the putative Boltzmann Eulerian quadrangulations are even more complex and varied than the boundary conditions for their triangulation counterpart. The extension of the results of Chapter 9 to more general boundary conditions, that we are still working on with Jérémie Bouttier, could also serve as a "warm-up" for this new enumerative challenge.

Deuxième partie

Triangulations colorées en dimension quelconque

CHAPITRE 6

Modèles aléatoires uniformes de complexes colorés

Ce chapitre est la reproduction de l'article [Car19] :
A. Carrance, *Uniform Random Colored complexes*,
Random Structures and Algorithms 55.3 (2019), pp 615-648. doi: 10.1002/rsa.20845.

Contents

6.1 Introduction

For $D \geq 1$, we call **$(D+1)$-colored graphs**, $(D+1)$-regular graphs, equipped with a proper $(D+1)$-coloring of their edges. $(D+1)$-colored graphs have been known from the 1970's, and the work of Pezzana [Pez74; Pez75], to be an encoding of piecewise-linear (PL) topological structures, that we will call **complexes** in a sense precised below. Among those structures are PL manifolds, which thus admit a combinatorial and graph-theoretical formulation. This formulation was further developed by Gagliardi and others (see [FGG86]), leading notably to classification results for 3- and 4-dimensional PL (hence smooth) manifolds with a small number of cells [CM15; CC15]. Additionally to these achievements in PL-topology, $(D+1)$-colored graphs have recently garnered interest from theoretical physicists, as they are at the heart of a new approach to quantum gravity, **colored tensor models** (see [GR12; Gur16] for detailed reviews). As the quantized space-time described by colored tensor models is a PL-structure corresponding to a random distribution on $(D+1)$-colored graphs, this is an incentive to study such distributions.

Our work can be related to other random models: first, we can compare it to Euclidean Dynamical Triangulations, that also have the purpose to define a quantum spacetime as the continuum limit of random triangulations in any dimension (see [Tho99] for a detailed review). In this approach, the topology is fixed to be spherical, and the random distribution depends on a parameter that tunes a curvature constraint, while we do not put any constraint on the topology nor the curvature. Note also that we do not work with any triangulations, but with a specific type of complexes that we will define below. Moreover, these models have mostly been studied numerically, while we make a probabilistic and combinatorial investigation of ours.

Likewise, we can relate this paper to works in random maps, as in dimension 2 our models can be seen as particular models of random maps. Furthermore, to look for a tentative continuum spacetime as the scaling limit of the discrete spacetime given by our model, we will consider the obtained complexes as metric spaces, just like the Brownian map is the scaling limit of several families of planar maps seen as metric spaces (see [LG13; Mie13] for instance). While the most studied models of random maps have conditions on the *face* degrees, with for instance random triangulations and quadrangulations, the graphs we consider for $D = 2$ have 3-valent *vertices*, so we are more naturally dealing with objects

dual to the ones typically studied in the random maps literature. Moreover, most works on random maps deal with maps of a fixed genus (most often planar maps), or whose genus is assumed to grow linearly with their size (like in [ACCR13]), whereas we do not fix the topology.

There is no fixed topology either in random simplicial complexes constructed as higher dimensional analogues of Erdös-Rényi graphs, such as [CF16; Kah14]. Such models also share with the present work the fact that they are defined in any dimension. However, they are constructed quite differently, as their realizations are subcomplexes of a standard simplex (see the definitions below), whereas we build a complex by randomly gluing simplexes together.

This gluing construction is very close to the various models of random gluings of polygons (see [PS06; CP16]), and we will indeed use similar techniques throughout this paper. Just like these random gluing models, our models can be seen as generalizations of the **configuration model**, which starts from a set of vertices with prescribed valences to form a random graph, by taking a uniform matching of the half-edges attached to these vertices. Some results on the configuration model will be of crucial use to prove some of our results.

Since the distributions arising the most naturally in colored tensor models are very involved from a mathematical point of view (notably, they are stongly non-uniform), we present here two simpler models on bipartite, vertex-labelled, $(D+1)$-colored graphs of fixed order $2p$. We focus on the limit $p \to \infty$, which is the first step towards the continuum limit for our tentative space-time. Our first model, which we analyze in Section 6.2, is the obvious, uniform one: as we will see, the associated topological structure has a very singular behavior as $p \to \infty$. Our second model, which we call the **quartic model**, is described in Section 6.3. It has more physical foundation, and is richer topologically, but is still ill-fitted for the purpose of quantum gravity. Over the course of the study of this model, we also obtain a Central Limit Theorem for the genus of a uniform map of order p, as $p \to \infty$ (see Section 6.3.3). We then study in Section 6.4 a generalization of the quartic model, that we call the class of **uniform-uncolored models**, which possess a similar asymptotical behavior.

Before going into technical details, let us fix some very general notations. We will say that an event A occurs *asymptotically almost surely* (a.a.s.), if $\mathbb{P}(A) \xrightarrow[p\to\infty]{} 1$. We will note $V(G)$ the vertex set of a graph G, $E(G)$ its edge set, and $k(G)$ its number of connected components (c.c.).

Colored graphs, bubbles and Gurau degree

We now give a few necessary definitions about colored graphs.

Definition 6.1.1 (Colored graphs)**.** Let G be a $(D+1)$-regular graph, and ζ a function $E(G) \to C$, where C is some set with cardinality $D+1$. The couple (G, ζ) is a **$(D+1)$-colored graph**, if, for all $v \in V(G)$, for all $c \in C$, there is one and only one edge e incident to v, such that $\zeta(e) = c$.
If there is no ambiguity, we will simply note G for the colored graph. In that case, if not specified, C will be the set of integers $\{0, 1, \dots, D\}$.

Remark. A very special class of $(D+1)$-colored graphs are those with only two vertices, and all edges joining the two vertices (see Figure 6.1.1). We call those graphs, **melons**.

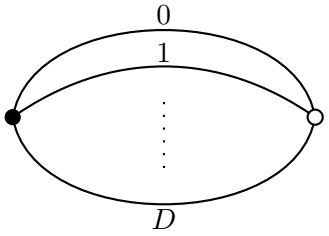

Figure 6.1.1 – Melons are the simplest example of $(D+1)$-colored graphs.

Definition 6.1.2 (Bubbles)**.** Let G be a $(D+1)$-colored graph, and let $\{i_1, \dots, i_k\}$ be a subset of the color set C. Consider the graph $G_{\hat{i}_1,\dots,\hat{i}_k}$ obtained from G by erasing all the i_l-colored edges, for $l = 1, \dots, k$. The connected components of $G_{\hat{i}_1,\dots,\hat{i}_k}$ are called **$(D+1-k)$-bubbles of G** (of colors $\{0,1,\dots,D\}\backslash\{i_1,\dots,i_d\}$). We will write $\mathcal{B}^{\hat{i}_1,\dots,\hat{i}_k}_{(\rho)}$ for a bubble of G of colors $\{0,1,\dots,D\}\backslash\{i_1,\dots,i_d\}$, with ρ indexing the different bubbles of the same color. We will note $b_k(G)$ the number of k-bubbles of G.
The vertices of G are its 0-bubbles, its edges are the 1-bubbles, and its 2-bubbles (which are bicolored cycles) are called its **faces**.

When dealing with bubbles, we will often write $\hat{\imath}_1 \dots \hat{\imath}_d$ for $\{0,1,\dots,D\}\backslash\{i_1,\dots,i_d\}$, to simplify notations.

Definition 6.1.3 (Embedding)**.** Let G be a graph, and S a Riemann surface. An **embedding of G into S** is a continuous and one-to-one function $i\colon G \to S$. We can then consider that G, as a topological space related to a 1-cellular complex, is included in S. The connected components of $S \setminus G$ are called the **regions** of the embedding. If all the regions are homeomorphic to an open disk, the embedding is said to be **2-cellular**.

Definition 6.1.4 (Regular embedding)**.** Let G be a $(D+1)$-colored graph. A 2-cellular embedding of G is said to be **regular** if there exists a $(D+1)$-cycle $\tau \in \mathfrak{S}_{D+1}$, such that any region is bounded by a bicolored cycle, of colors $\{i, \tau(i)\}$, for some $i \in C$. Any cycle τ gives rise to a regular embedding.

Remark. There is a two-to-two correspondence between regular embeddings of G and $(D+1)$-cycles, as a cycle and its reverse are associated to the same two embeddings.

If G is $(D+1)$-colored and bipartite, all its regular embeddings are necessarily into orientable surfaces (see for instance [Gag81]). This makes the following definition possible:

Definition 6.1.5 (Degree)**.** The **Gurau degree** $\omega(G)$ of a $(D+1)$-colored graph G is the sum of the genera of its regular embeddings:

$$\omega(G) = \frac{1}{2}\sum_{\tau} g_\tau$$

where the sum runs over the $(D+1)$-cycles of $\mathfrak{S}_{D+1}$. The factor $1/2$ is a matter of convention, here we follow [GR12].

The Gurau degree of G can also be written in terms of its number of vertices, edges and faces:

Lemma 6.1.6. [GR11] *For a connected bipartite $(D+1)$-colored graph G with $2p$ vertices, one has:*

$$\omega(G) = \frac{(D-1)!}{2}\left(\frac{D(D-1)}{2}p + D - b_2(G)\right).$$

Proof. G has $\frac{D!}{2}$ distinct regular embeddings, and each face of G corresponds to a region in $(D-1)!$ different regular embeddings. □

Trisps

With the bubbles of a $(D+1)$-colored graph G, we can build a D-dimensional triangulated space (trisp), which is a particular type of cellular complex with simplicial cells. For the sake of precision, let us fix some definitions and notations related to simplices that are needed for the definition of a trisp, for which we follow the conventions of [Koz08].

Definition 6.1.7 (Simplices)**.** A **geometrical n-simplex** σ is the convex enveloppe of a set A of $n+1$ affinely independent points in $\mathbb{R}^N$, for some $N \geq n$. The **dimension** of σ is $|A|-1=n$. The convex enveloppes of the subsets of A are called **sub-simplices** of σ, or its **faces**, and the points defining σ are called its **vertices**. We will note $\sigma \subseteq \tau$ to signify that σ is a face of τ. A d-face of σ is a face of dimension d, and the **d-skeleton** of σ is the set of its faces of dimension lower or equal to d.
We note $\langle x_1, \ldots, x_n \rangle$ the simplex with vertices $x_1, \ldots x_n$.
The **standard n-simplex** is $\langle (1,0,\ldots,0),(0,1,0,\ldots,0),\ldots,(0,\ldots,0,1)\rangle$, where the point coordinates are taken in the canonical basis of $\mathbb{R}^{n+1}$.

Let us start from some sets $(S_i)_{i\in\mathbb{N}}$ of geometrical simplices, where S_i contains i-simplices, seen as copies of the standard i-simplex. Then, for $m \leq n$, for each order-preserving injection $f\colon \{1,\ldots,m+1\} \to \{1,\ldots,n+1\}$, take a map $B_f\colon S_n \to S_m$, so that:

(i) if f, g are two such injections and are composable : $\{1,\ldots,l+1\} \xrightarrow{g} \{1,\ldots,m+1\} \xrightarrow{f} \{1,\ldots,n+1\}$, then: $B_{f\circ g} = B_g \circ B_f$

(ii) $B_{id_{\{1,\ldots,n+1\}}} = id_{S_n}$.

This abstract structure implicitly contains a topological space. Indeed, an order-preserving injection $f\colon \{1,\ldots,m+1\} \to \{1,\ldots,n+1\}$ induces a linear map $M_f\colon \mathbb{R}^{m+1} \to \mathbb{R}^{n+1}$, which sends the k-th vector of the canonical basis of $\mathbb{R}^{m+1}$ to the $f(k)$-th vector of the canonical basis of $\mathbb{R}^{n+1}$. This map can be restricted to a homeomorphism from the standard m-simplex to a certain m-sub-simplex of the standard n-simplex. For $\sigma \in S_n$, this homeomorphism therefore glues an m-sub-simplex of σ to the standard m-simplex $B_f(\sigma) \in S_m$. The condition $B_{f\circ g} = B_g \circ B_f$ ensures that these gluings are coherent.

Definition 6.1.8 (Trisp)**.** A complex defined in the above way is called a **triangulated space**, or **trisp**.

Let G be a $(D+1)$-colored graph. We now quickly map out the construction of a trisp $\Delta(G)$ with the bubbles of G. To each $(D+1-k)$-bubble $\mathcal{B}_{(\rho)}^{\hat{i}_1\ldots\hat{i}_k}$, we associate a $(k-1)$-simplex whose vertices are indexed by the missing colors $i_1,\ldots,i_k$. This yields some set S_k, with an order on the vertices of each simplex. The gluing maps are defined in the following way: if $f\colon \{1,\ldots,m+1\} \to \{1,\ldots,n+1\}$ is an order-preserving injection, and if $\sigma \in S_n$ corresponds to the bubble $\mathcal{B}_{(\rho)}^{\hat{i}_1\ldots\hat{i}_{n+1}}$, B_f sends it to the m-simplex corresponding to the $(D-m)$-bubble obtained from $\mathcal{B}_{(\rho)}^{\hat{i}_1\ldots\hat{i}_{n+1}}$ by adding the colors in $\{i_1,\ldots,i_{n+1}\} \setminus \{i_{f(1)},\ldots,i_{f(m+1)}\}$. By construction, the maps B_f satisfy conditions (i) and (ii) of Definition 6.1.8.

The trisp $\Delta(G)$ induced by a $(D+1)$-colored graph G has severable notable properties:

Theorem 6.1.9. [Gur10]
If G is connected, the induced trisp $\Delta(G)$ is a simplicial pseudo-manifold of dimension D, i.e.*:*

(i) $S_i = \varnothing$ *for* $i > D$, *and* $S_D \neq \varnothing$

(ii) $\Delta(G)$ *is* ***pure***, i.e. *any simplex is the face of a* D*-simplex*

(iii) it is ***strongly connected***, i.e. *any two* D*-simplices can be joined by a chain of* D*-simplices in which each pair of neighboring* D*-simplices has a common* $(D-1)$*-simplex*

(iv) it is ***non-branching***, i.e. *any* $(D-1)$*-simplex is a face of at most two* D*-simplices.*

Moreover, $\Delta(G)$ *is a simplicial pseudo-manifold* ***without boundary***, i.e. *each of its* $(D-1)$*-simplices is actually a face of exactly two* D*-simplices.*

Remarks.

- As the $(D+1-k)$-bubbles of G correspond to the $(k-1)$-simplices of $\Delta(G)$, we sometimes say that $\Delta(G)$ is the **dual complex** of G.
- If we cut open some edges of a bipartite $(D+1)$-colored graph G, the previous construction will yield a pseudomanifold with a boundary consisting of the $(D-1)$-simplices corresponding to the open half-edges.
- As said before, the physical motivations of our work lead us to consider the complex $\Delta(G)$ as a metric space, with the structure given by its graph distance: the elements of this metric space are the vertices of $\Delta(G)$, *i.e.* its 0-simplexes, and the distance between two points is the number of edges of the smallest path from one to the other in the 1-skeleton of $\Delta(G)$. The two first criteria to get a scaling limit will therefore be:
  (i) that the number of points of $\Delta(G)$ goes to infinity as $p \to \infty$
  (ii) that the typical distance between two points of $\Delta(G)$ goes to infinity as $p \to \infty$.

Permutations

Let us now note that the set of bipartite $(D+1)$-colored graphs with $2p$ labelled vertices (the positive and negative vertices being labelled independently from 1 to p each), is in bijection with the $(D+1)$-tuples of permutations $(\alpha_0, \ldots, \alpha_D) \in (\mathfrak{S}_p)^{D+1}$.

Indeed, given such a labelled graph, for each $i \in C$, define a permutation α_i by: $\alpha_i(k) = l$ if there is an i-colored edge linking the k-th negative vertex and the l-th positive one. Reciprocally, given such a tuple $(\alpha_0, \ldots, \alpha_D)$, we can consider p numbered negative vertices and p numbered positive ones, and link them according to the permutations.

In the sequel, we will use the permutation formulation to define random bipartite vertex-labelled $(D+1)$-colored graphs.

Remark. The labellings of the vertices, combined with the coloring of the edges, yield a labelling of the half-edges, and with this formulation we count the possible pairings of the half-edges, *i.e.* Wick contractions, in the language of quantum field theory.

6.2 Uniform model

We consider a $(D+1)$-tuple of random permutations $(\alpha_0, \ldots, \alpha_D)$, all independent and uniform on $\mathfrak{S}_p$, for $D \geq 1$. These permutations induce a $(D+1)$-colored, bipartite random graph U_p^D, with $2p$ labelled vertices. It is clear that U_p^D follows the uniform measure on this set of graphs.

Remark. We can note that this model is a "colored version" of the well-known configuration model [Wor99], that will appear more explicitly in Sections 6.3 and 6.4.

6.2.1 Connectedness

We show, similarly to Pippenger and Schleich [PS06], that a.a.s. U_p^D is connected, and more precisely:

Theorem 6.2.1. *Let U_p^D be the random graph defined above, with $D \geq 2$. Then*

$$\mathbb{P}\big(U_p^D \text{ connected}\big) = 1 - \frac{1}{p^{D-1}} + O\Big(\frac{1}{p^{2(D-1)}}\Big).$$

Proof. We first prove an upper bound on $\mathbb{P}\big(U_p^D \text{ not connected}\big)$. For U_p^D to be not connected (n.c.), it must be decomposable into at least two closed subgraph, and, considering the smallest of these subgraphs, it must have a closed subgraph with at most $2\lfloor p/2 \rfloor$ vertices. Thus

$$\begin{aligned}\mathbb{P}\big(U_p^D \text{ n.c.}\big) &\leq \sum_{1\leq k\leq \lfloor \frac{p}{2}\rfloor} \mathbb{P}(\exists \text{ closed subgraph with } 2k \text{ vertices}) \\ &\leq \sum_{1\leq k\leq \lfloor \frac{p}{2}\rfloor} F_k \text{ , where } F_k = \binom{p}{k}^{1-D}.\end{aligned}$$

Since

$$\frac{F_{k+1}}{F_k} = \frac{k+1}{p-k} \leq 1 \quad \forall k = 1, \dots, \Big\lfloor \frac{p}{2} \Big\rfloor - 1,$$

we get

$$\mathbb{P}\big(U_p^D \text{ n.c.}\big) \leq F_1 + F_2 + \Big(\frac{p}{2} - 2\Big) F_3 = \frac{1}{p^{D-1}} + \left(\frac{2}{p(p-1)}\right)^{D-1} + O\big(p^{-3D+4}\big),$$

and in particular

$$\mathbb{P}\big(U_p^D \text{ connected}\big) \xrightarrow[p\to\infty]{} 1.$$

Now, to get a lower bound on $\mathbb{P}\big(U_p^D \text{ n.c.}\big)$, consider the probability of having exactly one closed melon:

$$\begin{aligned}\mathbb{P}\big(U_p^D \text{ n.c.}\big) &\geq \mathbb{P}(\exists! \text{ closed melon}) \\ &= \mathbb{P}(\exists \text{ at least 1 closed melon}) - \mathbb{P}(\exists \text{ at least 2 closed melons}) \\ &\geq \frac{1}{p^{D-1}} - \frac{1}{2}\frac{1}{(p(p-1))^{D-1}}.\end{aligned}$$

Thus $\mathbb{P}\big(U_p^D \text{ connected}\big) = 1 - \frac{1}{p^{D-1}} + O\Big(\frac{1}{p^{2(D-1)}}\Big)$. □

Knowing that U_p^D is connected a.a.s., the next step is to investigate its average number of connected components. We have the following result:

Theorem 6.2.2. *For $D \geq 2$, one has:*

$$\mathbb{E}\big[k(U_p^D)\big] = 1 + O\Big(\frac{1}{p^{D-1}}\Big).$$

Proof. We derive upper bounds on $\mathbb{P}\big(k(U_p^D)=k\big)$, for $k \geq 2$. We already know that $\mathbb{P}\big(k(U_p^D)=2\big) \leq \frac{1}{p^{D-1}} + O\Big(\frac{1}{p^{2(D-1)}}\Big)$ from Theorem 6.2.1. We then get an upper bound for $k=3$, decomposing the event that U_p^D has 3 closed subgraphs:

$$\begin{aligned}
\mathbb{P}\big(k(U_p^D)=3\big) &\leq \mathbb{P}\big(k(U_p^D)\geq 3\big) = \mathbb{P}\big(U_p^D \text{ has 3 closed proper subgraphs}\big) \\
&\leq \sum_{1\leq k\leq \lfloor p/2\rfloor} \mathbb{P}\big(U_p^D \text{ has a closed subgraph } U' \text{ with } 2k \text{ vertices}\big) \\
&\quad \cdot \big(\mathbb{P}\big(U' \text{ n.c.}\big) + \mathbb{P}\big((U')^c \text{ n.c.}\big)\big) \\
&\leq \sum_{1\leq k\leq \lfloor p/2\rfloor} \left(\frac{k!(p-k)!}{p!}\right)^{D-1} \\
&\quad \cdot \left(\sum_{1\leq l\leq \lfloor k/2\rfloor} \left(\frac{l!(k-l)!}{k!}\right)^{D-1} + \sum_{1\leq l\leq \lfloor (p-k)/2\rfloor} \left(\frac{l!(p-k-l)!}{p-k!}\right)^{D-1}\right) \\
&\leq \frac{2}{p^{2(D-1)}} + O\Big(\frac{1}{p^{3(D-1)}}\Big).
\end{aligned}$$

And, similarly, for $k \geq 4$:

$$\begin{aligned}
\mathbb{P}\big(k(U_p^D)\geq 4\big) &\leq \sum_{1\leq k\leq \lfloor p/2\rfloor} \mathbb{P}\big(U_p^D \text{ has a closed subgraph } U' \text{ with } 2k \text{ vertices}\big) \\
&\quad \cdot \big[\mathbb{P}\big(U' \text{ has } \geq 3 \text{ c.c.}\big) + \mathbb{P}\big((U')^c \text{ has } \geq 3 \text{ c.c.}\big) + \mathbb{P}\big(U' \text{ n.c. and } (U')^c \text{ n.c.}\big)\big] \\
&\leq O\Big(\frac{1}{p^{3(D-1)}}\Big).
\end{aligned}$$

Thus

$$\begin{aligned}
\mathbb{E}\big[k(U_p^D)\big] &\leq 1 - \frac{1}{p^{D-1}} + \frac{2}{p^{D-1}} + O\Big(\frac{1}{p^{2(D-1)}}\Big) + \left(\frac{p(p+1)}{2} - 6\right) O\Big(\frac{1}{p^{3(D-1)}}\Big) \\
&\leq 1 + O\Big(\frac{1}{p^{D-1}}\Big) \quad \text{for } D \geq 2.
\end{aligned}$$

□

Remark. For $D=1$, we have two uniform permutations α_0 and α_1. The number of connected components of U_p^1 is the number of cycles of $\alpha_0\alpha_1^{-1}$, which is uniform too. Thus, one has: $\mathbb{P}\big(U_p^1 \text{ connected}\big) = \frac{1}{p}$, and, from well-known results on uniform permutations [ABT03]: $\mathbb{E}\big[k(U_p^1)\big] = \ln p + O(1)$.

For a given color $i \in [\![0, D]\!]$, the graph $(U_p^D)_{\hat{\imath}}$, see definition 6.1.2, has the same law as U_p^{D-1} (up to a color renaming). This means that Theorem 6.2.2 can also be used for the number $b_D(U_p^D)$ of D-bubbles of U_p^{D+1}, simply by summing over all colors. This is of particular interest, as these D-bubbles correspond to the vertices of the complex dual to our colored graph. It is straightforward to derive the following result:

Corollary 6.2.3. *For $D \geq 3$, one has:*

$$\mathbb{E}\big[b_D(U_p^D)\big] = D + 1 + O\Big(\frac{1}{p^{D-2}}\Big).$$

Remark. This means that for $D \geq 3$, there is typically only one point of each color in the dual complex. This thwarts the hope of defining a continuous D-dimensional random space from this simple model by going through the same steps that yield the Brownian Sphere from uniform planar maps. Note that, as stated in the introduction, this uniform model differs from that of uniform planar maps, in that it does not fix the topology.

However, the essential difference might lie in the dimension: indeed, in Euclidean Dynamical Triangulations, Monte Carlo simulations show evidence of a so-called **crumpled phase** in dimension 3 and 4 even for spherical models, as long as the sampling of the triangulation does not depend too strongly on its curvature (see [Tho99]), while for dimension 2 such a phase occurs only when there is no constraint on the topology.

6.2.2 Degree

We now investigate the Gurau degree of U_p^D, for $D \geq 2$. According to Lemma 6.1.6, this is equivalent to studying the number of faces of U_p^D, *i.e.* the number of its bicolored cycles. This quantity can be expressed in terms of the permutations $(\alpha_0, \dots, \alpha_D)$:

$$b_2(U_p^D) = \sum_{0 \leq i < j \leq D} \mathcal{O}\left(\alpha_i \alpha_j^{-1}\right),$$

where $\mathcal{O}(\alpha)$ is the number of orbits (cycles) of α. The use of well-known results about uniform permutations gives us the following estimations for the average and variance of the number of faces:

Proposition 6.2.4.

$$\mathbb{E}\big[b_2(U_p^D)\big] = \frac{D(D+1)}{2}(\ln p + \gamma) + o(1) \tag{6.2.1}$$

$$\mathrm{Var}\big(b_2(U_p^D)\big) = \frac{D(D+1)}{2} \ln p + o(\ln p). \tag{6.2.2}$$

In terms of the Gurau degree, this means that:

$$\mathbb{E}\big[\omega(U_p^D)\big] = \frac{(D-1)!}{2}\Big(\frac{D(D-1)}{2}p + D - \frac{D(D+1)}{2}(\ln p + \gamma)\Big) + o(1)$$

$$\mathrm{Var}\big(\omega(U_p^D)\big) = \frac{(D-1)!}{2}\frac{D(D+1)}{2} \ln p + o(\ln p).$$

Proof. If α is a uniform permutation of size p, then one has (see for instance [ABT03]):

$$\mathbb{E}[\mathcal{O}(\alpha)] = \sum_{j=1}^{p} \frac{1}{j} = \ln p + \gamma + o(1), \text{ where } \gamma \text{ is the Euler constant}$$

$$\mathrm{Var}(\mathcal{O}(\alpha)) = \sum_{j=1}^{p} \frac{j-1}{j^2} = \ln p + \gamma - \frac{\pi^2}{6} + o(1).$$

Equation (6.2.1) is obtained immediately from this. Equation (6.2.2) is obtained after simple calculations, once one notices that two permutations $\alpha_i \alpha_j^{-1}$ and $\alpha_k \alpha_l^{-1}$ are independent, as long as either $i \neq k$, or $j \neq l$. □

To get more precise information, we will now focus on the number of faces of a single regular embedding of U_p^D, instead of the total number of faces. We state our main result concerning this in Theorem 6.2.5 : the number of faces of any regular embedding $\mathcal{J}_p$ of

U_p^D has a normal limit when $p \to \infty$.

We can assume, without loss of generality, that $\mathcal{J}_p$ corresponds to the usual cyclic ordering of the colors $(0\,1\,\cdots\,D)$. Thus, we are interested in the law of:

$$F = \sum_{0\leq i\leq D} \mathcal{O}\left(\alpha_i \alpha_{i+1}^{-1}\right) =: \sum_{0\leq i\leq D} \mathcal{O}_{i,i+1}$$

where, by convention, $\alpha_{D+1} = \alpha_0$.
To prove its normal asymptotical behaviour, we consider the distribution of the last permutation, $\alpha_D \alpha_0^{-1} =: \alpha_{D,0}$, conditionally to a given realization $\{\mathcal{C}_{i,i+1}\}$ of the respective conjugacy classes $\pi(\alpha_{i,i+1})$ of the D first permutations $\alpha_i \alpha_{i+1}^{-1} =: \alpha_{i,i+1}$. We note this distribution $P_D^{\{\mathcal{C}_{i,i+1}\}}$.
As $\alpha_{D,0} = \left(\prod_{0\leq i\leq D-1} \alpha_{i,i+1}\right)^{-1}$, for some given $\{\mathcal{C}_{i,i+1}\}$, the parity of $\alpha_{D,0}$ is fixed. We will note $H := \mathcal{A}_p$ or $\mathcal{A}_p^c$, according to this parity condition (where $\mathcal{A}_p$ is the alternating group of degree p), and $\mathcal{U}_H$ the uniform distribution on H. Let us assume that, for $i = 0, \ldots, D-1$, $\mathcal{C}_{i,i+1}$ has less than $\ln p$ fixed points and 2-cycles. We note this hypothesis $(*)$. As stated in Proposition 6.2.7, under this assumption, $P_D^{\{\mathcal{C}_{i,i+1}\}}$ converges to $\mathcal{U}_H$ in total variation distance. We prove this using group representation techniques, similarly to Chmutov and Pittel in [CP16].
Well-known results on the number of cycles of fixed length in a uniform permutation then allow us to deduce Theorem 6.2.6, *i.e.* that, up to a parity condition, the law P_F of F converges to a convolution product of the laws $P_{i,i+1}$ of the $\mathcal{O}_{i,i+1}$. Finally, we prove the asymptotic normality of P_F, using a well-known expression of the number of cycles of a uniform permutation as a sum of Bernoulli variables.

Let us now state these results more precisely:

Theorem 6.2.5. *Let $\mathcal{J}_p$ be a regular embedding of U_p^D, and $F_{\mathcal{J}_p}$ be the number of faces (*i.e.* regions) of $\mathcal{J}_p$. Then the quantity $\frac{F_{\mathcal{J}_p} - \mathbb{E}\left[F_{\mathcal{J}_p}\right]}{\sqrt{\mathrm{Var}\left(F_{\mathcal{J}_p}\right)}}$ converges weakly to the standard normal distribution.*

Theorem 6.2.6. *With the notations given above, one has:*

$$\left\| P_F - 2 \cdot \mathbb{1}_{\{(D+1)p - F \text{ even}\}} P_{0,1} * P_{1,2} * \cdots * P_{D,0} \right\| = O\left(\frac{(\ln p)^D}{p^{D-1}}\right)$$

where $\|\cdot\|$ is the total variation distance.

Proposition 6.2.7. *Let us assume $(*)$. Then:*

$$\left\| P_D^{\{\mathcal{C}_{i,i+1}\}} - \mathcal{U}_H \right\| = O\left(\frac{(\ln p)^D}{p^{D-1}}\right).$$

Before starting the proof of Proposition 6.2.7, it should be noted that, while its steps closely follow those of the proof of Theorem 2.2 in [CP16], it employs a few stronger arguments, as we are here dealing with conjugacy classes with a logarithmic number of small cycles, whereas the permutations in [CP16] have no small cycles. We will detail those differences after the proof.

Proof. As proved in [CP16], we get from the Cauchy-Schwartz inequality and the Plancherel theorem:

$$\|P_D^{\{\mathcal{C}_{i,i+1}\}} - \mathcal{U}_H\|^2 \leq \frac{1}{4} \sum_{\lambda \vdash p,\, \lambda \neq <p>, <1^p>} f^\lambda \mathrm{tr}\left[\hat{P}_D^{\{\mathcal{C}_{i,i+1}\}}(\rho^\lambda)\hat{P}_D^{\{\mathcal{C}_{i,i+1}\}}(\rho^\lambda)^*\right]$$

where the sum is over the partitions $\lambda = (\lambda_1 \geq \lambda_2 \geq \dots)$ of p, ρ^λ is the irreducible representation of $\mathfrak{S}_p$ associated to λ, f^λ is the dimension of this representation, and, for a probability measure P on $\mathfrak{S}_p$, $\hat{P}$ is the Fourier transform of P:

$$\hat{P}(\rho) = \sum_{\sigma \in \mathfrak{S}_p} \rho(\sigma) P(\sigma)$$

for a representation ρ.

As the permutations $\alpha_{i,i+1}$, $i = 0, \dots, D-1$, are all independent, the law of $\alpha_{D,0}$ writes as a convolution product (even conditionally to the realization of $\{\mathcal{C}_{i,i+1}\}_{0 \leq i \leq D-1}$):

$$P_D^{\{\mathcal{C}_{i,i+1}\}} = P_{\alpha_{D,D-1}} * P_{\alpha_{D-1,D-2}} * \dots * P_{\alpha_{1,0}} = \mathcal{U}_{\mathcal{C}_{D-1,D}} * \mathcal{U}_{\mathcal{C}_{D-2,D-1}} * \dots * \mathcal{U}_{\mathcal{C}_{0,D1}}.$$

Indeed, for $i = 0, \dots, D-1$, $\alpha_{i,i+1}$ is uniform on $\mathcal{C}_{i,i+1}$, and so is its inverse $\alpha_{i+1,i}$. So, by applying the Fourier transform:

$$\hat{P}_D^{\{\mathcal{C}_{i,i+1}\}} = \hat{\mathcal{U}}_{\mathcal{C}_{D-1,D}} \cdot \hat{\mathcal{U}}_{\mathcal{C}_{D-2,D-1}} \cdot \dots \cdot \hat{\mathcal{U}}_{\mathcal{C}_{0,1}}.$$

Furthermore, as the $\mathcal{U}_{\mathcal{C}_{i,i+1}}$ are invariant under conjugacy, they are necessarily homothecies, by Schur's Lemma. We can therefore write:

$$\hat{\mathcal{U}}_{\mathcal{C}_{i,i+1}}(\rho^\lambda) = \frac{\chi^\lambda(\mathcal{C}_{i,i+1})}{f^\lambda} I_{f^\lambda}$$

where χ^λ is the character of ρ^λ. We derive from this:

$$\|P_D^{\{\mathcal{C}_{i,i+1}\}} - \mathcal{U}_H\|^2 \leq \frac{1}{4} \sum_{\lambda \vdash p,\, \lambda \neq <p>, <1^p>} \left(\frac{\prod_{0 \leq i \leq D-1} \chi^\lambda(\mathcal{C}_{i,i+1})}{(f^\lambda)^{D-1}}\right)^2.$$

We now decompose this sum into two parts:

$$\begin{aligned}
&\|P_D^{\{\mathcal{C}_{i,i+1}\}} - \mathcal{U}_H\|^2 \\
&\leq \frac{1}{4} \underbrace{\sum_{\substack{\lambda \neq <p>, <1^p> \\ \lambda_1, \lambda_1' \leq p-4}} \left(\frac{\prod_{0 \leq i \leq D-1} \chi^\lambda(\mathcal{C}_{i,i+1})}{(f^\lambda)^{D-1}}\right)^2}_{\Sigma_1} + \underbrace{\sum_{\substack{\lambda \neq <p>, <1^p> \\ \lambda_1 \geq p-3 \text{ or } \lambda_1' \geq p-3}} \left(\frac{\prod_{0 \leq i \leq D-1} \chi^\lambda(\mathcal{C}_{i,i+1})}{(f^\lambda)^{D-1}}\right)^2}_{\Sigma_2}
\end{aligned}$$

where λ' is the dual partition of λ. We will bound Σ_1 and Σ_2 with different inequalities from Gamburd [Gam06] and Larsen-Shalev [LS08]. We start with Σ_1. Since we have assumed that $\mathcal{C}_{i,i+1}$ has at most $p^{o(1)}$ cycles of size 1 or 2, from [LS08]:

$$|\chi^\lambda(\mathcal{C}_{i,i+1})| \leq \left(f^\lambda\right)^{\frac{1}{3}+o(1)} \text{ when } p \to \infty. \tag{6.2.3}$$

Therefore:

$$\forall \lambda \vdash p \quad \left(\frac{\prod_{0 \leq i \leq D-1} \chi^\lambda(\mathcal{C}_{i,i+1})}{(f^\lambda)^{D-1}}\right)^2 \leq \left(f^\lambda\right)^{-4D/3+2+o(1)} \text{ when } p \to \infty.$$

And, from [Gam06]:

$$\forall t > 0 \quad \sum_{\substack{\lambda \vdash p \\ \lambda_1, \lambda'_1 \leq p-m}} \left(f^\lambda\right)^{-t} = O\big(p^{-mt}\big).$$

Thus $\Sigma_1 = O\big(p^{-4D+6}\big)$.

For Σ_2, we use another inequality from [Gam06]:

$$f^\lambda \geq \binom{p-a}{a} \text{ if } \lambda_1 = p - a > \frac{p}{2}$$

which also gives a bound on f^λ when $\lambda'_1 \geq p-3$, since $f^\lambda = f^{\lambda'}$. Now, similarly to [CP16], we show that if $\lambda_1 = p - a$, with $a = 1$, 2 or 3:

$$|\chi^\lambda(\mathcal{C}_i)| = O((\ln p)^a).$$

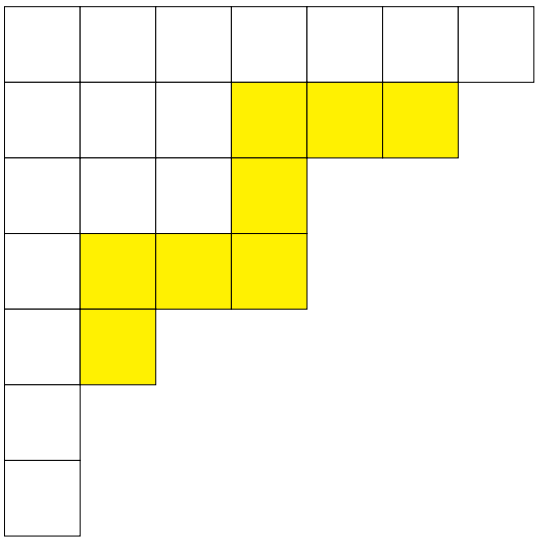

Figure 6.2.1 – Example of a rim hook.

Indeed, consider λ with $\lambda_1 \geq p-3$. Let $\zeta = (\zeta_1, \zeta_2, \dots)$ be an ordered sequence of the cycle lengths in $\mathcal{C}_{i,i+1}$ (with multiplicity). The Murnaghan-Nakayama rule implies:

$$|\chi^\lambda(\mathcal{C}_i)| \leq g^\lambda(\zeta) \tag{6.2.4}$$

where $g^\lambda(\zeta)$ is the number of ways of emptying the Young diagram $Y(\lambda)$ associated to λ by deleting rim hooks of successive sizes $(\zeta_1, \zeta_2, \dots)$. Here, by rim hooks of Y we mean the contiguous border strips R of Y that can be removed from Y leaving a proper subdiagram $Y \backslash R$ (see Figure 6.2.1).

As $\lambda_1 = p - a \geq p-3$, $Y(\lambda)$ is made of a first line of $p-a$ cells, and a small inferior subdiagram Z, with a cells. An ordered sequence of hook deletions emptying $Y(\lambda)$ according to ζ can be decomposed into two parts (see Figure 6.2.2):
- first, a sub-sequence of deletions that do no touch the a first cells of the first line;
- then, a sub-sequence of deletions starting with one that touches the cell $(1, a)$.

The first sub-sequence is composed of horizontal deletions in the first line, and possibly some deletions in Z too. Since at each step, the size of the deleted hook is fixed, the only freedom in this sub-sequence stems from the position of the deletions in Z. As $\mathcal{C}_{i,i+1}$ satisfies $(*)$, if $a = 1$ there are at most $O(\ln p)$ possible choices for the step at which the

only possible deletion in Z occurs, if $a = 2$ there are at most $O\big((\ln p)^2\big)$ possible choices (in the case where the two cells in Z are deleted one by one), and likewise for $a = 3$.

The second sub-sequence is composed of deletions in a sub-diagram containing at most a^2 cells, so the number of possibilities for this sub-sequence is a $O(1)$. Therefore $|\chi^\lambda(\mathcal{C}_i)| \leq g^\lambda(\zeta) = O((\ln p)^a)$.

We get the same result when $\lambda'_1 \geq p-3$, by considering the first column of $Y(\lambda)$. Hence

$$\Sigma_2 = O\Big(\frac{(\ln p)^{2D}}{p^{2D-2}}\Big),$$

which finally gives us $\|P^{(\mathcal{C}_1,\mathcal{C}_2)}_{\alpha_1\alpha_2^{-1}} - \mathcal{U}_H\| = O\Big(\frac{(\ln p)^D}{p^{D-1}}\Big)$. □

As mentioned above, some steps of this proof use stronger arguments than in [CP16]. Indeed, to estimate Σ_1, we are in the strongest case of application of the bound (6.2.3), when there is a number $p^{o(1)}$ of cycles under a given size, while the permutations in [CP16] have no cycles under a given size. Moreover, when we bound Σ_2 with a number of sequences of rim-hook deletions, we have to take into account the contribution to this number of rim-hooks of length 1 or 2, which do not appear in [CP16], for the same reason.

We can now prove Theorem 6.2.6.

Proof of Theorem 6.2.6. For $0 \leq l \leq (D+1)p$, we want to estimate the probability

$$\mathbb{P}(F = l) = \sum_{c_{0,1}+c_{1,2}+\cdots+c_{D,0}=l} \mathbb{P}(\mathcal{O}_{0,1} = c_{0,1}, \mathcal{O}_{1,2} = c_{1,2}, \dots, \mathcal{O}_{D,0} = c_{D,0}).$$

We decompose the event of having some given $\{c_{i,i+1}, 0 \leq i \leq D\}$ depending on the conjugacy classes $\pi(\alpha_{i,i+1})$ of the $\alpha_{i,i+1}$, for $0 \leq i \leq D-1$:

$$\mathbb{P}(F = l) = \sum_{c_{0,1}+c_{1,2}+\cdots+c_{D,0}=l} \sum_{\substack{\mathcal{C}_{i,i+1} \\ \mathcal{O}(\mathcal{C}_{i,i+1})=c_{i,i+1} \\ \text{for } i=0,\dots,D-1}} \mathbb{P}\big(\mathcal{O}_{D,0} = c_{D,0} \big| \{\mathcal{C}_{i,i+1}\}\big) \prod_{0\leq i\leq D-1} \mathbb{P}(\pi(\alpha_{i,i+1}) = \mathcal{C}_{i,i+1}).$$

Now, we separate the conjugacy classes into those that satisfy $(*)$ and those that do not:

$$\begin{aligned}\mathbb{P}(F = l) = &\sum_{c_{0,1}+c_{1,2}+\cdots+c_{D,0}=l} \sum_{\substack{\mathcal{O}(\mathcal{C}_{i,i+1})=c_{i,i+1} \\ \mathcal{C}_{i,i+1} \text{ satisfies } (*)\ \forall i}} \mathbb{P}\big(\mathcal{O}_{D,0} = c_{D,0} \big| \{\mathcal{C}_{i,i+1}\}\big) \prod_{0\leq i\leq D-1} \mathbb{P}(\pi(\alpha_{i,i+1}) = \mathcal{C}_{i,i+1}) \\ &+ \sum_{c_{0,1}+c_{1,2}+\cdots+c_{D,0}=l} \sum_{\substack{\mathcal{O}(\mathcal{C}_{i,i+1})=c_{i,i+1} \\ \exists i\ \mathcal{C}_{i,i+1} \text{ violating } (*)}} \mathbb{P}\big(\mathcal{O}_{D,0} = c_{D,0} \big| \{\mathcal{C}_{i,i+1}\}\big) \prod_{0\leq i\leq D-1} \mathbb{P}(\pi(\alpha_{i,i+1}) = \mathcal{C}_{i,i+1}) \\ &=: P_1 + P_2.\end{aligned}$$

From Proposition 6.2.7, if all the $\mathcal{C}_{i,i+1}$ satisfy $(*)$, then:

$$\begin{aligned}&\mathbb{P}\Big(\mathcal{O}\left(\alpha_{D,0}\right) = c_{D,0} \,\Big|\, \mathcal{C}(\alpha_{i,i+1}) = \mathcal{C}_{i,i+1}, 0 \leq i \leq D-1\Big) \\ &= \mathbb{P}\Big(\mathcal{O}\left(\alpha_{D,0}\right) = c_{D,0} \,\Big|\, \varepsilon(p - c_{D,0}) = \varepsilon(\mathcal{C}_{0,1}) \cdots \varepsilon(\mathcal{C}_{D-1,D})\Big) + O\Big(\frac{(\ln p)^D}{p^{D-1}}\Big) \\ &= 2 \cdot \mathbb{1}_{\{\varepsilon(p-c_{D,0}) = \varepsilon(\mathcal{C}_{0,1})\cdots\varepsilon(\mathcal{C}_{D-1,D})\}} \cdot \mathbb{P}(\mathcal{O}\left(\alpha_{D,0}\right) = c_{D,0}) + O\Big(\frac{(\ln p)^D}{p^{D-1}}\Big)\end{aligned}$$

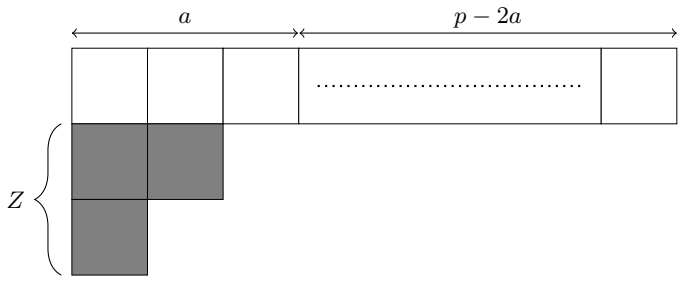

(a)

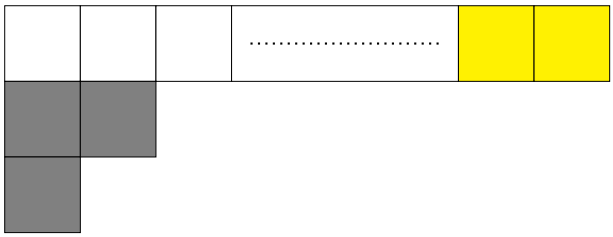

(b)

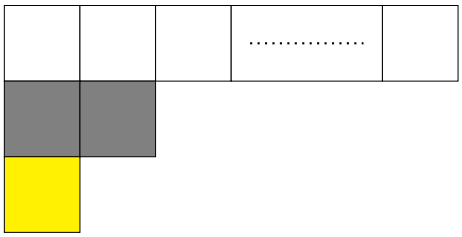

(c)

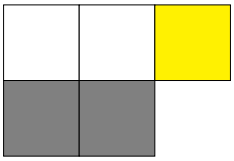

(d)

Figure 6.2.2 – The Young diagram $Y(\lambda)$ associated to λ (a), the 2 possible types of deletions of the first subsequence (b) and (c), and the first deletion of the second subsequence (d).

where $\varepsilon(n)$ is the parity of n. Thus, for P_1, we know that the only dependency left in $c_{D,0}$ is a parity condition:

$$\sum_{c_{0,1}+c_{1,2}+\cdots+c_{D,0}=l} \sum_{\substack{\mathcal{O}(\mathcal{C}_{i,i+1})=c_{i,i+1} \\ \mathcal{C}_{i,i+1} \text{ satisfies } (*)\,\forall i}} \mathbb{P}\big(\mathcal{O}_{D,0}=c_{D,0}\big|\{\mathcal{C}_{i,i+1}\}\big) \prod_{0\le i\le D-1} \mathbb{P}(\pi(\alpha_{i,i+1})=\mathcal{C}_{i,i+1})$$

$$= \sum_{c_{0,1}+c_{1,2}+\cdots+c_{D,0}=l} 2\cdot \mathbb{1}_{\{p-c_{D,0}\equiv Dp-\sum c_{i,i+1}\,[2]\}}$$

$$\cdot \sum_{\substack{\mathcal{O}(\mathcal{C}_{i,i+1})=c_{i,i+1} \\ \mathcal{C}_{i,i+1} \text{ satisfies } (*)\,\forall i}} \left(\mathbb{P}(\mathcal{O}_{D,0}=c_{D,0})+O\!\left(\frac{(\ln p)^D}{p^{D-1}}\right)\right) \prod_{0\le i\le D-1} \mathbb{P}(\pi(\alpha_{i,i+1})=\mathcal{C}_{i,i+1})$$

$$= \sum_{c_{0,1}+c_{1,2}+\cdots+c_{D,0}=l} 2\cdot \mathbb{1}_{\{p-c_{D,0}\equiv Dp-\sum c_{i,i+1}\,[2]\}}$$

$$\cdot \left(\sum_{\substack{\mathcal{O}(\mathcal{C}_{i,i+1})=c_{i,i+1} \\ \mathcal{C}_{i,i+1} \text{ satisfies } (*)\,\forall i}} \mathbb{P}(\mathcal{O}_{D,0}=c_{D,0}) \prod_{0\le i\le D-1} \mathbb{P}(\pi(\alpha_{i,i+1})=\mathcal{C}_{i,i+1}) \right)$$

$$+ O\!\left(\frac{(\ln p)^D}{p^{D-1}}\right).$$

To control P_2, we use the fact that for a fixed l, the number of cycles of length l in a uniform permutation $\alpha \in \mathfrak{S}_p$ asymptotically follows a Poisson law of parameter $1/l$ (see [ABT03]).
This implies that: $\mathbb{P}(\alpha \text{ has more than } \ln p \text{ cycles of size 1 and 2}) = O(1/(\ln p)!)$. Therefore:

$$\begin{aligned} P_2 &= \mathbb{P}(F=l \text{ and } \exists i\in\{0,1,\dots,D-1\} \;\; \alpha_{i,i+1} \text{ violates } (*)) \\ &\le \mathbb{P}(\exists i\in\{0,1,\dots,D-1\} \;\; \alpha_{i,i+1} \text{ violates } (*)) = O\!\left(\frac{1}{(\ln p)!}\right) \end{aligned}$$

and, similarly,

$$\sum_{c_{0,1}+c_{1,2}+\cdots+c_{D,0}=l} \sum_{\substack{\mathcal{O}(\mathcal{C}_{i,i+1})=c_{i,i+1} \\ \exists i\ \mathcal{C}_{i,i+1} \text{ violating } (*)}} 2\cdot \mathbb{1}_{\{p-c_{D,0}\equiv Dp-\sum c_{i,i+1}\,[2]\}} \mathbb{P}(\mathcal{O}_{D,0}=c_{D,0})\cdot$$

$$\prod_{0\le i\le D-1} \mathbb{P}(\pi(\alpha_{i,i+1})=\mathcal{C}_{i,i+1}) = O\!\left(\frac{1}{(\ln p)!}\right).$$

Hence

$$\mathbb{P}(F=l) = \sum_{c_{0,1}+c_{1,2}+\cdots+c_{D,0}=l} 2\cdot \mathbb{1}_{\{p-c_{D,0}\equiv Dp-\sum c_{i,i+1}\,[2]\}}\, \mathbb{P}(\mathcal{O}_{D,0}=c_{D,0})\cdot$$

$$\prod_{0\le i\le D-1} \mathbb{P}(\mathcal{O}_{i,i+1}=c_{i,i+1}) + O\!\left(\frac{\ln p^D}{p^{D-1}}\right).$$

Finally, notice that the parity condition on the $c_{i,i+1}$ is: "$(D+1)p-\sum_{0\le i\le D} c_{i,i+1}$ is

even", that is: "$(D+1)p-l$ is even". So

$$\mathbb{P}(F=l) = 2\cdot \mathbb{1}_{\{(D+1)p-l \text{ even}\}} \sum_{\sum_{0\le i\le D} c_{i,i+1}=l} \mathbb{P}(\mathcal{O}_{D,0}=c_{D,0})\cdot \prod_{0\le i\le D-1} \mathbb{P}(\mathcal{O}_{i,i+1}=c_{i,i+1}) + O\Big(\frac{\ln p^D}{p^{D-1}}\Big).$$

□

We now prove Theorem 6.2.5:

Proof of Theorem 6.2.5. We have obtained that:

$$\|P_F - P_{\mathcal{F}}\| = O\Big(\frac{(\ln p)^D}{p^{D-1}}\Big),$$

where $P_{\mathcal{F}} = 2\cdot\mathbb{1}_{\{(D+1)p-\mathcal{F} \text{ even}\}} P_{0,1} * P_{1,2} * \cdots * P_{D,0}$, *i.e.* $\mathcal{F}$ is, up to a parity condition, the sum of $D+1$ i.i.d. variables of law $P_{0,1}$. Therefore, F converges (uniformly) in distribution to $\mathcal{F}$:

$$|\Phi_F - \Phi_{\mathcal{F}}| = O\Big(\frac{(\ln p)^D}{p^{D-1}}\Big)$$

where $\Phi_X(a) = \mathbb{P}(X \le a)$, *i.e.* Φ_X is the cumulative distribution function of X.

We thus want to show that $\frac{\mathcal{F}-\mathbb{E}[\mathcal{F}]}{\sqrt{\mathrm{Var}(\mathcal{F})}}$ converges weakly to the normal distribution. Now, for a uniform permutation $\sigma \in \mathfrak{S}_p$, $\mathcal{O}(\sigma)$ has the same distribution as a certain sum of independent Bernoulli variables:

$$\mathbb{P}(\mathcal{O}(\sigma)=l) = \mathbb{P}\left(\sum_{1\le j\le p} B_j = l\right)$$

where the B_j are independent Bernoulli variables, with B_j of parameter $1/j$. Therefore, $\mathcal{F}$ has the same distribution as $\mathcal{S}\cdot\mathbb{1}_{\{(D+1)p-\mathcal{S} \text{ even}\}}$, with:

$$\mathcal{S} = \sum_{1\le j\le p} C_j$$

where the C_j are independent binomial variables, with C_j of parameters $(D+1, 1/j)$.

Applying the Lindeberg Central Limit Theorem to $\mathcal{S}$, we show that $\frac{\mathcal{S}-\mathbb{E}[\mathcal{S}]}{\sqrt{\mathrm{Var}(\mathcal{S})}}$ converges in distribution to the standard normal law. Then, by applying the Local Limit Theorem (see [McD05, Theorem 3.1]), we show that:

$$\mathbb{P}(\mathcal{S}=l) = \frac{(1+o(1))\exp\left(\frac{-(l-\mathbb{E}[\mathcal{S}])^2}{2\,\mathrm{Var}(\mathcal{S})}\right)}{\sqrt{2\pi\,\mathrm{Var}(\mathcal{S})}}$$

uniformly in l. Therefore, as

$$\mathbb{P}(\mathcal{F}=l) = 2\cdot\mathbb{1}_{\{(D+1)p-l \text{ even}\}}\cdot\mathbb{P}(\mathcal{S}=l),$$

this local limit theorem holds for $\mathcal{F}$ as well.

This implies that $\frac{\mathcal{F}-\mathbb{E}[\mathcal{S}]}{\sqrt{\mathrm{Var}(\mathcal{S})}}$ converges in distribution to the standard normal law, so this is also the case for F, and, as $\mathbb{E}[F]=\mathbb{E}[\mathcal{S}]$ and $\mathrm{Var}(F)=\mathrm{Var}(\mathcal{S})$, we get the final result. □

6.3 Quartic model

The uniform model presented in the previous section is easy to manipulate, but, as we have seen, it yields a relatively unsatisfying geometrical structure. Moreover, it is very far from the distributions arising in colored tensor models, as all of these yield an average number of faces linear with p (see for instance [BDR15]), to be compared with the logarithmic behavior of the uniform case, which thus has little physical relevance. These two sources of dissatisfaction are incentives to consider a slightly more complicated model, that we call the **quartic model**, and whose structure is quite familiar to physicists working on colored tensor models [DGR13; DGR14; OSVT13; RVT19]. Note however that the quartic model from the physics literature has degree-dependent weights, whereas ours is uniform on the possible realizations.

More precisely, our quartic model can be defined as follows: we consider a bipartite $(D+1)$-colored graph, where the D-bubbles without color 0 are all quartic, *i.e.* contain 4 vertices, put into two pairs linked by $D-1$ edges, with the two edges of the remaining color c connecting the pairs (see Figure 6.3.1). The D-bubbles without color 0, that we call **$\hat{0}$-bubbles**, are the "interaction vertices" of the model from the point of view of quantum field theory, while the 0-edges are its "propagators". In each $\hat{0}$-bubble, we want every color $c \in \{1, 2, \dots, D\}$ to be drawn equiprobably as the distinguished color, the bubbles being all independent. We also want the edges of color 0 to be sampled uniformly and independently of the rest.

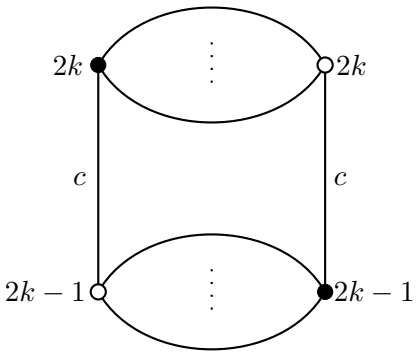

Figure 6.3.1 – The structure of each $\hat{0}$-bubble of Q_p^D.

Thus, our random graph Q_p^D ($(D+1)$-colored, with p $\hat{0}$-bubbles, hence $4p$ vertices) can be described by a permutation α_0 uniform on $\mathfrak{S}_{2p}$, independent from a set of D permutations $\{\alpha_1, \alpha_2, \dots, \alpha_D\} \subseteq \mathfrak{S}_{2p}$, each being a product of transpositions of the form $(2k-1 \quad 2k)$, with the constraints:

$$\forall k \in \{1, 2, \dots, p\}\ \exists! i \in \{1, 2, \dots, D\}, \alpha_i(2k-1) = 2k$$
$$\forall k \in \{1, 2, \dots, p\}, \forall i \in \{1, 2, \dots, D\},\ \mathbb{P}(\alpha_i(2k-1) = 2k) = \frac{1}{D}.$$

Following the structure of the previous section, we now present results on the connectedness and the degree of Q_p^D, as $p \to \infty$.

6.3.1 Connectedness

We show that Q_p^D is connected a.a.s., very similarly to the uniform case:

Theorem 6.3.1. *For all $D \geq 2$, one has:*

$$\mathbb{P}\big(Q_p^D \text{ connected}\big) = 1 - \frac{1}{2p-1} + O\Big(\frac{1}{p}\Big).$$

Proof. We use the same arguments as for Theorem 6.2.1, with the slight difference that we consider the number of $\hat{0}$-bubbles contained in a subgraph, instead of the number of vertices. Thus, for the upper bound on $\mathbb{P}\big(Q_p^D \text{ n.c.}\big)$

$$\begin{aligned}\mathbb{P}\big(Q_p^D \text{ n.c.}\big) &\leq \sum_{1\leq k\leq \lfloor \frac{p}{2}\rfloor} \mathbb{P}\big(\exists \text{ closed subgraph with } k \ \hat{0}\text{-bubbles}\big)\\ &\leq \sum_{1\leq k\leq \lfloor \frac{p}{2}\rfloor} \binom{p}{k} \frac{(2k)!(2(p-k))!}{(2p)!} = \frac{1}{2p-1} + O\Big(\frac{1}{p^2}\Big),\end{aligned}$$

and, for the lower bound

$$\begin{aligned}\mathbb{P}\big(Q_p^D \text{ n.c.}\big) &\geq \mathbb{P}\big(\exists! \text{ isolated } \hat{0}\text{-bubble}\big)\\ &= \mathbb{P}(\exists \text{ at least 1 isolated bubble}) - \mathbb{P}(\exists \text{ at least 2 isolated bubbles})\\ &\geq \frac{1}{2p-1} - \frac{1}{2(2p-1)(2p-3)}\,.\end{aligned}$$

□

As was the case for the uniform model, the probability of Q_p^D having k connected components decreases fast enough with k to get an asympotic expectation value of 1 for its number of connected components:

Theorem 6.3.2. *For all $D \geq 2$, one has:*

$$\mathbb{E}\big[k(Q_p^D)\big] = 1 + O\Big(\frac{1}{p}\Big).$$

Proof. Calculations similar to those of Section 6.2.1 give:

$$\mathbb{P}\big(k(Q_p^D) \geq 3\big) = O\Big(\frac{1}{p^2}\Big), \quad \mathbb{P}\big(k(Q_p^D) \geq 4\big) = O\Big(\frac{1}{p^3}\Big).$$

Hence

$$\begin{aligned}\mathbb{E}\big[k(Q_p^D)\big] &= 1 + O\Big(\frac{1}{p}\Big) + O\Big(\frac{1}{p^2}\Big) + \Big(\frac{p(p+1)}{2} - 6\Big)\, O\Big(\frac{1}{p^3}\Big)\\ &= 1 + O\Big(\frac{1}{p}\Big).\end{aligned}$$

□

If we now move on to the number of D-bubbles of Q_p^D, we get a picture which is very different from the uniform case. Indeed, since removing from Q_p^D the edges of one given color does not yield Q_p^{D-1}, one cannot rely on Theorem 6.3.2 to infer a result for $b_D(Q_p^D)$, and one must therefore tackle this problem with new tools.
Let us first deal with the case $D = 2$, which is much simpler than the higher dimensions. As a matter of fact, for $D = 2$ removing one color other than 0 (that is, either 1 or 2) yields $2p$ edges linked by a uniform permutation (see Figure 6.3.2), hence:

$$\mathbb{E}\big[b_D(Q_p^2)\big] = p + 2(\ln p + \gamma) + o(1),$$

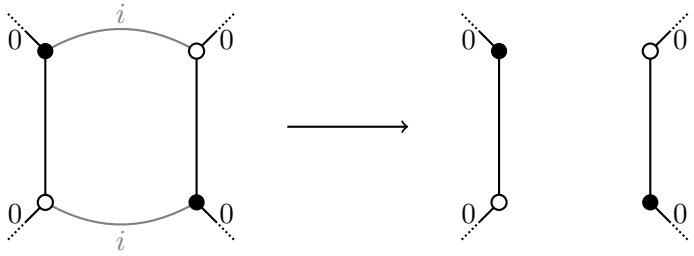

Figure 6.3.2 – Removing a color other than 0 in Q_p^2.

using once again our knowledge of the number of cycles of uniform permutations.

To answer our question for the general case $D \geq 3$, let us start with a quick analysis of the structure of $\left(Q_p^D\right)_{\hat{\imath}}$, for $i \in \{0, 1, \ldots, D\}$:

- if $i = 0$, then we just have p disconnected quartic bubbles;
- if $i \neq 0$, then $\left(Q_p^D\right)_{\hat{\imath}}$ is composed of $(D-1)$-melons (coming from the splitting of the $\hat{0}$-bubbles in which i is distinguished) and quartic $(D-1)$-bubbles (coming from the $\hat{0}$-bubbles in which i is not distinguished), completed with edges of color 0.

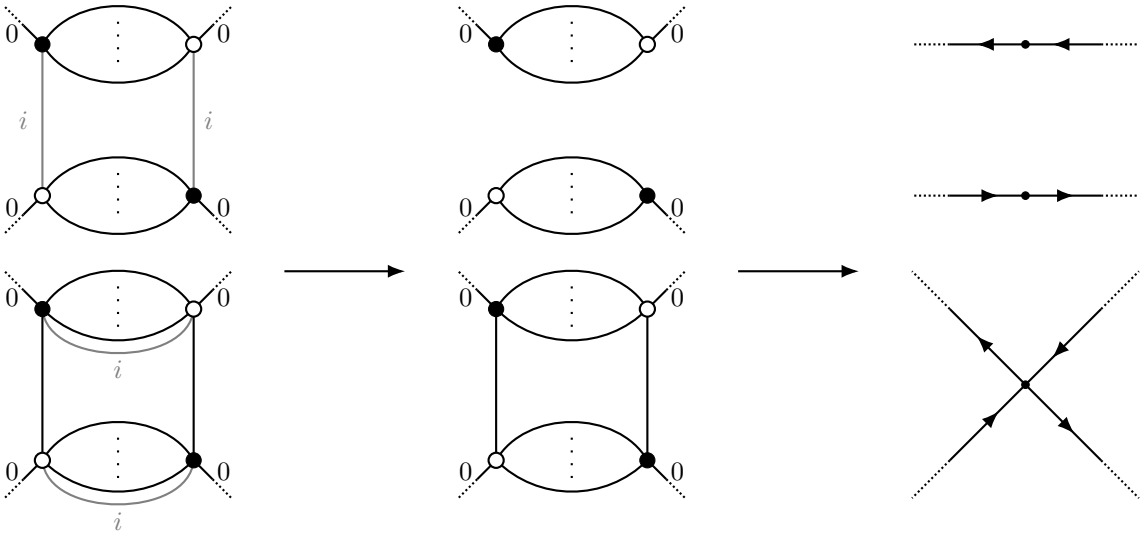

Figure 6.3.3 – Going from Q_p^D to $\left(Q_p^D\right)_{\hat{\imath}}$, and from $\left(Q_p^D\right)_{\hat{\imath}}$ to $S_p^{D,i}$.

For $i \neq 0$, as we are here only interested in the connected components of $\left(Q_p^D\right)_{\hat{\imath}}$, we can study a simpler (directed) graph $S_p^{D,i}$, which possesses vertices in lieu of quartic bubbles and melons, and whose edges correspond to the 0-edges of $\left(Q_p^D\right)_{\hat{\imath}}$.
More precisely, the quartic bubbles of $\left(Q_p^D\right)_{\hat{\imath}}$ are represented in $S_p^{D,i}$ by vertices with in-degree and out-degree of 2, and its melons, by vertices with in-degree and out-degree of 1. We can decide for instance that each white (resp. black) vertex gives rise to an in- (resp. out-)half edge, and thus the half edges of $S_p^{D,i}$ unambiguously inherit a labelling. The uniformity of α_0 is then translated into a uniform matching of the in- and out-half edges. This construction, illustrated in Figure 6.3.3, clearly preserves the connected components of $\left(Q_p^D\right)_{\hat{\imath}}$.
Crucially, $S_p^{D,i}$ is a very special case of the (directed) configuration model, and general

results by Cooper and Frieze [CF04], combined with the recent ones of Federico and van der Hofstad [FH17], allow us to obtain the following asymptotic results for the connected components of $\left(Q_p^D\right)_{\hat{\imath}}$:

Theorem 6.3.3. *For $D \geq 3$, for any $i \in \{1, 2, \ldots, D\}$, Q_p^D has a giant $\hat{\imath}$-bubble containing $4p - O\big(\sqrt{p \ln p}\big)$ vertices. Moreover, the expectation value of the number of $\hat{\imath}$-bubbles of Q_p^D is:*

$$\mathbb{E}\big[k(S_p^{D,i})\big] = \ln\left(\frac{D}{D-1}\right) + 1 + o(1).$$

We therefore get, for the total number of D-bubbles of Q_p^D:

Corollary 6.3.4. *For $D \geq 3$:*

$$\mathbb{E}\big[b_D(Q_p^D)\big] = p + D\left(\ln\left(\frac{D}{D-1}\right) + 1\right) + o(1).$$

As stated above, to prove Theorem 6.3.3, we will make use of results on the directed configuration model, that we define now. The directed configuration model describes a random digraph D_n with n vertices, among which, for $i, j \geq 0$, $l_{i,j}$ have in-degree i and out-degree j. D_n is obtained from these vertices by taking each matching of the in- and out-half-edges equiprobably. For D_n to be well-defined,there must be an equal number of in- and out-half edges, *i.e.*: $\sum_{i,j} i l_{i,j} = \sum_{i,j} j l_{i,j} =: \theta \cdot n$. The average directed degree in D_n is then $d := \sum_{i,j} ij \frac{l_{i,j}}{\theta n}$.

$S_p^{D,i}$ is an example of a directed configuration model, with $q = 2q_1 + q_2$ vertices, where q_1 is the number $\hat{0}$-bubbles that were split by removing i-edges, and $q_2 = p - q_1$ is the number of bubbles that were not split. Now, by construction, q_1 is the sum of p independent Bernoulli variables of parameter $1/D$, so, from the Hoeffding inequality:

$$\mathbb{P}\left(\left|\frac{q_1}{p} - \frac{1}{D}\right| \geq \sqrt{\frac{\ln p}{p}}\right) \leq \frac{2}{p^2}.$$

Thus, a.a.s. $q_1 \sim p/D$, and in that case $l_{1,1} = \frac{2p}{D}(1 + o(1))$, $l_{2,2} = \frac{(D-1)p}{D}(1 + o(1))$, $\theta = \frac{2p}{q} = \frac{2D}{D+1}(1 + o(1))$, and $d = \frac{2q_1+4q_2}{2p} = \left(\frac{2D-1}{D}\right)(1 + o(1))$.

To prove Theorem 6.3.3, we use a result proved in [CF04], which implies that $S_p^{D,i}$ a.a.s. contains one giant connected component of size of order q, as well as smaller cycles. Then, we will adapt a result from [FH17] to know the number of those cycles.

Theorem 6.3.5. [CF04]
Let D_n be a configuration model digraph defined by a sequence $(l_{i,j})$, satisfying:

(i) the degrees in D_n are bounded, i.e. $\exists\, i_m, j_m$ *such that* $i > i_m$ *or* $j > j_m \Rightarrow l_{i,j} = 0$

(ii) $\exists$ *constants θ_0, d_0 such that: $\theta = \theta_0(1 + o(1))$ and $d = d_0(1 + o(1))$, with $d_0 > 1$*

(iii) $\forall\, i \;\; l_{i,0} = 0$ *and* $\forall\, j \;\; l_{0,j} = 0$.

Then a.a.s. the structure of D_n is as follows:

(i) There is a unique giant strongly connected component S in D_n, of size $n - O\Big(\sqrt{n \ln n}\Big)$.

(ii) There is a collection C of vertex-disjoint directed cycles. The vertices of a cycle in C are all of in-degree 1 or all of out-degree 1. Moreover, each cycle in C is connected to S by zero or more directed paths, all such paths having the same direction with respect to the given cycle.

To understand Theorem 6.3.5, it is important to note that it deals with *strongly* connected components of D_n, *i.e.* subgraphs of D_n in which any two vertices can be joined by directed paths in both directions. Thus, the cycles in C can be connected to S by paths, but not strongly connected.

From our analysis of $S_p^{D,i}$, Theorem 6.3.5 applies to our case, as only $l_{1,1}$ and $l_{2,2}$ are non-zero, $\theta \to \frac{2D}{D+1}$, and $d \to 2 - \frac{1}{D}$. Moreover, as all the vertices of $S_p^{D,i}$ have same in-degree and out-degree, its strongly connected components are the same as its merely connected ones. Therefore, $S_p^{D,i}$ is comprised of one giant connected component, together with a collection of small cycles. To obtain the number of connected components of $S_p^{D,i}$, we thus have to determine its number of cycles. To do so, we adapt a result from [FH17] on the undirected configuration model, to the directed case:

Proposition 6.3.6. *Let D_n be a configuration model digraph defined by a sequence $(l_{i,j})$, satisfying the hypothesis (ii) from Theorem 6.3.5, and such that: $\frac{l_{1,1}}{n} \xrightarrow[p\to\infty]{} p_{1,1} \in [0,1]$. Let $C_k(n)$ be the number of cycles (composed of vertices of in- and out-degree 1) of length k in D_n. Then:*

$$(C_k(n))_{k\geq 1} \xrightarrow{(d)} (C_k)_{k\geq 1}$$

where the C_k are independent Poisson variables, of respective parameter $\frac{p_{1,1}^k}{k\theta_0^k}$.

To prove Proposition 6.3.6, we use the following Lemma, similarly to the proof of Theorem 3.3 in [FH17]:

Lemma 6.3.7. [Hof16] *A sequence of vectors of non-negative integer-valued random variables $(X_1^{(n)}, X_2^{(n)}, \dots, X_k^{(n)})_{n\geq 1}$ converges in distribution to a vector of independent Poisson random variables with parameters $(\lambda_1, \lambda_2, \dots, \lambda_k)$ when, for all possible choices of $(r_1, r_2, \dots, r_k) \in \mathbb{N}^k$:*

$$\lim_{n\to\infty} \mathbb{E}\Big[(X_1^{(n)})_{r_1}(X_2^{(n)})_{r_2}\cdots(X_k^{(n)})_{r_k}\Big] = \prod_{i=1}^{k} \lambda_i^{r_i}$$

where $(X)_r = X(X-1)\cdots(X-r+1)$.

Proof of Proposition 6.3.6. From Lemma 6.3.7, it suffices to show that, for all $k \geq 1$ and all possible choices of $(r_1, r_2, \dots, r_k) \in \mathbb{N}^k$:

$$\lim_{n\to\infty} \mathbb{E}[(C_1(n))_{r_1}(C_2(n))_{r_2}\cdots(C_k(n))_{r_k}] = \left(\frac{p_{1,1}}{\theta_0}\right)^{r_1+2r_2+\cdots+kr_k} \frac{1}{2^{r_2}\cdots k^{r_k}}.$$

We will proceed by induction on k. We first define $\mathscr{C}_k$ the set of candidates for cycles of length k in D_n, *i.e.* $\mathscr{C}_k = \{\{v_1, v_2, \dots, v_k\} | v_i \text{ has in- and out-degree } 1\}$, so that:

$$C_k(n) = \sum_{c\in\mathscr{C}_k} \mathbb{1}_{\{c \text{ is in } D_n\}}.$$

This formulation highlights the fact that we are dealing with the factorial moments of sums of indicators, which implies that (see [Hof16, Section 2.1]):

$$\mathbb{E}[(C_1(n))_{r_1}(C_2(n))_{r_2}\cdots(C_k(n))_{r_k}] = \sum_{\substack{c_1(1),\dots,c_1(r_1)\in\mathscr{C}_1\\ \text{distinct}}} \cdots \sum_{\substack{c_k(1),\dots,c_k(r_k)\in\mathscr{C}_k\\ \text{distinct}}} \mathbb{P}(c_i(s) \text{ is in } D_n,\ \forall\, i=1,\dots,k,\ \forall s=1,\dots,r_k). \quad (6.3.1)$$

We note $W_k(\overrightarrow{r})$ the set of candidates for a collection of cycles like in Equation (6.3.1): $W_k(\overrightarrow{r}) := \{\{c_1(1),\dots,c_1(r_1),\dots,c_k(1),\dots,c_k(r_k)\}\,|\,c_i(j)\in\mathscr{C}_i,\ 1\le i\le k,\ 1\le j\le r_i,$ the $c_i(s)$ are distinct$\}$, and for $w\in W_k(\overrightarrow{r})$ we note $\mathscr{E}(w)$ the event that all the cycles of w are in D_n. Then

$$\begin{aligned}
&\mathbb{E}[(C_1(n))_{r_1}(C_2(n))_{r_2}\cdots(C_k(n))_{r_k}]\\
&= \sum_{w_k\in W_k(\overrightarrow{r})} \mathbb{P}(\mathscr{E}(w_k))\\
&= \sum_{w_{k-1}\in W_{k-1}(\overrightarrow{r})} \mathbb{P}(\mathscr{E}(w_{k-1})) \underbrace{\sum_{\substack{c_1,\dots,c_{r_k}\in\mathscr{C}_k\\ \text{distinct}}} \mathbb{E}\Big[\mathbb{1}_{\{c_1 \text{ in } D_n\}}\cdots\mathbb{1}_{\{c_{r_k} \text{ in } D_n\}}|\mathscr{E}(w_{k-1})\Big]}_{S_k}.
\end{aligned}$$

We now calculate S_k. It can be decomposed into the possible choices of cycles, that is, choices of collections of vertices of in- and out-degree of 1, multiplied by the probability of having those cycles in D_n. The choice of vertices is only constrained by the vertices already appearing in cycles of w_k, as those cannot be chosen. As for the probability of the cycles, they correspond to successive restrictions on the uniform permutation representing the matchings of the half-edges. Thus:

$$S_k = \frac{(l_{1,1}-a_{1,1})!}{(l_{1,1}-a_{1,1}-kr_k)!(k!)^{r_k}}\cdot\frac{((k-1)!)^{r_k}(\theta n-a_{1,1}-k)!}{(\theta n-a_{1,1})!}$$

where $a_{1,1}$ is the number of vertices appearing in w_{k-1}. Therefore, for fixed k,

$$S_k = \frac{l_{1,1}^{kr_k}}{k^{r_k}(\theta n)^{kr_k}}(1+o(1)) = \left(\frac{p_{1,1}^k}{k\theta_0^k}\right)^{r_k}(1+o(1)),$$

i.e.

$$\mathbb{E}[(C_1(n))_{r_1}(C_2(n))_{r_2}\cdots(C_k(n))_{r_k}] = \mathbb{E}\big[(C_1(n))_{r_1}(C_2(n))_{r_2}\cdots(C_{k-1}(n))_{r_{k-1}}\big]\cdot\left(\frac{p_{1,1}^k}{k\theta_0^k}\right)^{r_k}(1+o(1)).$$

□

From Theorem 6.3.5 and Proposition 6.3.6, we deduce that the number of connected components of $S_p^{D,i}$ has an expectation value of:

$$\mathbb{E}\big[k(S_p^{D,i})\big] = 1+\sum_{k\ge1}\mathbb{E}[C_k(q)]\Big|_{|q-\frac{D+1}{D}p|=O\left(\sqrt{p\ln p}\right)} + O\left(p\cdot\frac{1}{p^2}\right) = 1+\sum_{k\ge1}\frac{1}{kD^k}+o(1),$$

i.e.

$$\mathbb{E}\big[k(S_p^{D,i})\big] = 1+\ln\left(\frac{D}{D-1}\right)+o(1)$$

which gives Theorem 6.3.3, and therefore Corollary 6.3.4.

6.3.2 Geometry of the complex

With a view towards scaling limits, it is encouraging that the number of points in the complex $\Delta(Q_p^D)$ grows linearly with p, as stated in Corollary 6.3.4. However, to make it possible to hope for a continuum scaling limit, the typical distances in $\Delta(Q_p^D)$ must grow to infinity with p. This is why we investigate the behavior of distances in this complex.

We show that, unfortunately, the average distance between two points of the complex is bounded, and more precisely, as stated in Theorem 6.3.8, equal to 2. This can be predicted by considering the "typical landscape" of the complex. Indeed, there always are p 0-points, while the number of i-points, for $i \neq 0$, grows sublinearly with p, as a consequence of Theorem 6.3.5. Thus, a uniform point is a.a.s. of color 0. Moreover, Theorem 6.3.5 also implies that, for $i \neq 0$, there is a "hub" i-point corresponding to the giant component of $S_p^{D,i}$, which is linked to most of the 0-points, and much more isolated i-points, corresponding to the small cycles of $S_p^{D,i}$. Hence, typically two independent and uniform points of $\Delta(Q_p^D)$ will be of color 0, and will have the "hub" i-points, for $i \neq 0$, as common neighbors. We formalize this heuristic in the proof of the following theorem:

Theorem 6.3.8. *Let u, v be two vertices of $\Delta(Q_p^D)$ chosen uniformly at random and independently. Then, a.a.s.:*

$$d(u, v) = 2.$$

Proof. To prove this result, we show that a.a.s. u and v are points of color 0, and have a common neighbor of color $i \neq 0$. The fact that they are 0-colored a.a.s. is a simple consequence of Theorem 6.3.5, and more precisely the fact that a.a.s. the giant component of $S_p^{D,i}$ has size $q - O\big(\sqrt{q \ln q}\big)$ (where q is the number of vertices of $S_p^{D,i}$), so that a.a.s. there are less than $O\big(\sqrt{p \ln p}\big)$ $\hat{\imath}$-bubbles for $i \neq 0$, while there are p $\hat{0}$-bubbles.

It now remains to show that u and v have a common neighbor. To do so, let us consider the D-bubbles $\mathcal{B}_u, \mathcal{B}_v$ of Q_p^D they respectively correspond to. For any color $i \neq 0$, $\mathcal{B}_u$ corresponds to either 1 or 2 vertices in $S_p^{D,i}$, depending on whether i is the distinguished color in $\mathcal{B}_u$ or not. If $\mathcal{B}_u$ corresponds to a single vertex $u \in S_p^{D,i}$, then conditionally to the existence of a giant component like in Theorem 6.3.5, u is necessarily in that giant component, as it is a quartic vertex. Now, conditionally to the fact that $\mathcal{B}_u$ corresponds to 2 vertices $w, x \in S_p^{D,i}$, both w and x are uniform on the quadratic vertices of $S_p^{D,i}$, and are thus a.a.s. in the giant component of $S_p^{D,i}$, from Theorem 6.3.5. Therefore, a.a.s. $\mathcal{B}_u$ and the $\hat{\imath}$-bubble $\mathcal{B}_{g,i}$ corresponding to the giant component of $S_p^{D,i}$ have an $(\hat{\imath}, \hat{0})$-bubble in common. In terms of simplices of $\Delta(Q_p^D)$, this means that a.a.s., a 1-simplex of the complex links u to the vertex $t_{g,i}$ corresponding to $\mathcal{B}_{g,i}$, *i.e.* that these two vertices are nearest neighbors. Following the same reasoning for v, a.a.s. it is also a direct neighbor of $t_{g,i}$, so that u and v are at distance 2 in $\Delta(Q_p^D)$. □

6.3.3 Degree

We now look into the number of faces of Q_p^D. Like for the uniform model, we present results on the expectation value and the variance of the total number of faces, as well as one on the asymptotic behavior of the number of faces of a given jacket. As we will see, upon proving these results we also obtain the asymptotic behavior of the genus of a uniform map of size p, as $p \to \infty$ (see Theorem 6.3.14).

Theorem 6.3.9 (Number of faces of Q_p^D)**.**

$$\mathbb{E}\big[[b_2(Q_p^D)]\big] = (D-1)^2 p + D(\ln(2p) + \gamma) + o(1) \tag{6.3.2}$$
$$\mathrm{Var}\big(b_2(Q_p^D)\big) = O\big((\ln p)^3\big). \tag{6.3.3}$$

We also get a normal limit for the number of faces of one jacket:

Theorem 6.3.10. *Let $\mathcal{J}_p$ be a regular embedding of Q_p^D, and $F_{\mathcal{J}_p}$ be the number of faces of $\mathcal{J}_p$. Then the quantity $\frac{F_{\mathcal{J}_p} - \mathbb{E}\left[F_{\mathcal{J}_p}\right]}{\sqrt{\mathrm{Var}\left(F_{\mathcal{J}_p}\right)}}$ converges weakly to the standard normal distribution.*

To prove both (6.3.9) and (6.3.10), we will need to determine the asymptotical behavior of the joint law of $\mathcal{O}(\alpha_0\alpha_i^{-1}), \mathcal{O}(\alpha_j\alpha_i^{-1}), \mathcal{O}(\alpha_j\alpha_0^{-1})$, for $1 \leq i < j \leq D$. By conjugating all permutations by a uniform permutation $\beta \in \mathfrak{S}_{2p}$, independent from the rest, this amounts to answering the same question for $\mathcal{O}(\varphi), \mathcal{O}(\alpha), \mathcal{O}(\alpha\varphi^{-1})$, for α, φ two independent permutations in $\mathfrak{S}_{2p}$, with φ uniform, and α an involution with $n = 2b$ fixed points, where b is the sum of p independent Bernoulli variables of parameter $\frac{D-2}{D}$. This slight change of setting leads to considering the following result:

Proposition 6.3.11. *Let p be a positive integer, and $0 \leq b \leq p$ fixed. Let α be uniform on the conjugacy class of involutions on $\{1, \ldots, 2p\}$ with $2b$ fixed points, and let φ be a uniform permutation on $\{1, \ldots, 2p\}$, independent from α. Then $(\mathcal{O}(\varphi) + \mathcal{O}(\alpha\varphi^{-1}))$ has the same law as $(\mathcal{O}(\psi) + \mathcal{O}(\delta\psi^{-1}))$, where δ is uniform on the fixed-point-free involutions on $\{1, \ldots, 2(p-b)\}$, and ψ is uniform on $\mathfrak{S}_{2(p-b)}$, and independent from δ.*

Proof. The key idea of the proof is that $\alpha, \varphi, \alpha\varphi^{-1}$ respectively describe the (half-)edges, faces and vertices, of an (half-edge) labelled ribbon graph G with $(p-b)$ edges and $2b$ unmatched half-edges. By erasing the unmatched half-edges of G, we obtain a ribbon graph H with $(p-b)$ edges.

As α and φ are independent and uniform on their respective sets of possible realizations, G is uniform on the set of labelled ribbon graphs with $(p-b)$ edges and $2b$ unmatched half-edges. Therefore, if we relabel the half-edges of H, by keeping their order, so that the labels are in $\{1, 2, \ldots, 2(p-b)\}$, we get a ribbon graph H', uniform on the labelled ribbon graphs with $(p-b)$ edges. H' can thus be identified to a triple $(\delta, \psi, \delta\psi^{-1})$ satisfying the hypotheses mentioned above. As the transformation from G to H' preserves the Euler characteristic, we have

$$\begin{aligned}\chi(G) &= \mathcal{O}(\varphi) - (\mathcal{O}(\alpha) - 2b) + \mathcal{O}(\alpha\varphi^{-1}) \\ &= \chi(H') = \mathcal{O}(\psi) - \mathcal{O}(\delta) + \mathcal{O}(\delta\psi^{-1}),\end{aligned}$$

that is

$$\mathcal{O}(\varphi) + \mathcal{O}(\alpha\varphi^{-1}) = \mathcal{O}(\psi) + \mathcal{O}(\delta\psi^{-1}).$$

□

Let us go back to the permutations that define Q_p^D. We deduce from Proposition 6.3.11 an intermediate result that will be necessary to prove Theorem 6.3.9:

Proposition 6.3.12. *Let $\mathcal{O}_{i,j}$ be the number of cycles of $\alpha_i\alpha_j^{-1}$. Then:*

$$\mathbb{E}[\mathcal{O}_{0,1}\mathcal{O}_{D,0}] = O\big((\ln p)^3\big).$$

Proof. We first write:

$$\mathbb{E}[\mathcal{O}_{0,1}\mathcal{O}_{D,0}] = \frac{1}{2}\left(\mathbb{E}\Big[(\mathcal{O}_{0,1}+\mathcal{O}_{D,0})^2\Big] - \mathbb{E}\big[\mathcal{O}_{0,1}^2\big] + \mathbb{E}\big[\mathcal{O}_{D,0}^2\big]\right).$$

Then, from Proposition 6.3.11, when the number $2b$ of fixed points of $\alpha_D\alpha_1^{-1}$ is fixed, we have:

$$\mathbb{E}\Big[(\mathcal{O}_{0,1}+\mathcal{O}_{D,0})^2 \mid \alpha_{D,1} \text{ has } 2b \text{ fixed points } \Big] = \mathbb{E}\Big[\big(\mathcal{O}(\psi)+\mathcal{O}(\delta\psi^{-1})\big)^2\Big]$$

with the notations of Proposition 6.3.11. Now, with the same techniques as in Section 6.2.2, we prove that, conditionally to the conjugacy class $\mathcal{C}_\psi$ of ψ, $\delta\psi^{-1}$ is asymptotically uniform on $H = \mathcal{A}_{2(p-b)}$ (resp. $H = (\mathcal{A}_{2(p-b)})^c$) if ψ and δ are of the same parity (resp. of opposite parities). More precisely,

$$\|P_{\delta\psi^{-1}} - \mathcal{U}_H\| = O\left(\frac{(\ln(p-b))^2}{p-b}\right).$$

Thus

$$\begin{aligned}
\mathbb{E}\big[\mathcal{O}(\psi)\mathcal{O}(\delta\psi^{-1})\big] &= \sum_{1\le c_1,c_2\le 2(p-b)} c_1c_2\,\mathbb{P}\big(\mathcal{O}(\psi)=c_1,\mathcal{O}(\delta\psi^{-1})=c_2\big)\\
&= \sum_{1\le c_1\le 2(p-b)} c_1\,\mathbb{P}(\mathcal{O}(\psi)=c_1)\Big[\,O\big((\ln(p-b))^2\big)\\
&\quad + \sum_{1\le c_2\le 2(p-b)} 2\cdot\mathbb{1}_{\{(-1)^{c_1+c_2}=(-1)^{p-b}\}}\cdot c_2\,\mathbb{P}\big(\mathcal{O}(\delta\psi^{-1})=c_2\big)\Big]\\
&= \sum_{1\le c_1\le 2(p-b)} c_1\,\mathbb{P}(\mathcal{O}(\psi)=c_1)\Big[\,O\big((\ln(p-b))^2\big)+O(\ln(p-b))\Big]\\
&= O\big((\ln(p-b))^2\big)\sum_{1\le c_1\le 2(p-b)} c_1\,\mathbb{P}(\mathcal{O}(\psi)=c_1)\\
&= O\big((\ln(p-b))^3\big).
\end{aligned}$$

This implies that

$$\mathbb{E}\Big[\big(\mathcal{O}(\psi)+\mathcal{O}(\delta\psi^{-1})\big)^2\Big] = O\big((\ln(p-b))^3\big),$$

and so $\mathbb{E}[\mathcal{O}_{0,1}\mathcal{O}_{D,0}] = O\big((\ln(p-b))^3\big)$ as well. □

We can now prove Theorem 6.3.9.

Proof of Theorem 6.3.9. To prove Equation (6.3.2), we first make a clear list of the different types of faces:

- the faces without color 0 are, by definition, subsets of the $\hat{0}$-bubbles. They either contain the distinguished color of their $\hat{0}$-bubble, in which case they have 4 vertices, or they do not, in which case they have 2 vertices. There are, in each $\hat{0}$-bubble, $D-1$ faces of the first type, and $(D-1)(D-2)$ of the second.
- For each $i \neq 0$, one can see the bicolored graph $(Q_p^D)_{i,0}$ as $2p$ vertices with one in- and one out-half-edge, with a uniform matching of the half-edges, similarly to the construction of $S_p^{D,j}$. The faces of color $\{0,i\}$ are thus given by the cycles of a uniform permutation of size $2p$.

Therefore:

$$\begin{aligned}\mathbb{E}\big[b_2(Q_p^D)\big] &= \left((D-1)(D-2)+(D-1)\right)p + D\left(\sum_{j=1}^{2p}\frac{1}{j}\right)\\ &= (D-1)^2p + D(\ln(2p)+\gamma)+o(1).\end{aligned}$$

To obtain the variance, we now have to calculate $\mathbb{E}\Big[\big(b_2(Q_p^D)\big)^2\Big]$. We decompose it into different parts as follows:

$$\begin{aligned}\mathbb{E}\Big[\big(b_2(Q_p^D)\big)^2\Big] &= \mathbb{E}\left[\left(\sum_{0\le i<j\le D}\mathcal{O}\left(\alpha_i\alpha_j^{-1}\right)\right)^2\right]\\ &= \underbrace{\mathbb{E}\left[\left(\sum_{1\le i<j\le D}\mathcal{O}\left(\alpha_i\alpha_j^{-1}\right)\right)^2\right]}_{E_1} + \underbrace{2\ \mathbb{E}\left[\sum_{\substack{1\le i\le D\\ 1\le k<l\le D}}\mathcal{O}\left(\alpha_0\alpha_i^{-1}\right)\mathcal{O}\left(\alpha_k\alpha_l^{-1}\right)\right]}_{E_2}\\ &\quad + \underbrace{\sum_{1\le i\le D}\mathbb{E}\Big[\mathcal{O}\left(\alpha_0\alpha_i^{-1}\right)^2\Big]}_{E_3} + \underbrace{2\sum_{1\le i<j\le D}\mathbb{E}\Big[\mathcal{O}\left(\alpha_0\alpha_i^{-1}\right)\mathcal{O}(\alpha_0\alpha_j^{-1})\Big]}_{E_4}.\end{aligned}$$

In the first term, E_1, there are all the faces without color 0. By definition, the number of those is fixed:

$$\sum_{1\le i<j\le D}\mathcal{O}\left(\alpha_i\alpha_j^{-1}\right) = p((D-1)(D-2)+(D-1)) = p(D-1)^2,$$

so that $E_1 = p^2(D-1)^4$. Moving on to E_2, for any $i,k,l\in\{1,2,\dots,D\}$, the permutations $\alpha_0\alpha_i^{-1}$ and $\alpha_k\alpha_l^{-1}$ are independent, so:

$$\begin{aligned}E_2 &= 2\ \mathbb{E}\left[\sum_{1\le i\le D}\mathcal{O}\left(\alpha_0\alpha_i^{-1}\right)\right]\cdot\mathbb{E}\left[\sum_{1\le k<l\le D}\mathcal{O}\left(\alpha_k\alpha_l^{-1}\right)\right]\\ &= 2D\left(\sum_{j=1}^{2p}\frac{1}{j}\right)\cdot(D-1)^2p,\end{aligned}$$

using, for the first part, the fact that all $i\in\{1,2,\dots,D\}$, $\alpha_0\alpha_i^{-1}$ is uniform, and, for the second part, the same argument as for E_1. Thus

$$E_2 = 2D(D-1)^2p\left(\sum_{j=1}^{2p}\frac{1}{j}\right).$$

For E_3, we are dealing with uniform permutations, so:

$$\begin{aligned}E_3 &= D((\ln 2p)^2 + (2\gamma-1)\ln(2p) + o(\ln p))\\ &= D(\ln p)^2 + O(\ln p).\end{aligned}$$

We are now left with E_4, which we estimate thanks to Proposition 6.3.11: $E_4 = O\big((\ln p)^3\big)$.

Therefore

$$\begin{aligned}\mathrm{Var}\big(b_2(Q_p^D)\big) &= \left(p^2(D-1)^4 + 2D(D-1)^2 p\left(\sum_{j=1}^{2p}\frac{1}{j}\right) + O\big((\ln p)^3\big)\right) \\ &\quad - \left((D-1)^2 p + D\left(\sum_{j=1}^{2p}\frac{1}{j}\right)\right)^2 \\ &= O\big((\ln p)^3\big).\end{aligned}$$

□

Proof of Theorem 6.3.10. Like in Section 6.2.2, by symmetry, we assume without loss of generality that $\mathcal{J}_p$ corresponds to the usual cyclic ordering $(0\,1\,\ldots\,D)$, and in that case we are interested in the quantity:

$$F = \sum_{0\leq i\leq D} \mathcal{O}_{i,i+1}$$

where, by convention, $\mathcal{O}_{D,D+1} = \mathcal{O}_{D,0}$. From the structure of the α_i, for $1 \leq i \leq D$, we deduce

$$\sum_{1\leq i\leq D-1} \mathcal{O}_{i,i+1} + \mathcal{O}_{D,1} = 2p(D-1),$$

hence:

$$F = \mathcal{O}_{0,1} + \mathcal{O}_{D,0} + 2p(D-1) - \mathcal{O}_{D,1}.$$

Thus, up to a constant, F follows the same law as $f := \mathcal{O}_{0,1} + \mathcal{O}_{D,0} - \mathcal{O}_{D,1}$. Now, conditionally to the number $2b$ of fixed points of $\alpha_D\alpha_1^{-1}$, Proposition 6.3.11 gives us the behavior of f. Indeed, it has the same law as $\mathcal{O}(\psi) + \mathcal{O}(\delta\psi^{-1}) - (p+b)$, with the notations of Proposition 6.3.11.

As explained above in the proof of Proposition 6.3.12, conditionally to the conjugacy class $\mathcal{C}_\psi$ of ψ, the law of $\delta\psi^{-1}$ converges for the total variation distance to the uniform measure either on $\mathcal{A}_{2(p-b)}$ (if $\mathcal{C}_\psi$ has the same parity as δ), or on $(\mathcal{A}_{2(p-b)})^c$ (if they are of opposite parities). Thus:

$$\begin{aligned}\mathbb{P}(f=l) &= \sum_{1\leq b\leq p} \mathbb{P}(\mathcal{O}_{D,1} = p+b)\,\mathbb{P}\big(\mathcal{O}(\psi) + \mathcal{O}(\delta\psi^{-1}) = l+p+b\big) \\ &= \sum_{1\leq b\leq p} \mathbb{P}(\mathcal{O}_{D,1} = p+b)\Big[2\cdot\mathbb{1}_{\{l \text{ even}\}}\left(P_\psi * P_{\delta\psi^{-1}}\right)(l+p+b) + \\ &\qquad\qquad O\left(\frac{(\ln(p-b))^2}{p-b}\right)\Big] \qquad (6.3.4)\end{aligned}$$

where P_σ is the law of the number of cycles of σ.

Now, let us recall that for a uniform permutation $\sigma \in \mathfrak{S}_n$, $\mathcal{O}(\sigma)$ has the same distribution as $\sum_{j=1}^n B_j$, where the B_j are independent Bernoulli variables, with B_j of parameter $1/j$. We use this fact to bound the dependence on b of P_ψ and $P_{\delta\psi^{-1}}$. Indeed, as we will later use Hoeffding's inequality for b, we consider the case $|b - p\left(\frac{D-2}{D}\right)| \leq \sqrt{p\ln p}$. We can couple $\mathcal{O}(\psi)$ with a variable of the form $\sum_{j=1}^{\lfloor\frac{4p}{D}\rfloor} B_j$,by taking or adding some B_j to the sum

to get $\mathcal{O}(\psi)$, and in that case:

$$\mathbb{P}\left(\left|\mathcal{O}(\psi) - \sum_{j=1}^{\lfloor \frac{4p}{D} \rfloor} B_j\right| \geq 1\right) = O\left(\sqrt{\frac{\ln p}{p}}\right). \tag{6.3.5}$$

Indeed:

$$\left|\mathcal{O}(\psi) - \sum_{j=1}^{\lfloor \frac{4p}{D} \rfloor} B_j\right| \leq B\left(O\left(\sqrt{p \ln p}\right), \left\lfloor \frac{4p}{D} \right\rfloor\right)$$

where $B(O(\sqrt{p \ln p}), \lfloor \frac{4p}{D} \rfloor)$ follows a binomial distribution of parameters $(O(\sqrt{p \ln p}), (\lfloor \frac{4p}{D} \rfloor)^{-1})$. Then, applying Markov's inequality to $B(O(\sqrt{p \ln p}), \lfloor \frac{4p}{D} \rfloor)$:

$$\mathbb{P}\left(B\left(O\left(\sqrt{p \ln p}\right), \left\lfloor \frac{4p}{D} \right\rfloor\right) \geq 1\right) = o\left(\frac{1}{\sqrt{\ln p}}\right).$$

Let us note g_p^D the law of $\sum_{j=1}^{\lfloor \frac{4p}{D} \rfloor} B_j$. Similarly to what we did in the proof of Theorem 6.2.5, we show that g_p^D converges uniformly to a discrete gaussian distribution, of mean $E_p = \ln p + \gamma + \ln(\frac{4}{D}) + o(1)$, and of variance $V_p = \ln p + \gamma + \ln(\frac{4}{D}) - \pi^2/6 + o(1)$:

$$g_p^D(c) = \frac{(1 + o(1)) \exp\left(\frac{-(c - E_p)^2}{2V_p}\right)}{\sqrt{2\pi V_p}}. \tag{6.3.6}$$

As Equation (6.3.6) implies in particular that $g_p^D(c)$ is slowly varying, we deduce from Equation (6.3.5):

$$P_\psi(c) = g_p^D(c) + o\left(\frac{1}{\sqrt{\ln p}}\right). \tag{6.3.7}$$

Now, applying Hoeffding's inequality to b, we get:

$$\mathbb{P}\left(\left|b - p\left(\frac{D-2}{D}\right)\right| \geq \sqrt{p \ln p}\right) = O\left(\frac{1}{p^2}\right). \tag{6.3.8}$$

Combining Equations (6.3.4), (6.3.7) and (6.3.8), we can write:

$$\mathbb{P}(f = l) = 2 \cdot \mathbb{1}_{\{l \text{ even}\}}(\tilde{P}_{D,1} * g_p^D * g_p^D)(l) + o\left(\frac{1}{\sqrt{\ln p}}\right)$$

where $\tilde{P}_{D,1}$ is the law of $-\mathcal{O}_{D,1}$.

Thus:

$$\left\| P_f - 2P_h \cdot \mathbb{1}_{\{h \text{ even}\}} \right\| = o\left(\frac{1}{\sqrt{\ln p}}\right),$$

where $h = \sum_{1 \leq j \leq \lfloor \frac{4p}{D} \rfloor} X_j + Y + p$, with the X_j and Y being independent binomial variables, with X_j of parameters $(2, 1/j)$ and Y of parameters $(p, (D-2)/D)$. The Lindeberg Central Limit Theorem and the Local Limit Theorem apply once again, and the resulting convergence of P_h to a discrete gaussian implies that of P_f.
Finally, as $\mathbb{E}[f] = 2p(D-1)/D + 2\ln p + O(1) = \mathbb{E}[h] + O(1)$, and $\mathrm{Var}(f) = 2p(D-2)/D^2 + O\big((\ln p)^3\big) = \mathrm{Var}(h) + O\big((\ln p)^3\big)$, we have a weak convergence result for $(f - \mathbb{E}[f])/\sqrt{\mathrm{Var}(f)}$. □

As anounced before, the arguments we have used here to get results on the degree of Q_p^D also imply a Central Limit Theorem for the genus of a uniform random map, in a sense that we make more precise now. Consider, for a given $p \geq 1$, a uniform fixed-point-free involution of $\{1, \dots, 2p\}$, δ, and a uniform permutation $\psi \in \mathfrak{S}_{2p}$, independent from δ. Then $\delta, \psi, \delta\psi^{-1}$ respectively describe the edges, faces and vertices of a (half-edge-labelled) ribbon graph M_p with p edges, which is clearly uniform on the set of such graphs.

We first prove that M_p is *a.a.s.* connected:

Proposition 6.3.13. *One has:*

$$\mathbb{P}(M_p \text{ connected}) = 1 - \frac{1}{2p-1} + O\Big(\frac{1}{p}\Big). \tag{6.3.9}$$

Proof. Notice that the probability of M_p being connected is exactly the same as the probability of Q_p^D being connected (for any $D \geq 2$). Indeed, in both cases we consider the set of indices $\{1, \dots, 2p\}$ grouped into pairs (by δ for M_p and by the structure of the $\hat{0}$-bubbles for Q_p^D), and then add connections according to a uniform permutation independent from the pairing (ψ for M_p and α_0 for Q_p^D). We therefore deduce Equation (6.3.9) directly from Theorem 6.3.1. □

Now that we know that M_p is connected *a.a.s.*, we can consider its genus, for which we prove the following theorem:

Theorem 6.3.14. *Let g_p be the genus of M_p. Then the quantity $\frac{g_p - \mathbb{E}[g_p]}{\sqrt{\mathrm{Var}(g_p)}}$ converges weakly to the standard normal distribution. Moreover, we have the following estimations:*

$$\begin{aligned} \mathbb{E}[g_p] &= \frac{p}{2} - (\ln 2p + \gamma) + 1 + o(1), \\ \mathrm{Var}(g_p) &= O\big((\ln p)^3\big). \end{aligned}$$

Proof. Let us start with the first statement of the theorem. As explained in the proof of Proposition 6.3.12, conditionally to the conjugacy class $\mathcal{C}_\psi$ of ψ, $\delta\psi^{-1}$ is asymptotically uniform on $H = \mathcal{A}_{2p}$ (resp. $H = (\mathcal{A}_{2p})^c$) if ψ and δ are of the same parity (resp. of opposite parities), indeed:

$$\|P_{\delta\psi^{-1}} - \mathcal{U}_H\| = O\bigg(\frac{(\ln p)^2}{p}\bigg).$$

Therefore, just like we derived Theorem 6.2.6 from Proposition 6.2.7, we get:

$$\|P_{\delta,\psi} - 2 \cdot \mathbb{1}_{\{C_{\delta,\psi}+p \text{ even}\}} P_\psi * P_{\delta\psi^{-1}}\| = O\bigg(\frac{(\ln p)^2}{p}\bigg)$$

where $P_{\delta,\psi}$ is the law of $C_{\delta,\psi} := \mathcal{O}(\psi) + \mathcal{O}(\delta\psi^{-1})$.

Now, following the same arguments as in the proof of Theorem 6.2.5, we obtain that the quantity $\frac{C_{\delta,\psi} - \mathbb{E}[C_{\delta,\psi}]}{\sqrt{C_{\delta,\psi}}}$ converges weakly to the standard normal law. Finally, as $g_p = \frac{1}{2}(p - C_{\delta,\psi}) + 1$, we have a weak convergence result for g_p as well. As for the estimations of $\mathbb{E}[g_p]$ and $\mathrm{Var}(g_p)$, the first is a direct consequence of the fact that ψ and $\delta\psi^{-1}$ are uniform permutations, and the second was proved in the proof of Proposition 6.3.12. □

6.4 Uniform-uncolored models

Random D-complexes studied by physicists are mainly of the type of the quartic model: the $\hat{0}$-bubbles of the corresponding colored graphs all belong to a fixed finite set of D-colored graphs. In the quartic model studied in section 6.3, this set is reduced to a singleton, namely the quartic melonic graph of Figure 6.3.1. Melonic $D+1$-colored graphs are dual to special colored triangulations of the D-sphere [GR12]. A natural question is the following: do the results obtained for the quartic model also hold in the case of more generic $\hat{0}$-bubbles set and particularly if this set contains non melonic graphs? To answer this question, we now consider a type of model similar to the quartic one, where the $\hat{0}$-bubbles are all identical, up to color permutations.

More precisely, we start from a fixed, connected bipartite D-colored graph G with $2t \geq 4$ vertices, and we consider a random $(D+1)$-colored graph G_p, with p $\hat{0}$-bubbles $\mathcal{B}_1^{\hat{0}}, \dots, \mathcal{B}_p^{\hat{0}}$, which are all copies of G up to a color permutation: if an edge e of G has color $c(e) \in \{1, \dots, D\}$, then the corresponding edge e' of $\mathcal{B}_k^{\hat{0}}$ will have color $c_k(e') = \gamma_k(c(e))$, where $\gamma_1, \dots, \gamma_p$ are i.i.d. uniform permutations in $\mathfrak{S}_D$ (see Figure 6.4.1 for an illustration).
Similarly to the quartic case, the 0-colored edges of G_p are given by a permutation α_0 uniform on $\mathfrak{S}_{p \cdot t}$, and independent from the rest (we can choose an arbitrary labelling $v_1^B, \dots, v_t^B, v_1^W, \dots, v_t^W$ of the vertices of G to obtain a canonical labelling of the vertices of G_p).

The connectivity properties of this model are very similar to the specific case of the quartic model seen in Section 6.3.1, as detailed in Section 6.4.1. In particular, the complex of the general uniform-uncolored model $\Delta(G_p)$ exhibits the same asymptotic structure as for the quartic model, *i.e.* a majority of 0-points, most of which having the "colored hubs" as common neighbors, as explained in Section 6.4.2. As for the behaviors of the degree and of the genera of the jackets, they are difficult to obtain in the general case, as we do not have an explicit description of G_p in terms of $D+1$ random permutations $(\alpha_0, \alpha_1, \dots, \alpha_D) \in \mathfrak{S}_p^{D+1}$. Even if we use such a description for a particular case, the laws of the α_i will typically be much more complicated than for Q_p^D, and might not yield explicit results or estimations as easily. Moreover, because of the unsatisfying connectivity properties of this model, it does not seem very worthwhile to undertake such a laborious task.

6.4.1 Connectedness

Just like in the quartic case, we show that G_p is connected a.a.s., and moreover that the expectation value of its number of components converges to 1:

Theorem 6.4.1. *One has:*

$$\mathbb{P}(G_p \text{ connected}) = 1 - \frac{p}{\binom{tp}{t}} + O\left(\frac{1}{p^{2(t-1)}}\right),$$

$$\mathbb{E}[k(G_p)] = 1 + O\left(\frac{1}{p^{t-1}}\right).$$

Proof. We proceed in the same way as for (6.3.1) and (6.3.2), using the fact that, for $1 \leq k \leq \lfloor \frac{p}{2} \rfloor$, $\mathbb{P}(G_p \text{ has a closed subgraph containing } k \text{ copies of } G) = \binom{p}{k} / \binom{tp}{tk}$. □

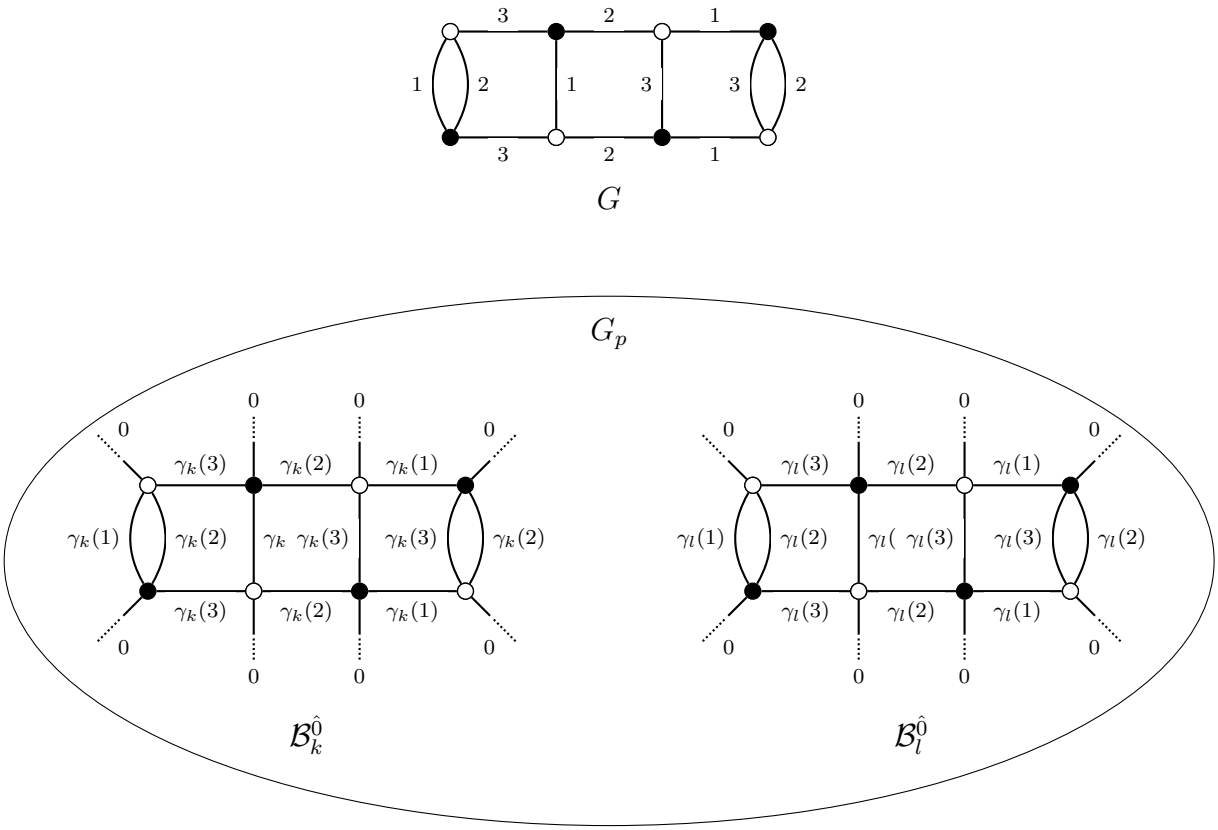

Figure 6.4.1 – Starting from a D-colored graph G (here $D = 3$), we construct a $(D+1)$-colored graph G_p, whose p $\hat{0}$-bubbles are copies of G in which the colors have been permuted.

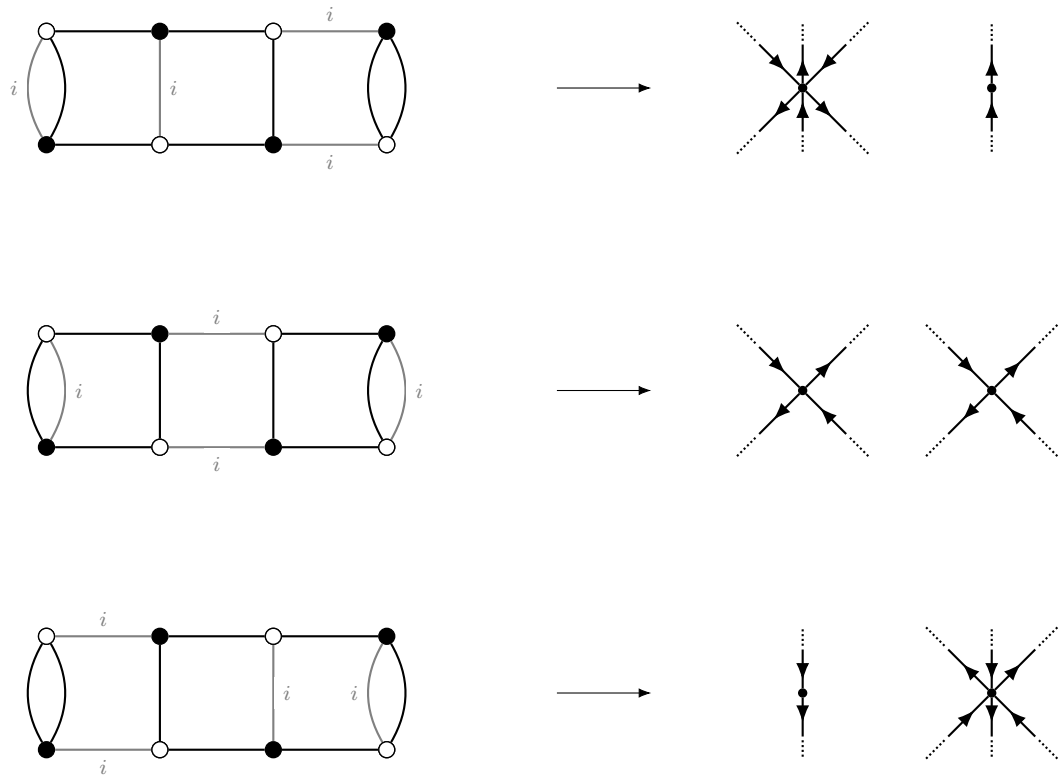

Figure 6.4.2 – For the purpose of studying the $\hat{\imath}$-bubbles of G_p, we replace each of its $\hat{0}$-bubbles by vertices, whose number, in- and out-degrees are prescribed by the positions of the i-edges in the $\hat{0}$-bubble. In this example we have taken the same base graph G as in Figure 6.4.1.

Now, to obtain results about the asymptotic number of $\hat{\imath}$-bubbles of G_p, for a fixed $i \in \{1, 2, \dots, D\}$, we will consider the simplified graph S_p^i, defined like in the quartic case: the deletion of the edges of color i decomposes any $\hat{0}$-bubble $\mathcal{B}_k$ into a certain number r_i of connected components $\mathcal{B}_k^{(1)}, \dots, \mathcal{B}_k^{(r_i)}$, having respectively, say, $2n_1, \dots, 2n_{r_i}$ vertices (with $\sum_k n_k = t$). We associate to each component $\mathcal{B}_k^{(s)}$ a vertex $v_{k,s}$ with n_s out- (resp. in-)going half-edges, corresponding to its black (resp. white) vertices, so that each half-edge inherits the labelling of its corresponding vertex (see Figure 6.4.2 for an example). We then consider the graph S_p^i on the vertices $(v_{k,s})$ (corresponding to all the components of all the $\hat{0}$-bubbles of $(G_p)_{\hat{\imath}}$), obtained by taking a uniform matching of the in- and out-half-edges: as explained in Section 6.3.1 for the quartic case, this translates the uniformity of α_0, and thus the connected components of $(G_p)_{\hat{\imath}}$ correspond to those of S_p^i.

Now, just like in the quartic case, we want to apply Theorem 6.3.5 to prove that S_p^i has a giant component. First, let us translate the characteristics of S_p^i in the notation of the directed configuration model. If deleting the color j in G gives rise to r_j vertices of respective degrees $(\delta_1^j, \delta_1^j), \dots, (\delta_r^j, \delta_r^j)$ in our simplified formulation, then S_p^i will have $q = \sum_{1 \leq j \leq D} q_j r_j$ vertices, where $q_j = \#\{k \in \{1, 2, \dots, p\} \big| \gamma_k(j) = i\}$. And for each possible degree $1 \leq \delta \leq t$, the number of vertices of degree (δ, δ) in S_p^i will be: $l_{\delta,\delta} = \sum_{1 \leq j \leq D} q_j N_{\delta,j}$, with $N_{\delta,j} = \#\{v \in \{1, \dots, r_j\} \big| \delta_v^j = \delta\}$.

Now, note that, as the γ_k are uniform, a given $i \in \{1, 2, \dots, D\}$ has an equal probability to replace any color $j \in \{1, 2, \dots, D\}$ in a given $\hat{0}$-bubble. Moreover, the γ_k are independent, so that, for given $i, j \in \{1, 2, \dots, D\}$, the number of $\hat{0}$-bubbles in which i replaces j is a binomial variable of parameters $(\frac{1}{D}, p)$:

$$\#\{k \in \{1, 2, \dots, p\} \big| \gamma_k(j) = i\} \sim \mathrm{Bin}\left(\frac{1}{D}, p\right).$$

Thus, applying Hoeffding's inequality, we have once again:

$$\mathbb{P}\left(\left|\frac{q_j}{p} - \frac{1}{D}\right| \geq \sqrt{\frac{\ln p}{p}}\right) \leq \frac{2}{p^2},$$

and for $q_j \sim p/D$, we can write $l_{\delta,\delta} = p \cdot c_\delta(1+o(1))$, $q = p \cdot c_q(1+o(1))$, $\theta = \theta_0(1+o(1))$, $d = d_0(1 + o(1))$, where:

$$c_\delta = \frac{1}{D} \sum_{1 \leq j \leq D} N_{\delta,j}, \qquad c_q = \sum_{1 \leq \delta \leq t} c_\delta$$
$$\theta_0 = \frac{\sum_\delta \delta c_\delta}{\sum_\delta c_\delta}, \qquad d_0 = \frac{\sum_\delta \delta^2 c_\delta}{\sum_\delta \delta c_\delta}.$$

Thus, S_p^i satisfies the hypotheses of Theorem 6.3.5 as long as $d_0 > 1$, *i.e.* as long as $c_1 < \sum_\delta c_\delta$. In other words, we can apply Theorem 6.3.5 if there is at least one color $j \in \{1, 2, \dots, D\}$ such that $G_{\hat{\jmath}}$ is not made of melons only, which is always the case when $D \geq 2$. Indeed, if there is one color j such that $G_{\hat{\jmath}}$ is only made of melons, then G is necessarily a "pearl necklace" (see Figure 6.4.3), and in that case, for any other color $k \in \{1, 2, \dots, D\} \setminus \{j\}$, $G_{\hat{k}}$ is connected, and in particular not made of melons only.

Proposition 6.3.6 also applies, as we have, in the notation of the proposition: $\frac{l_{1,1}}{n} = \frac{c_1}{c_q} + o(1)$. This yields the following theorem, analogous to Theorem 6.3.3:

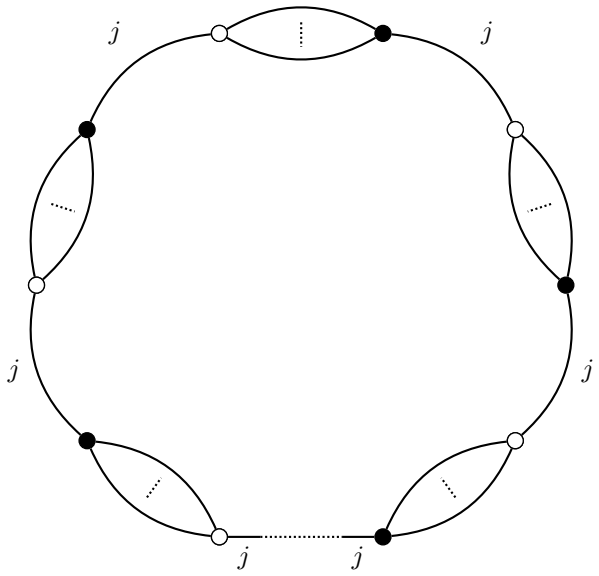

Figure 6.4.3 – A pearl necklace of color j.

Theorem 6.4.2. *For $D \geq 3$, for any $i \in \{1, 2, \ldots, D\}$, G_p has a giant $\hat{\imath}$-bubble containing $2tp - O\big(\sqrt{p \ln p}\big)$ vertices. Moreover, the expectation value of the number of $\hat{\imath}$-bubbles of G_p is:*

$$\mathbb{E}\big[k(S_p^i)\big] = c_G + 1 + o(1)$$

where $c_G = \sum_{k \geq 2} \frac{c_1^k}{k(c_q \theta_0)^k} < \infty$ as $c_1 < c_q \theta_0$.

Hence, for the total number of D-bubbles of G_p:

Corollary 6.4.3. *For $D \geq 3$, $\mathbb{E}[b_D(G_p)] = p + D\,(c_G + 1) + o(1)$.*

6.4.2 Geometry of the complex

Just like in the particular case of the quartic model, the previous study of the D-bubbles of G_p gives us insight on the typical geometry of the associated complex $\Delta(G_p)$. Indeed, once again there are p 0-points in $\Delta(G_p)$, while for any $i \in \{1, 2, \ldots, D\}$ there are at most $O\big(\sqrt{p \ln p}\big)$ i-points, one of which is the "hub" i-point having most 0-points as neighbors. The result of Theorem 6.3.8 thus also holds for any uniform-uncolored model, as long as $D \geq 3$:

Theorem 6.4.4. *Let u, v be two vertices of $\Delta(G_p)$ chosen uniformly at random and independently. Then, if $D \geq 3$, $d(u, v) = 2$ a.a.s..*

Remark. Let us note that what we have done for one fixed, connected base graph G can be generalized further to models where this base graph G is not necessarily connected (in which case, the copies of G are not $\hat{0}$-bubbles but *sets* of $\hat{0}$-bubbles), or where each $\hat{0}$-bubble is uniformly drawn from a finite set of (finite) D-colored graphs (with, once again, a randomization of the different colors): similar results will still apply, as long as the criterion $d_0 > 1$ is verified for the corresponding oriented configuration model. This is typically the case for all "interaction vertices" appearing in colored tensor models generalizing the quartic one.

This brings an end to the pursuit of continuum scaling limits in the spirit of the Brownian sphere in uniform-uncolored models. As noted in Section 6.2.1, the results of

numerical simulations for Euclidean Dynamical Triangulations had already hinted that in higher dimensions, models of random triangulations with no or low constraints on curvature yield quite degenerate limit spaces. We can thus see both our uniform and uniform-uncolored models as instances of a crumpled phase, which would be the first ones to be investigated mathematically and not by simulations.

To find promising scaling limits, we must turn to more complicated models, and works in theoretical physics suggest that the Gurau degree (which is a way to quantify the curvature of trisps) must play a central role in our tentative distributions.

6.5 Conclusion

We have studied in this work two random models on bipartite $(D+1)$-colored graphs and the associated complexes. The first one, U_p^D, is uniform on the bipartite $(D+1)$-colored graphs with $2p$ labelled vertices. We have proved that, *a.a.s.*, U_p^D is connected and the associated complex $\Delta(U_p^D)$ has exactly one point of each color, which is a quite singular behavior, and is not satisfactory for the purpose of finding scaling limits. We have also obtained a Central Limit Theorem for the genus of one jacket of U_p^D. In the second one, G_p, we have fixed the $\hat{0}$-bubbles to be copies of a given D-colored graph G, and kept the matching of the 0-half-edges uniform. G_p is also connected *a.a.s.*, but the number of points of $\Delta(G_p)$ grows linearly with p. However, the average distance between two points of $\Delta(G_p)$ is *a.a.s.* 2, which also halts our quest for a continuum limit. We have more extensively studied the special case of Q_p^D, in which G is quartic. In that particular case, we have also obtained a Central Limit Theorem for the genus of one jacket, and the arguments we employed also yielded a Central Limit Theorem for the genus of a uniform map of size p, as $p \to \infty$.

In the context of quantum gravity, we wish to find random models on colored complexes exhibiting a scaling limit, that can be interpreted as a continuum space-time. We have seen that these models do not fit this purpose. However, their study involved the adaptation of several combinatorial and probabilistic tools to the subject of edge-colored graphs, which will surely prove to be valuable when tackling more complicated models, as we plan to do. Those new models will undoubtely have to involve the Gurau degree more deeply, as it is a crucial quantity in the theory of colored tensor models.

Troisième partie

Triangulations eulériennes

CHAPITRE 7

Convergence des triangulations eulériennes planaires

Contents

7.1 Introduction

7.1.1 Context

Eulerian triangulations are maps whose faces are all of degree 3, and whose vertices are all of even degree. They can be encountered in several contexts. As their definition is quite straightforward, they are already an object of interest in themselves in enumerative combinatorics (see [Tut62; BDFG04; BMS00; AB12]). Moreover, they are in bijection with combinatorial objects such as **constellations** and **bipartite maps**, and geometrical objects such as **Belyi surfaces**. They also correspond to the two-dimensional case of **colored tensor models**, an approach to quantum gravity that generalizes matrix models to any dimension, detailed in Chapter 4.

The main aim of this chapter is to show that large planar rooted Eulerian triangulations converge to the Brownian map (see Theorem 7.3.1 for a more precise statement). Along the way, we explore uncharted properties of planar Eulerian triangulations. This allows us to construct, in the case of Eulerian triangulations, many random objects and structures whose equivalents already exist for other families of planar maps.

Let us now briefly sketch how this exploration ties in together with proving Theorem 7.3.1.

If one wants to prove that a family of planar maps converges to the Brownian map, the classical method is to use a **bijection** between this family, and a family of labeled

trees, whose labels keep track of the distances in the map. Obtaining a joint scaling limit for the trees and their label functions is a classical procedure, however, it then remains to deduce from this limit, a scaling limit for the metric space induced by the maps. This was first done independently by Le Gall for triangulations and $2p$-angulations [LG13], and Miermont for quadrangulations [Mie13], using different technical tools. The list of families amenable to this method has been expanded since then to general maps, general bipartite maps, simple triangulations and odd p-angulations [BJM14; Abr16; ABA17; ABA][1].

A more recent method applies to local modifications of distances, in families that are already known to converge to the Brownian map. This method, established by Curien and Le Gall in [CLG19] for usual triangulations, uses a **layer decomposition** of the maps, rather than a bijection with trees. This makes it possible to use an ergodic subbaditivity argument, to obtain that the modified and original distances are asymptotically proportional.

In the case of Eulerian triangulations, there exists a bijection with a family of labeled trees, but, as we will explain in the sequel, these labels do not correspond to the usual graph distance from the root, but to an oriented pseudo-distance. This implies that we cannot a priori recover the distances from the labels, so that, while it is still easy to get a scaling limit at the level of labeled trees, we are stuck there without any additional ingredient. This ingredient turns out to be the layer decomposition. Indeed, the oriented pseudo-distance can be seen as a local modification of the usual graph distance, so that the layer decomposition method applies to Eulerian triangulations equipped with these two distances, and this yields that the oriented pseudo-distance is asymptotically proportional to the usual graph distance, so that the labels do keep track of it up to a small error. This proves to be enough to obtain convergence to the Brownian map.

This is the first time that a combination of these two methods is needed to show such a convergence. It would be interesting to apply this to other families of maps, such as Eulerian quadrangulations.

Note that one could want to prove the convergence of planar Eulerian triangulations to the Brownian map using their bijection with bipartite maps, as the convergence for these has already been proven in [Abr16]. However, this would necessitate to treat the distances on an Eulerian triangulation as a local modification of the distances on the corresponding bipartite map, and thus use a layer decomposition of bipartite maps. As this has not been achieved yet, this route is a priori not easier than the one undertaken here, which has the advantage of uncovering a lot of properties of Eulerian triangulations. However, achieving a layer decomposition of bipartite maps would be interesting in itself.

7.1.2 Outline

In the whole chapter, $\mathbf{c}_0$ refers to the constant $\mathbf{c}_0 \in [2/3, 1]$ of Proposition 7.8.1. The main result of this chapter is Theorem 7.3.1. As the full statement of this theorem necessitates a bit of notation, we postpone it to Section 7.3. We can however now give a weak version of it:

Theorem 7.1.1. *Let $\mathcal{T}_n$ be a uniform random rooted Eulerian planar triangulation with n black faces, equipped with its usual graph distance d_n. Let $(\mathbf{m}_\infty, D^*)$ be the Brownian map. The following convergence holds*

$$n^{-1/4} \cdot (V(\mathcal{T}_n), d_n) \xrightarrow[n\to\infty]{(d)} \mathbf{c}_0 \cdot (\mathbf{m}_\infty, D^*),$$

[1] Note that we stay purposefully vague here, and that some of these results rely on bijections with other types of decorated trees

for the Gromov-Hausdorff distance on the space of isometry classes of compact metric spaces.

We will see how this can be obtained from the following result:

Theorem 7.1.2. *Let $\mathcal{T}_n$ be a uniform random rooted Eulerian planar triangulation with n black faces, and let $V(\mathcal{T}_n)$ be its vertex set. For every $\varepsilon > 0$, we have*

$$\mathbb{P}\left(\sup_{x,y \in V(\mathcal{T}_n)} |d_n(x,y) - \mathbf{c}_0 \vec{d}_n(x,y)| > \varepsilon n^{1/4} \right) \xrightarrow[n\to\infty]{} 0.$$

After giving a precise description of the structure of Eulerian triangulations endowed their oriented pseudo-distance in Section 7.2, in Section 7.3 we will give the complete statement of Theorem 7.3.1, and explain how to prove it using Theorem 7.1.2. The rest of the chapter is then devoted to proving Theorem 7.1.2.

Let us sketch the different steps of this proof. After some technical statements in Section 7.4, we detail in Section 7.5 the decomposition of finite rooted planar Eulerian triangulations (possibly with a boundary) into *layers*, determined by the oriented distance from the root. This decomposition makes it possible to describe the random triangulation $\mathcal{T}_n$, uniform over planar Eulerian triangulations with n black faces, in terms of a branching process whose generations are associated to the layers of $\mathcal{T}_n$. This nice description of $\mathcal{T}_n$ allows us to take the limit $n \to \infty$, to define the Uniform Infinite Planar Eulerian triangulation, $\mathcal{T}_\infty$, that is naturally endowed with a decomposition into an infinite number of layers. Now, in Section 7.6, we take a local limit of $\mathcal{T}_\infty$ where we view these layers "from infinity", which yields the Lower Half-Planar Eulerian Triangulation $\mathcal{L}$. In Section 7.8, we explain how the construction of this half-plane model makes it possible to obtain Theorem 7.1.2. First, the layers of $\mathcal{L}$ are i.i.d., which makes it straightforward to apply an ergodic subbadditivity argument to the graph distance d between the root of $\mathcal{L}$ and the n-th layer of $\mathcal{L}$. Then, we detail how this result can carry over to finite Eulerian triangulations, first for the graph distance between the root and a random uniform vertex, then between any two vertices, as stated in Theorem 7.1.2. The transfer of the results from $\mathcal{L}$ to finite triangulations necessitates estimates on the distances in $\mathcal{L}$ that are derived in Section 7.7.

As our use of the layer decomposition to get the asymptotic "proportionality" of the oriented and usual distances follows closely the chain of arguments of [CLG19] (albeit with additional difficulties), we purposefully use similar notation, and will omit some details of proofs when they are very similar and do not present any additional subtleties in our case. This is especially the case in Section 7.7.2 and Section 7.8.

7.2 Structure of Eulerian triangulations and bijection with trees

For basic definitions related to graphs and maps, we refer to Section 3.1 in the introduction. We consider here rooted planar Eulerian triangulations, that is, maps whose faces have all degree 3, and whose vertices have all even degree. Bouttier, Di Francesco and Guitter [BDFG04] have established a bijection between this family of maps and a particular class of labeled trees, whose construction we now briefly recall.

7.2.1 Bijection with trees

Let A be such a rooted planar Eulerian triangulation. The orientation of the root edge of A fixes a **canonical orientation** of all its edges, by requiring that orientations alternate around each vertex. By construction, edges around a given face are necessarily oriented either all clockwise, or all anti-clockwise. This induces a natural bicoloration of the faces of A, by setting for instance that clockwise faces are black, and anti-clockwise faces, white.

From now on, any mention of orientation refers to this canonical orientation.

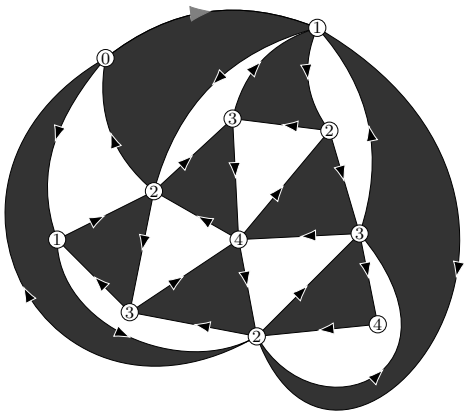

Figure 7.2.1 – An Eulerian triangulation with its canonical orientation, bicoloration and oriented geodesic distances.

We define the **oriented geodesic distance** $\vec{d}$ of any vertex of A from the origin (that is, the root vertex ρ), as the minimal length of an oriented path from the origin to that vertex. This gives a labeling of the vertices of A, such that the sequence of labels around any triangle, starting from the minimal label, is of the form $n \to n+1 \to n+2$.

Let us state a useful fact. Denoting by d the usual graph distance, in any Eulerian triangulation, we always have:

$$d \leq \vec{d} \leq 2d, \tag{7.2.1}$$

as, in the worst case, the oriented distance forces a path to go through two edges of a triangle instead of just taking the third one.

Let us now introduce a bit of notation that will be of use in the sequel.

Definition 7.2.1. In a rooted Eulerian triangulation A, a **vertex of type n** is a vertex whose canonical labeling by the oriented geodesic distance is n. An **edge of type $n \to m$** is an oriented edge that starts at a vertex of type n and ends at a vertex of type m. A **triangle of type n** is a triangle adjacent to a vertex of type $n-1$, one of type n and one of type $n+1$.

By keeping only the edge of type $n+1 \to n+2$ in each black face of type $n+1$, we construct a graph T whose vertices are labeled by integers, and which is **well-labeled** in the sense that the labels of adjacent vertices differ by exactly 1. Moreover, by construction those labels are positive.

Lemma 7.2.2 ([BDFG04]). *For any planar rooted Eulerian triangulations A, the corresponding labeled graph T is a plane tree.*

This tree is naturally rooted at the corner of a 1-vertex, that corresponds to the root edge of A (see Figure 7.2.2).

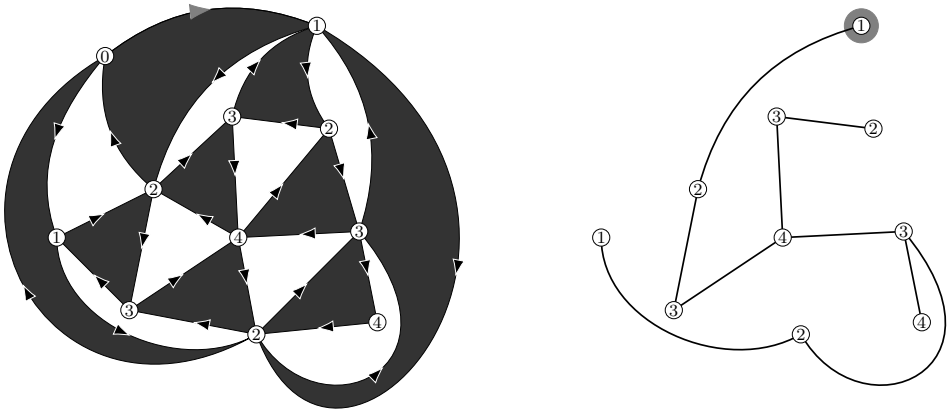

Figure 7.2.2 – The construction of the well-labeled tree associated to the triangulation of Figure 7.2.1.

The inverse construction consists in building iteratively the black triangles of A. Starting from a well-labeled rooted plane tree with positive integers, the first step consists in adding an origin (labeled 0). We then create a black triangle of type 1 to the right of each edge of type $1 \to 2$, by adding edges between the origin and the two vertices of the edge. The creation of these black triangles splits the original external face into a number of white faces. By construction, the clockwise sequence of labels around any of these white faces is of the form $0 \to 2 \to \cdots \to 2 \to 1$, where all the labels between the first and last "2" are greater or equal to 2, and all increments but the first are ± 1. For each white face F that is not already a triangle, and for each type-$(2 \to 3)$ edge whose right side is adjacent to F, we create a black triangle of type 2 to the right of this edge, by adding edges between its vertices and the unique vertex labeled 1 around F. This induces a splitting of F into smaller white faces, and we repeat the procedure again, until all labels are exhausted. This yields an Eulerian triangulation A rooted at the $0 \to 1$ edge linking the origin to the root of T (see Figure 7.2.3).

As the second construction only consists of adding edges of type $n \to n+1$ and $n+2 \to n$ to the edges of the tree (that are of type $n+1 \to n+2$), it is clear that starting from a tree T, applying this construction to obtain a triangulation A, then applying the first construction to A, gives back T. A counting argument suffices to conclude that we do have a bijection. Indeed, from [Tut62], the number of Eulerian triangulations with n black triangles is

$$\#\mathbb{T}_n = 3 \cdot 2^{n-1} \cdot \frac{(2n)!}{n!(n+2)!},$$

and, as derived in [BDFG04], the number of well-labeled trees with n edges and positive labels agrees with this formula.

In the sequel, it will be more convenient to deal with trees whose labels are not necessarily positive. For that purpose, we choose some vertex v in A, and shift all the distance

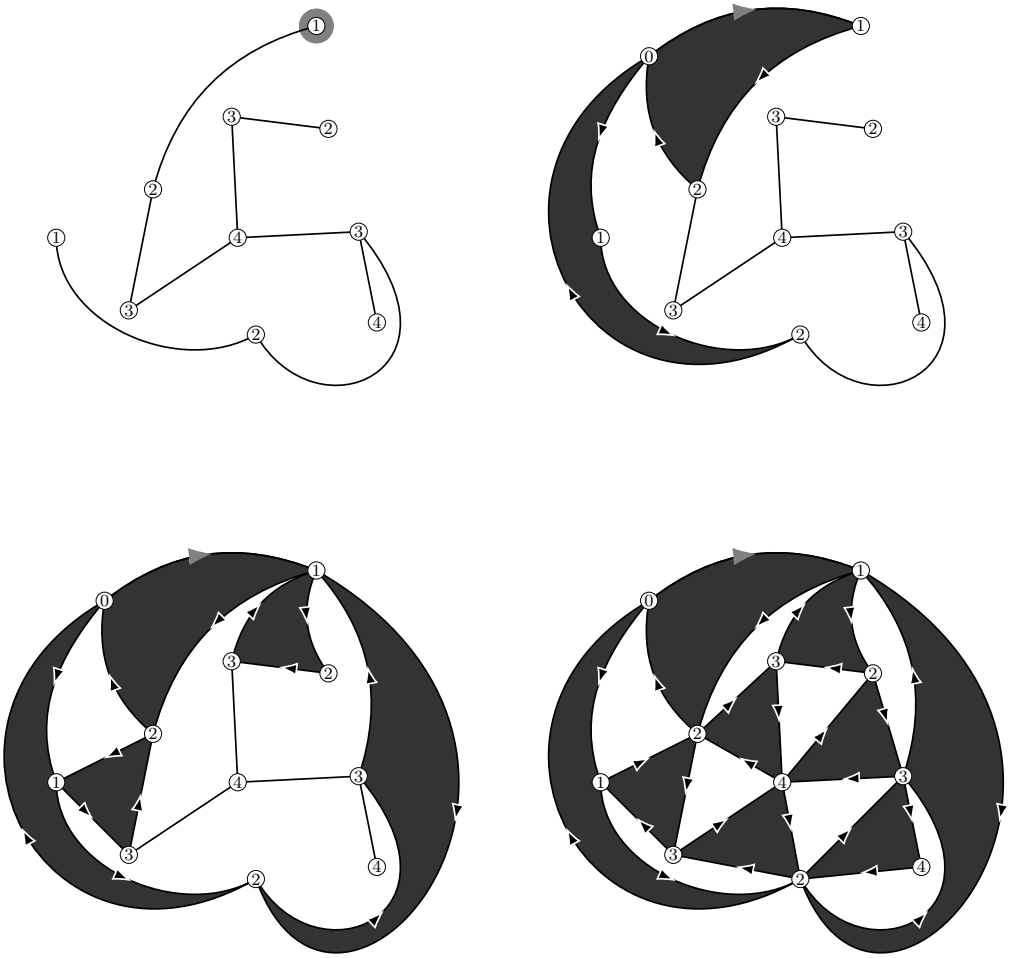

Figure 7.2.3 – The inverse construction of the triangulation of Figure 7.2.1 from the labeled tree.

labels by $\vec{d}(\rho, v)$, that is, define a new labeling l on the vertices of T by:

$$l(u) := \vec{d}(\rho, u) - \vec{d}(\rho, v).$$

With this shifting, we obtain a bijection between rooted, pointed planar Eulerian triangulations with n black faces, and well-labeled trees with n edges.

Note that, for every vertex u of T, the distance from the root of A to u is given by:

$$\vec{d}(\rho, u) = l(u) - \min_{v \in V(T)} l(v) + 1. \tag{7.2.2}$$

To get more general information on the oriented distances in A from the labels of T, we need a bit of additional notation.

First observe that, with the construction of A from T, a corner c of T is always incident in A to an edge oriented from the first corner c' encountered when going anticlockwise around T, starting at c, and that has label $l(c) - 1$. Indeed, either this corner was already adjacent to c in T, or we create an edge between them when adding a black triangle to the right of the edge of type $l(c) \to l(c) + 1$ that starts at c.

We call c', the **predecessor** of c, and denote it by $p(c)$. (The predecessor of a corner of minimal label is naturally the corner of the origin to which it is linked in the first step of the construction.) We also call $p^k(c)$ the k-th predecessor of c, whenever it is defined.

For a corner c of T, the edge $p(c) \to c$ in A is obviously of type $\vec{d}(c) - 1 \to \vec{d}(c)$. This implies that the path from the origin to c going through all its predecessors: $\rho \to p^{\vec{d}(c)-1}(c) \to \cdots \to p(c) \to c$ is a geodesic for $\vec{d}$ in A.

For any pair of corners c, c' in T, we denote by $[c, c']$ the set of corners of T encountered when starting from c, going anticlockwise around T, and stopping at c'. The property (7.2.2) yields the following bound on oriented distances in A:

Proposition 7.2.3. *Let c, c' be two corners of T, with corresponding vertices u, v. Then*

$$\vec{d}(u, v) \leq 2 \left(l(u) + l(v) - 2 \min_{c'' \in [c, c']} l(c'') + 2 \right).$$

Proof. Let $m = \min_{c'' \in [c, c']} l(c'')$, and let c'' be the first corner in $[c, c']$ such that $l(c'') = m$. Then c'' is the $(l(c) - m)$-th predecessor of c. Moreover, by definition, $p(c'')$ does not belong to $[c, c']$, so that it is also the $(l(c') - m)$-th predecessor of c'. Thus, the predecessor geodesic $p(c'') \to c'' \to \cdots \to c$, concatenated with the similar geodesic $p(c'') \to \cdots \to c'$, is a simple path in A made of $l(c) + l(c') - 2m + 2$ edges. However, part of it is not oriented from c to c', so that we lose a multiplicative factor of 2 when deducing a bound on the distance from u to v. □

As will be clearer in the proof of Theorem 7.3.1, this factor of 2 is really the stumbling block that prevents us from reaching the convergence to the Brownian map using only the bijective approach.

7.2.2 Convergence of the labeled trees

From what precedes, starting from a uniform random rooted, pointed planar Eulerian triangulation with n black faces, we get a uniform random well-labeled tree $\mathscr{T}_n$ with n edges. Let us now explain how we can make sense of taking a continuum scaling limit of the latter. We first define the **contour process** of $\mathscr{T}_n$: let $e_0, e_1, \cdots, e_{2n-1}$ be the sequence of oriented edges bounding the unique face of $\mathscr{T}_n$, starting with the root edge,

and ordered counterclockwise around this face. Then let $u_i = e_i^-$ be the i-th visited vertex in this contour exploration, and set the **contour process** of $\mathscr{T}_n$ at time i:

$$C_n(i) := d_{\mathscr{T}_n}(u_0, u_i),\ 0 \leq i \leq 2n-1,$$

with the convention that $u_{2n} = u_0$ and $C_n(2n) = 0$. We also extend C_n by linear interpolation between integer times: for $0 \leq s \leq 2n$

$$C_n(s) = (1 - \{s\})C_n(\lfloor s \rfloor) + \{s\}C_n(\lfloor s \rfloor + 1),$$

where $\{s\} = s - \lfloor s \rfloor$ is the fractional part of s. Thus, the contour process C_n is a non-negative path of length $2n$, starting and ending at 0, with increments of 1 between integer times. We will use the **rescaled contour process** of $\mathscr{T}_n$:

$$C_{(n)}(t) = \frac{C_n(2nt)}{\sqrt{2n}},\ 0 \leq t \leq 1.$$

We define similarly the **rescaled label function** of $\mathscr{T}_n$:

$$L_{(n)}(t) = \frac{L_n(2nt)}{n^{1/4}},\ 0 \leq t \leq 1,$$

where, similarly, we start by defining $L_n(i)$ as the label of u_i for $i \in \{0, 1, \ldots, 2n\}$, then interpolate between integer times.

Finally, for a continuous, non-negative function $f : [0,1] \to \mathbb{R}_+$ such that $f(0) = f(1) = 0$, for any $s, t \in [0,1]$, we set

$$\check{f}(s,t) = \inf\{f(u) | s \wedge t \leq u \leq s \vee t\}.$$

Then we have the following result:

Theorem 7.2.4. [JM05] *It holds that*

$$\left(C_{(n)}, L_{(n)}\right) \xrightarrow[n\to\infty]{(d)} (\mathbb{e}, Z), \tag{7.2.3}$$

in distribution in $\mathcal{C}([0,1], \mathbb{R})^2$*, where* $\mathbb{e}$ *is a standard Brownian excursion, and, conditionally on* $\mathbb{e}$*,* Z *is a continuous, centered Gaussian process with covariance*

$$Cov(Z_s, Z_t) = \check{\mathbb{e}}_{s,t},\ s, t \in [0,1].$$

As this convergence will be crucial to ultimately prove the convergence of Eulerian triangulations to the Brownian map, to describe and analyse these triangulations, we will need to use their *oriented* distances, instead of the usual graph distance.

7.2.3 Structure for oriented distance

Let us consider a rooted Eulerian triangulation A, equipped with its canonical orientation and oriented geodesic distance $\vec{d}$. For each type-n black face f of A, there is exactly one white face f' that shares its $n+1 \to n-1$ edge. We call the union of f and f' a **type-n module**. Now, imagine that for each type-n module of A, we trace the "diagonal" linking its two type-n vertices, and orient it from the black triangle to the white one (see Figure 7.2.4). We will call this, orienting the module **left-to-right**.

We now explain how to describe the union of the diagonals of type-n modules as a set of simple closed curves. First note that, by construction, this union of diagonals only goes through vertices of type n. Moreover, around each vertex u of type n, these oriented

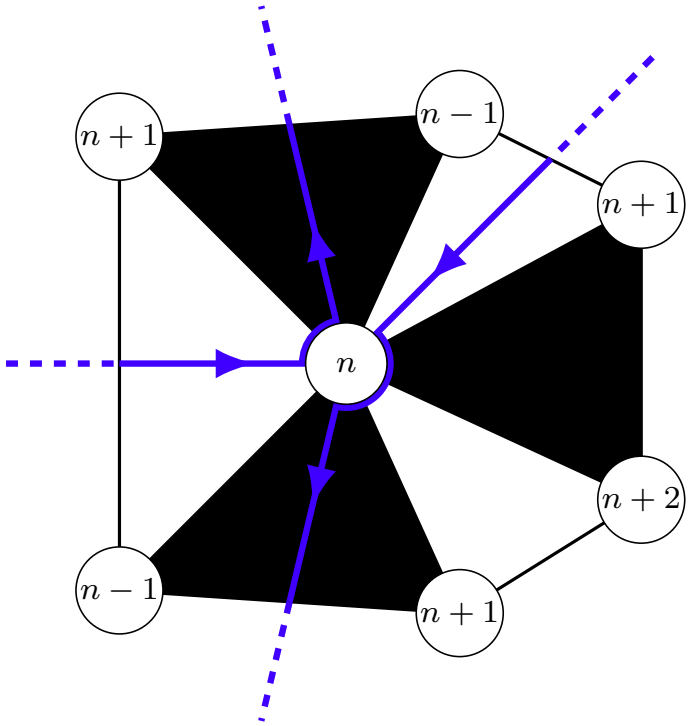

Figure 7.2.4 – The union of type-n module diagonals can be decomposed into a set of simple closed curves by pairing, at each vertex of type n, each ingoing diagonal with the next one clockwise, which is necessarily outgoing.

diagonals alternate between ingoing and outgoing. Indeed, around u, after each black type-n triangle, there is necessarily a white type-n triangle before the next black type-n triangle. This stems from the fact that the triangles around u can only be of type $n-1$, n or $n+1$, and that along each edge, the oriented geodesic distance can only change by 1 or 2 (see Figure 7.2.4). Now, to resolve the intersections at type-n vertices, we can take the convention that if a curve arrives at a vertex u by an ingoing diagonal δ, it will immediately leave u by the first outgoing diagonal that we encounter going clockwise around u, starting at δ (see Figure 7.2.4).

This yields a set of closed curves that we denote by $\boldsymbol{\mathcal{C}_n(A)}$. By construction, the curves in $\mathcal{C}_n(A)$ separate vertices at oriented distance $n+1$ or higher from the origin, and they go counter-clokwise around these vertices.

Lemma 7.2.5. *Let A be a planar rooted Eulerian triangulation. For a given vertex v at (oriented) distance at least $n+1$ from the root, there is a unique curve in $\mathcal{C}_n(A)$ that separates v from the root.*

Moreover, all curves in $\mathcal{C}_n(A)$ are simple.

Proof. First consider two disjoint curves in $\mathcal{C}_n(A)$ that separate the same vertex v from the origin. Necessarily, a geodesic path from the root to a vertex belonging to one of them should go through the other, and thus have length at least $n+1$ (see Figure 7.2.5).

Now, if two curves of $\mathcal{C}_n(A)$ intersect at a vertex of type n, then by our resolution rule, they cannot go counterclockwise around the same region of A (see Figure 7.2.6), and, as explained before, these are precisely the regions they separate from the origin.

This rule also implies that a curve $\mathscr{C}$ in $\mathcal{C}_n(A)$ cannot go twice through the same type-n vertex. Indeed, if that were the case, then $\mathscr{C}$ would separate from the origin vertices of oriented distance $n-1$ and less, so that any oriented geodesic from the origin to these vertices should be of length at least $n+1$ (see Figure 7.2.6). □

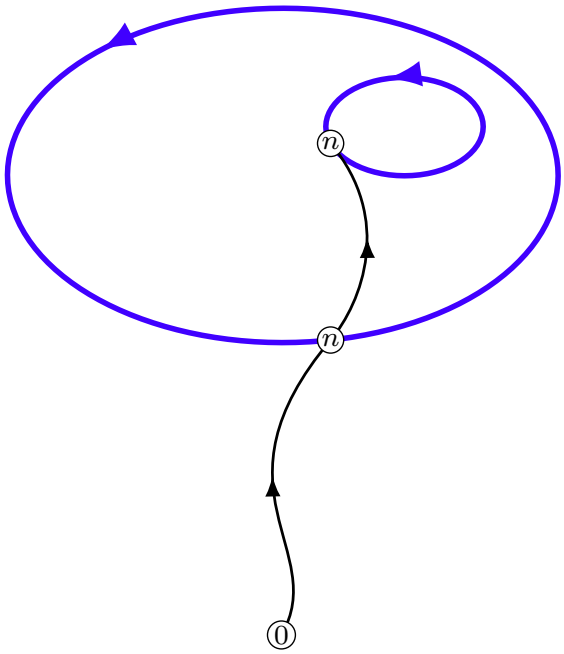

Figure 7.2.5 – Two disjoint curves in $\mathcal{C}_n(A)$ cannot encircle one other.

We define the **ball $\mathcal{B}_n(A)$** as the submap of A obtained by keeping only the faces and edges of A incident to at least a vertex at distance $n-1$ or less from the origin, cutting along the edges of type $n \to n+1$, and filling in the produced holes by simple faces (see Figure 7.2.7 for a local depiction of this procedure). Thus, in $\mathcal{B}_n(A)$, for each closed curve $\mathscr{C} \in \mathcal{C}_n(A)$, we have replaced all faces that $\mathscr{C}$ separates from the root, by a single, simple face. In particular, if two faces of A of type n share a type-$(n \to n+1)$ edge, in $\mathcal{B}_n(A)$ their respective type-$(n \to n+1)$ edges are not identified, so that their common type-$(n+1)$ vertex gives rise to two vertices in $\mathcal{B}_n(A)$ (see Figure 7.2.8). Two type-n faces f, f' may also share a type-$(n+1)$ vertex v but no edge: in that case, it means that v is also shared by faces of types $n+1$, so that we would need to add these faces and the type $n \to n+1$ edges they share with f and/or f', in order to identify the type-$(n+1)$ vertices of f and f' into v. Note that as $\mathcal{B}_n(A)$ contains all the type-$(n-1 \to n)$ edges of A, type-n vertices of A are never duplicated in $\mathcal{B}_n(A)$.

Thus, $\mathcal{B}_n(A)$ is an Eulerian triangulation with simple boundaries[2] (as many as curves in $\mathcal{C}_n(A)$), and the faces adjacent of $\mathcal{B}_n(A)$ to these boundaries compose the type-n modules of A, so that each part of $\partial\mathcal{B}_n(A)$ is **alternating**, that is, the adjacent faces alternate between black and white.

Let us also formalize the definition of the complement of $\mathcal{B}_n(A)$. It is naturally obtained from A by removing the faces and edges of A that are incident to at least a vertex at distance $n-1$ or less from the origin. Note that it is made of as many connected components as there are curves in $\mathcal{C}_n(A)$, as it is also the number of boundaries of $\mathcal{B}_n(A)$. Consider some $\mathscr{C} \in \mathcal{C}_n(A)$, and write $M(A, \mathscr{C})$ for the corresponding connected component of $A \setminus \mathcal{B}_n(A)$. $M(A, \mathscr{C})$ is a planar Eulerian triangulation with a boundary, which has the same length as the corresponding one of $\mathcal{B}_n(A)$, and is also alternating. However, the boundary of $M(A, \mathscr{C})$ is not necessarily simple. More precisely, a type-$(n+1)$ vertex v of A that sits on the boundary of $M(A, \mathscr{C})$ is attached to the type-$(n \to n+1)$ edges and type-$(n+1)$ faces that are adjacent to v in A, as they were excluded from $\mathcal{B}_n(A)$, so that v may be a separating vertex in the external face of $M(A, \mathscr{C})$. This is not the case

[2]Note that these boundaries may share a vertex, but not an edge.

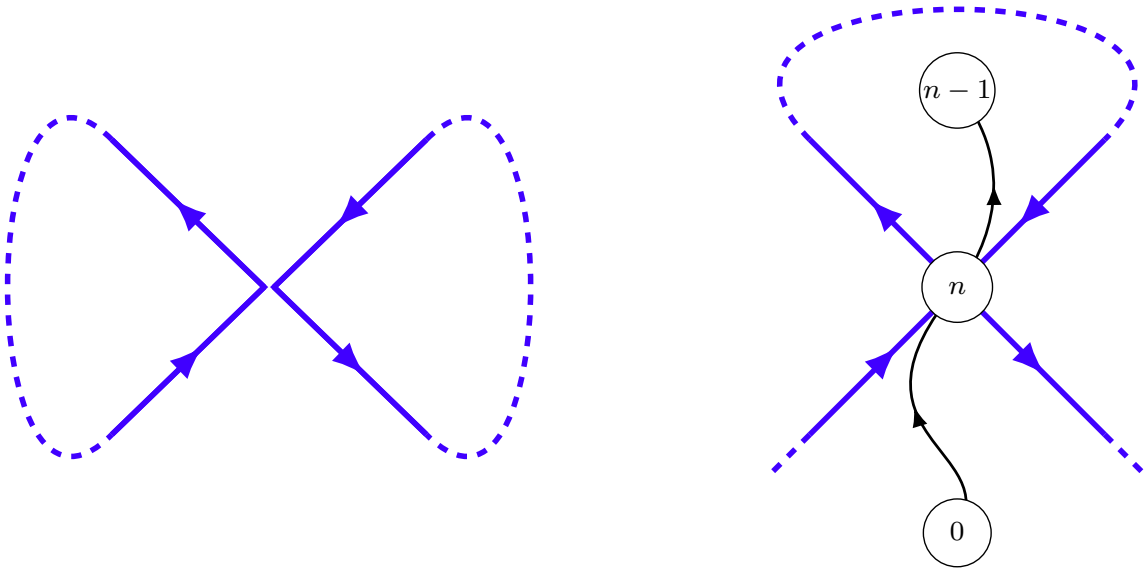

Figure 7.2.6 – From the rule we have chosen to resolve intersections, two curves in $\mathcal{C}_n(A)$ going through the same vertex cannot encircle one other (left), and one curve cannot go through the same vertex twice (right).

for type-n vertices, as $\mathcal{B}_n(A)$ contains all the type-$(n-1 \to n)$ edges and type-n faces of A. Thus, the boundary of $M(A, \mathscr{C})$ can have separating vertices, but only on boundary vertices that have a white triangle before them and a black one after (as it corresponds to the type-$(n+1)$ vertices of A). We call such boundary conditions **semi-simple**.

Let v be a distinguished vertex of A at oriented distance at least $n+2$ from the root. We can now define the **hull $\mathcal{B}_n^\bullet(A)$** of $\mathcal{B}_n(A)$, as the union of $\mathcal{B}_n(A)$ and all the connected components of its complement that do not contain v. More precisely, for each curve $\mathscr{C} \in \mathcal{C}_n(A)$ that does not separate v from the origin, we glue the boundary of $M(A, \mathscr{C})$ to the corresponding boundary of $\mathcal{B}_n(A)$. This operation is well-defined, as the latter is simple, and they both have the same length. The resulting map $\mathcal{B}_n^\bullet(A)$ has only one boundary, that corresponds to $\mathscr{C}^*$, the unique curve of $\mathcal{C}_n(A)$ that separates v from the origin.

In the sequel, we will use the notion of **local distance** between rooted maps. Let $\mathcal{M}$ be the set of finite rooted maps, for $m, m' \in \mathcal{M}$, we define the **local distance** between m and m' as

$$d_{loc}(m, m') = \frac{1}{1 + \sup\{R \geq 1 | \mathcal{B}_R^d(m) = \mathcal{B}_R^d(m')\}},$$

where $\mathcal{B}_R^d(m)$ is defined similarly as before, replacing $\vec{d}$ by the usual graph distance. It is clearly a distance on $\mathcal{M}$, and the completion $(\overline{\mathcal{M}}, d_{loc})$ of the space $(\mathcal{M}, d_{loc})$ is a Polish space. The notion of convergence in this space will be called **local limit**. The elements of $\overline{\mathcal{M}} \setminus \mathcal{M}$ are thus **infinite** maps that can be defined as the local limit of finite rooted maps.

Note that, from (7.2.1), if A_n is a sequence of rooted Eulerian triangulations (possibly with a boundary), and A a rooted planar map, the property that all oriented balls of A_n converge to those of A, as n tends to infinity, is equivalent to the same property for non-oriented balls, which is precisely the definition of the convergence of A_n to A in the sense of local limits of rooted planar maps.

As the topology induced by the local distance is what will really matter in the sequel,

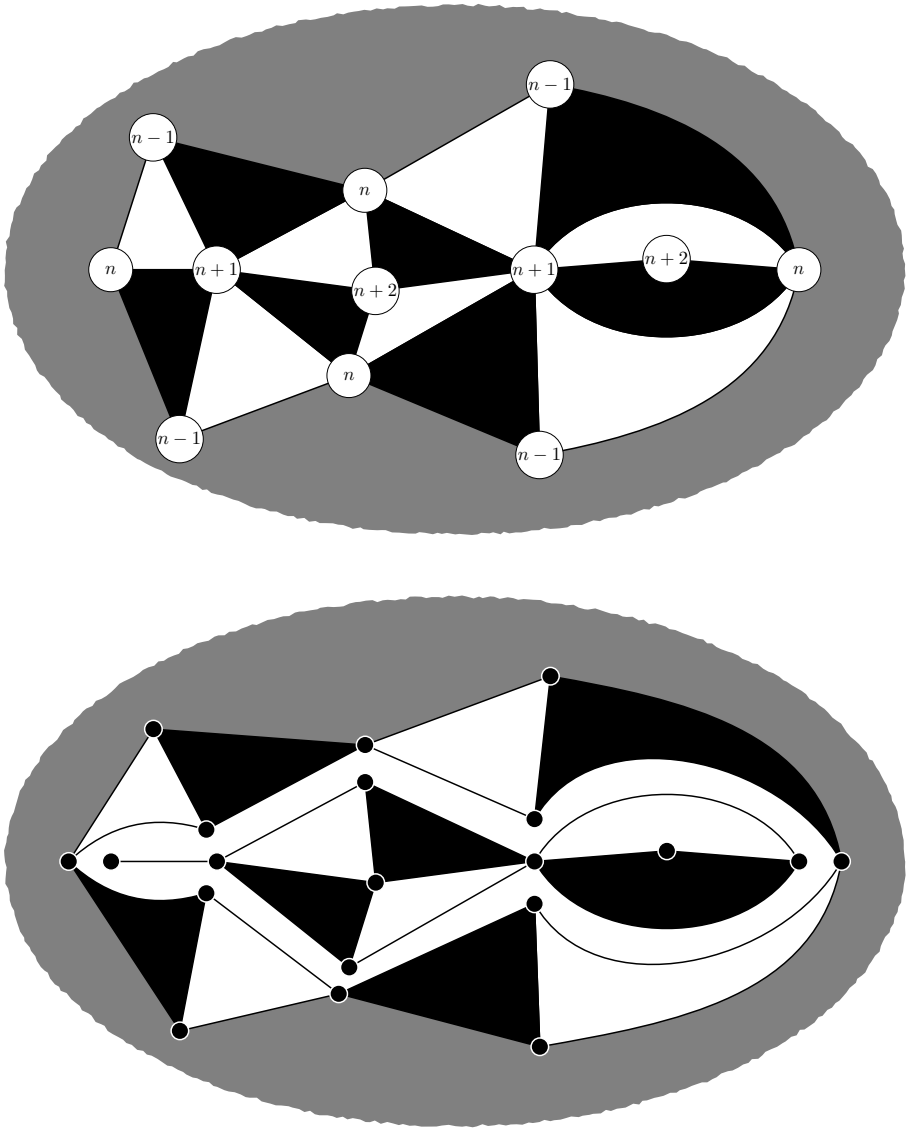

Figure 7.2.7 – In an Eulerian triangulation (top), we cut along the edges of type $n \to n+1$ to separate the ball of radius n from the components of its complement (bottom). This possibly induces the duplication of edges and vertices in the ball.

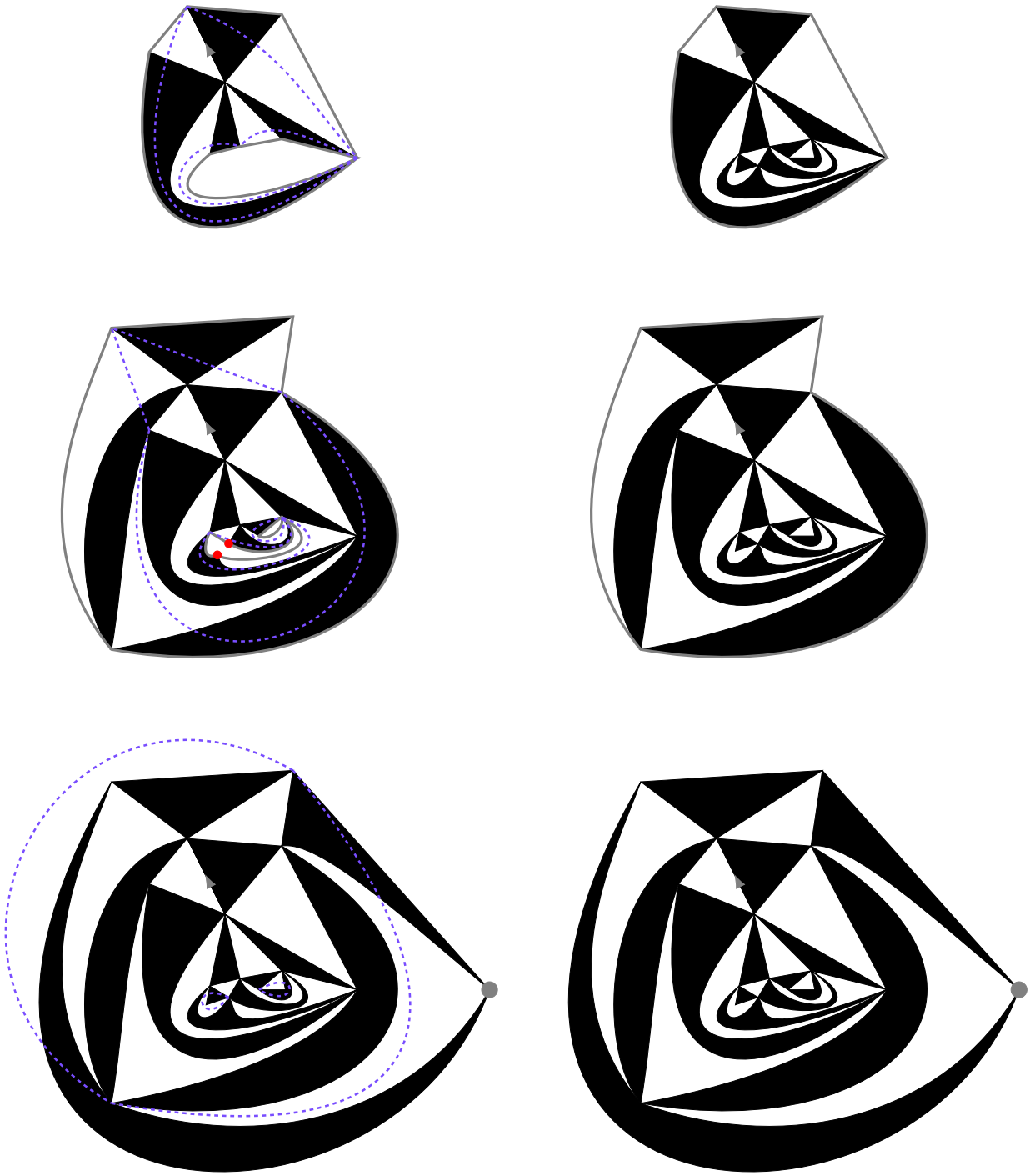

Figure 7.2.8 – A rooted, pointed Eulerian triangulation (bottom right) and its balls (left) and corresponding hulls (right). The module "diagonals" are in dashed purple, and the boundaries of the balls and hulls in solid gray. We can see an example of duplication of vertices in the ball of radius 2, marked in red.

rather than the actual value of the local distance between two maps, we can forget the general definition of the local distance, and just compare the oriented balls of Eulerian triangulations.

7.3 Convergence to the Brownian map

We will now state and give the proof of the main result of this chapter.

Before doing so, let us recall the construction of the Brownian map, and introduce some notation. As in Section 7.2.2, we write $\mathbb{e}$ for a standard Brownian excursion, and Z for the "head" of the Brownian snake driven by $\mathbb{e}$, *i.e.*, conditionally on $\mathbb{e}$, Z a continuous, centered Gaussian process on $[0,1]$ with covariance

$$Cov(Z_s, Z_t) = \check{\mathbb{e}}_{s,t},\ s,t \in [0,1].$$

The Brownian excursion $\mathbb{e}$ encodes the **Continuum Random Tree** $(\mathscr{T}_{\mathbb{e}}, d_{\mathbb{e}})$, defined by:

$$d_{\mathbb{e}}(s,t) = \mathbb{e}(s) + \mathbb{e}(t) - 2\check{\mathbb{e}}_{s,t}$$
$$\mathscr{T}_{\mathbb{e}} = [0,1]/\{d_{\mathbb{e}} = 0\}.$$

The function $d_{\mathbb{e}}$, which is a pseudo-distance on $[0,1]$, induces a true distance on $\mathscr{T}_{\mathbb{e}}$ via the canonical projection $p_{\mathbb{e}} : [0,1] \to \mathscr{T}_{\mathbb{e}}$, to $\mathscr{T}_{\mathbb{e}}$.

Almost surely, there is a unique $s \in [0,1]$ such that $Z_s = \inf Z$ [LGW06]. We then denote this point by s_*, and $x_* = p_{\mathbb{e}}(s_*)$ its projection on $\mathscr{T}_{\mathbb{e}}$.

We define, for $s \leq t \in [0,1]$,

$$D^\circ(s,t) = D^\circ(t,s) := Z_s + Z_t - 2\max(\min_{r\in[s,t]} Z_r, \min_{r\in[t,1]\cap[0,s]} Z_r).$$

This function does not satisfy the triangle inequality, which leads us to introduce

$$D^*(s,t) := \inf\left\{ \sum_{i=1}^{k} D^\circ(s_i,t_i) \,\middle|\, k \geq 1,\ s_1 = s, t_k = t,\ d_{\mathbb{e}}(t_i, s_{i+1}) = 0 \ \ \forall i \in \{1,2,\dots,k\} \right\}.$$

We can now define the **Brownian map**, by setting $\mathbf{m}_\infty = [0,1]/\{D^* = 0\}$, and equipping this space with the distance induced by D^*, which is still noted D^*.

Let $\mathcal{T}_n$ be a uniform random rooted Eulerian planar triangulation with n black faces, equipped with its usual graph distance d_n, and its oriented pseudo-distance $\vec{d}_n$. Let $\overline{\mathcal{T}}_n$ be the triangulation $\mathcal{T}_n$ together with a distinguished vertex o_n picked uniformly at random. Recall from Section 7.2.1 that $\overline{\mathcal{T}}_n$ is the image, by the BDG bijection, of a random labeled tree $\mathscr{T}_n$, uniformly distributed over the set of well-labeled rooted plane trees with n edges. We denote by l_n the labels of the vertices of $\mathscr{T}_n$, and enumerate as in Section 7.2.1 the vertices (or rather, the corners) of $\mathscr{T}_n$, by setting $u_i^{(n)}$ to be the i-th vertex visited by the contour process of $\mathscr{T}_n$, for $0 \leq i \leq 2n$. As before, we denote by $L_{(n)}$ the rescaled labels of the vertices of $\mathscr{T}_n$.

We define the symmetrization $\overleftrightarrow{d}_n$ of $\vec{d}_n$, by

$$\overleftrightarrow{d}_n(u,v) = \frac{\vec{d}_n(u,v) + \vec{d}_n(v,u)}{2}.$$

We also define a rescaled oriented distance $\vec{D}_{(n)}$ on $[0,1]^2$, by first setting, for $i,j \in \{0,1,\dots,2n\}$:

$$\vec{D}_{(n)}\left(\frac{i}{n},\frac{j}{n}\right) = \frac{\vec{d}_n(u_i^{(n)},u_j^{(n)})}{n^{1/4}},$$

then linearly interpolating to extend $\vec{D}_{(n)}$ to $[0,1]^2$.

We define similarly $D_{(n)}$ from d_n.

Theorem 7.3.1. *Let $(\mathbf{m}_\infty, D^*)$ be the Brownian map. There exists some constant $\mathbf{c}_0 \in [2/3,1]$, such that the following convergence in distribution holds:*

$$\left(C_{(n)}, L_{(n)}, \vec{D}_{(n)}, D_{(n)}\right) \xrightarrow[n\to\infty]{(d)} (\mathbb{e}, Z, D^*, \mathbf{c}_0 D^*)\,.$$

Consequently, we have the following joint convergences

$$n^{-1/4}\cdot(V(\mathcal{T}_n), \overleftrightarrow{d}_n) \xrightarrow[n\to\infty]{(d)} (\mathbf{m}_\infty, D^*)$$
$$n^{-1/4}\cdot(V(\mathcal{T}_n), d_n) \xrightarrow[n\to\infty]{(d)} \mathbf{c}_0\cdot(\mathbf{m}_\infty, D^*),$$

for the Gromov-Hausdorff distance on the space of isometry classes of compact metric spaces.

Note that we would like to have a statement similar to the one on $\overleftrightarrow{d}_n$ for $\vec{d}_n$. However, as $\vec{d}_n$ is not a proper distance, it does not induce a metric space structure on $V(\mathcal{T}_n)$. Thus, we would need to generalize the Gromov-Hausdorff topology to spaces equipped with a non-symmetric pseudo-distance, to be able to write such a statement.

Proof. We admit here Theorem 7.1.2, that will be proven later in the paper: for every $\varepsilon > 0$, we have

$$\mathbb{P}\left(\sup_{x,y\in V(\mathcal{T}_n)} |d_n(x,y) - \mathbf{c}_0\vec{d}_n(x,y)| > \varepsilon n^{1/4}\right) \xrightarrow[n\to\infty]{} 0. \tag{7.3.1}$$

We proceed similarly to the case of usual triangulations in [LG13].

For this whole proof, we work with the pointed triangulation $\overline{\mathcal{T}}_n$, but, as all Eulerian triangulations with n black faces have the same number of vertices, this does not introduce any bias for the underlying, non-pointed triangulation, so that the final statement also holds for $\mathcal{T}_n$.

We have, from Proposition 7.2.3, for any $0 \le i < j \le 2n$:

$$\vec{D}_{(n)}\left(\frac{i}{n},\frac{j}{n}\right) \le \frac{2}{n^{1/4}}\left(l_n(u_i^{(n)}) + l_n(u_j^{(n)}) - 2\max(\min_{k\in\{i,\dots,j\}} l_n(u_k^{(n)}), \min_{k\in\{j,\dots,2n\}\cup\{0,\dots,i\}} l_n(u_k^{(n)})) + 2\right). \tag{7.3.2}$$

As noted before, if we did not have the global multiplicative factor of 2 in (7.3.2), we could then proceed as for usual triangulations and other well-known families of planar maps. Thus, the rest of this proof will consist in proving that Theorem 7.1.2 makes it possible to "get rid" of this cumbersome factor.

We claim that the sequence of the rescaled distances $(\vec{D}_{(n)}(s,t))_{s,t\in[0,1]}$ is tight. Indeed, for any $s,s',t,t' \in [0,1]$, we have

$$|\vec{D}_{(n)}(s,t) - \vec{D}_{(n)}(s',t')| \le \vec{D}_{(n)}(s,s') + \vec{D}_{(n)}(t',t), \tag{7.3.3}$$

as $\vec{D}_n$, like $\vec{d}_n$, satisfies the triangle inequality. Then, using (7.3.2) and Theorem 7.2.4, we get that, if $|s-s'| \vee |t-t'| \leq \eta$, then, for n large enough, the right-hand side of (7.3.3) is smaller than $2\omega(Z,\eta)+\varepsilon$, where we denote by $\omega(Z,\eta)$ the supremum $\sup_{|I|\leq\eta} \omega(Z,I)$, and $\omega(f,I)$ is the modulus of continuity of f on the interval I.

Thus, along a subsequence, we have the joint convergence:

$$\left(C_{(n)}, L_{(n)}, \vec{D}_{(n)}\right) \xrightarrow[n\to\infty]{(d)} (\mathbb{e}, Z, D), \tag{7.3.4}$$

for some random continuous process D on $[0,1]^2$. In the rest of this proof, we fix a subsequence so that (7.3.4) holds, and work along this subsequence.

Note that, from Theorem 7.1.2, we also have the joint convergence of $D_{(n)}$ to $\mathbf{c}_0 D$. This already implies that D is symmetric, and thus is a pseudo-metric. We now want to show that $D = D^*$ a.s., which will conclude the proof, since this will imply the uniqueness of the limit D.

First, it is straightforward to get from (7.2.2) and (7.3.4) that, for any $s \in [0,1]$:

$$D(s_*, s) = Z_s - \inf Z. \tag{7.3.5}$$

We will now show that a.s., for every $s,t \in [0,1]$,

$$D(s,t) \leq D^\circ(s,t). \tag{7.3.6}$$

To prove this claim, let us get back to $\overline{\mathcal{T}}_n$ and $\mathscr{T}_n$. From (7.3.1), for any $\varepsilon > 0$ and any $\delta \in (0,1)$, for any n large enough, the event

$$\left| d_n(u,v) - \mathbf{c}_0 \vec{d}_n(v,u) \right| \leq \varepsilon n^{1/4} \quad \forall u,v \in V(\overline{\mathcal{T}}_n)$$

holds with probability at least $1-\delta$.

On that event, we have, for any $u,v,w \in V(\overline{\mathcal{T}}_n)$,

$$\begin{aligned} \vec{d}_n(u,v) &\leq \vec{d}_n(u,w) + \vec{d}_n(w,v) \leq \mathbf{c}_0 d_n(u,w) + \vec{d}_n(w,v) + \varepsilon n^{1/4} \\ &\leq \vec{d}_n(w,u) + \vec{d}_n(w,v) + 2\varepsilon n^{1/4}. \end{aligned} \tag{7.3.7}$$

Thus, going back to the proof of Proposition 7.2.3, when estimating oriented distances from the length of the concatenation of two predecessor geodesics, rather than having to multiply this length by 2, we just need to add $2\varepsilon n^{1/4}$.

Therefore, for any $0 \leq i < j \leq 2n$,

$$\begin{aligned} &\vec{D}_{(n)}\left(\frac{i}{n}, \frac{j}{n}\right) \\ \leq &L_{(n)}\left(\frac{i}{n}\right) + L_{(n)}\left(\frac{j}{n}\right) - 2\max\left(\min_{k\in\{i,\dots,j\}} L_{(n)}\left(\frac{k}{n}\right), \min_{k\in\{j,\dots,2n\}\cup\{0,\dots,i\}} L_{(n)}\left(\frac{k}{n}\right)\right) + \frac{2}{n^{1/4}} + 2\varepsilon. \end{aligned}$$

Thus, letting $n \to \infty$ (along our subsequence), for any $\varepsilon > 0$, we have $D \leq D^\circ + \varepsilon$ a.s., so that we get the desired inequality (7.3.6).

Moreover, as D satisfies the triangle inequality, we have

$$D(s,t) \leq D^*(s,t) \qquad \forall s,t \in [0,1] \text{ a.s.} \tag{7.3.8}$$

To replace this inequality by an equality, it now suffices to show that, for U,V chosen uniformly and independently at random in $[0,1]$, and independently from the rest, $D(U,V) \overset{(d)}{=} D^*(U,V)$. Indeed, this would imply $D = D^*$ a.e., and thus $D = D^*$ since both are continuous. To prove this, from (7.3.5), it is enough to show that $D(U,V) \overset{(d)}{=} D(s_*, U)$.

To prove this, let us get back to the discrete level for a moment. Let u_n, v_n be two vertices of $\mathcal{T}_n$ chosen indepently and uniformly at random. As $\mathcal{T}_n$ re-rooted at u_n has the same law as $\mathcal{T}_n$, we have

$$\vec{d}_n(u_n, v_n) \overset{(d)}{=} \vec{d}_n(\rho_n, v_n), \tag{7.3.9}$$

where ρ_n is the root of $\mathcal{T}_n$.

Similarly to the case of usual triangulations in [LG13], this implies the desired equality in distribution $D(U,V) \overset{(d)}{=} D(s_*, U)$. Indeed, set $U_n = \lceil (2n-1)U \rceil$ and $V_n = \lceil (2n-1)V \rceil$, which are both uniformly distributed over $\{1, 2, \dots, 2n-1\}$, so that

$$\frac{U_n}{n} \xrightarrow[n\to\infty]{(P)} U, \quad \frac{V_n}{n} \xrightarrow[n\to\infty]{(P)} V.$$

Then, from (7.3.4), we have

$$\vec{D}_{(n)}\left(\frac{U_n}{n}, \frac{V_n}{n}\right) \xrightarrow[n\to\infty]{(P)} \vec{D}(U,V).$$

Now, from (7.3.9), we have that the distribution of $\vec{D}(U,V)$ is also the limiting distribution of

$$L_{(n)}(\frac{U_n}{n}) - \min L_{(n)} + 1,$$

so that $\vec{D}(U,V)$ has the same distribution as $Z_U - \inf Z$, which is also the distribution of $D(s_*, U)$, from (7.3.5). This concludes the proof. □

7.4 Technical preliminaries

7.4.1 Consequences of the convergence of the rescaled labels

We now prove a few technical properties of $\vec{d}$ that stem from the convergence given in Theorem 7.2.4.

For any integer $n \geq 1$, let ρ_n be the root vertex of the random triangulation $\mathcal{T}_n$, uniform over the rooted planar Eulerian triangulations with n black faces. We denote by $\overline{\mathcal{T}}_n$, the triangulation $\mathcal{T}_n$ together with a distinguished vertex o_n, picked uniformly at random in $\mathcal{T}_n$. We then have the following result:

Proposition 7.4.1. *The following convergence holds:*

$$n^{-1/4}\vec{d}(\rho_n, o_n) \xrightarrow[n\to\infty]{(d)} \sup Z.$$

Consequently, the sequence $(n^{-1/4}\vec{d}(\rho_n, o_n))_{n\geq 1}$ is bounded in probability and bounded away from zero in probability.

Proof. Recall that $\overline{\mathcal{T}}_n$ is in correspondence with a random tree $\mathscr{T}_n$, uniform over the well-labeled plane trees with n edges, whose labelling we denote by l_n. We have, from (7.2.2), that

$$\vec{d}(\rho_n, o_n) = l_n(o_n) - \min_{v\in V(\mathscr{T}_n)} l(v) + 1,$$

including the case $o_n = \rho_n$ by setting $l_n(\rho_n) = \min_{v\in V(\mathscr{T}_n)} l(v) - 1$.

Then, using the convergence of Theorem 7.2.4, we get that the quantity

$$n^{-1/4}\left(l_n(o_n) - \min_{v\in V(\mathscr{T}_n)} l(v) + 1\right)$$

converges in distribution to $Z_U - \inf Z$, where U is uniform on $[0,1]$ and independent from Z. We then use the fact that $Z_U - \inf Z \overset{(d)}{=} \sup Z$, which is proven for instance in [LGW06]. □

For a rooted Eulerian triangulation (possibly with a boundary) Δ, let $N(\Delta)$ be the number of black triangles of Δ. Then:

Proposition 7.4.2. *Let $\alpha > 0$. For any $\varepsilon \in (0,1)$, there exists some $b \in (0,1)$ such that*

$$\liminf_{n\to\infty} \mathbb{P}\big(N(\mathcal{B}_{\alpha n^{1/4}}(\overline{\mathcal{T}}_n)) > bn\big) \geq 1 - \varepsilon.$$

Proof. Let us roughly sketch the idea of the proof. Recall that $\overline{\mathcal{T}}_n$ is in correspondence with a random tree $\mathscr{T}_n$, uniform over the well-labeled plane trees with n edges. We will use a slight variant of the contour process C_n of $\mathscr{T}_n$ to bound from below the number of vertices of $\overline{\mathcal{T}}_n$ at distance less than $\alpha n^{1/4}$ from the root, by an integral depending on the label function $L_{(n)}$. We can then use the convergence of Theorem 7.2.4 to relate this to equivalent integral for the Brownian snake Z.

Let us now get into the details of the proof. For $s \in [0, 2n)$, we define $< s >= \lceil s \rceil$ if C_n has slope $+1$ right after s, and $< s >= \lfloor s \rfloor$ otherwise. Then, for any $u \in V(\mathscr{T}_n) \setminus \{u_0^{(n)}\}$, we have

$$\mathrm{Leb}\{s \in [0,2n) \Big| u^{(n)}_{<s>} = u\} = 2.$$

Thus, using (7.2.2), we have

$$\frac{1}{n} \cdot N(\mathcal{B}_{\alpha n^{1/4}}(\overline{\mathcal{T}}_n)) \geq \int_0^1 \mathbb{1}_{\{l_n(<2ns>) - \min l_n \leq \alpha n^{1/4} - 1\}} \mathrm{d}s.$$

Note that we have, for any $s \in [0,1)$:

$$|l_n(< 2ns >) - n^{1/4} L_{(n)}(s)| \leq 1,$$

so that:

$$\int_0^1 \mathbb{1}_{\{l_n(<2ns>) - \min l_n \leq \alpha n^{1/4} - 1\}} \mathrm{d}s \geq \int_0^1 \mathbb{1}_{\{L_{(n)}(s) - \min L_{(n)} \leq \alpha - 2/n^{1/4}\}} \mathrm{d}s.$$

Therefore:

$$\mathbb{P}\big(N(\mathcal{B}_{\alpha n^{1/4}}(\overline{\mathcal{T}}_n)) > bn\big) \geq \mathbb{P}\bigg(\int_0^1 \mathbb{1}_{\{L_{(n)}(s) - \min L_{(n)} \leq \alpha - 2/n^{1/4}\}} \mathrm{d}s > b\bigg).$$

Now, the liminf of the probability on the right-handside of the previous equation can be bounded below by

$$\mathbb{P}\bigg(\int_0^1 \mathbb{1}_{\{Z_s - \inf Z \leq \frac{\alpha}{2}\}} \mathrm{d}s > b\bigg),$$

which tends to 1 as b tends to 0, as Z is continuous.

This concludes the proof. □

Proposition 7.4.3. *For any $\varepsilon > 0$ and any $\delta \in (0,1)$ there exists an integer $k \geq 1$ such that, for any sufficiently large n, if $o_n^1, \ldots, o_n^k$ are chosen uniformly and independently in $V(\mathcal{T}_n)$, we have*

$$\mathbb{P}\bigg(\sup_{x \in V(\mathcal{T}_n)} \Big(\inf_{1 \leq j \leq k} \vec{d}(x, o_n^j)\Big) > \varepsilon n^{1/4}\bigg) \leq \delta.$$

Proof. Let us fix an integer $K \geq 1$. Recall that we write $(u_i^{(n)})_{0\leq i\leq 2n-1}$ for the vertices of $\mathscr{T}_n$ along its contour exploration. Then, for k large enough, for any sufficiently large n,

$$\mathbb{P}\Big(\forall i \in \{0,\dots,2K-1\}\,\exists j \in \{1,\dots,k\}\,\exists m \in \{\lfloor \frac{in}{k}\rfloor,\dots,\lfloor\frac{(i+1)n}{k}\rfloor\},\, o_n^j = v_m^{(n)}\Big) \geq 1-\frac{\delta}{2}. \tag{7.4.1}$$

We will now argue on the event in (7.4.1).

Using (7.2.2), we have, for any $i,j \in \{0,1,\dots,2n\}$,

$$\vec{d}_n(u_i^{(n)},u_j^{(n)}) \leq 2(l_n(u_i^{(n)})+l_n(u_j^{(n)})-2\check{l}_n(i,j)+2),$$

so that, for any n sufficiently large:

$$\sup_{x\in V(\mathcal{T}_n)}\left(\inf_{1\leq j\leq k}\vec{d}(x,o_n^j)\right) \leq 4\max_{0\leq i\leq 2K-1}\omega\left(l_n,\left[\lfloor\frac{in}{K}\rfloor,\lfloor\frac{(i+1)n}{K}\rfloor\right]\right)+4$$

where $\omega(f,I)$ is the modulus of continuity of the function f on the interval I.

Therefore, we have

$$\liminf_n \mathbb{P}\left(\sup_{x\in V(\mathcal{T}_n)}\left(\inf_{1\leq j\leq k}\vec{d}(x,o_n^j)\right)<\varepsilon n^{1/4}\right) \geq \mathbb{P}\Big(\omega(Z,\frac{1}{K})<\frac{\varepsilon}{5}\Big),$$

by using once again the convergence of Theorem 7.2.4. (We denote by $\omega(Z,\eta)$ the supremum $\sup_{|I|\leq\eta}\omega(Z,I)$.)

Now, as Z is a.s. continuous on $[0,1]$, it is uniformly continuous, so that, for any $\varepsilon>0$, for K large enough,

$$\mathbb{P}\Big(\omega(Z,\frac{1}{K})<\frac{\varepsilon}{5}\Big)\geq 1-\frac{\delta}{2},$$

which concludes the proof. □

7.4.2 Enumeration results

We will need some asymptotic results on the generating series $B(t,z)$ of Eulerian triangulations with a semi-simple alternating boundary, as defined in Section 7.2.3:

$$B(t,z)=\sum_{n,p\geq 0}B_{n,p}t^n z^p,$$

where $B_{n,p}$ is the number of Eulerian triangulations with semi-simple alternating boundary of length $2p$ and with n black triangles. With techniques "à la Tutte", Jérémie Bouttier and the author obtain a rational parametrization of $B(t,z)$, which yields the following asymptotic result (see Chapter 9 for a preliminary version of this work):

Theorem 7.4.4.

$$[t^n]B(t,z)=\sum_{p\geq 0}B_{n,p}z^p \underset{n\to\infty}{\sim}\frac{3}{2}\frac{z}{\sqrt{\pi(z-1)(4z-1)^3}}8^n n^{-5/2} \quad \forall\, z\in[0,\frac{1}{4}). \tag{7.4.2}$$

This implies that:

$$\begin{cases} B_{n,p}\underset{n\to\infty}{\sim}C(p)8^n n^{-5/2} \quad \forall\, p \\ C(p)\underset{p\to\infty}{\sim}\frac{\sqrt{3}}{2\pi}4^p\sqrt{p} \text{ and } \sum_{p\geq 1}C(p)z^p=\frac{3}{2}\frac{z}{\sqrt{\pi(z-1)(4z-1)^3}} \quad \forall\, z\in[0,\frac{1}{4}) \end{cases} \tag{7.4.3}$$

Note that (7.4.2) is much stronger than (7.4.3). Indeed, it states that, for any $\varepsilon > 0$, for any n large enough, we have, for all $z \in [0, 1/4)$,

$$(1-\varepsilon)8^n n^{-5/2} f(z) \leq g_n(z) \leq (1+\varepsilon)8^n n^{-5/2} f(z), \tag{7.4.4}$$

where

$$f(z) = \frac{3}{2} \frac{z}{\sqrt{\pi(z-1)(4z-1)^3}}$$

and

$$g_n(z) = \sum_{p \geq 0} B_{n,p} z^p.$$

Thus, as both f and g_n are analytic functions on $[0, 1/4)$, by taking the successive derivatives of the terms in (7.4.4), we obtain equivalent bounds for the successive coefficients of f and g_n seen as power series:

$$(1-\varepsilon)8^n n^{-5/2}([z^p]f(z)) \leq B_{n,p} \leq (1+\varepsilon)8^n n^{-5/2}([z^p]f(z)),$$

for any n large enough and for any p.

This yields that, for all $n, p \geq 1$,

$$c\, C(p) 8^n n^{-5/2} \leq B_{n,p} \leq c'\, C(p) 8^n n^{-5/2}, \tag{7.4.5}$$

for some constants $0 < c < c'$ independent of n and p.

We also deduce from (7.4.2) that

$$\begin{cases} \sum_{p \geq 0} Z(p) z^p \equiv \sum_{p \geq 0,\, n \geq 0} \left(\frac{1}{8}\right)^n B_{n,p} z^p = \frac{1+7z-8z^2+\sqrt{(z-1)(4z-1)^3}}{2(1-z)} & \forall\, z \in [0, \frac{1}{4}) \\ Z(p) \underset{p \to \infty}{\sim} \frac{1}{4}\sqrt{\frac{3}{\pi}} 4^p p^{-5/2} \text{ and } Z(0) = 1. \end{cases} \tag{7.4.6}$$

In particular, for any $p \geq 1$, the sum $Z(p) = \sum_n B_{n,p} 8^{-n}$ is finite, which makes it possible to define the **Boltzmann distribution** on Eulerian triangulations of the p-gon (with a semi-simple alternating boundary), that assigns a weight $8^{-n}/Z(p)$ to each such triangulation having n black triangles. A random triangulation sampled according to this measure will be called a **Boltzmann Eulerian triangulation of perimeter p**.

Note that there is a natural bijection between Eulerian triangulations of the 2-gon (with an alternating boundary), and rooted planar Eulerian triangulations, which simply consists in "zipping" or "unzipping" the root edge (see Figure 7.4.1). This simple observation will be useful in the sequel.

7.5 Skeleton decomposition

We previously considered the balls of planar rooted Eulerian triangulations, and the associated hulls, defined with the oriented distance from the root. To obtain the layer decomposition of finite planar Eulerian triangulations that will be crucial to the rest of this chapter, we will now focus on similar notions, but for some Eulerian triangulation A with one boundary: we will be interested in the union of faces of A incident to vertices at (oriented) distance less than n from the *boundary*, instead of the root. We will denote this union $B_{n+1}(A)$. As was the case for usual balls, the faces of $B_{n+1}(A)$ adjacent to its boundary parts, other than the original boundary ∂A, will correspond to modules of

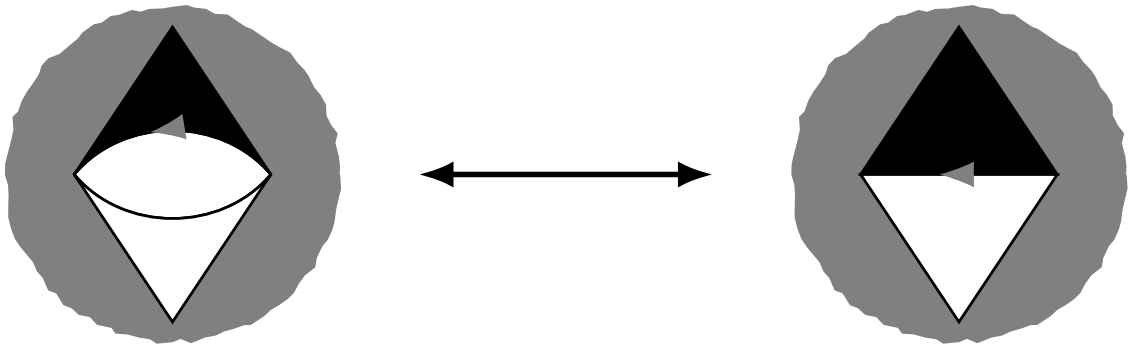

Figure 7.4.1 – The bijection between Eulerian triangulations of the 2-gon with an alternating boundary, and rooted planar Eulerian triangulations.

type $n+1$, for the oriented distance from ∂A. Once again, we will have the convention that these boundary parts are simple, and we will glue them to semi-simple boundaries. If A is pointed at a vertex v at oriented distance at least $n+2$ from the boundary, we can also define a notion of hull for $B_{n+1}(A)$, which will be an Eulerian triangulation with two boundaries of specific types. In this section, we will first develop the description of such triangulations, before dealing with random Eulerian triangulations with one boundary, and their hulls.

7.5.1 Cylinder triangulations

Definition 7.5.1. We call **Eulerian cylinder triangulation of height $r \geq 1$**, an Eulerian triangulation with two boundaries, one (the bottom of the cylinder) being alternating and semi-simple, the other one (the top) being a succession of modules (see Figure 7.5.1), and such that any module adjacent to the top boundary is of distance type $(r-1, r, r+1)$ with respect to the bottom.

We denote by $\partial\Delta$ its bottom boundary, and by $\partial^*\Delta$ its top boundary. The root is an edge on $\partial\Delta$ oriented such that the bottom face sits on its right.

Let Δ be an Eulerian cylinder triangulation of height r. Let $2p$ be the bottom boundary length, and $2q$ the top boundary length. For $1 \leq j \leq r$, the ball $B_j(\Delta)$ is defined as the union of all edges and faces of Δ incident to at least a vertex at distance $< j$ from the bottom boundary, and the hull $B_j^\bullet(\Delta)$ is obtained from $B_j(\Delta)$ by adding all the connected components of its complement except the one containing the top boundary. Therefore $B_j^\bullet(\Delta)$ is a cylinder triangulation of height j, and we denote by $\partial_j\Delta$ the set of modules adjacent to its top boundary. Let $\mathcal{M}(\Delta)$ be the set of modules of Δ belonging to some $\partial_j(\Delta)$, for $0 \leq j \leq r$. (For convenience, we will associate a "ghost" module to each pair of successive edges of the bottom boundary respectively adjacent to a white and a black triangle, and the set $\partial_0(\Delta)$ of these p ghost modules will be included in $\mathcal{M}(\Delta)$.)

We define a genealogical order on $\mathcal{M}(\Delta)$: a module m of $\partial_j(\Delta)$ is the parent of a module m' of $\partial_{j-1}(\Delta)$ if m is the first module of $\partial_j(\Delta)$ that we encounter when going left-to-right along the modules of $\partial_{j-1}(\Delta)$, starting by the top vertex of m'. This order yields a forest $\mathcal{F}$ of q plane trees, whose vertices correspond to the modules belonging to $\mathcal{M}(\Delta)$. The maximal height of this forest is r, and a vertex of height $r-j$ corresponds to a module of $\partial_j(\Delta)$. We denote by $\tau_1, \tau_2, \ldots, \tau_q$ the trees of the forest listed clockwise around $\partial_r(\Delta)$, with τ_1 the tree containing the vertex corresponding to the root. Therefore, the tree τ_1 has height r, with a distinguished vertex (the one corresponding to the root) at height r.

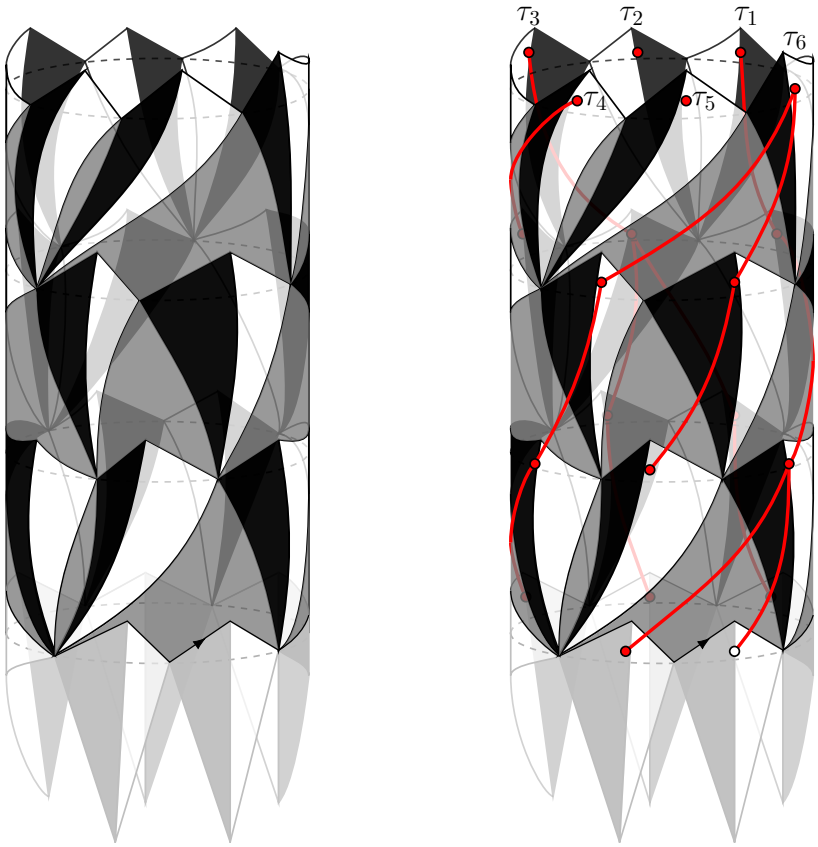

Figure 7.5.1 – Left, a cylinder Eulerian triangulation of height 3, top length 12 and bottom length 10: the foreground parts of the slots are in medium grey while the background ones are left white for legibility, and the ghost modules are in pale grey at the bottom. Right, the construction of the associated forest (with its distinguished vertex at height 3, in white).

Apart from the modules of $\mathcal{M}(\Delta)$, Δ is composed of triangulations with a semi-simple alternating boundary that fill in the "slots" bounded by the modules of $\mathcal{M}(\Delta)$. To a module m in $\partial_j(\Delta)$, we associate the slot bounded by m, its children if any, and the module to the left of m in $\partial_j(\Delta)$. This slot M_m is thus filled in by a triangulation with a semi-simple alternating boundary, of perimeter $2(c_m+1)$, where c_m is the number of children of m. We denote by $T(M_m)$ the number of black triangles of this triangulation with a boundary.

We will say a forest $\mathcal{F}$ with a distinguished vertex is a **(p,q,r)-admissible forest** if it consists of an ordered sequence $(\tau_1,\tau_2,\dots,\tau_q)$ of q rooted plane trees of maximal height r, with p vertices at height r, with the distinguished vertex at height r in τ_1.

If $\mathcal{F}$ is a (p,q,r)-admissible forest, we write $\mathcal{F}^*$ for the set of all vertices of $\mathcal{F}$ at height strictly smaller than r.

From the preceding decomposition, we obtain the following result:

Proposition 7.5.2. *The Eulerian triangulations of the cylinder Δ of height r with a bottom boundary length $2p$ and a top boundary length $2q$, are in bijection with pairs consisting of a (p,q,r)-admissible forest $\mathcal{F}$ and a collection $(M_v)_{v\in\mathcal{F}^*}$ such that, for every $v\in\mathcal{F}^*$, M_v is an Eulerian triangulation of the $2(c_v+1)$-gon with a semi-simple alternating boundary, with c_v being the number of children of v in $\mathcal{F}$.*

Following the existing literature on other families of maps, we call this bijection the **skeleton decomposition**, and say that $\mathcal{F}$ is the **skeleton** of the triangulation Δ. We will also call **skeleton modules** the modules of $\mathcal{M}(\Delta)$.

7.5.2 Skeleton decomposition of random triangulations

We will now use the bijection derived in Section 7.5.1 to obtain the asymptotic behavior of the laws of the hulls of random uniform Eulerian triangulations with a boundary.

We first need a bit of additional notation.

Consider an Eulerian triangulation with a boundary Δ pointed in v. We can define the hull $B_r^\bullet(\Delta)$ of Δ like for cylinder triangulations, if $\vec{d}(\partial\Delta,v)>r+1$. If $\vec{d}(\partial\Delta,v)\le r+1$, we can set $B_r^\bullet(\Delta)=\Delta$.

Let $\mathcal{T}_n^{(p)}$ be a uniform random triangulation over the set of Eulerian triangulations with a semi-simple alternating boundary of length $2p$ and with n black triangles. We denote by $\overline{\mathcal{T}}_n^{(p)}$ the pointed triangulation obtained by choosing a uniform random inner vertex of $\mathcal{T}_n^{(p)}$. Let Δ be a cylinder triangulation of height r, of respective bottom and top boundary lengths $2p$ and $2q$, with N black triangles, with $n\ge N$. Using the skeleton decomposition, we associate to Δ a (p,q,r)-admissible forest $\mathcal{F}$, together with triangulations $(M_v)_{v\in\mathcal{F}}$ filling in the "slots" between the modules of $\mathcal{M}(\Delta)$. We write $T(M_v)$ for the number of black triangles of M_v, for every $v\in\mathcal{F}^*$.

Lemma 7.5.3. *We have*

$$\lim_{n\to\infty}\mathbb{P}\left(B_r^\bullet(\overline{\mathcal{T}}_n^{(p)})=\Delta\right)=\frac{4^{-q}C(q)}{4^{-p}C(p)}\prod_{v\in\mathcal{F}^*}\theta(c_v)\frac{8^{-T(M_v)}}{Z(c_v+1)},\tag{7.5.1}$$

where

$$\theta(k)=\frac{1}{8}4^{-k+1}Z(k+1),\tag{7.5.2}$$

with $Z(k)$ defined as in (7.4.6).

Proof. To simplify notation, let us note in this proof $\rho = 8$ and $\alpha = 4$.
The property $B_r^\bullet(\overline{\mathcal{T}}_n^{(p)}) = \Delta$ holds if and only if $\mathcal{T}_n^{(p)}$ is obtained from Δ by gluing to the top boundary an arbitrary triangulation with a semi-simple alternating boundary of length $2q$, and with $n - N$ black triangles, and if the distinguished vertex is chosen among the inner vertices of the glued triangulation. Thus:

$$\mathbb{P}\left(B_r^\bullet(\overline{\mathcal{T}}_n^{(p)}) = \Delta\right) = \frac{B_{n-N,q}}{B_{n,p}} \cdot \frac{\#\text{inner vertices in glued triangulation}}{\#\text{inner vertices in total triangulation}}. \tag{7.5.3}$$

Therefore:

$$\lim_{n\to\infty} \mathbb{P}\left(B_r^\bullet(\overline{\mathcal{T}}_n^{(p)}) = \Delta\right) = \frac{C(q)}{C(p)}\rho^{-N}. \tag{7.5.4}$$

As we have

$$N = \#\mathcal{M}(\Delta) - p + \sum_{v\in\mathcal{F}^*} T(M_v) = \sum_{1\le i\le q} \#\tau_i - p + \sum_{v\in\mathcal{F}^*} T(M_v) = q + \sum_{v\in\mathcal{F}^*} (c_v + T(M_v)) - p,$$

we get

$$\lim_{n\to\infty} \mathbb{P}\left(B_r^\bullet(\overline{\mathcal{T}}_n^{(p)}) = \Delta\right) = \frac{\rho^{-q}C(q)}{\rho^{-p}C(p)} \prod_{v\in\mathcal{F}^*} \rho^{-c_v}\rho^{-T(M_v)}.$$

Now, since $\sum_{v\in\mathcal{F}^*}(c_v - 1) = p - q$, we can multiply the right-hand side by $(\alpha\rho)^{p-q-\sum_{v\in\mathcal{F}^*}(c_v-1)}$, which yields

$$\lim_{n\to\infty} \mathbb{P}\left(B_r^\bullet(\overline{\mathcal{T}}_n^{(p)}) = \Delta\right) = \frac{\alpha^{-q}C(q)}{\alpha^{-p}C(p)} \prod_{v\in\mathcal{F}^*} \rho^{-1}\alpha^{-c_v+1}\rho^{-T(M_v)},$$

that is

$$\lim_{n\to\infty} \mathbb{P}\left(B_r^\bullet(\overline{\mathcal{T}}_n^{(p)}) = \Delta\right) = \frac{\alpha^{-q}C(q)}{\alpha^{-p}C(p)} \prod_{v\in\mathcal{F}^*} \theta(c_v)\frac{\rho^{-T(M_v)}}{Z(c_v+1)},$$

for $\theta(k) = \rho^{-1}\alpha^{-k+1}Z(k+1)$. □

Let us give a few properties of θ that will be useful in the sequel.
First, the asymptotics of Z give:

$$\theta(k) \underset{k\to\infty}{\sim} \frac{1}{2}\sqrt{\frac{3}{\pi}}k^{-5/2}. \tag{7.5.5}$$

Moreover, θ has the following generating function g_θ:

$$g_\theta(x) = \sum_{k=0}^{\infty} \theta(k)x^k = 1 - \frac{3}{\left(\sqrt{\frac{4-x}{1-x}} + 1\right)^2 - 1} \quad \forall x \in [0,1). \tag{7.5.6}$$

Indeed, the generating function of θ may be written, for $0 \leq x < 1$:

$$\begin{aligned}\sum_{k\geq 0}\theta(k)x^k &= \sum_{k\geq 0}\rho^{-1}\alpha^{-k+1}Z(k+1)x^k = \frac{\alpha}{\rho}\sum_{k\geq 0}\left(\frac{x}{\alpha}\right)^k Z(k+1)\\ &= \frac{\alpha^2}{x\rho}\sum_{k\geq 1}\left(\frac{x}{\alpha}\right)^k Z(k) = \frac{\alpha^2}{x\rho}\left(\sum_{k\geq 0}\left(\frac{x}{\alpha}\right)^k Z(k) - Z(0)\right)\\ &= \frac{2}{x}\left(\frac{1}{2}\left(\frac{1+\frac{7}{4}x-\frac{x^2}{2}+\sqrt{(\frac{x}{4}-1)(x-1)^3}}{1-\frac{x}{4}}\right)-1\right)\\ &= \frac{-4+9x-2x^2+2\sqrt{(x-4)(x-1)^3}}{x(4-x)}\\ &= 1-\frac{3}{\left(\sqrt{\frac{4-x}{1-x}}+1\right)^2-1} = g_\theta(x).\end{aligned}$$

It is straightforward to obtain from this that θ is a probability distribution with mean 1, so that, considered as the offspring distribution of a branching process, it is critical.

Let $Y = (Y_r)_{r\geq 0}$ be a Galton-Watson process with offspring distribution θ, and let us write $\mathcal{P}_k(\cdot)$ for the law of Y given $Y_0 = k$, and $\mathcal{E}_k[\,\cdot\,]$ for the corresponding expectation. Then, for every $r \geq 1$, the generating function of Y_r under $\mathcal{P}_1$ is the r-th iterate $g_\theta^{(r)}$ of g_θ. It is easy to show that this iterate has a very nice expression for any positive integer r:

$$\mathcal{E}_1\left[x^{Y_r}\right] = g_\theta^{(r)}(x) = 1-\frac{3}{\left(\sqrt{\frac{4-x}{1-x}}+r\right)^2-1} \quad \forall x\in[0,1). \tag{7.5.7}$$

Note that a similarly nice expression for the r-th iterate of the generating function also exists for the offspring distributions associated to the skeleton decompositions of usual triangulations and of quadrangulations [CLG19; LGL].

Using the transfer theorem (see Theorem VI.3 in [FS09]), we deduce from (7.5.7) that

$$\mathcal{P}_1\left(Y_r = k\right) \underset{k\to\infty}{\sim} \sqrt{\frac{3}{\pi}}\frac{r}{2}k^{-5/2}. \tag{7.5.8}$$

Let us denote by $\mathbb{F}_{p,q,r}$ the set of (p,q,r)-admissible forests. We also define the set $\mathbb{F}'_{p,q,r}$ of pointed forests satisfying the same conditions as (p,q,r)-admissible forests, except that the tree with a distinguished vertex is not necessarily τ_1, and the set $\mathbb{F}''_{p,q,r}$ of forests which satisfy the same conditions but do not have a distinguished vertex.

We now prove that the "skeleton part" of (7.5.1) defines a probability measure on $\mathbb{F}_{p,r} = \cup_{q\geq 1}\mathbb{F}_{p,q,r}$:

Lemma 7.5.4. *For every $p \geq 1$ and $r \geq 1$,*

$$\sum_{q=1}^{\infty}\sum_{\mathcal{F}\in\mathbb{F}_{p,q,r}}\frac{4^{-q}C(q)}{4^{-p}C(p)}\prod_{v\in\mathcal{F}^*}\theta(c_v) = 1. \tag{7.5.9}$$

Proof. Notice that, for a forest $\mathcal{F}\in\mathbb{F}_{p,q,r}$, there are exactly q forests $\mathcal{F}'$ in $\mathbb{F}'_{p,q,r}$ that are obtained from $\mathcal{F}$ by a cyclic permutations of the trees. Thus

$$\sum_{q=1}^{\infty}\sum_{\mathcal{F}\in\mathbb{F}_{p,q,r}}\frac{4^{-q}C(q)}{4^{-p}C(p)}\prod_{v\in\mathcal{F}^*}\theta(c_v) = \sum_{q=1}^{\infty}\sum_{\mathcal{F}'\in\mathbb{F}'_{p,q,r}}\frac{1}{q}\frac{4^{-q}C(q)}{4^{-p}C(p)}\prod_{v\in\mathcal{F}^*}\theta(c_v).$$

Now, each forest $\mathcal{F}'' \in \mathbb{F}''_{p,q,r}$ can be obtained from p different forests $\mathcal{F}'$ of $\mathbb{F}'_{p,q,r}$ by forgetting the distinguished vertex. Hence,

$$\sum_{q=1}^{\infty} \sum_{\mathcal{F}' \in \mathbb{F}'_{p,q,r}} \frac{1}{q} \frac{4^{-q}C(q)}{4^{-p}C(p)} \prod_{v \in \mathcal{F}^*} \theta(c_v) = \sum_{q=1}^{\infty} \sum_{\mathcal{F}'' \in \mathbb{F}''_{p,q,r}} \frac{p}{q} \frac{4^{-q}C(q)}{4^{-p}C(p)} \prod_{v \in \mathcal{F}^*} \theta(c_v) = \sum_{q=1}^{\infty} \sum_{\mathcal{F}'' \in \mathbb{F}''_{p,q,r}} \frac{h(q)}{h(p)} \prod_{v \in \mathcal{F}^*} \theta(c_v) \tag{7.5.10}$$

with

$$h(k) = 2\sqrt{\pi} \frac{4^{-k}C(k)}{k}. \tag{7.5.11}$$

Thus, showing (7.5.9) amounts to show that

$$\sum_{q=1}^{\infty} \frac{h(q)}{h(p)} \mathcal{P}_q \left(Y_r = p\right) = 1,$$

that is

$$\sum_{q=1}^{\infty} h(q) \mathcal{P}_q \left(Y_r = p\right) = h(p), \tag{7.5.12}$$

or in other words that h is an infinite stationary measure for Y.

Let Π be the generating function of the sequence $(h(k))_{k \geq 1}$:

$$\Pi(x) := \sum_{k=1}^{\infty} h(k) x^k = \sum_{k=1}^{\infty} \frac{1}{k} C(k) \left(\frac{x}{4}\right)^k.$$

By integrating (7.4.3), we obtain for every $0 < x < 1$

$$\Pi(x) = \sqrt{\frac{4-x}{1-x}} - 2.$$

To prove that h is an infinite stationary measure for Y, it is enough to check that $\Pi\left(g_\theta(x)\right) - \Pi\left(g_\theta(0)\right) = \Pi(x)$ for every $x \in [0,1)$, which follows from the explicit formulas for g_θ and Π. □

With Lemma 7.5.4, we can define a probability measure $\mathbf{P}_{p,r}$ on $\mathbb{F}_{p,r}$ by setting, for any $\mathcal{F} \in \mathbb{F}_{p,q,r}$,

$$\mathbf{P}_{p,r}(\mathcal{F}) := \frac{4^{-q}C(q)}{4^{-p}C(p)} \prod_{v \in \mathcal{F}^*} \theta(c_v). \tag{7.5.13}$$

Let us note $\mathbb{C}_{p,r}$ the set of Eulerian triangulations of the cylinder of height r and bottom boundary length $2p$. We can define a probability measure $\mathbb{P}_{p,r}$ on $\mathbb{C}_{p,r}$, by first setting the skeleton to be distributed according to $\mathbf{P}_{p,r}$, then, conditionally on the skeleton, filling the slots by independent Boltzmann triangulations (whose boundary lengths are prescribed by the skeleton). Thus, Lemma 7.5.3 amounts to stating that, if $\Delta \in \mathbb{C}_{p,r}$,

$$\lim_{n \to \infty} \mathbb{P}\left(B_r^\bullet(\overline{\mathcal{T}}_n^{(p)}) = \Delta\right) = \mathbb{P}_{p,r}(\Delta). \tag{7.5.14}$$

In other words, the law of $B_r^\bullet(\overline{\mathcal{T}}_n^{(p)})$ converges weakly to $\mathbb{P}_{p,r}$ as $n \to \infty$.

Note that the expression (7.5.13) implies that, if a random cylinder triangulation A is distributed as $\mathbb{P}_{p,r}$, then, for all $1 \leq s \leq r$, its hull $B_s^\bullet(A)$ will be distributed as $\mathbb{P}_{p,s}$, or, in other words, the laws $(\mathbb{P}_{p,r})_{r \geq 1}$ are consistent. This implies that the sequence of random maps $(\mathcal{T}_n^{(p)})_n$ has a local distributional limit. To express this result more precisely, we

need to generalize the notion of hulls to some infinite maps. First, for any infinite planar Eulerian triangulation A with a boundary, we can define its ball $B_r(A)$ like in the finite case. Then, if A has a unique end, only one connected component of $A \setminus B_r(A)$ is infinite, so that we can fill all the finite holes, to get the hull $B_r^\bullet(A)$.

We then have the following result:

Proposition 7.5.5. *For any integer $p \geq 1$, the sequence of random maps $(\mathcal{T}_n^{(p)})_n$ converges in distribution, in the sense of local limits of rooted maps, to an infinite map that we call the **uniform infinite Eulerian triangulation of the 2p-gon**, and that we denote by $\mathcal{T}_\infty^{(p)}$. It is a random infinite Eulerian triangulation of the plane, with an alternating, semi-simple boundary of length $2p$, that has a unique end almost surely, and such that $B_r^\bullet(\mathcal{T}_\infty^{(p)})$ has law $\mathbb{P}_{p,r}$, for every integer $r \geq 1$.*

For $p = 1$, we can perform the transformation described in Figure 7.4.1, which yields a random infinite planar Eulerian triangulation, which we denote by $\mathcal{T}_\infty$. This random infinite map is the local limit of uniform rooted planar Eulerian triangulations with n black faces when $n \to \infty$, therefore we call it the **Uniform Infinite Planar Eulerian Triangulation** (UIPET).

The UIPET is the equivalent of well-known models of random infinite planar maps such as the UIPT or the UIPQ (see [Ang03; Kri]), in the case of Eulerian triangulations. Note that this present work gives the first construction of the UIPET.

Let $L_r^{(p)}$ be the length of the top cycle of $B_r^\bullet(\mathcal{T}_\infty^{(p)})$. When $p = 1$, we write L_r for $L_r^{(1)}$ for simplicity.

Let us first note that $\mathcal{T}_\infty^{(p)}$ exhibits a spatial Markov property. Let r, s be integers with $1 \leq r < s$, and $\Delta \in \mathbb{C}_{p,s}$. Let $2q$ be the length of the boundary $\partial_r\Delta$. We can obtain Δ by gluing a triangulation $\Delta'' \in \mathbb{C}_{q,s-r}$ on top of a triangulation $\Delta' \in \mathbb{C}_{p,r}$, whose top boundary has length q. From the explicit formula of (7.5.13), we get

$$\mathbb{P}_{p,s}(\Delta) = \mathbb{P}_{p,r}(\Delta') \cdot \mathbb{P}_{q,s-r}(\Delta''). \tag{7.5.15}$$

Therefore, conditionally on $\{L_r^{(p)} = q\}$, $B_s^\bullet(\mathcal{T}_\infty^{(p)}) \setminus B_r^\bullet(\mathcal{T}_\infty^{(p)})$ follows $\mathbb{P}_{q,s-r}$, and is independent of $B_r^\bullet(\mathcal{T}_\infty^{(p)})$. By letting $s \to \infty$, we obtain that, conditionally on $\{L_r^{(p)} = q\}$, the triangulation $\mathcal{T}_\infty^{(p)} \setminus B_r^\bullet(\mathcal{T}_\infty^{(p)})$ is distributed as $\mathcal{T}_\infty^{(q)}$ and is independent of $\mathcal{T}_\infty^{(p)}$.

We now give a technical but useful result on the law of L_r.

Lemma 7.5.6. *There exists a constant $C_0 > 0$ such that for any $\alpha \geq 0$, and for any integers $r, p \geq 1$,*

$$\mathbb{P}\left(L_r = p\right) \leq \frac{C_0}{r^2} \tag{7.5.16}$$

and

$$\mathbb{P}\left(L_r \geq \alpha r^2\right) \leq C_0 e^{-\alpha/4}. \tag{7.5.17}$$

Let us fix some notation before getting to the proof of Lemma 7.5.6. For $1 \leq r < s$, let $\mathcal{F}_{r,s}^{(1)}$ be the skeleton of $B_s^\bullet(\mathcal{T}_\infty^{(1)}) \setminus B_r^\bullet(\mathcal{T}_\infty^{(1)})$. We let $\widetilde{\mathcal{F}}_{r,s}^{(1)}$ by the non-pointed forest obtained by a uniform cyclic permutation of $\mathcal{F}_{r,s}^{(1)}$, and by forgetting the distinguished vertex. Thus, on the event $\{L_r = p\} \cap \{L_s = q\}$, $\widetilde{\mathcal{F}}_{r,s}^{(1)}$ is a random element of $\mathbb{F}''_{p,q,s-r}$.

Proof. Observe that

$$\mathbb{P}(L_r = p) = \sum_{\mathcal{F} \in \mathbb{F}''_{1,p,r}} \mathbb{P}\Big(\widetilde{\mathcal{F}}_{0,r}^{(1)} = \mathcal{F}\Big) = \sum_{\mathcal{F} \in \mathbb{F}''_{1,p,r}} \frac{h(p)}{h(1)} \prod_{v \in \mathcal{F}^*} \theta(c_v).$$

Thus

$$\mathbb{P}(L_r = p) = \frac{h(p)}{h(1)} \mathcal{P}_p\left(Y_r = 1\right).$$

From the definition of h and the asymptotics of $C(p)$, there exists a constant C_1 such that, for every $p \geq 1$,

$$h(p) \leq \frac{C_1}{\sqrt{p}}.$$

Moreover, from (7.5.7), we have

$$\mathcal{P}_1\left(Y_r = 0\right) = 1 - \frac{3}{(r+2)^2 - 1}, \tag{7.5.18}$$

hence

$$\begin{aligned}
\mathcal{P}_p\left(Y_r = 1\right) &= \lim_{x \downarrow 0} x^{-1} \left(\mathbb{E}_p\left[x^{Y_r}\right] - \mathcal{P}_p\left(Y_r = 0\right)\right) \\
&= \lim_{x \downarrow 0} x^{-1} \left(\left(1 - \frac{3}{\left(\sqrt{\frac{4-x}{1-x}} + r\right)^2 - 1} \right)^p - \left(1 - \frac{3}{(r+2)^2 - 1}\right)^p \right) \\
&= \frac{9p(r+2)}{2((r+2)^2 - 1)^2} \left(1 - \frac{3}{(r+2)^2 - 1}\right)^p.
\end{aligned}$$

Therefore, for some constant $C_3 > 0$,

$$\mathbb{P}(L_r = p) \leq \frac{C_2}{h(1)} \sqrt{p} \frac{9(r+2)}{((r+2)^2 - 1)^2} \left(1 - \frac{3}{(r+2)^2 - 1}\right)^{p-1} \leq \frac{C_3}{r^2} \sqrt{\frac{p}{r^2}} e^{-3p/r^2}.$$

The bound (7.5.16) immediately follows. As for (7.5.17), since the function $x \mapsto \sqrt{x} e^{-x/3}$ is decreasing for $x \geq 3/2$, we have, for $\alpha \geq 3/2$, for some constant $C_4 > 0$,

$$\mathbb{P}\big(L_r > \alpha r^2\big) \leq \sum_{p=\alpha r^2 + 1}^{\infty} \frac{C_3}{r^2} \sqrt{\frac{p}{r^2}} e^{-3p/r^2} \leq \frac{C_3}{r^2} \int_{\alpha r^2}^{\infty} \sqrt{\frac{x}{r^2}} e^{-3x/r^2} \mathrm{d}x \leq C_4 e^{-\alpha/4}.$$

□

We now fix a positive constant $a \in (0,1)$. For every integer $r \geq 1$, let $N_r^{(a)}$ be uniform random in $\{\lfloor ar^2 \rfloor + 1, \ldots, \lfloor a^{-1} r^2 \rfloor\}$. We also consider a sequence $\tau_1, \tau_2, \ldots$ of independent Galton-Watson trees with offspring distribution θ, independent of $N_r^{(a)}$. For every integer $j \geq 0$, we write $[\tau_i]_j$ for the tree τ_i truncated at generation j.

Proposition 7.5.7. *There exists a constant C_1, which only depends on a, such that, for every sufficiently large integer r, for every choice of $s \in \{r+1, r+2, \ldots\}$, for every choice of the integers p and q with $ar^2 < p, q \leq a^{-1} r^2$, for every forest $\mathcal{F} \in \mathbb{F}''_{p,q,s-r}$,*

$$\mathbb{P}\Big(\widetilde{\mathcal{F}}_{r,s}^{(1)} = \mathcal{F}\Big) \leq C_1 \, \mathbb{P}\Big(([\tau_1]_{s-r}, \ldots, [\tau_{N_r^{(a)}}]_{s-r}) = \mathcal{F}\Big). \tag{7.5.19}$$

Proof. We have

$$\begin{aligned}
\mathbb{P}\Big(([\tau_1]_{s-r}, \ldots, [\tau_{N_r^{(a)}}]_{s-r}) = \mathcal{F}\Big) &= \mathbb{P}\Big(N_r^{(a)} = p\Big) \, \mathbb{P}(([\tau_1]_{s-r}, \ldots, [\tau_p]_{s-r}) = \mathcal{F}) && (7.5.20) \\
&= \frac{1}{\lfloor a^{-1} r^2 \rfloor - \lfloor ar^2 \rfloor} \cdot \prod_{v \in \mathcal{F}^*} \theta(c_v). && (7.5.21)
\end{aligned}$$

On the other hand, let $\mathcal{F}^\circ$ be any pointed forest in $\mathbb{F}_{p,q,s-r}$ that coincides with $\mathcal{F}$ up to a cyclic permutation of the trees. We know that, conditionally on $L_r = p$, $B_s^\bullet(\mathcal{T}_\infty^{(1)}) \backslash B_r^\bullet(\mathcal{T}_\infty^{(1)})$ follows $\mathbb{P}_{p,s-r}$, thus

$$\mathbb{P}\Big(\mathcal{F}_{r,s}^{(1)} = \mathcal{F}^\circ | L_r = p\Big) = \mathbf{P}_{p,s-r}\left(\mathcal{F}^\circ\right) = \frac{4^{-q}C(q)}{4^{-p}C(p)} \prod_{v \in \mathcal{F}^*} \theta(c_v).$$

Therefore, by arguments similar to those of the proof of Lemma 7.5.4, we have

$$\mathbb{P}\Big(\widetilde{\mathcal{F}}_{r,s}^{(1)} = \mathcal{F} | L_r = p\Big) = \frac{p}{q}\,\mathbb{P}\Big(\mathcal{F}_{r,s}^{(1)} = \mathcal{F}^\circ | L_r = p\Big) = \frac{h(q)}{h(p)} \prod_{v \in \mathcal{F}^*} \theta(c_v).$$

By our conditions on p and q, the ratio $h(q)/h(p)$ is bounded above by some constant C_5 (which depends on a). Applying the bound of (7.5.16), we obtain

$$\mathbb{P}\Big(\widetilde{\mathcal{F}}_{r,s}^{(1)} = \mathcal{F}\Big) \leq \frac{C_0}{r^2} C_5 \prod_{v \in \mathcal{F}^*} \theta(c_v).$$

Comparing this with (7.5.20), we obtain the desired bound. □

7.5.3 Leftmost mirror geodesics

We now define a type of paths in Eulerian cylinder triangulations that will be useful in the sequel.

Let Δ be an Eulerian cylinder triangulation of heighr $r \geq 1$. Let x be a vertex of $\partial_j\Delta$, with $1 \leq j \leq r$. We define the **leftmost mirror geodesic** from x to the bottom cycle in the following way. Enumerate in clockwise order around x all the half-edges incident to it, starting from the half-edge of $\partial_j\Delta$ that is to the right of x. The first edge on the leftmost mirror geodesic starting from x is the last edge connecting x to $\partial_{j-1}\Delta$ arising in this order. The path is then continued by induction. Note that, taken in the reverse order, this path is an oriented geodesic, hence the name *mirror* geodesic.

The coalescence of leftmost geodesics from distinct vertices can be characterized by the skeleton of Δ. Indeed, let u, v be two distinct vertices of $\partial^*\Delta$. Let $\mathcal{F}$ be the skeleton of Δ, $\mathcal{F}'$ the subforest of $\mathcal{F}$ consisting of the trees rooted between u and v left-to-right in $\partial^*\Delta$, and $\mathcal{F}''$ be the rest of the trees in $\mathcal{F}$. Then, for any $k \in \{1, 2, \ldots, r\}$, the leftmost mirror geodesics from u and v merge before step k (possibly exactly at step k) if and only if at least one of the two forests $\mathcal{F}'$ and $\mathcal{F}''$ have height strictly smaller than k.

7.6 The Lower Half-Plane Eulerian Triangulation

We now construct a triangulation of the lower half-plane $\mathbb{R} \times \mathbb{R}_-$ that will be crucial to prove Theorem 7.1.2, and that also is an object of interest in itself.

We start with a doubly infinite sequence $(\mathscr{T}_i)_{i \in \mathbb{Z}}$ of independent Galton-Watson trees with offspring distribution θ. They are embedded in the lower half-plane so that, for every $i \in \mathbb{Z}$, the root of $\mathscr{T}_i$ is $(\frac{1}{2} + i, 0)$, and such that the collection of all vertices of all the $\mathscr{T}_i$ is $(\frac{1}{2} + \mathbb{Z}) \times \mathbb{Z}_{\leq 0}$, with vertices at height k being of the form $(\frac{1}{2} + i, -k)$. We also assume that the embedding is such that the collection of vertices of the $\mathscr{T}_i$, for $i \geq 0$, is $(\frac{1}{2} + \mathbb{Z}_{\geq 0}) \times \mathbb{Z}_{\leq 0}$ (see Figure 7.6.1).

We can now build the triangulation itself. We start with the "distinguished" modules, which will play the role of skeleton modules for our infinite triangulation. They are naturally associated with the vertices of the infinite collection of trees in the following way. To

each vertex $(\frac{1}{2}+i, j)$ in one of the trees, we associate a module whose type $n+1$ vertices are (i, j) and $(i+1, j)$. The type n vertex is $(k, j-1)$, where k is the minimal integer such that $(\frac{1}{2}+k, j-1)$ is the child of $(\frac{1}{2}+i', j)$, for some $i' > i$. The last vertex, of type $n+2$, is set to be $(\frac{1}{2}+i, j+\varepsilon)$, for an arbitrary $0 < \varepsilon < 1$. As for the (outer) edges of these skeleton modules, we draw them such that they are all distinct, and do not cross. Having completely determined the configuration of the skeleton edges from the infinite collection of trees, we fill in the slots bounded by these modules, with independent Boltzmann Eulerian triangulation of appropriate perimeters. (Note that each point of the form (i, j), with $j \geq 1$, is at the top of a slot of perimeter $2(c_{i,j}+1)$, where $c_{i,j}$ is the number of children of $(\frac{1}{2}+i, j)$ in the infinite collection of trees.)

We obtain an Eulerian triangulation of the lower-half plane, which we will note $\mathcal{L}$ and call the **Lower Half-Plane Eulerian Triangulation** (LHPET). It is rooted at the edge from $(0, 0)$ to $(\frac{1}{2}, \varepsilon)$.

We will denote by $\mathcal{L}_{[0,r]}$ the infinite rooted planar map obtained by keeping only the first r layers of $\mathcal{L}$ (having the skeleton modules at level r as ghost modules), and denote by $\mathcal{L}_r$ the lower boundary of $\mathcal{L}_{[0,r]}$.

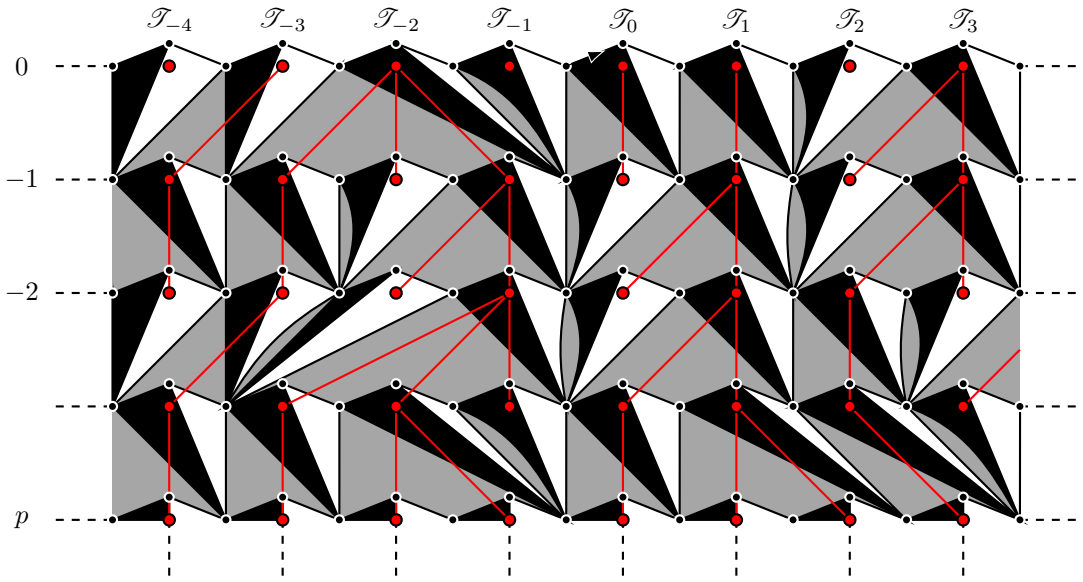

Figure 7.6.1 – Construction of the LHPET.

While we will not use this result in the sequel, note that $\mathcal{L}$ is the local limit of $\mathcal{T}_\infty^{(p)}$ "seen from infinity". This statement is made more precise in the following proposition:

Proposition 7.6.1. *Set $p \geq 1$, and for every $r \geq 1$, define $\widetilde{B}_s^\bullet\left(\mathcal{T}_\infty^{(p)}\right)$ as the hull $B_s^\bullet\left(\mathcal{T}_\infty^{(p)}\right)$ re-rooted at an edge uniform on those of $\partial_s\left(\mathcal{T}_\infty^{(p)}\right)$ that are oriented so that the top face is lying on their left. Then*

$$\widetilde{B}_s^\bullet\left(\mathcal{T}_\infty^{(p)}\right) \xrightarrow[s\to\infty]{(d)} \mathcal{L}$$

in the sense of local limits of rooted planar maps.

An equivalent result was stated for usual triangulations in [CLG19], but its proof was not detailed, since it is similar to the proof of the equivalent convergence to the *Upper* Half-Plane Triangulation. We give a proof of our result both for the sake of completeness, and because it involves nonetheless a few arguments that are different from the ones for the upper half-plane models.

Proof. Recall that, for an Eulerian triangulation A (possibly with a boundary) and an integer $r \geq 1$, we denote by $\mathcal{B}_r(A)$ the ball of radius r of A, that is, the union of all edges and faces of A incident to a vertex at (oriented) distance strictly less than r from the root. Proving the proposition amounts to showing that, for every $r \geq 1$, for every rooted planar map A,

$$\mathbb{P}\Big(\mathcal{B}_r\left(\widetilde{B}_s^\bullet\left(\mathcal{T}_\infty^{(p)}\right)\right) = A\Big) \xrightarrow[s\to\infty]{} \mathbb{P}(\mathcal{B}_r(\mathcal{L}) = A). \tag{7.6.1}$$

To obtain this convergence, we will need a bit of additional notation. We fix $r \geq 1$, and note $[\mathscr{T}]_r$ for the tree $\mathscr{T}$ truncated at height r, and similarly for a forest. For any $s \geq 1$, we write $\mathcal{F}_{0,s}^{(p)} = \left(\mathscr{T}_0^{(p)}, \mathscr{T}_1^{(p)}, \dots, \mathscr{T}_{L_s^{(p)}}^{(p)}\right)$ for the skeleton of $B_s^\bullet\left(\mathcal{T}_\infty^{(p)}\right)$. Let us fix $k \geq 1$. For any $q \geq 1$, for any forest $\mathcal{F} = (\sigma_0, \dots, \sigma_{l-1}) \in \mathbb{F}_{q,l,r}$ with $l \geq 2k+1$, we write $\Phi_k(\mathcal{F}) = (\sigma_{i-k}, \dots, \sigma_{i-1}, \sigma_i, \dots, \sigma_{i+k})$, where i is a uniform index on $0, \dots, l-1$, and the indices for the σ_j are extended to $\mathbb{Z}$ by periodicity.

We will prove that, for every collection $\mathcal{F}_k = (\tau_{-k}, \dots, \tau_0, \dots, \tau_k)$ of $2k+1$ plane trees of maximal height r,

$$\mathbb{P}\Big(\{\Phi_k\left([\mathcal{F}_{0,s}]_r\right) = \mathcal{F}_k\} \cap \{L_s^{(p)} \geq 2k+1\}\Big) \xrightarrow[s\to\infty]{} \mathbb{P}(([\mathscr{T}_{-k}]_r, \dots, [\mathscr{T}_0]_r, \dots, [\mathscr{T}_k]_r) = \mathcal{F}_k). \tag{7.6.2}$$

If k is large enough, we can find a set $\mathbf{F}_k$ of forests such that the probability of the event

$$([\mathscr{T}_{-k}]_r, \dots, [\mathscr{T}_0]_r, \dots, [\mathscr{T}_k]_r) \in \mathbf{F}_k$$

is close to 1, and such that, on that event, the ball $\mathcal{B}_r(\mathcal{L})$ is a deterministic function of the truncated trees $[\mathscr{T}_{-k}]_r, \dots, [\mathscr{T}_0]_r, \dots, [\mathscr{T}_k]_r$ and of the triangulations with a boundary filling in the slots associated with the vertices of these trees. (Note that we need k to be large, so that the $(2k+1)$ central trees of the skeleton of $\mathcal{L}$ and the associated slots are enough to cover the ball $\mathcal{B}_r(\mathcal{L})$, not only vertically, which is a given, but also horizontally.) Likewise, on the event $\{\Phi_k\left([\mathcal{F}_{0,s}]_r\right) \in \mathbf{F}_k\} \cap \{L_s^{(p)} \geq 2k+1\}$, the ball $\mathcal{B}_r\left(\widetilde{B}_s^\bullet\left(\mathcal{T}_\infty^{(p)}\right)\right)$ is given by the same deterministic function of the trees in $\Phi_k\left([\mathcal{F}_{0,s}]_r\right)$ and of the associated triangulations with a boundary.

Moreover, we claim that, for every fixed $p \geq 1$ and $j \geq 1$,

$$\mathbb{P}\Big(L_s^{(p)} = j\Big) \xrightarrow[s\to\infty]{} 0. \tag{7.6.3}$$

Indeed, we can write

$$\mathbb{P}\Big(L_s^{(p)} = j\Big) = \frac{h(j)}{h(p)} \mathcal{P}_j\left(Y_s = p\right),$$

and, from $\mathbb{E}_j[x^{Y_s}] = (g_\theta^{(s)}(x))^j$, we get that $\mathcal{P}_j\left(Y_s = p\right) \xrightarrow[s\to\infty]{} 0$.

Thus, the desired convergence of (7.6.1) will follow from (7.6.2) and (7.6.3).

It remains to prove (7.6.2). Let us fix $\mathcal{F}_k$ as above. From the definition of the $\mathscr{T}_i$, we have

$$\mathbb{P}(([\mathscr{T}_{-k}]_r, \dots, [\mathscr{T}_0]_r, \dots, [\mathscr{T}_k]_r) = \mathcal{F}_k) = \prod_{v \in (\tau_{-k}, \dots, \tau_k)^*} \theta(c_v), \tag{7.6.4}$$

where, as before, for a forest $\mathcal{F}$, $\mathcal{F}^*$ denotes the set of vertices in $\mathcal{F}$ that are not at the maximal height, and, for such a vertex v, c_v is its number of children.

Now, using the definition of the law $\mathbf{P}_{p,s}$ of $B_s^\bullet\left(\mathcal{T}_\infty^{(p)}\right)$, the left-hand side of (7.6.2) is equal to

$$\sum_{l=2k+1}^{\infty} \sum_{\mathcal{F}\in\mathbb{F}_{p,l,s},\Phi_k(\mathcal{F})=\mathcal{F}_k} \frac{4^{-l}C(l)}{4^{-p}C(p)} \prod_{v\in\mathcal{F}^*} \theta(c_v)$$

$$= \left(\prod_{v\in(\tau_{-k},\dots,\tau_k)^*} \theta(c_v)\right) \cdot \left(\sum_{l=2k+1}^{\infty} \frac{4^{-l}C(l)}{4^{-p}C(p)} \prod_{\substack{v\in(\sigma_0,\dots,\sigma_{l-2k-1})^* \bigcup(\tilde\sigma_1,\dots,\tilde\sigma_{m_k})^* \\ \#\sigma_0(s)+\cdots+\#\sigma_{l-2k-1}(s)+\#\tilde\sigma_1(s-r)+\cdots+\#\tilde\sigma_{m_k}(s-r)=p}} \theta(c_v)\right),$$

where m_k is the number of vertices at generation r in $\mathcal{F}_k$, while $\sigma_0,\dots,\sigma_{l-2k-1}$ stand for the trees (of maximal height s) not selected in $\mathcal{F}_k$, and $\tilde\sigma_1,\dots,\tilde\sigma_{m_k}$ stand for the trees (of maximal height $s-r$) obtained after truncation of the selected trees.

Let us denote by A_s the second term of the second line of the previous equation. To conclude the proof, it suffices to show that

$$\liminf_s A_s \geq 1. \tag{7.6.5}$$

Indeed, in that case the liminf of the quantities in the left-hand side of (7.6.2) are greater than or equal to the right-hand side, for any choice of the forest $\mathcal{F}_k$. As the sum of the quantities on the right-hand side of (7.6.2) over these choices is equal to 1, necessarily the desired convergence holds.

Let us thus show (7.6.5). Set $\varphi(l) := 4^{-l}C(l)$. We have

$$A_s = \sum_{l=2k+1}^{\infty} \frac{\varphi(l)}{\varphi(p)} \sum_{q=0}^{p} \mathcal{P}_{l-(2k+1)}\left(Y_s = q\right) \mathcal{P}_{m_k}\left(Y_{s-r} = p-q\right).$$

First, as θ is a critical offspring distribution, we get from [Pap68] that, for any $q \geq 0$,

$$\frac{\mathcal{P}_{m_k}\left(Y_{s-r} = p-q\right)}{\mathcal{P}_{m_k}\left(Y_s = p-q\right)} \xrightarrow[s\to\infty]{} 1.$$

Thus, for any $l \geq 2k+1$, for every $\varepsilon > 0$, for any sufficiently large s,

$$\sum_{q=0}^{p} \mathcal{P}_{l-(2k+1)}\left(Y_s = q\right) \mathcal{P}_{m_k}\left(Y_{s-r} = p-q\right) \geq (1-\varepsilon)\mathcal{P}_{l-(2k+1)}\left(Y_s = q\right) \mathcal{P}_{m_k}\left(Y_s = p-q\right)$$
$$\geq (1-\varepsilon)\mathcal{P}_{l-(2k+1)+m_k}\left(Y_s = p\right).$$

This implies that:

$$A_s \geq (1-\varepsilon) \sum_{l=2k+1}^{\infty} \frac{\varphi(l)}{\varphi(p)} \mathcal{P}_{l-(2k+1)+m_k}\left(Y_s = p\right).$$

Now, from the asymptotics of $C(l)$, we have that, for some $l_0 \geq 0$, for any $l \geq l_0$, we have

$$\varphi(l) \geq (1-\varepsilon)\varphi(l-(2k+1)+m_k),$$

so that,

$$A_s \geq (1-\varepsilon)^2 \sum_{l=m_k\vee l_0}^{\infty} \frac{\varphi(l)}{\varphi(p)} \mathcal{P}_l\left(Y_s = p\right).$$

Recall that $\varphi(l) = lh(l)$, which yields:

$$\begin{aligned} A_s &\geq (1-\varepsilon)^2 \sum_{l=m_k\vee l_0\vee p}^{\infty} \frac{h(l)}{h(p)} \mathcal{P}_l\left(Y_s = p\right) \\ &= (1-\varepsilon)^2 \left(1 - \sum_{l=0}^{m_k\vee l_0\vee p-1} \frac{h(l)}{h(p)} \mathcal{P}_l\left(Y_s = p\right)\right), \end{aligned}$$

the last equality stemming from (7.5.12).

Finally, we use once again the fact that, for any fixed l,

$$\mathcal{P}_l\left(Y_s = p\right) \xrightarrow[s\to\infty]{} 0,$$

to get that, for any $\varepsilon > 0$,

$$\liminf_s A_s \geq (1-\varepsilon)^2.$$

As ε was completely arbitrary in the above chain of arguments, we get that

$$\liminf_s A_s \geq 1.$$

This completes the proof of the proposition. □

7.7 Distances along the half-plane boundary

To fulfill our goal of showing the asymptotic equivalence between the oriented and non-oriented distances in uniform Eulerian triangulations, we need as a technical ingredient some estimates on the (oriented) distances along the boundary of $\mathcal{L}$.

Note that the vertices on $\partial\mathcal{L}$ are of two types, those of coordinates $(i, 0)$ for some $i \in \mathbb{Z}$, and those of coordinates $(i + 1/2, \varepsilon)$, for some $i \in \mathbb{Z}$. To simplify notation, the results in this section only deal with the distances between vertices of the first type, since we are interested in asymptotic estimates, and including the vertices of the second type only adds 1 or 2 to the considered distances. We will lay the stress on this generalization whenever it arises later in the paper.

In the sequel, we will use leftmost mirror geodesics, that were defined in Section 7.5 for finite cylinder triangulations, and that we generalize now to $\mathcal{L}$. For any $i \in \mathbb{Z}$, the leftmost mirror geodesic from $(i, 0)$ in $\mathcal{L}$ is an infinite path ω in $\mathcal{L}$, whose reverse is an oriented geodesic, and that visits a vertex $\omega(n)$ in $\mathcal{L}_n$ at every step $n \geq 0$. It starts at $(i, 0)$, and is obtained by choosing at step $n + 1$ the lefmost edge between $\omega(n)$ and $\mathcal{L}_{n+1}$. As before, for $i < j$, the leftmost mirror geodesics from $(i, 0)$ and $(j, 0)$ will coalesce before hitting $\mathcal{L}_r$, if and only if all the trees $\mathscr{T}_i, \mathscr{T}_{i+1}, \ldots, \mathscr{T}_{j-1}$ all have height strictly smaller than r.

7.7.1 Block decomposition and lower bounds

We first want to obtain upper bounds on the distances along the boundary of $\mathcal{L}$. For that purpose, we adapt the **block decomposition** of causal triangulations [CHN], to $\mathcal{L}$.

For $r \geq 1$, we define the random map $\mathcal{G}_r$ to be the planar map obtained from $\mathcal{L}_{[0,r]}$ by keeping only the faces and edges that are between $\mathscr{T}_0$ and $\mathscr{T}_{i_r}$, where i_r is the smallest integer $i > 0$ such that $\mathscr{T}_i \neq \varnothing$. More precisely, we only keep the skeleton modules that are at height smaller than or equal to r, belonging to trees $\mathscr{T}_i$, with $0 \leq i \leq i_r$, and the slots that are to the left of all these skeleton modules (see Figure 7.7.1 for an example).

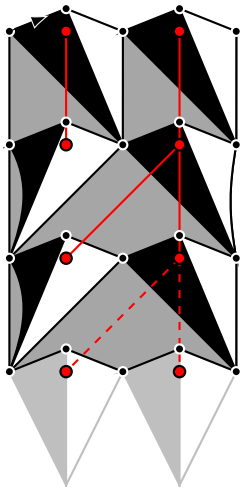

Figure 7.7.1 – The block of height 3 between $\mathscr{T}_0$ and $\mathscr{T}_1$ in the triangulation of Figure 7.6.1. As before, ghost modules are shown in pale grey.

Thus, $\mathcal{G}_r$ has one boundary that is naturally divided into four parts: the upper and lower parts that it shares with $\mathcal{L}_{[0,r]}$, and the left and right parts.

Note that $\mathcal{L}$ contains a lot of submaps that have the same law as $\mathcal{G}_r$: if $\mathscr{T}_i$, $\mathscr{T}_j$ are two consecutive trees reaching height $r-1$ in the skeleton of $\mathcal{L}$ (with $i<j$), we can define the submap of $\mathcal{L}_{[0,r]}$ encased between $\mathscr{T}_i$ (strictly) and $\mathscr{T}_j$ (included), which is obtained by keeping only the skeleton modules belonging to trees $\mathscr{T}_k$, with $i<k\leq j$, and the slots that are to the left of all these skeleton modules. Such a map has the same law as $\mathcal{G}_r$.

We call any map with the same law as $\mathcal{G}_r$, a **block of height r**.

We define the **diameter** of $\mathcal{G}_r$, denoted $\mathbf{Diam}(\mathcal{G}_r)$ to be the minimal oriented distance from a vertex on its left boundary, to a vertex on its right boundary. Note that this diameter is not uniformly large when r is large. However, we will now show that a long block is also typically wide. To do so, we consider the **median diameter** of a block.

Definition 7.7.1. For any $r\geq 1$, let $f(r)$ be the median diameter of $\mathcal{G}_r$, that is, the largest number such that

$$\mathbb{P}(\mathrm{Diam}(\mathcal{G}_r)\geq f(r))\geq \frac{1}{2}.$$

We show the following upper bound on the median diameter:

Theorem 7.7.2. *There exists $c>0$ such that*

$$f(r)\geq cr,$$

for all r sufficently large.

To prove this, we will use, like in [CHN], a renormalization scheme, splitting $\mathcal{G}_r$ into smaller blocks.

Proposition 7.7.3. *There exists $c>0$ such that, for any integer m with $1\leq m\leq cr$, we have*

$$f(r)\geq c\cdot\min\{m,\left(\frac{r}{m}\right)^2 f(m)\}.$$

Let us introduce a bit of notation before delving into the proof of this proposition. For any $m\geq 1$ and $h\geq 0$, consider the layer $\mathcal{L}_{[h,h+m]}$. It is composed of a sequence of

blocks of height m, denoted by $\mathcal{G}_m(i,h)$, for integers $i \geq 1$. For fixed h, m, these blocks are independent and distributed as $\mathcal{G}_m$. We denote by $N_r(m,h)$ the maximal index i such that the block $\mathcal{G}_m(i,h)$ is a sub-block of $\mathcal{G}_r$.

Proof of Proposition 7.7.3. Fix $r > m \geq 1$, and suppose for simplicity that m divides r. We get a lower bound for the diameter of $\mathcal{G}_r$ using the diameters of the blocks $\mathcal{G}_{2m}(i,h)$, for h of the form $l \cdot m$, with $0 \leq l \leq (r/m) - 2$. More precisely, we pick a vertex x on the left boundary of $\mathcal{G}_r$, at a height $0 \leq j \leq r$. Then, we can find an integer l such that x is located in the layer $\mathcal{L}_{[lm,(l+2)m]}$, with $0 \leq l \leq (r/m) - 2$ and so that $|lm - j| \geq m/3$ and $|(l+2)m - j| \geq m/3$. Consider then the shortest (oriented) path from x to the right boundary of $\mathcal{G}_r$. Either it stays in that layer, or it leaves it at some point. In the second case, we know that the length of the path is at least $m/3$, using our assumptions on j and h, and the fact that the distance between two vertices is at least their height difference. In the first case, the length of the path is bounded below by

$$\sum_{i=1}^{N_r(2m,lm)} \mathrm{Diam}(\mathcal{G}_{2m}(i,lm)).$$

Indeed, the path must cross, from left to right, every sub-block of height $2m$ of that layer, that also belongs to $\mathcal{G}_r$.

As noted before, for fixed h, m, the blocks $\mathcal{G}_{2m}(i,h)$ are independent and distributed as $\mathcal{G}_{2m}$. Thus, by the definition of the function f,

$$\mathbb{P}\left(\sum_{i=1}^{k} \mathrm{Diam}(\mathcal{G}_{2m}(i,h)) \leq \frac{k \cdot f(2m)}{4}\right) \leq \mathbb{P}(\mathrm{Bin}(k,1/2) \leq k/4) \leq e^{-\eta k},$$

for some $\eta > 0$ independent of k, h and m. Summing over the possibilities for $h = l \cdot m$, we obtain that, with probability at least $1 - (r/m)e^{-\eta k}$, we have

$$\forall\, 0 \leq l \leq (r/m) - 2 \quad \sum_{i=1}^{k} \mathrm{Diam}(\mathcal{G}_{2m}(i,lm)) \geq \frac{k \cdot f(2m)}{4}. \tag{7.7.1}$$

We now estimate $N_r(2m, lm)$:

Lemma 7.7.4. *There exists $c > 0$ such that, for every $1 \leq m \leq cr$, we have*

$$\mathbb{P}\left(\inf_{0 \leq l \leq (r/m)-2} N_r(2m,lm) \geq c\left(\frac{r}{m}\right)^2\right) \geq \frac{7}{8}.$$

Proof. Consider the case $m = 1$: in that case, $N_r(1,h)$ is just the horizontal width of the block $\mathcal{G}_r$ at height h. Like in [CHN], since θ is in the domain of attraction of a 3/2-stable law, we can find $c > 0$ sufficiently small that

$$\mathbb{P}\left(\inf_{0 \leq h \leq r-1} N_r(1,h) \geq cr^2\right) \geq \frac{15}{16} \tag{7.7.2}$$

for every $r \geq 1$. For other values of m, let us consider the intersection the event considered in (7.7.2). The variable $N_r(2m,h)$ counts the number of (sub-)trees in the skeleton of $\mathcal{L}$, starting at height h at an index between 0 and $N_r(1,h)-1$, and that reach (relative) height $2m$. Since $N_r(1,h) \geq cr^2$, using (7.5.18), we obtain that there are more than $c'(r/m)^2$ such trees on average, for some $c' > 0$. It then follows that

$$\mathbb{P}\big(N_r(2m,h) \leq c''(r/m)^2\big) \leq e^{-\delta(r/m)^2}$$

for some $c'' > 0$ and $\delta > 0$, independent of r and m. Then, for sufficiently large values of r/m, we have $(r/m)e^{-\delta(r/m)^2} < 1/16$, so that, when considering the different values for $h = lm$, we get

$$\begin{aligned}&\mathbb{P}\Big(\exists\, 0 \le l \le (r/m) - 2 \;\; N_r(2m, lm) \le c''\left(\frac{r}{m}\right)^2\Big)\\ &\le \mathbb{P}\Big(\inf_{0\le h\le r-1} N_r(1,h) < cr^2\Big) + \Big(\frac{r}{m} - 1\Big)\,\mathbb{P}\big(N_r(2m,h) \le c''(r/m)^2,\, N_r(1,h) \ge cr^2\big) \le \frac{1}{8},\end{aligned}$$

which proves the lemma. □

Let us now return to the proof of Proposition 7.7.3. Take $k = c(r/m)^2$, and assume that r/m is large enough to ensure that $(r/m)e^{-\eta k} \le 1/8$. Then, using Lemma 7.7.4 and intersecting with the event in (7.7.1) yields

$$\mathbb{P}\Big(\mathrm{Diam}(\mathcal{G}_r) \le \frac{m}{3} \wedge \frac{k\cdot f(2m)}{4}\Big) \le \mathbb{P}\Big(\inf_{0\le l\le (r/m)-2} N_r(2m, lm) \ge c\left(\frac{r}{m}\right)^2\Big) + \frac{r}{m}e^{-\eta k} \le \frac{1}{4}.$$

By definition of the function f, we have thus obtained that

$$f(r) \ge \frac{m}{3} \wedge \frac{c}{4}\left(\frac{r}{m}\right)^2 f(2m),$$

which directly gives the wanted inequality when $2m$ divides r, and the case where $2m$ does not divide r is a straightforward generalization. □

We can now prove Theorem 7.7.2.

Proof of Theorem 7.7.2. Let k be an integer that is larger than c^{-1}. Let $a_n = f(k^n)/k^n$. Then

$$\liminf_{n\to\infty} a_n > 0.$$

Indeed, applying Proposition 7.7.3 to $r = k^{n+1}$ and $m = k^n$, we obtain

$$a_{n+1} \ge \min\{\frac{ck^n}{k^{n+1}}, ck^{-1}\left(\frac{k^{n+1}}{k^n}\right)^2 a_n\} \ge \min\{\frac{c}{k}, a_n\}.$$

Note that $f(r) > 0$ for some $r \ge 1$, so that $a_n > 0$ for some $n \ge 1$, which yields that $\liminf_{n\to\infty} a_n > 0$ as claimed. This gives the desired inequality for values of r of the form k^n. The inequality for general values of r follows by taking $m = k^{\lfloor \log_k r - 1\rfloor}$ in Proposition 7.7.3. □

From Theorem 7.7.2, we obtain the following lower bounds for the distances along the boundary of $\mathcal{L}$:

Proposition 7.7.5. *For every $\varepsilon > 0$, there exists an integer $K > 0$ such that, for every $r \ge 1$,*

$$\mathbb{P}\Big(\min_{|j|\ge Kr^2} \vec{d}_{\mathcal{L}}((0,0),(j,0)) \ge r\Big) \ge 1 - \varepsilon.$$

Consequently, for $K' = 9K$, we also have, for every $r \ge 1$,

$$\mathbb{P}\Big(\min_{|j|\ge 2K'r^2} \;\; \min_{-K'r^2\le i\le K'r^2} \vec{d}_{\mathcal{L}}((i,0),(j,0)) \ge r\Big) \ge 1 - 2\varepsilon.$$

Proof. Let us start with the first assertion. Let $\varepsilon > 0$. Fix $r \geq 1$, and $K \geq 1$. Then, from (7.5.18), the number $N_{(K,r)}$ of trees that reach height r between $(0,0)$ and $(j,0)$ is bounded below by a binomial variable of parameters $(Kr^2, 3/((r+2)^2-1))$, so that, using Chebyshev's inequality, for any $a > 0$,

$$\mathbb{P}\left(N_{(K,r)} \leq \frac{3}{8}K - a\right) \leq \frac{3K}{a^2}.$$

(Note that the binomial variable in question has expectation greater than or equal to $3K/8$, with equality when $r = 1$, and a variance smaller than $3K$.)

Taking $a = \sqrt{(6K/\varepsilon)}$, for K large enough that $a \leq (1/8)K + 1$, we get

$$\mathbb{P}\left(N_{(K,r)} \leq \frac{1}{4}K + 1\right) \leq \frac{\varepsilon}{2}. \tag{7.7.3}$$

Now, on the event that $N_{(K,r)} > K/4$, for any $j \geq Kr^2$, we have

$$\vec{d}_{\mathcal{L}}((0,0),(j,0)) \geq \sum_{i=1}^{\lfloor \frac{K}{4} \rfloor + 1} \mathrm{Diam}(\mathcal{G}_r(i)) \wedge r,$$

so that, using Theorem 7.7.2,

$$\mathbb{P}\left(\vec{d}_{\mathcal{L}}((0,0),(j,0)) < cr\frac{K}{4} \wedge r\right) \leq \frac{1}{2^{K/4}}.$$

Now, taking K even larger if necessary, we can also have $cK/4 \geq 1$, and $1/2^{K/4} \leq \varepsilon/2$, which does give that, with probability at least $1-\varepsilon$, for all $j \geq Kr^2$, $\vec{d}_{\mathcal{L}}((0,0),(j,0)) \geq r$. The case of negative j can be treated in the same way.

Let us now turn to the second assertion. Assume that there exist $j \geq 2K'r^2$ and $i \in \{-K'r^2, \ldots, K'r^2\}$, such that $\vec{d}_{\mathcal{L}}((i,0),(j,0)) < r$. Then, any geodesic from $(i,0)$ to $(j,0)$ must stay in the layer $\mathcal{L}_{[0,r]}$, and therefore must intersect the leftmost mirror geodesic from $(K'r^2,0)$ to the line $\mathcal{L}_r$, so that

$$\vec{d}_{\mathcal{L}}((K'r^2,0),(j,0)) < 3r.$$

But then, by the first assertion of the proposition, the probability of such an event is bounded above by ε. Considering also the case $j < -K'r^2$, we obtain the desired result. □

An alternative proof of this result, adapting to Eulerian triangulations the method used in [CLG19] for usual triangulations, can be found in Chapter 8.

7.7.2 Upper bounds

After having proved in the previous subsection lower bounds for the distances along the boundary of $\mathcal{L}$, we now prove upper bounds for these quantities, that will carry to the UIPT of the digon $\mathcal{T}_\infty^{(1)}$ thanks to Proposition 7.5.7.

Proposition 7.7.6. *Let $\delta > 0$ and $\gamma > 0$. We can choose an integer $A \geq 1$ such that, for every sufficiently large n, with probability at least $1-\delta$:*

$\forall\, i \in \{-n+1, -n+2, \ldots, n\}$, the leftmost mirror geodesic starting from $(i,0)$ coalesces with the one starting from $(-n + \lfloor 2ln/A \rfloor, 0)$, for some $0 \leq l \leq A$, before hitting $\mathcal{L}_{\lfloor \gamma\sqrt{n} \rfloor}$.

Proof. Let $U_1^{(n)} < U_2^{(n)} < \cdots < U_{m_n}^{(n)}$ be all the indices in $\{1, 2, \ldots, 2n-1\}$ such that the height of $\mathscr{T}_{-n+i}$ is greater than or equal to $\lfloor \gamma\sqrt{n} \rfloor$. Defining, for $t \in \{0, 1, \ldots, 2n\}$, $N_t^{(n)} := \#\{i \in \{1, 2, \ldots, m_n\} | U_i^{(n)} \leq t\}$, it follows from (7.5.18) that $(N_{\lfloor nt \rfloor}^{(n)})_{0 \leq t \leq 2}$ converges in distribution in the Skorokhod sense to a Poisson process of parameter $3\gamma^{-2}$ (see [Bil99], Theorem 13.2). This implies that we can choose η small enough that, for every sufficiently large n, the property

$$U_{i+1}^{(n)} - U_i^{(n)} > \eta n \quad \forall\, i \in \{0, 1, \ldots, m_n\} \tag{7.7.4}$$

holds with probability at least $1 - \delta$. (Here we have set for convenience $U_0^{(n)} = 0$ and $U_{m_n+1}^{(n)} = 2n$.)

By the characterization of the coalescence of the lefmost mirror geodesics, if $U_j^{(n)} < i \leq i' \leq U_{j+1}^{(n)}$, the leftmost geodesic from $(-n+i, 0)$ coalesces with the one from $(-n+i', 0)$ before hitting the line $\mathcal{L}_{\lfloor \gamma\sqrt{n} \rfloor}$. Set $A = \lfloor 2/\eta \rfloor + 1$, so that $2/A < \eta$. On the event where (7.7.4) holds, each interval $(U_j^{(n)}, U_{j+1}^{(n)}]$, $0 \leq j \leq m_n$, contains at least one of the points $\lfloor 2ln/A \rfloor$, $1 \leq l \leq A$, which gives the desired result. □

We now derive a similar result for $\mathcal{T}_\infty^{(1)}$. Recall the notation L_r for the number of skeleton modules on $\partial^* B_r^\bullet(\mathcal{T}_\infty^{(1)})$.

For any integer $n \geq 1$, we write $u_0(n)$ for a vertex chosen uniformly at random in the vertices of type n of $\partial^* B_n^\bullet(\mathcal{T}_\infty^{(1)})$, and $u_1(n), \ldots, u_{L_n-1}(n)$ for the other type-n vertices of $\partial^* B_n^\bullet(\mathcal{T}_\infty^{(1)})$, enumerated clockwise, starting from $u_0(n)$. We extend the definition of $u_i(n)$ to $i \in \mathbb{Z}$ by periodicity.

Proposition 7.7.7. *Let $\gamma \in (0, 1/2)$ and $\delta > 0$. For every integer $A \geq 1$, let $H_{n,A}$ be the event where any leftmost mirror geodesic to the root starting from a type-n vertex of $\partial^* B_n^\bullet(\mathcal{T}_\infty^{(1)})$ coalesces before time $\lfloor \gamma n \rfloor$ with the leftmost mirror geodesic to the root starting from $u_{\lfloor kn^2/A \rfloor}(n)$, for some $0 \leq k \leq \lfloor n^{-2} L_n A \rfloor$. Then, we can choose A large enough that, for every sufficiently large n,*

$$\mathbb{P}(H_{n,A}) \leq 1 - \delta.$$

Proof. The idea of the proof is to carry the result of Proposition 7.7.6 over to the case of $\mathcal{T}_\infty^{(1)}$, using the *comparison principle* of Proposition 7.5.7. To apply it, one needs to consider the intersection of $H_{n,A}$ with an event of the form

$$\{\lfloor an^2 \rfloor < L_n \leq \lfloor a^{-1} n^2 \rfloor\} \cap \{\lfloor an^2 \rfloor < L_{n - \lfloor \gamma n \rfloor} \leq \lfloor a^{-1} n^2 \rfloor\}. \tag{7.7.5}$$

Lemma 7.5.6 ensures that we can choose an $a > 0$ such that this latter event holds with probability at least $1 - \delta/2$.

The details of the proof can be adapted verbatim from the proof of Proposition 17 in [CLG19]. □

7.8 Asymptotic equivalence between oriented and non-oriented distances

Recall that, on any Eulerian triangulation with a boundary A, we write $\vec{d}_A$ for the oriented distance on A, and d_A for the usual graph distance. We will show that these two distances are asymptotically proportional, first on the layers of the LHPET $\mathcal{L}$, then on the ones of the UIPET $\mathcal{T}_\infty^{(1)}$, and finally in large finite Eulerian triangulations.

7.8.1 Subbadditivity in the LHPET and the UIPET

Recall that we write ρ for the root vertex $(0,0)$ of the LPHET $\mathcal{L}$, and that $\mathcal{L}_r$ is the lower boundary of the layer $\mathcal{L}_{[0,r]}$. We have the following result:

Proposition 7.8.1. *There exists a constant $\mathbf{c}_0 \in [2/3, 1]$ such that*

$$r^{-1} d_{\mathcal{L}}(\rho, \mathcal{L}_r) \xrightarrow[r\to\infty]{a.s.} \mathbf{c}_0.$$

Proof. For integers $0 \leq m < n$, we define $\mathcal{L}_{[m,n]}$ similarly to the layers $\mathcal{L}_{[0,r]}$. The non-oriented distance $d_{\mathcal{L}_{[m,n]}}$ on this strip is defined by considering the shortest non-oriented paths that stay in $\mathcal{L}_{[m,n]}$. Thus, for two vertices $v, v' \in \mathcal{L}_{[m,n]}$, we have $d_{\mathcal{L}_{[m,n]}}(v, v') \geq d_{\mathcal{L}}(v, v')$.

Let then $m, n \geq 1$, and let x_m be the leftmost vertex x of $\mathcal{L}_m$ such that $d_{\mathcal{L}}(\rho, \mathcal{L}_m) = d_{\mathcal{L}}(\rho, x)$. We have

$$d_{\mathcal{L}}(\rho, \mathcal{L}_{m+n}) \leq d_{\mathcal{L}}(\rho, \mathcal{L}_m) + d_{\mathcal{L}_{[m,m+n]}}(x_m, \mathcal{L}_{m+n}).$$

As x_m is a function of $\mathcal{L}_{[0,m]}$ only, and the layers in $\mathcal{L}$ are independent, the random variable $d_{\mathcal{L}_{[m,m+n]}}(x_m, \mathcal{L}_{m+n})$ is independent of $\mathcal{L}_{[0,m]}$, and has the same distribution as $d_{\mathcal{L}}(\rho, \mathcal{L}_n)$.

We can then apply Liggett's version of Kingman's subbadditive theorem [Lig85], to get the desired convergence: the fact that the limit is a constant follows from Kolmogorov's zero-one law. As for the bounds for $\mathbf{c}_0$, it is clear from (7.2.1) that $\mathbf{c}_0 \in [1/2, 1]$. Our proof that $\mathbf{c}_0$ must be at least $2/3$ relies on a result of asymptotic proportionality in *finite* Eulerian triangulations, that will be stated further in Theorem 7.1.2. We thus postpone this argument to after Theorem 7.1.2.

It would be interesting to also refine the upper bound on $\mathbf{c}_0$. However, this seems to necessitate deeper arguments than our refinement of the lower bound. □

To carry this asymptotic proportionality over to large finite Eulerian triangulations, we will make a stop at the UIPET of the digon $\mathcal{T}_\infty^{(1)}$. In the remainder of this subsection, we write d for the non-oriented distance on $\mathcal{T}_\infty^{(1)}$, $B_n^\bullet$ for $B_n^\bullet(\mathcal{T}_\infty^{(1)})$ and $\partial^* B_n^\bullet$ for $\partial^* B_n^\bullet(\mathcal{T}_\infty^{(1)})$, to simplify notation.

Proposition 7.8.2. *Let $\varepsilon, \delta \in (0,1)$. We can find $\eta \in (0, 1/2)$ such that, for every sufficiently large n, the property*

$$(1-\varepsilon)\mathbf{c}_0 \eta n \leq d(v, \partial^* B^\bullet_{n-\lfloor \eta n \rfloor}) \leq (1+\varepsilon)\mathbf{c}_0 \eta n \qquad \forall\, v \in \partial^* B_n^\bullet$$

holds with probability at least $1-\delta$.

Proof. Let us give a sketch of the proof, as it is very similar to the proof of Proposition 20 in [CLG19]. Recall the notation $u_j^{(n)}$ for the type-n vertices of $\partial^* B_n^\bullet$. The first key step is to use Proposition 7.7.5 to get that a non-oriented shortest path from some $u_j^{(n)}$ to $\partial^* B^\bullet_{n-\lfloor \eta n \rfloor}$ that stays in $B_n^\bullet$ cannot meander too much in the layer $B_n^\bullet \setminus B^\bullet_{n-\lfloor \eta n \rfloor}$, and, more precisely, that it must stay in the region bounded by the leftmost mirror geodesics starting at $u^{(n)}_{j-\lfloor cn^2 \rfloor}$ and $u^{(n)}_{j+\lfloor cn^2 \rfloor}$ respectively, for some $c > 0$. Then, to bound probabilities of events on that sector of $B_n^\bullet \setminus B^\bullet_{n-\lfloor \eta n \rfloor}$, Proposition 7.5.7 together with Lemma 7.5.6 allows us to replace the skeleton of $B_n^\bullet \setminus B^\bullet_{n-\lfloor \eta n \rfloor}$ by independent Galton-Watson trees. We can therefore transfer the property of Proposition 7.8.1 from $\mathcal{L}$ to $B_n^\bullet \setminus B^\bullet_{n-\lfloor \eta n \rfloor}$. Finally, to consider all vertices of $\partial^* B_n^\bullet$, we use the coalescence property obtained in Proposition 7.7.7, which amounts to saying that it suffices to consider for the values of j a fixed number C, large but independent of n.

The details of the proof can be adapted verbatim from the proof of Proposition 20 in [CLG19] (replacing d_{gr} by $\vec{d}$, and d_{fpp} by d), with a small caveat.

Indeed, when using the coalescence property of Proposition 7.7.7 (which corresponds to (57) in [CLG19]), one must pay attention to two things.

First, Proposition 7.7.7 only gives an upper bound on the distances between vertices of $\partial^* B_n^\bullet$ *of type* n, and the C chosen $u_j^{(n)}$. To also include the vertices of type $n+1$, one must add an additional margin of 1 to the bounds, which, for any fixed ε, can be smaller than $\varepsilon \mathbf{c}_0 \eta n/2$, for n large enough.

A second restriction of the application of Proposition 7.7.7 is that it ensures that *oriented* geodesics *from the root* to a type-n vertex v of $\partial^* B_n^\bullet$ and to one of the chosen $u_j^{(n)}$, are merged up to a level γn. Thus, the upper bound on the oriented distance between v and $u_j^{(n)}$ is not $2\gamma n$ but $3\gamma n$.

Thus, rather than $\gamma = \varepsilon \mathbf{c}_0 \eta/2$, we take $\gamma = \varepsilon \mathbf{c}_0 \eta/6$, to obtain the equivalent of (57) in [CLG19] for all vertices of $\partial^* B_n^\bullet$. □

We now derive a more global result from the one of Proposition 7.8.2:

Proposition 7.8.3. *For every* $\varepsilon \in (0,1)$,

$$\mathbb{P}((\mathbf{c}_0 - \varepsilon)n \le d(\rho, v) \le (\mathbf{c}_0 + \varepsilon)n \text{ for every vertex } v \in \partial^* B_n^\bullet) \xrightarrow[n\to\infty]{} 1.$$

Proof. Let v be a vertex in $\partial^* B_n^\bullet$. The idea of the proof is to use Proposition 7.8.2 to estimate the distance $d(\rho, v)$ by going through the successive layers $\mathcal{L}_{\lfloor n_i - \lfloor \eta n_i \rfloor \rfloor}$, where n_i is defined inductively by $n_0 = n$ and $n_{i+1} = n_i - \lfloor \eta n_i \rfloor$.

The details of the proof can be adapted from Proposition 20 of [CLG19], replacing d_{gr} by $\vec{d}$, and d_{fpp} by d. □

7.8.2 Asymptotic proportionality of distances in finite triangulations

We now turn to finite triangulations. More precisely, we consider $\mathcal{T}_n^{(1)}$, uniform on the Eulerian triangulations of the digon with n black triangles. Recall that such triangulations are in bijection with (rooted) Eulerian triangulations with n black faces, from Figure 7.4.1. We write ρ_n for the root of $\mathcal{T}_n^{(1)}$, and d for the non-oriented distance on $\mathcal{T}_n^{(1)}$.

Proposition 7.8.4. *Let* o_n *be uniform over the inner vertices of* $\mathcal{T}_n^{(1)}$. *Then, for every* $\varepsilon > 0$,

$$\mathbb{P}\Big(|d(\rho_n, o_n) - \mathbf{c}_0 \vec{d}(\rho, o_n)| > \varepsilon n^{1/4}\Big) \xrightarrow[n\to\infty]{} 0.$$

To derive this from the previous results on $\mathcal{T}_\infty^{(1)}$, we will first establish an absolute continuity relation between finite triangulations and this infinite model.

Recall that $\mathbb{C}_{1,r}$ is the set of Eulerian triangulations of the cylinder of height r and bottom boundary length 2. For $\Delta \in \mathbb{C}_{1,r}$, we denote by $N(\Delta)$ the number of black triangles in Δ. Finally, we write $\overline{\mathcal{T}}_n^{(1)}$ for the triangulation $\mathcal{T}_n^{(1)}$ together with a distinguished vertex o_n. The hull $B_r^\bullet(\overline{\mathcal{T}}_n^{(1)})$ is well-defined when $\vec{d}(\rho_n, o_n) > r+1$, otherwise we set it to be $\overline{\mathcal{T}}_n^{(1)}$.

Lemma 7.8.5. *There exists a constant* $\bar{c} > 0$ *such that, for every* $n, r, p \ge 1$ *and every* $\Delta \in \mathbb{C}_{1,r}$ *with top boundary half-length* p, *such that* $n > N(\Delta) + p$,

$$\mathbb{P}\Big(B_r^\bullet(\overline{\mathcal{T}}_n^{(1)}) = \Delta\Big) \le \bar{c} \left(\frac{n}{n - N(\Delta) + 1}\right)^{3/2} \cdot \mathbb{P}\Big(B_r^\bullet(\mathcal{T}_\infty^{(1)}) = \Delta\Big). \tag{7.8.1}$$

Proof. Fix $r \geq 1$ and $\Delta \in \mathbb{C}_{1,r}$ with top boundary half-length p. We will write N for $N(\Delta)$ to simplify notation. Using (7.5.4) and the fact that $\mathcal{T}_\infty^{(1)}$ is the local limit of $\mathcal{T}_n^{(1)}$, we have

$$\mathbb{P}\Big(B_r^\bullet(\mathcal{T}_\infty^{(1)}) = \Delta\Big) = \frac{C(p)}{C(1)} 8^{-N(\Delta)}. \tag{7.8.2}$$

On the other hand, (7.5.3) gives the formula

$$\begin{aligned}\mathbb{P}\left(B_r^\bullet(\overline{\mathcal{T}}_n^{(1)}) = \Delta\right) &= \frac{B_{n-N,p}}{B_{n,1}} \cdot \frac{\#\text{inner vertices in } \mathcal{T}_n^{(1)} \setminus \Delta}{\#\text{inner vertices in } \mathcal{T}_n^{(1)}} \\ &\leq \frac{B_{n-N,p}}{B_{n,1}} \cdot \frac{n-N}{n},\end{aligned}$$

where the last inequality is given by Euler's formula and the fact that at most p vertices of $\partial^*\Delta$ are identified together in $\mathcal{T}_n^{(1)}$. (We still need $n > N + p$ since $\mathcal{T}_n^{(1)} \setminus \Delta$ will have $n - N - p$ inner vertices if none of these identifications occur.)

Then, using the bounds of (7.4.5) and the asymptotics of (7.4.3), we get that

$$\mathbb{P}\left(B_r^\bullet(\overline{\mathcal{T}}_n^{(1)}) = \Delta\right) \leq c^* C(p) \left(\frac{n}{n-N}\right)^{3/2} 8^{-N}$$

for some constant c^*. Comparing the last bound with (7.8.2) gives the desired result. □

Proof of Proposition 7.8.4. We will only sketch the main arguments of the proof, as it follows closely the proof of Proposition 21 in [CLG19].

Fix $\varepsilon > 0$ and $\nu > 0$. Its suffices to prove that, for all n sufficiently large, we have

$$\mathbb{P}\left(\left|\frac{d(\rho_n, o_n)}{\vec{d}(\rho_n, o_n)} - \mathbf{c}_0\right| > 2\varepsilon\right) < \nu. \tag{7.8.3}$$

Indeed, as stated in Theorem 7.2.4, the rescaled oriented distances from the origin converge to a Brownian snake. This implies, as detailed in Proposition 7.4.1, that the sequence $n^{-1/4}\vec{d}(\rho_n, o_n)$ is bounded in probability, so that the statement of the proposition will follow from (7.8.3).

Let us give an idea of how to obtain (7.8.3). We first want to use Lemma 7.8.5 to bound the probability of the event

$$E_{n,r,\varepsilon} := \left\{\sup_{x \in \partial^*\Delta} \left|\frac{d(\rho_n, x)}{\vec{d}(\rho_n, x)} - \mathbf{c}_0\right| \geq \varepsilon\right\},$$

using Proposition 7.8.3.

However, Lemma 7.8.5 can only give us that, for any $b \in (0, 1)$,

$$\lim_{r \to \infty} \left(\sup_{n \geq 1} \mathbb{P}(E_{n,r,\varepsilon} \cap F_{n,r,b})\right) = 0, \tag{7.8.4}$$

where

$$F_{n,r,b} := \left\{N(B_r^\bullet(\overline{\mathcal{T}}_n^{(1)})) \leq (1-b)n\right\}.$$

We now want to replace $F_{n,r,b}$ by events that are more manageable, to get to (7.8.3).

Fix some constants $0 < \alpha < \beta < \gamma$. We write $\mathfrak{B}_r(\mathcal{T}_n^{(1)}, o_n)$ for the ball of radius r centered at o_n in $\mathcal{T}_n^{(1)}$ (for the oriented distance). For every $n \geq 1$, we define the event

$$D_{\beta,\gamma,n} := \left\{\beta n^{1/4} < \vec{d}(\rho_n, o_n) \leq \gamma n^{1/4}\right\}.$$

We have that

$$\Big(D_{\beta,\gamma,n} \cap \{N(\mathfrak{B}_{\lfloor(\beta-\alpha)n^{1/4}\rfloor}(\mathcal{T}_n^{(1)}, o_n)) > bn\}\Big) \subset F_{n,\lfloor\alpha n^{1/4}\rfloor,b},$$

since, on $D_{\beta,\gamma,n}$, $\mathfrak{B}_{\lfloor(\beta-\alpha)n^{1/4}\rfloor}(\mathcal{T}_n^{(1)}, o_n)$ is entirely contained in the complement of $B^{\bullet}_{\lfloor\alpha n^{1/4}\rfloor}(\overline{\mathcal{T}}_n^{(1)})$.

Hence, we get from (7.8.4) that

$$\lim_{r\to\infty} \mathbb{P}\Big(E_{n,\lfloor\alpha n^{1/4}\rfloor,\varepsilon} \cap D_{\beta,\gamma,n} \cap \{N(\mathfrak{B}_{\lfloor(\beta-\alpha)n^{1/4}\rfloor}(\mathcal{T}_n^{(1)}, o_n)) > bn\}\Big) = 0 \tag{7.8.5}$$

as well.

The idea is then to get rid of the condition on $N(\mathfrak{B}_{\lfloor(\beta-\alpha)n^{1/4}\rfloor}(\mathcal{T}_n^{(1)}, o_n))$ by taking b small enough. Then, we choose a family of events $(D_{\beta_j,\gamma_j,n})_j$ such that their union occurs with high probability, to get that the event

$$\bigcup_j \Big(\Big(E_{n,\lfloor\alpha n^{1/4}\rfloor,\varepsilon}\Big)^c \cap D_{\beta_j,\gamma_j,n}\Big) \tag{7.8.6}$$

occurs with high probability as well.

Then, to conclude the proof, we show that when the event (7.8.6) occurs, the event in (7.8.3) does not hold.

For the first step, note that, given any $y < 1$, we can choose $b \in (0,1)$ such that

$$\liminf_{n\to\infty} \mathbb{P}\Big(N(\mathfrak{B}_{\lfloor(\beta-\alpha)n^{1/4}\rfloor}(\mathcal{T}_n^{(1)}, o_n)) > bn\Big) \geq y. \tag{7.8.7}$$

This is a consequence of the convergence of the rescaled oriented distances from the origin to a Brownian snake, as shown in Proposition 7.4.2.

As (7.8.7) holds for y arbitrarily close to 1, (7.8.5) implies that we also have, as announced,

$$\lim_{n\to\infty} \mathbb{P}\Big(E_{n,\lfloor\alpha n^{1/4}\rfloor,\varepsilon} \cap D_{\beta,\gamma,n}\Big) = 0. \tag{7.8.8}$$

To choose our family of events $(D_{\beta_j,\gamma_j,n})_j$, note that Proposition 7.4.1 implies that there exist constants $0 < \delta < \eta$ such that

$$\mathbb{P}\Big(\delta n^{1/4} < \vec{d}(\rho_n, o_n) \leq \eta n^{1/4}\Big) \geq 1 - \frac{\nu}{2}.$$

Thus, we just have to choose a range of β_j, γ_j such that the union $\cup_j D_{\beta_j,\gamma_j,n}$ contains the event of the previous display.

It then remains to show that we have

$$\left|\frac{d(\rho_n, o_n)}{\vec{d}(\rho_n, o_n)} - \mathbf{c}_0\right| > 2\varepsilon$$

on the event (7.8.6).

This last step can be adapted verbatim from the proof of Proposition 21 in [CLG19], replacing once again d_{gr} by $\vec{d}$, and d_{fpp} by d. □

We will now derive our final result of asymptotic proportionality between the oriented and non-oriented distances, Theorem 7.1.2. This one is in the context of $\mathcal{T}_n$, the uniform rooted plane Eulerian triangulation with n black faces, that is in correspondence with $\mathcal{T}_n^{(1)}$ as shown in Figure 7.4.1. As previously, we use d to denote the non-oriented graph distance.

Proof of Theorem 7.1.2. Let us give an idea of the proof of this theorem, which follows once again the arguments of the proof of Theorem 1 in [CLG19].

From Proposition 7.8.4 and the correspondence between $\mathcal{T}_n^{(1)}$ and $\mathcal{T}_n$, we get that, if o_n' is a uniform vertex of $\mathcal{T}_n$, we have

$$\mathbb{P}\Big(|d(\rho_n, o_n') - \mathbf{c}_0 \vec{d}(\rho_n, o_n')| > \varepsilon n^{1/4}\Big) \xrightarrow[n\to\infty]{} 0. \tag{7.8.9}$$

Observe now that $\overline{\mathcal{T}}_n$, re-rooted at a random uniform edge e_n (remember that all edges of $\mathcal{T}_n$ have a canonical orientation), still pointed at o_n', has the same distribution as $\overline{\mathcal{T}}_n$. This allows us to deduce from (7.8.9) a similar statement on distances between two random uniform vertices o_n', o_n'' of $\mathcal{T}_n$:

$$\mathbb{P}\Big(|d(o_n', o_n'') - \mathbf{c}_0 \vec{d}(o_n', o_n'')| > \varepsilon n^{1/4}\Big) \xrightarrow[n\to\infty]{} 0. \tag{7.8.10}$$

We now want to make this statement into a global one on all the vertices of $\mathcal{T}_n$.

Let us fix $\delta \in (0, 1/2)$. We can choose an integer $k \geq 1$ such that, for every n sufficiently large, we can pick k random vertices $(o_n^1, \dots, o_n^k)$ uniformly in $\mathcal{T}_n$ and independently from one another, satisfying

$$\mathbb{P}\left(\sup_{x\in V(\mathcal{T}_n)} \left(\inf_{1\leq j\leq k} \vec{d}(x, o_n^j)\right) < \varepsilon n^{1/4}\right) > 1 - \delta. \tag{7.8.11}$$

This follows from the convergence of the rescaled oriented distances from the origin to a Brownian snake, see Proposition 7.4.3.

Then, (7.8.10) implies that we also have, for all sufficiently large n,

$$\mathbb{P}\left(\bigcap_{1\leq i\leq j\leq k} \{|d(o_n^i, o_n^j) - \mathbf{c}_0 \vec{d}(o_n^i, o_n^j)| \leq \varepsilon n^{1/4}\}\right) > 1 - \delta.$$

Observe now that

$$\sup_{x,y\in V(\mathcal{T}_n)} |d(x,y) - \mathbf{c}_0 \vec{d}(x,y)| \leq \sup_{1\leq i,j\leq N} |d(o_n^i, o_n^j) - \mathbf{c}_0 \vec{d}(o_n^i, o_n^j)| + 5 \sup_{x\in V(\mathcal{T}_n)} \left(\inf_{1\leq j\leq N} \vec{d}(x, o_n^j)\right).$$

Using the previous two bounds, the right-hand side of this inequality can be bounded by 6ε outside a set of probability at least 2δ for all sufficiently large n, which concludes the proof. □

Let us finally give a short proof of why $\mathbf{c}_0 \geq 2/3$. Consider $\mathcal{T}_n$, the uniform rooted plane Eulerian triangulation with n black faces. From Theorem 7.1.2, for any $\varepsilon, \delta \in (0,1)$, for n large enough,

$$|d_n(x,y) - \mathbf{c}_0 \vec{d}_n(x,y)| \leq \varepsilon n^{1/4}, \quad \forall x, y \in (\mathcal{T}_n), \tag{7.8.12}$$

outside an event of probability less than δ.

Suppose $\mathbf{c}_0 < 2/3$. Then, on the event of (7.8.12), for any $x, y \in (\mathcal{T}_n)$ such that

$$d_n(x,y) \geq c n^{1/4}, \tag{7.8.13}$$

for some $c > 0$, we have:

$$\vec{d}_n(x,y) \geq \left(\frac{1}{\mathbf{c}_0} - \frac{\varepsilon}{c}\right) d_n(x,y).$$

This means that, for any geodesic γ for the distance d_n from x to y in $\mathcal{T}_n$, a proportion larger than or equal to $(1/\mathbf{c}_0 - 1 - \varepsilon/c)$ of the edges of γ are oriented from y to x. But, as the above bound also applies when we exchange x and y, the same proportion of edges of γ must be oriented from x to y, which is not possible if $(1/\mathbf{c}_0 - 1 - \varepsilon/c) > 1/2$, that is, $\varepsilon/c < 1/\mathbf{c}_0 - 3/2$.

Since, for any $c \in (0, 1)$, for n large enough, a positive proportion of pairs of vertices of $\mathcal{T}_n$ satisfy (7.8.13), we deduce that (7.8.12) cannot have a high probability, if $\mathbf{c}_0 < 2/3$.

CHAPITRE 8

Études des boules de la triangulation eulérienne infinie du demi-plan supérieur

Contents

8.1 Setting

This chapter is closely related to the previous one, and as such we will use the same notation without introducing it again. In particular, recall that we have defined in Chapter 7 the Lower Half-Plane Eulerian Triangulation $\mathcal{L}$, whose skeleton is defined by a bi-infinite sequence of independent Galton-Watson trees $(\mathscr{T}_i)_{i\in\mathbb{Z}}$, with critical offspring distribution θ.

In this chapter, we define a new random Eulerian triangulation of the half-plane, the **Upper Half-Plane Eulerian Triangulation $\mathcal{U}$**. As its name indicates, it is the equivalent of well-known models such as the UHPT or UHPQ, in the case of Eulerian triangulations.

In Section 8.5 and Section 8.6, we proceed similarly to Section 4 of [CLG19], to obtain estimates on the (oriented) distances along the boundary of $\mathcal{U}$, that will be carried to $\mathcal{L}$ by an "absolute continuity" property: we derived these estimates in $\mathcal{L}$ in Chapter 7, using an independent proof involving the block decomposition of $\mathcal{L}$.

Using $\mathcal{U}$ to obtain these estimates necessitates a precise understanding of its structure. In Section 8.2, after defining $\mathcal{U}$, we show that it is the local limit of the infinite Eulerian triangulation of the $2p$-gon, $\mathcal{T}_\infty^p$, as $p \to \infty$. Then, in Section 8.3, we will investigate the structure of the balls and hulls of $\mathcal{U}$, and see that they involve Eulerian triangulations with new types of boundary conditions. In Section 8.4, we recall the asymptotic enumeration results derived for these new boundary conditions in Chapter 9, and prove some additional bounds relating the generating functions for these new boundary conditions, to the generating function for the semi-simple alternating boundary condition.

Notably, the alternative proof carried out in this chapter allows us to gain insight on the structure of $\mathcal{U}$, by decomposing it into spherical layers described by a branching process, together with Boltzmann Eulerian triangulations with several types of boundary conditions. This is expressed more precisely in Theorem 8.5.1, whose statement requires the introduction of a good bit of notation.

8.2 The Upper Half-Plane Eulerian Triangulation

We thus construct a triangulation of the upper half-plane $\mathbb{R} \times \mathbb{R}_+$. A key step in this construction is an infinite tree embedded in the half-plane, whose vertex set is $\{(\frac{1}{2}+i, j), i \in \mathbb{Z}, j \in \mathbb{Z}_{\geq 0}\}$. We start with the construction of this tree.

The tree has an infinite "spine" that consists of all the vertices of the (discrete) half-line $\{(\frac{1}{2}, j), j \in \mathbb{Z}_{\geq 0}\}$. We can view the tree as growing downwards, and thus for every $j \geq 1$ the vertex $(\frac{1}{2}, j)$ is the parent of $(\frac{1}{2}, j-1)$. Let $\bar{\theta}$ be the size-biased distribution associated with θ, that is: $\bar{\theta}(k) = k \cdot \theta(k)$ for all $k \geq 1$. Each vertex $(\frac{1}{2}, j)$ of the spine has, independently of all the others, a random number m_j of children distributed according to

$\bar{\theta}$, and these children are the vertices $(\frac{1}{2}+k, j-1)$, for $l_j - m_j \leq k \leq l_j - 1$, where l_j is uniform in $\{1, 2, \ldots, m_j\}$. The pairs $(m_j, l_j), j \in \mathbb{Z}_{\geq 0}$ are assumed to be independent.

Then, to each vertex $(\frac{1}{2}+k, j)$ with $k \neq 0$ which is a child of a vertex of the spine, we attach (independently and independently of the pairs $(m_i, l_i), i \in \mathbb{Z}_{\geq 0}$) a Galton-Watson tree with offspring distribution θ truncated at height j, such that the vertices at height r (for $0 \leq r \leq j$) in this tree will be points of the form $(\frac{1}{2}+i, j-r)$. Without going into the details, it is possible to draw these trees in the half-plane so that no two edges cross, and so that vertices are exactly all the points of the form $(\frac{1}{2}+i, j), i \in \mathbb{Z}, j \in \mathbb{Z}_{\geq 0}$ (see Figure 8.2.1).

We now construct the triangulation itself, similarly to $\mathcal{L}$. We start with the "distinguished" modules, which will play the role of skeleton modules for our infinite triangulation. For each $(i, j) \in \mathbb{Z} \times \mathbb{Z}_{>0}$, we construct a module for which the points $(i-1, j)$ and (i, j) will be the vertices of type $n+1$. The vertex of type n of the module will be the point $(k, j-1)$, where k is the minimal integer such that the tree vertex $(\frac{1}{2}+k, j)$ is a child of $(\frac{1}{2}+i', j)$, for some $i' > i$. The last vertex of this module, the type $n+2$ one, is set as the point $(\frac{1}{2}+i, j+\varepsilon)$, for some arbitrary $0 < \varepsilon < 1$. We draw the edges of these modules in a such a way that they are all distinct, and do not cross. Note that, keeping the same convention as for finite triangulations, the vertices of the form $(\frac{1}{2}+i, 0)$ in the infinite tree are associated in the same way with "ghost" skeleton modules which are below the boundary. We finish the construction of the triangulation by filling in the slots bounded by the skeleton modules, with independent Boltzmann Eulerian triangulations of appropriate perimeters[1].

The resulting triangulation of the upper half-plane, which we will denote by $\mathcal{U}$, is called the **Upper Half-Plane Eulerian Triangulation** (UHPET). It is rooted at the edge from $(0, 0)$ to $(\frac{1}{2}, \varepsilon)$.

Proposition 8.2.1. *We have*

$$\mathcal{T}_\infty^{(p)} \xrightarrow[p\to\infty]{(d)} \mathcal{U}$$

in the sense of local limits of rooted planar maps.

Proof. Let us just give an idea of the proof, as it is very similar to the one of Proposition 6 in [CLG19]. It is also similar to the proof of the convergence to $\mathcal{L}$ in Chapter 7: proving the desired convergence amounts to show that, for any Eulerian triangulation A with boundaries,

$$\mathbb{P}\Big(\mathcal{B}_r(\mathcal{T}_\infty^{(p)}) = A\Big) \xrightarrow[p\to\infty]{} \mathbb{P}(\mathcal{B}_r(\mathcal{U}) = A). \tag{8.2.1}$$

To do so, like for the convergence to $\mathcal{L}$, we actually show that the liminf of the left-hand side is larger than or equal to the right-hand side.

Despite this similarity in principle, this proof involves calculations that are disjoint from the ones concerning $\mathcal{L}$, as we take here the limit $p \to \infty$ (recall that $\widetilde{B}_s^\bullet\left(\mathcal{T}_\infty^{(p)}\right) \xrightarrow[s\to\infty]{(d)} \mathcal{L}$).

Let us introduce a bit of notation, similar to the notation we used in the proof of Proposition 7.6.1 in Chapter 7. Consider $r \geq 1$ fixed and denote by $\mathcal{F}_{0,r}^{(p)} = \left(\mathscr{T}_0^{(p)}, \mathscr{T}_1^{(p)}, \ldots, \mathscr{T}_{L_r^{(p)}-1}^{(p)}\right)$ the skeleton of $B_r^\bullet\left(\mathcal{T}_\infty^{(p)}\right)$. In $\mathcal{U}$, we denote by $\Gamma_{(i,j)}$ the subtree of descendants of $(\frac{1}{2}+i, j)$ in the infinite tree, and it is understood that $\Gamma_{(0,j)}$ has a distinguished vertex corresponding to $(\frac{1}{2}, 0)$. In the sequel, we will just consider the $\Gamma_{(i,j)}$ as abstract plane trees, without their specific embedding in $\mathbb{R} \times \mathbb{R}_+$.

[1] Note that, as the boundary of Boltzmann Eulerian triangulations is *semi*-simple, this can have the effect of identifying vertices with coordinates of the form $(\frac{1}{2}+i, j+\varepsilon)$, $(\frac{1}{2}+i', j'+\varepsilon)$, so that vertices of this type may be associated to several sets of coordinates

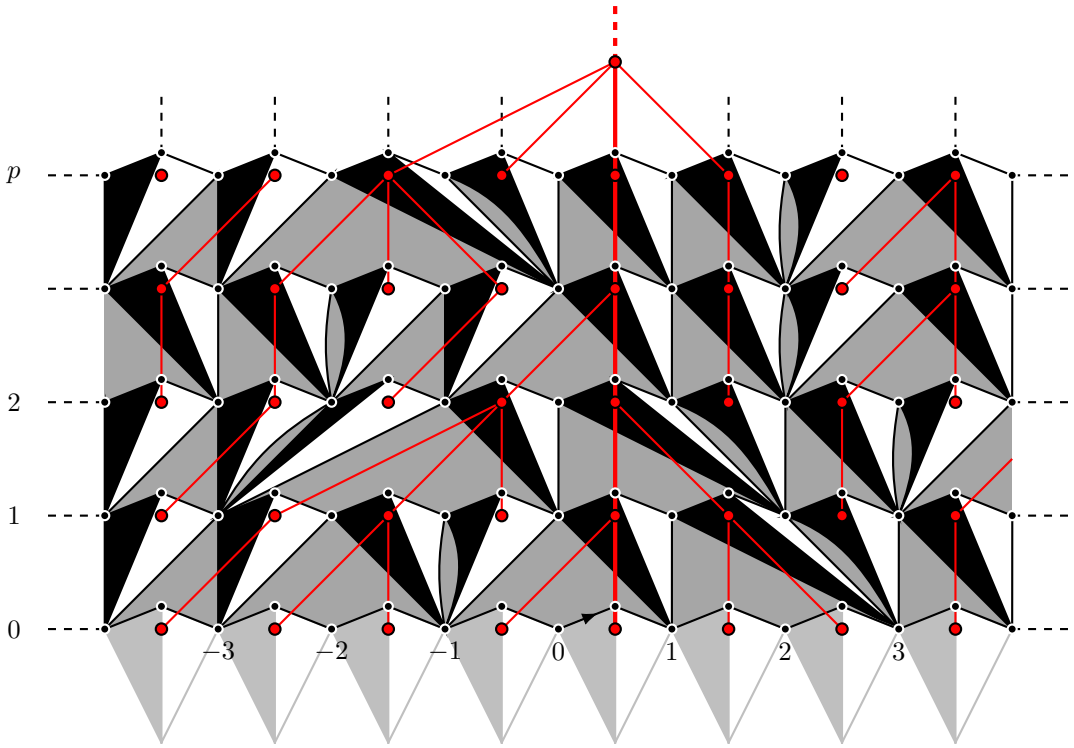

Figure 8.2.1 – Construction of the UHPET

Let us fix $k \geq 1$. For any forest $\mathcal{F} = (\sigma_0, \dots, \sigma_{l-1}) \in \mathbb{F}_{p,l,r}$ with $l \geq 2k+1$, we write $\Phi_k(\mathcal{F}) = (\sigma_{l-k}, \dots, \sigma_{l-1}, \sigma_0, \dots, \sigma_k)$ where it is understood that, in $\Phi_k(\mathcal{F})$ like in $\mathcal{F}$, σ_0 comes with a distinguished vertex at height r.

We claim that it is enough to prove that, for every finite set $\mathcal{F}_k = (\tau_{-k}, \dots, \tau_0, \dots, \tau_k)$ of $2k+1$ plane trees of maximal height r, with a distinguished vertex at height r in τ_0,

$$\mathbb{P}\Big(\{\Phi_k\left(\mathcal{F}_{0,r}^{(p)}\right) = \mathcal{F}_k\} \cap \{L_r^{(p)} \geq 2k+1\}\Big) \xrightarrow[p\to\infty]{} \mathbb{P}\big(\big(\Gamma_{(-k,r)}, \dots, \Gamma_{(0,r)}, \dots, \Gamma_{(k,r)}\big) = \mathcal{F}_k\big). \tag{8.2.2}$$

(Note that the equalities between these collections of trees entail that they have the same distinguished vertex in their central tree.)

Indeed, if k is large enough, we can find a collection $\mathbf{F}_k$ of forests $\mathcal{F}_k$ such that the probability of the event $\{\big(\Gamma_{(-k,r)}, \dots, \Gamma_{(0,r)}, \dots, \Gamma_{(k,r)}\big) \in \mathbf{F}_k\}$ is close to 1, and, on that event, the ball $\mathcal{B}_r(\mathcal{U})$ is a deterministic function of the trees $\Gamma_{(-k,r)}, \dots, \Gamma_{(k,r)}$ and of the triangulations with a boundary filling in the slots associated with the vertices of these trees. (Note that we need k to be large, so that the $(2k+1)$ subtrees of the skeleton of $\mathcal{U}$ and the associated slots are enough to cover the ball $\mathcal{B}_r(\mathcal{U})$, not only vertically, which is a given, but also horizontally.) Likewise, on the event $\{\Phi_k\left(\mathcal{F}_{0,r}^{(p)}\right) \in \mathbf{F}_k\} \cap \{L_r^{(p)} \geq 2k+1\}$, the ball $\mathcal{B}_r\left(\mathcal{T}_\infty^{(p)}\right)$ is given by the same deterministic function of the trees in $\Phi_k\left(\mathcal{F}_{0,r}^{(p)}\right)$ and of the associated triangulation with a boundary. Thus, the desired convergence of (8.2.1) will follow from (8.2.2), together with the fact that, for every fixed $r \geq 1$ and $j \geq 1$,

$$\mathbb{P}\Big(L_r^{(p)} = j\Big) \xrightarrow{p\to\infty} 0,$$

where, as in Chapter 7, $L_r^{(p)}$ is the length of the top cycle of $B_r^\bullet(\mathcal{T}_\infty^{(p)})$. This last convergence easily follows, like in [CLG19], from the asymptotic behavior of θ.

To prove (8.2.2), we expand its left-hand and right-hand sides. The right-hand side can be written very straightforwarly:

$$\mathbb{P}\big(\big(\Gamma_{(-k,r)},\dots,\Gamma_{(0,r)},\dots,\Gamma_{(k,r)}\big)=\mathcal{F}_k\big)=\prod_{v\in(\tau_{-k},\dots,\tau_k)^*}\theta(c_v), \tag{8.2.3}$$

where, as before, for a collection $\mathcal{F}$ of trees, $\mathcal{F}^*$ stands for the set of vertices in $\mathcal{F}$ that are not at the maximal height, and, for such a vertex v, c_v is the number of children of v.

Now, using the definition of the law $\mathbf{P}_{p,r}$ of $B_r^\bullet\left(\mathcal{T}_\infty^{(p)}\right)$, the left-hand side of (8.2.2) is equal to

$$\begin{aligned}&\sum_{l=2k+1}^{\infty}\sum_{\mathcal{F}\in\mathbb{F}_{p,l,r},\,\Phi_k\left(\mathcal{F}_{0,r}^{(p)}\right)=\mathcal{F}_k}\frac{4^{-l}C(l)}{4^{-p}C(p)}\prod_{v\in\mathcal{F}^*}\theta(c_v)\\&=\left(\prod_{v\in(\tau_{-k},\dots,\tau_k)^*}\theta(c_v)\right)\cdot\left(\sum_{l=2k+1}^{\infty}\frac{4^{-l}C(l)}{4^{-p}C(p)}\sum_{\sigma_{k+1},\sigma_{k+2},\dots,\sigma_{l-k-1}}\prod_{v\in(\sigma_{k+1},\dots,\sigma_{l-k-1})^*}\theta(c_v)\right)\end{aligned} \tag{8.2.4}$$

where the second sum in the last line runs over all possible choices for the set of plane trees $\{\sigma_{k+1},\sigma_{k+2},\dots,\sigma_{l-k-1}\}$ of maximal height at most r, with $p-m_k$ vertices at height r, m_k being the number of vertices at generation r in $\mathcal{F}_k$.

Let us denote by A_p the second term of the second line in (8.2.4): to conclude the proof, as advertised, it suffices to prove that $\liminf_p A_p\geq 1$.

Setting $\varphi(l):=4^{-l}C(l)$ as in Chapter 7, we have

$$\begin{aligned}A_p=\sum_{l=2k+1}^{\infty}\frac{\varphi(l)}{\varphi(p)}\mathcal{P}_{l-(2k+1)}\left(Y_r=p-m_k\right)&=\sum_{l=0}^{\infty}\frac{\varphi(l+2k+1)}{\varphi(p)}\mathcal{P}_{l-(2k+1)}\left(Y_r=p-m_k\right)\\&\geq\sum_{l=0}^{\infty}\frac{\varphi(l)}{\varphi(p)}\mathcal{P}_l\left(Y_r=p-m_k\right),\end{aligned}$$

the last inequality relying on the fact that φ is monotone increasing. Indeed, as, for all $0\leq z<1$,

$$\sum_{l\geq 0}\varphi(l)z^l=\frac{3}{8}\frac{z}{\sqrt{\pi(1-\frac{z}{4})(1-z)^3}},$$

we have

$$\sum_{l\geq 0}(\varphi(l+1)-\varphi(l))z^l=\frac{3}{8}\frac{1}{\sqrt{\pi(1-\frac{z}{4})(1-z)^3}}(1-z)=\frac{3}{8}\frac{1}{\sqrt{\pi(1-\frac{z}{4})(1-z)}}.$$

This last generating function has nonnegative coefficients, since it is the case for $z\mapsto\frac{1}{\sqrt{1-z}}$, which means that φ is indeed monotone increasing. Note that this argument is slightly more involved than the equivalent one in [CLG19], as we do not have a simple expression for $\varphi(l)$.

We then use the asymptotic behavior of θ to conclude that $\liminf_p A_p\geq 1$: the details of this last part of the proof can be adapted verbatim from the proof of Proposition 6 in [CLG19]. □

8.3 Structure of the balls of the UHPET

For any integer $r \geq 1$, we define the **ball of radius** r of $\mathcal{U}$, $\mathcal{B}_r(\mathcal{U})$, as the submap of $\mathcal{U}$ obtained by keeping only the faces and edges of $\mathcal{U}$ incident to at least a vertex at oriented distance less than $r-1$ from the root. We also define its **hull** $\mathcal{B}_r^\bullet(\mathcal{U})$ as the union of $\mathcal{B}_r(\mathcal{U})$ and all the finite connected components of its complement. Note that this is the notion we detailed in Chapter 7 for Eulerian triangulations *without boundary*, and not the notion of "vertical" balls and hulls $B_r, B_r^\bullet$ that would simply yield the layers of $\mathcal{U}$.

As $\mathcal{U}$ has a boundary, we can expect that its "spherical" balls and hulls will have a slightly different structure than what we described for planar Eulerian triangulations without boundary in Chapter 7. We now investigate this possibly new structure.

We can straightforwardly use again the notion of type-r modules, module diagonals, and orient them "left-to-right". Then, we still want to see the union of these oriented diagonals as a set of oriented curves $\mathcal{C}_r(\mathcal{U})$. The idea is that, instead of being closed, some of these curves start and end on the half-plane boundary. Let us explain how this occurs.

We must first examine what happens at vertices of $\mathcal{U}$ of type r. For inner vertices, the arguments of Chapter 7 still stand, and we have an alternation of ingoing and outgoing diagonals. However, for boundary vertices, we must be more careful.

Consider a boundary vertex v of type r. If the leftmost type-r triangle incident to v is black (and so corresponds to a module diagonal that goes out of v), it will be unpaired by our resolution rule, and thus it will be the starting point of a curve. Similarly, if the rightmost type-r triangle incident to v is white, it will be unpaired, and be the end point of a curve (see Figure 8.3.1).

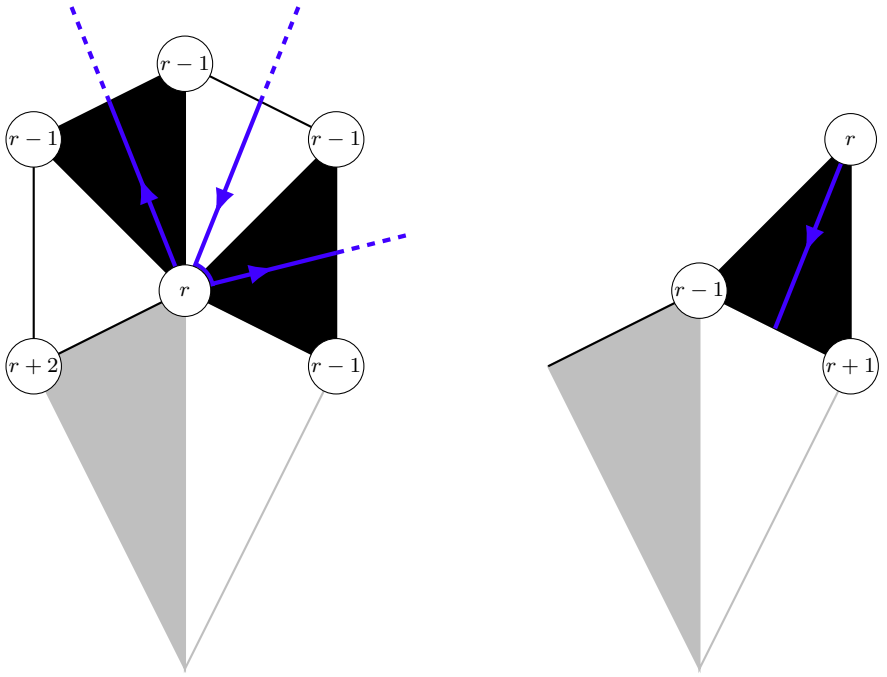

Figure 8.3.1 – In $\mathcal{U}$, the curves in $\mathcal{C}_r(\mathcal{U})$ can end on $\partial\mathcal{U}$, either on a type-r vertex (left), or on an unpaired type-r triangle (right).

(As $\partial\mathcal{U}$ is semi-simple, if v has coordinates of the type $(i, 0)$, it might be the end of an isthmus of the infinite face of $\mathcal{U}$: in that case the only edge incident to v is oriented away from it, so that the oriented distance from the origin to v is a priori ill-defined... we can resolve this by setting $\vec{d}(\rho, v) = \vec{d}(\rho, u) + 2$, where u is the only neighbor of v, and

has "coordinates" $(i \pm 1/2, \varepsilon)$. In any case, v is not adjacent to an infinite component of $\mathcal{U} \setminus \mathcal{B}_r(\mathcal{U})$, so that this pathological case will not appear on the boundary of the hull $\mathcal{B}_r^\bullet(\mathcal{U})$, which is what really interests us.)

Another new feature to take into account is that not all triangles of $\mathcal{U}$ are paired into modules. Indeed, if a triangle f of type r shares its edge of type $r-1 \to r+1$ with $\partial\mathcal{U}$, then f does not belong to a type-r module, so that the "half-diagonal" crossing f starts (resp. ends) at $\partial\mathcal{U}$ if f is white (resp. black) (see Figure 8.3.1).

As the union of module diagonals is even (and with alternating orientation) on inner vertices of type r, the curves in $\mathcal{C}_r(\mathcal{U})$ are either closed (but may "rebound" on $\partial\mathcal{U}$ on boundary vertices of type r), or they start and end at $\partial\mathcal{U}$, either at vertices of type r, or at the edge of type $r-1 \to r+1$ of an unpaired triangle of type r. For the same reasons as in Chapter 7, it is still the case that the closed curves in $\mathcal{C}_r(\mathcal{U})$ cannot encircle one another, and that each closed curve must be simple.

Let note that, by our choice of orientation of the module diagonals, a semi-circular curve $\mathscr{C} \in \mathcal{C}_r(\mathcal{U})$ either goes right to left between two points on the boundary that are on the same side of the origin, or it goes from a point that is on the left of the origin, to one that is on the right. With this observation, together with a slight variation of the arguments for closed curves, we can show that a "semi-circular" curve in $\mathcal{C}_r(\mathcal{U})$ must also be simple, and cannot rebound on $\partial\mathcal{U}$ (see Figures 8.3.2 and 8.3.3), and that neither two semi-circular curves, nor a semi-circular one and closed one, can separate the same vertex from the origin (see Figure 8.3.4).

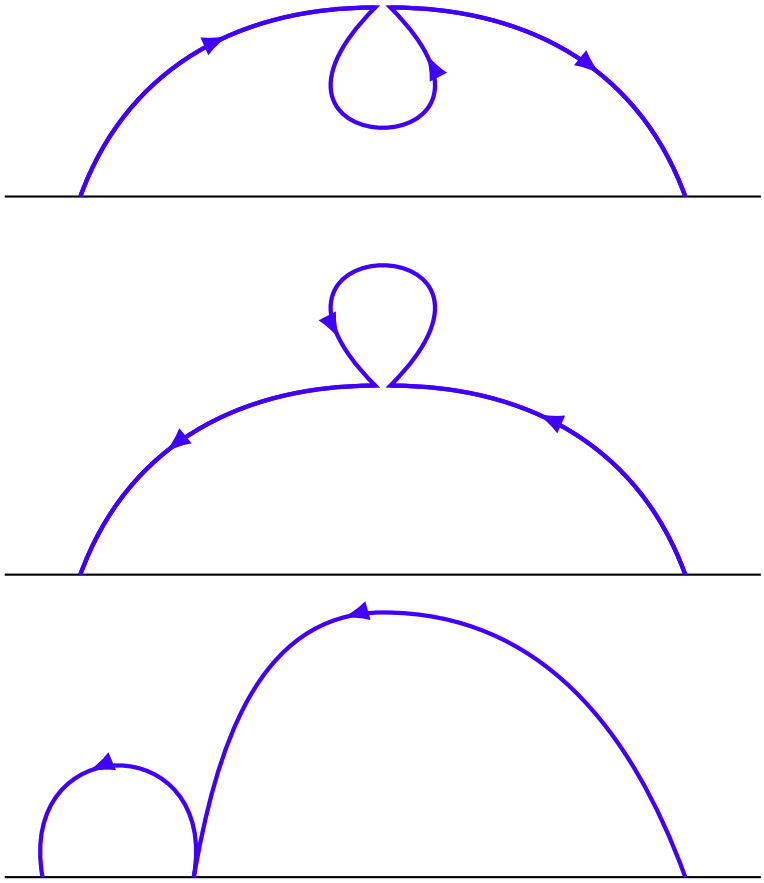

Figure 8.3.2 – Half of the possible self-intersections for a semi-circular curve, as well as rebounding on $\partial\mathcal{U}$ after a right-to-left semi-circle, are forbidden because they do not follow our resolution rule.

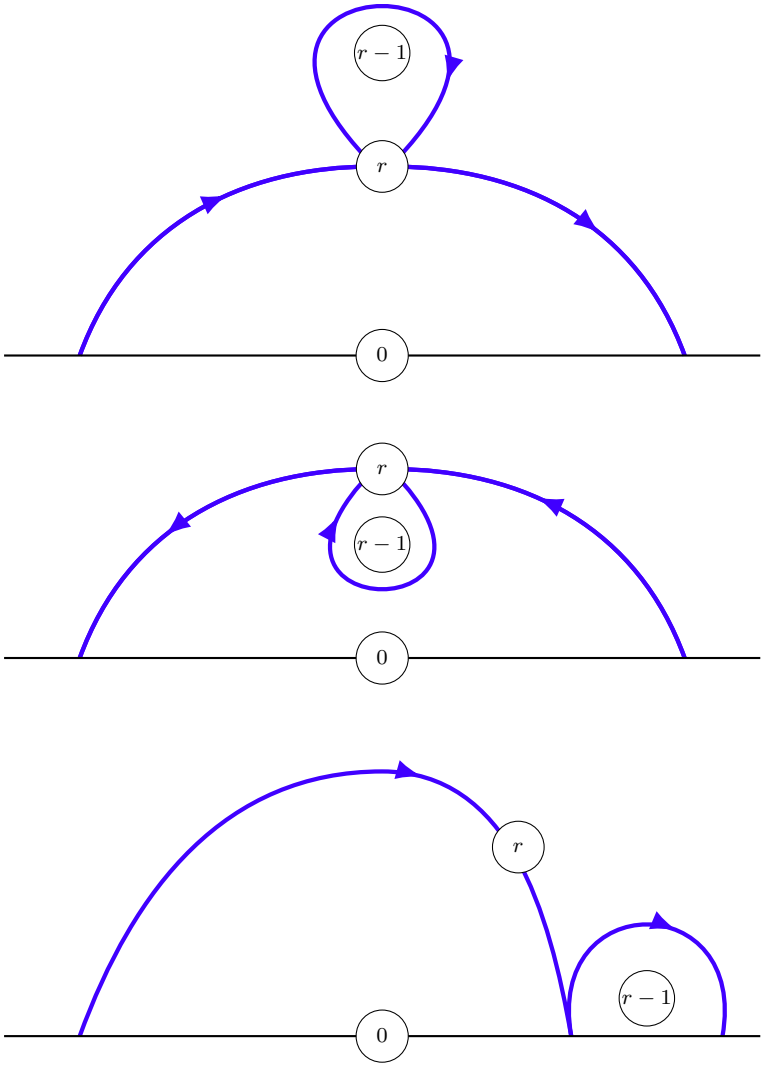

Figure 8.3.3 – The other half of the possible self-intersections for a semi-circular curve, as well as rebounding on $\partial\mathcal{U}$ after a left-to-right semi-circle, are forbidden because they would prevent the existence of oriented geodesics from the origin to some vertex of type $r-1$.

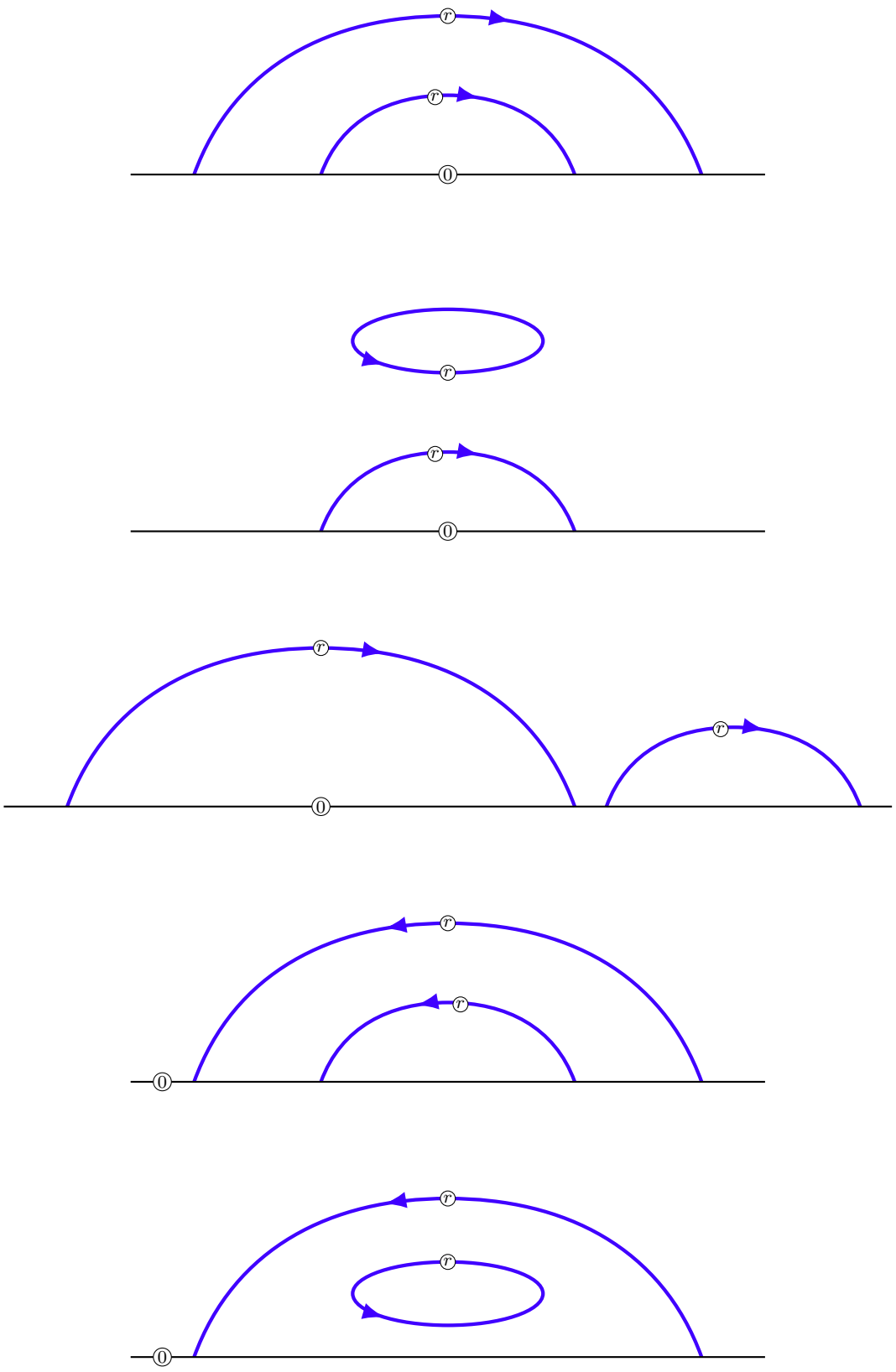

Figure 8.3.4 – In each of the five possible configurations where a semi-circular curve and anothe curve in $\mathcal{C}_r(\mathcal{U})$ would separate the same vertex from the origin, is forbidden because it would prevent the existence of oriented geodesics from the origin to some vertex of type r.

Our previous remarks imply that there is a unique semi-circular curve $\mathscr{C}^*$ that encircles the origin, and it is the unique curve in $\mathcal{C}_r(\mathcal{U})$ that separates an infinite submap of $\mathcal{U}$ from the root (it is clear that every closed curve separates a finite submap from the root).

Thus, we can state without any ambiguity that, like in the boundary-less case, we can obtain $\mathcal{B}_r(\mathcal{U})$ from $\mathcal{U}$ by doing one of the following operations, for each curve $\mathscr{C} \in \mathcal{C}_r(\mathcal{U})$:

- replace all the faces that $\mathscr{C}$ separates from the origin by a single, simple face if $\mathscr{C}$ is closed
- replace all the faces that $\mathscr{C}$ separates from the origin by a single, simple face and merge it with the infinite face of $\mathcal{U}$ if $\mathscr{C}$ is semi-circular

This yields a (finite) planar Eulerian triangulation with boundaries: the ones corresponding to closed curves are simple and alternating, while the one obtained from all the operations related to the semi-circular curves may have **defects** in the alternation of colors, corresponding to the points where the curves meet $\partial\mathcal{U}$ (see Figure 8.3.5), and also has semi-simple portions, corresponding to parts of $\partial\mathcal{U}$.

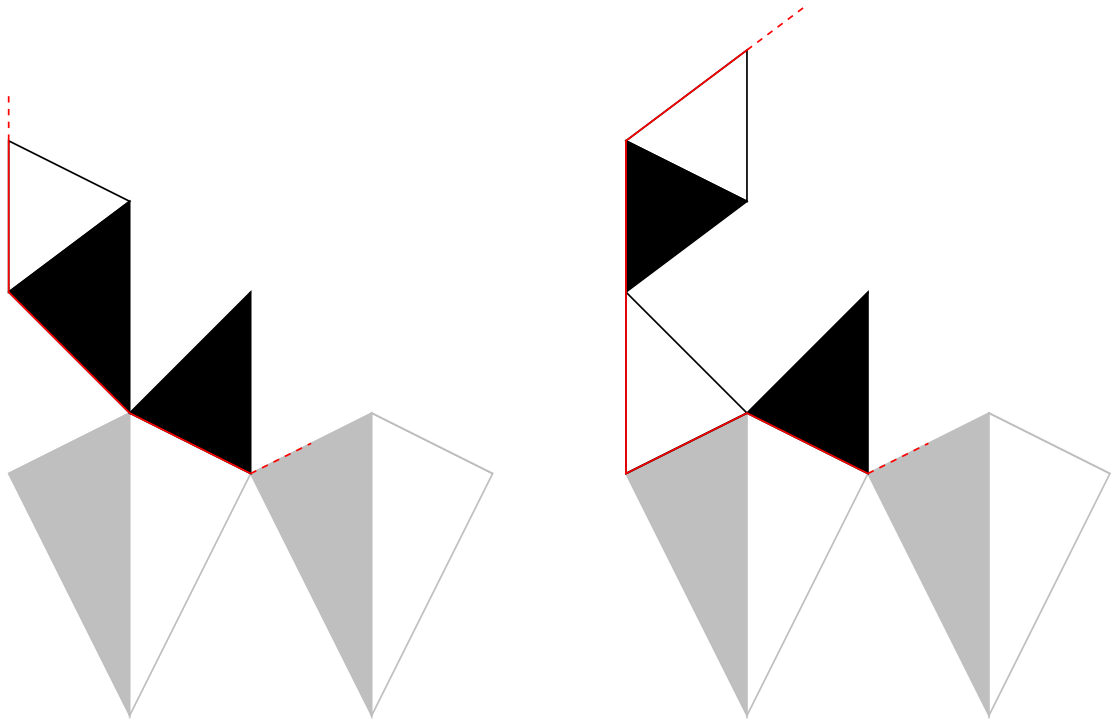

Figure 8.3.5 – There are cases where the boundary of $\mathcal{B}_r^\bullet(\mathcal{U})$ (depicted in red) has defects (depicted by red stars) in the alternation of colors, at the vertex where the two portions of the boundary meet.

Now, the hull $\mathcal{B}_r^\bullet(\mathcal{U})$, which is obtained from $\mathcal{B}_r(\mathcal{U})$ by gluing to it all the finite components of its complement, has one boundary, which has two parts: one that is also a part of $\partial\mathcal{U}$, and is thus alternating and semi-simple, and another one which is delimited by $\mathscr{C}^*$, and it thus alternating and simple. We will keep with $\mathcal{B}_r^\bullet(\mathcal{U})$ the information of two distinguished boundary vertices, namely the ones that separate the two parts of its boundary. As mentioned before, at these two distinguished points, the boundary of $\mathcal{B}_r^\bullet(\mathcal{U})$ might have defects in the alternation of colors. We will now explain how the presence or absence of defects, and the overall structure of $\mathcal{B}_r^\bullet(\mathcal{U})$, depends on the value of r.

Let us start by looking at $\mathcal{B}_1^\bullet(\mathcal{U})$. We know that the faces of $\mathcal{U}$ adjacent to the semi-circular part of the boundary of $\mathcal{B}_1^\bullet(\mathcal{U})$ form a chain of modules of type 1, which thus all share the origin as their "bottom" vertex. What remains to determine is therefore where exactly this chain meets $\partial\mathcal{U}$, left and right of the origin: is it at a vertex of coordinates $(i, 0)$, or of coordinates $(i + 1/2, \varepsilon)$, or at an unpaired triangle of type n?

To resolve this, let us focus on the slot M delimited by $\partial\mathcal{U}$ and the rightmost module of $\partial\mathcal{B}_1^\bullet(\mathcal{U})$: it is, obviously, a planar Eulerian triangulation with a boundary. We denote by $E_\circ$ the number of edges on this boundary that are adjacent to a white triangle, $E_\bullet$ the number of edges on this boundary that are adjacent to a black triangle, E the total number of edges of M, $T_\circ$ its number of white triangles, and $T_\bullet$ its number of black triangles. Then, observe that the edges of M that are not adjacent to a white triangle, are precisely the boundary edges adjacent to a black triangle, and *vice versa*. Thus:

$$\begin{aligned} E &= 3T_\circ + E_\bullet \\ &= 3T_\bullet + E_\circ, \end{aligned}$$

so that

$$E_\bullet \equiv E_\circ \pmod 3. \tag{8.3.1}$$

As shown in Figure 8.3.6, this is only possible if the leftmost and rightmost modules of $\partial\mathcal{B}_1^\bullet(\mathcal{U})$ meet $\partial\mathcal{U}$ at vertices of coordinates of the form $(i + 1/2, \varepsilon)$. Note that this implies that $\partial\mathcal{B}_1^\bullet(\mathcal{U})$ has defects in the alternation of colors at these two points, while all the slots between the boundary modules, including the two extreme ones, have strictly alternating boundaries.

Applying the same criterion for the leftmost and rightmost slots between the boundary modules of $\mathcal{B}_1^\bullet(\mathcal{U})$ and $\mathcal{B}_2^\bullet(\mathcal{U})$, we see that this time, it is necessary that the intersection of the chain of modules of $\partial\mathcal{B}_2^\bullet(\mathcal{U})$ and $\partial\mathcal{U}$ occurs on both sides at unpaired triangles. We have still one defect of alternation at each of these intersections, and this time the two extreme slots have defects too (also at the leftmost and rightmost points shared by their boundary and $\partial\mathcal{U}$).

Then, going to $\mathcal{B}_3^\bullet(\mathcal{U})$, we see that the only possible configuration is stll a different one, with intersections at vertices with coordinates of the form $(i, 0)$. This time, the boundary of the hull is strictly alternating, while the two extreme slots present defects at the leftmost and rightmost points shared by their boundary and $\partial\mathcal{U}$.

For larger values of r, it is clear that we get back to the same situation for $r = 4$ as we had for $r = 1$, and so on.

Note that, to proceed like in Section 7.5 of Chapter 7, the objects that we really want to enumerate to derive asymptotic expressions for probabilities, are the *complements* of the hulls of $\mathcal{U}$, rather than the hulls themselves. Thus, let us note that the boundary of $\mathcal{U} \setminus \mathcal{B}_r^\bullet(\mathcal{U})$ is also made of two parts: a "spherical" part that matches the one in $\partial\mathcal{B}_r^\bullet(\mathcal{U})$, and a horizontal, infinite one which is $\partial\mathcal{U} \setminus (\partial\mathcal{U} \cap \partial\mathcal{B}_r^\bullet(\mathcal{U}))$. These two parts are still alternating, and their meeting points present defects in the alternation of colors if and only if, there are defects at the same points in $\partial\mathcal{B}_r^\bullet(\mathcal{U})$.

For the boundary of these complements, we also keep the information about the two distinguished boundary vertices that separate the two parts of the boundary.

We have talked so far of the color conditions for the boundaries of the complements of the hulls of $\mathcal{U}$ and of the slots of these hulls, and have seen that some of them present two defects in the alternation of colors, as in the general layout shown in Figure 8.3.7: we thus call them Eulerian triangulations with an **alternating boundary with defects of size 1**.

We must also pay attention to the *simplicity* conditions of the boundaries of these Eulerian triangulations.

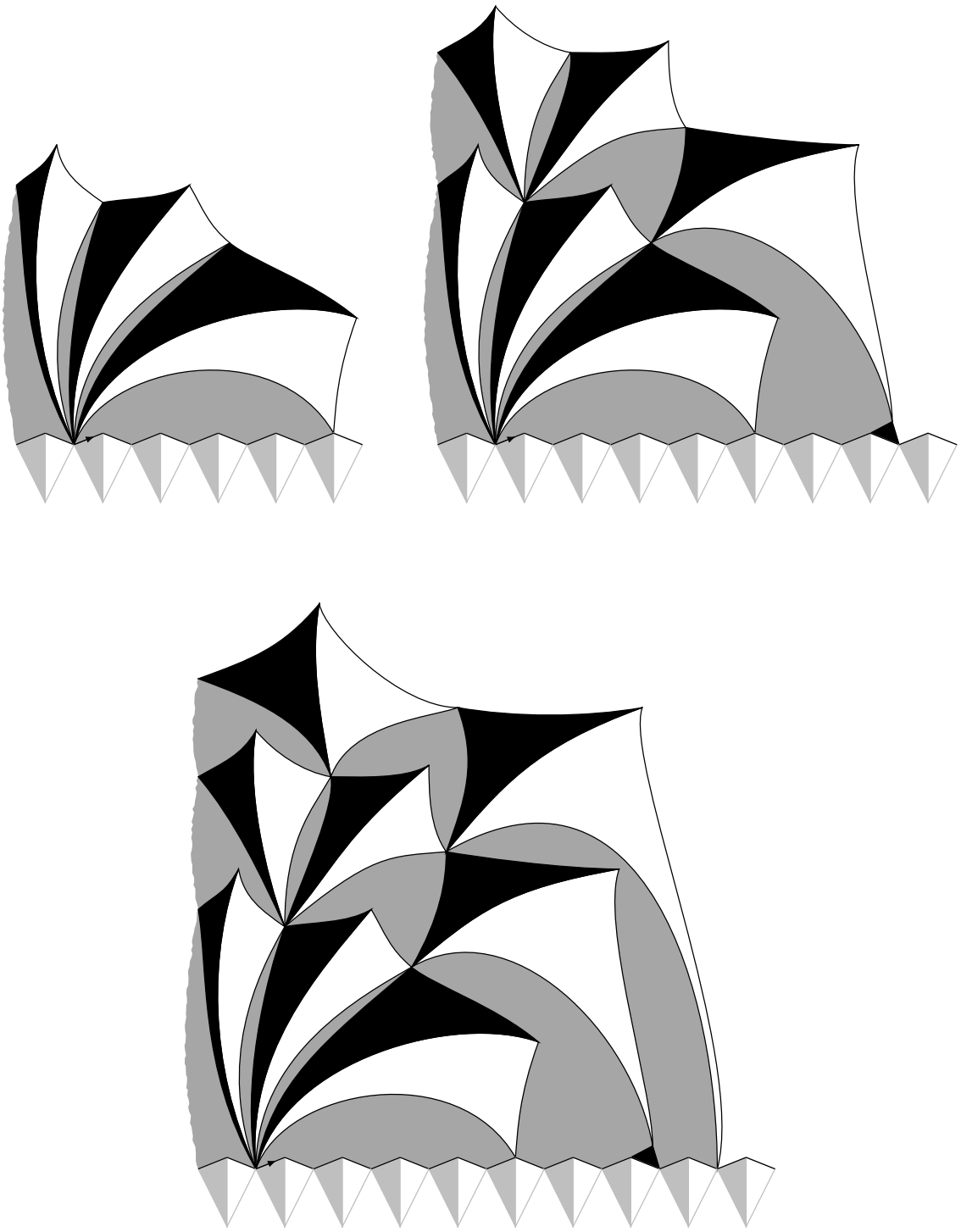

Figure 8.3.6 – Configurations for the first hulls of $\mathcal{U}$: only the right part is shown, as the left part has symmetric conditions. As before, slots are in medium grey and ghost modules in pale grey.

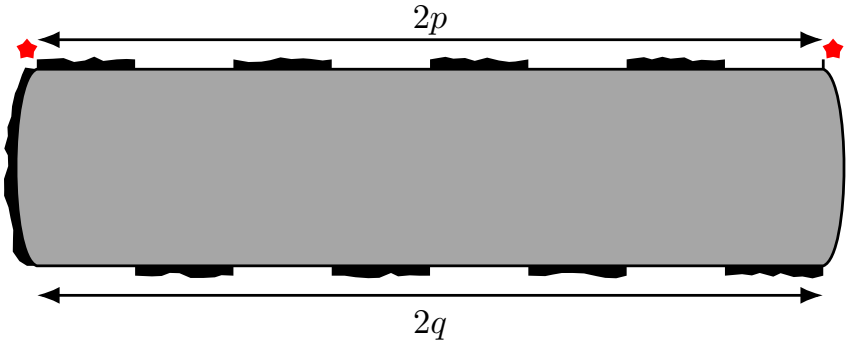

Figure 8.3.7 – General layout of a boundary with defects for an Eulerian triangulation, where the black regions represent boundary edges that are adjacent to white faces of the triangulation, and the white segments in-between them represent boundary edges that are adjacent to black faces.

Let us start with the boundary of $\mathcal{U} \setminus \mathcal{B}_r^\bullet(\mathcal{U})$, for $r \equiv 1 \pmod 3$. Thinking of its possible pinch-points as identifications of boundary vertices starting from a simple boundary (like the layout of Figure 8.3.7), we see that identifications between vertices of the spherical part still follow the semi-simplicity conditions, for the same reasons that the boundary of the complement of a hull of an Eulerian triangulation without boundary is semi-simple. Moreover, by construction, the horizontal part of the boundary of $\mathcal{U} \setminus \mathcal{B}_r^\bullet(\mathcal{U})$ is semi-simple as well. What remains to determine are the possible identifications/pinching between these two parts of the boundary. We then see that such identifications are not possible, because if that were the case, the curve running through the modules that are adjacent to the boundary of $\mathcal{B}_r^\bullet(\mathcal{U})$ could not be the unique curve $\mathscr{C}^* \in \mathcal{C}_r(\mathcal{U})$ that separates the origin from infinity (see Figure 8.3.8).

Putting all these rules together, the simplicity conditions of the boundary of $\mathcal{U} \setminus \mathcal{B}_r^\bullet(\mathcal{U})$ can be summed up in Figure 8.3.9. We call such simplicity conditions **non-chaining**, for reasons that shoud be clear very soon.

Note that the leftmost and rightmost slots between the boundary modules of $\mathcal{B}_{r-1}^\bullet(\mathcal{U})$ and $\mathcal{B}_r^\bullet(\mathcal{U})$ will naturally have the same boundary conditions, for $r \equiv 2 \pmod 3$.

Now, let us consider the boundary of $\mathcal{U} \setminus \mathcal{B}_r^\bullet(\mathcal{U})$ for $r \equiv 2 \pmod 3$. The spherical and horizontal parts of this boundary are once again semi-simple. As for the identifications between these two parts, they are now allowed, since they are not in conflict with the properties that helped us define $\mathcal{B}_r^\bullet(\mathcal{U})$ (see Figure 8.3.10).

This new set of simplicity conditions is summed up graphically in Figure 8.3.11. Note that the possibility of identifying vertices of the two parts of the boundary means that we can have configurations where the triangulation actually looks like a "chain" of Eulerian triangulations with defects, so that we call this set of simplicity conditions **chaining**.

Once again, the leftmost and rightmost slots between the boundary modules of $\mathcal{B}_{r-1}^\bullet(\mathcal{U})$ and $\mathcal{B}_r^\bullet(\mathcal{U})$ will naturally have the same boundary conditions, for $r \equiv 0 \pmod 3$.

8.4 Enumeration results

Before delving into the calculations of probabilities for the hulls of $\mathcal{U}$, we thus need asymptotic enumeration results for the new families of Eulerian triangulations with a boundary that we have encountered.

We are interested in the generating series $B^{(1)}(t, y, z)$ of Eulerian triangulations with either a "semi-simple non-chaining" or "semi-simple chaining" alternating boundary with

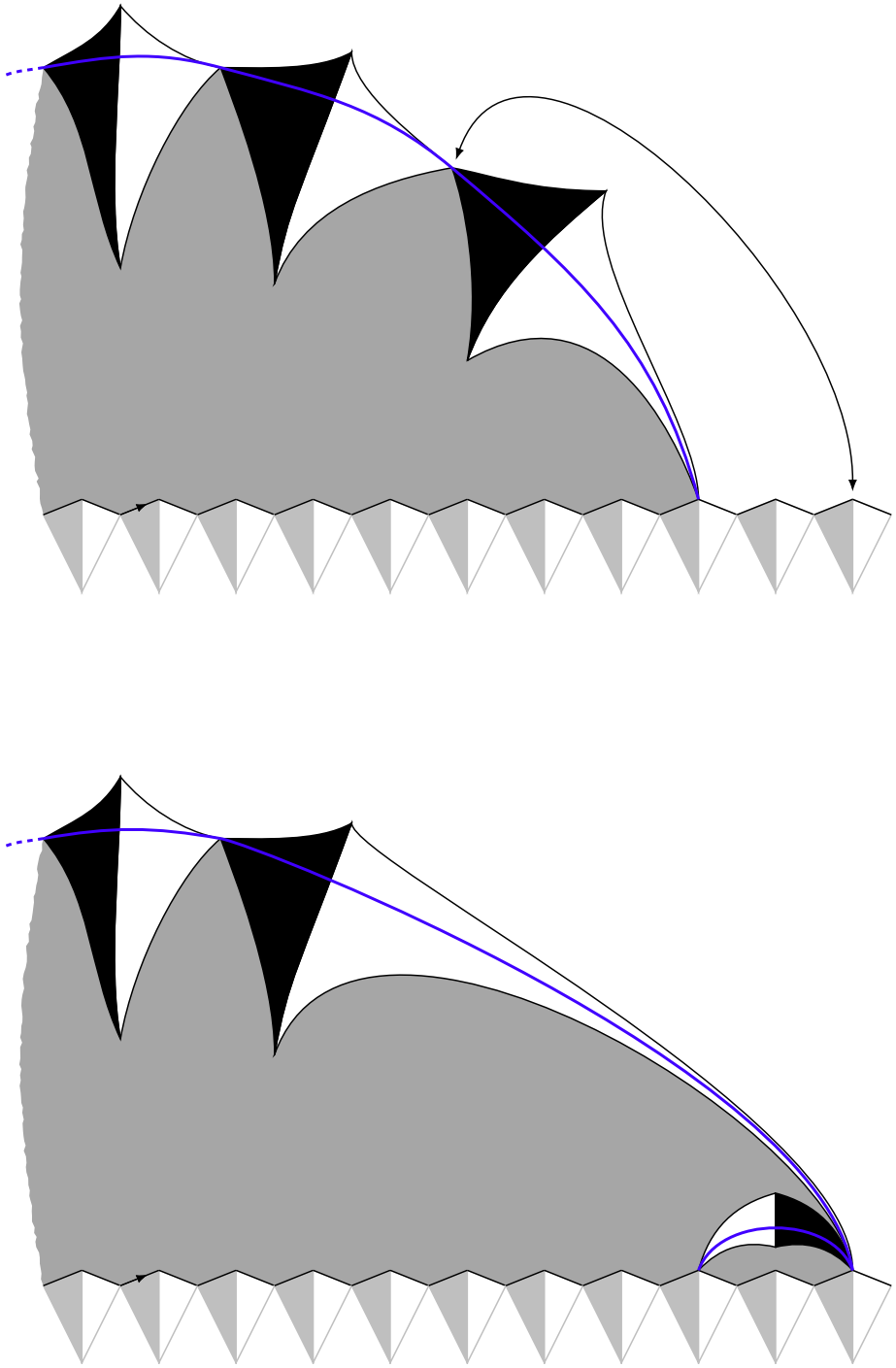

Figure 8.3.8 – Top-bottom identifications on the boundary of $\mathcal{U} \setminus \mathcal{B}_r^\bullet(\mathcal{U})$ are forbidden when $r \equiv 1 \pmod 3$, since they contradict the fact that the curve running through the modules that are adjacent to this boundary is the unique curve $\mathscr{C}^* \in \mathcal{C}_r(\mathcal{U})$ that separates the origin from infinity.

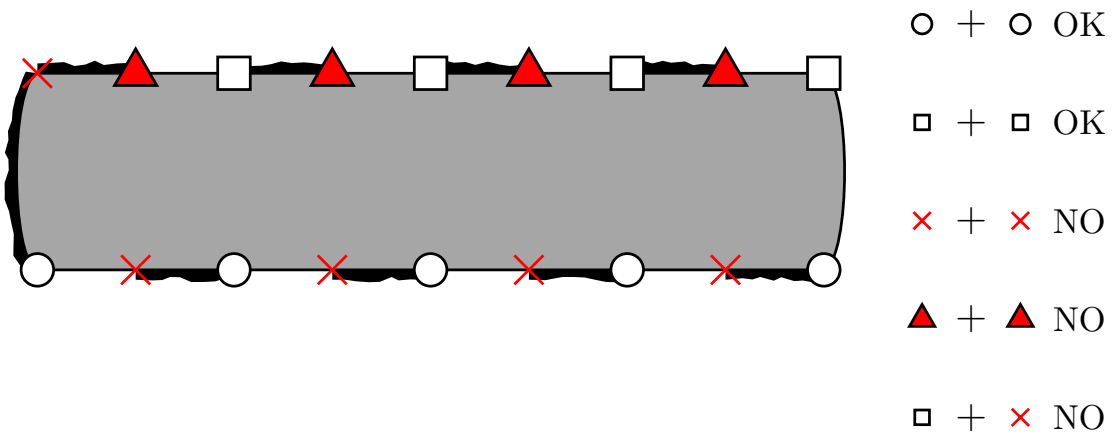

Figure 8.3.9 – The possible identifications of boundary vertices in $\mathcal{U} \setminus \mathcal{B}_r^\bullet(\mathcal{U})$ for $r \equiv 1 \pmod 3$ and the extreme slots for $r \equiv 2 \pmod 3$. The prohibition of the "square-cross" identifications means that we have no chaining configurations here.

defects of size 1 (see Figure 8.3.7), respectively

$$B^{(1)}(t,y,z) = \sum_{n,p,q\geq 0} B^{(1)}_{n,p,q} t^n y^p z^q$$

and

$$B^{(1,c)}(t,y,z) = \sum_{n,p,q\geq 0} B^{(1,c)}_{n,p,q} t^n y^p z^q$$

where t enumerates the number of black triangles, y the half-length of the upper boundary, and z the half-length of the lower boundary.

We obtain in Chapter 9:

$$\begin{cases} B^{(1)}_{n,p,q} \underset{n\to\infty}{\sim} D(p,q) 8^n n^{-5/2} \quad \forall\, p,q \\ D(p,q) \underset{q\to\infty}{\sim} E(p) 4^q \sqrt{q} \quad \forall\, p \\ E(p) \underset{p\to\infty}{\sim} \frac{27\sqrt{6}}{32\pi} 4^p. \end{cases} \tag{8.4.1}$$

We are also interested in the behavior of the coefficients

$$\widetilde{Z}(p,q) = \sum_n \frac{1}{8^n} B^{(1)}_{n,p,q}.$$

We obtain that,

$$\begin{cases} \frac{1}{4^p} \sum_q \widetilde{Z}(p,q) \left(\frac{1}{4}\right)^q \underset{p\to\infty}{\sim} \frac{9\sqrt{3}}{8\sqrt{\pi} p^{3/2}} \\ \frac{1}{4^q} \sum_p \widetilde{Z}(p,q) \left(\frac{1}{4}\right)^p \underset{q\to\infty}{\sim} \frac{9\sqrt{3}}{8\sqrt{\pi} q^{3/2}} \\ \sum_{p,q} \widetilde{Z}(p,q) \left(\frac{1}{4}\right)^p \left(\frac{1}{4}\right)^q = \frac{27}{8}. \end{cases} \tag{8.4.2}$$

As for $B^{(1,c)}$, we get asymptotic results similar to the ones for $B^{(1)}$:

$$\begin{cases} B^{(1,c)}_{n,p,q} \underset{n\to\infty}{\sim} D_c(p,q) 8^n n^{-5/2} \quad \forall\, p,q \\ D_c(p,q) \underset{q\to\infty}{\sim} E_c(p) 4^q \sqrt{q} \quad \forall\, p \\ E_c(p) \underset{p\to\infty}{\sim} \frac{144\sqrt{6}}{49\pi} 4^p, \end{cases} \tag{8.4.3}$$

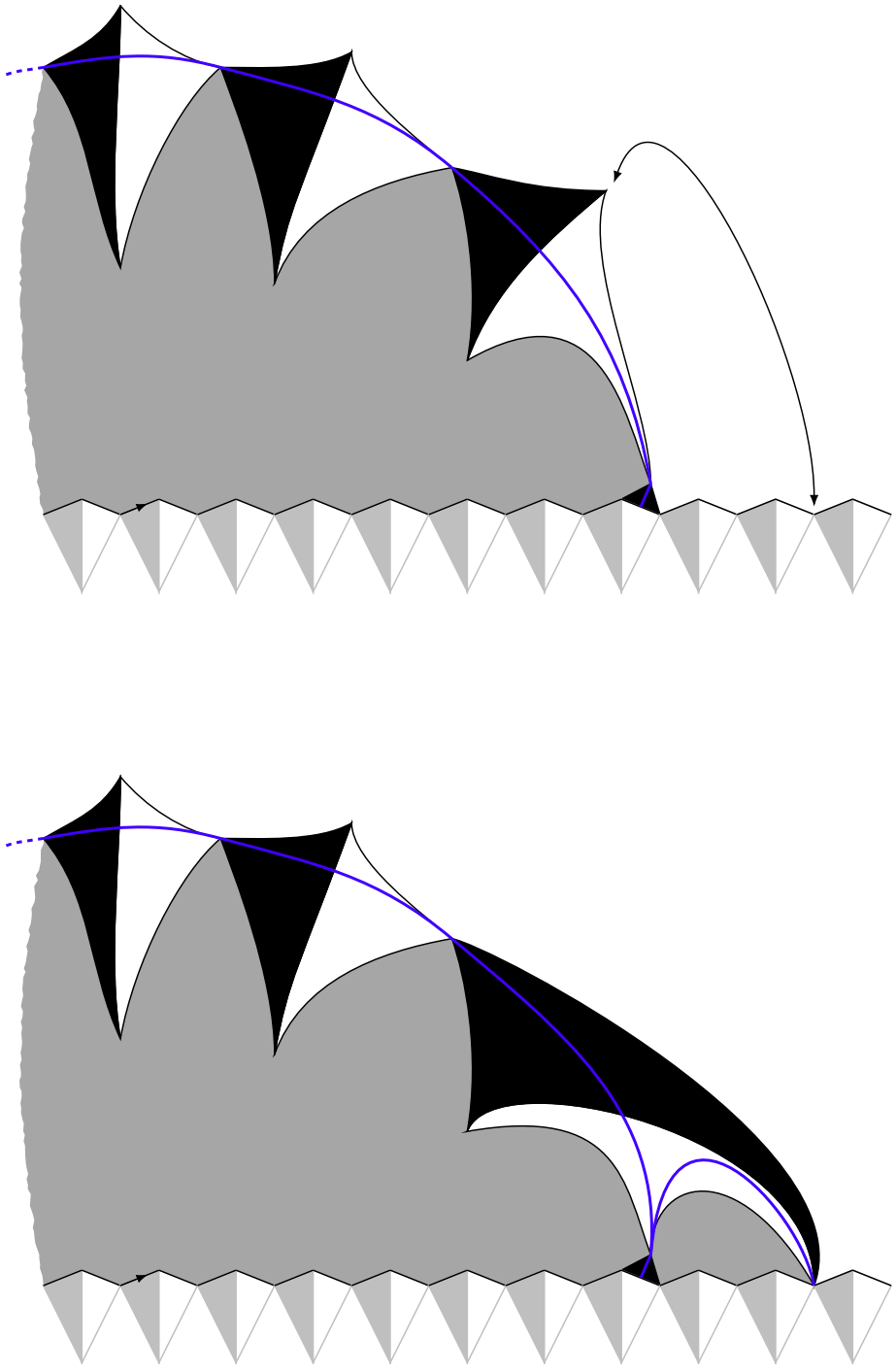

Figure 8.3.10 – Top-bottom identifications on the boundary of $\mathcal{U} \setminus \mathcal{B}_r^\bullet(\mathcal{U})$ are allowed when $r \equiv 2 \pmod 3$, since in that case there is no contradiction.

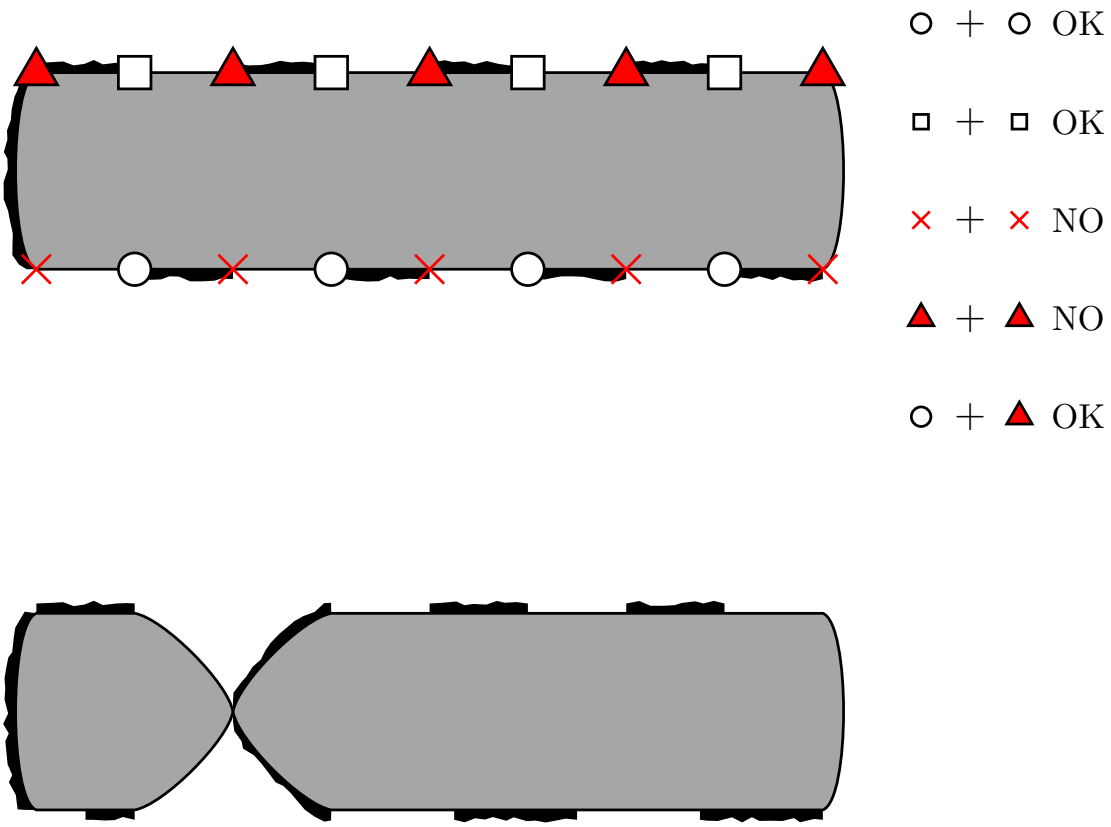

Figure 8.3.11 – The possible identifications of boundary vertices in $\mathcal{U} \setminus \mathcal{B}_r^\bullet(\mathcal{U})$ for $r \equiv 2 \pmod 3$ and the extreme slots for $r \equiv 0 \pmod 3$, and an example of a chaining configuration, corresponding to a "circle-triangle" identification. Note that the colors in this picture are reversed compared to Figure 8.3.6, so that the boundary conditions can be more easily compared to the non-chaining case.

and

$$\begin{cases} \frac{1}{4^p}\sum_q \widetilde{Z}_c(p,q)\left(\frac{1}{4}\right)^q \underset{p\to\infty}{\sim} \frac{9\sqrt{3}}{8\sqrt{\pi}p^{3/2}} \\ \frac{1}{4^q}\sum_p \widetilde{Z}_c(p,q)\left(\frac{1}{4}\right)^p \underset{q\to\infty}{\sim} \frac{9\sqrt{3}}{8\sqrt{\pi}q^{3/2}} \\ \sum_{p,q} \widetilde{Z}_c(p,q)\left(\frac{1}{4}\right)^p\left(\frac{1}{4}\right)^q = \frac{27}{8}, \end{cases} \tag{8.4.4}$$

where $\widetilde{Z}_c$ is defined similarly to the non-chaining case.

We will need to compare $\widetilde{Z}$ and $\widetilde{Z}_c$ with Z. We have the following bounds:

Proposition 8.4.1. *For every $p, q \geq 1$,*

$$Z(p+q+1) \leq \widetilde{Z}(p,q) \leq Z(p+q-1) \tag{8.4.5}$$

$$\frac{1}{8}Z(p+q+1) \leq \widetilde{Z}_c(p,q) \leq 8^4\, Z(p+q-1). \tag{8.4.6}$$

Proof. Let us start with the upper bounds. We will transform injectively any triangulation A with defects, either chaining or non-chaining, of boundary parameters (p,q), into a triangulation an with alternating semi-simple boundary of length $2(p+q-1)$. To do so, consider the leftmost simple oriented path from the bottom left corner to the vertex just left of the bottom right corner of A in Figure 8.4.1. Such a path may have edges on the top boundary of A, and vertices on its bottom boundary boundary, but never edges on the bottom: indeed, due to the semi-simplicity conditions, there cannot be any bridge in the external face (see Figure 8.4.1). Note that this is always true in the non-chaining case, but in the chaining one, due to the simplicity conditions, the starting and ending corners of the path might be isthmuses in the external face. To circumvent this, in the chaining we systematically add some additional triangles to A (see Figure 8.4.3), so that if A has n black triangles, we will obtain an alternating triangulation with $n+4$ triangles, which reflects on the obtained bound.

Having constructed a directed path as above in either case, we know that all its edges have a black triangle on the right, and the path itself cuts A into a (possibly disconnected) top part, and a bottom part (also possibly disconnected, but containing all the triangles adjacent to the bottom boundary). If we cut A along the path, all the bottom components have both black triangles along the top, and a black triangle in their bottom left corner. Thus, we can rotate them by one edge anticlockwise, and reglue them to the rest of A. As depicted in Figure 8.4.3, this yields a triangulation that has two additional defects adjacent to the already present ones. Note that if an edge on the top boundary belonged to the path, it was adjacent to a black triangle, which is still the case after the transformation, so that the top boundary colors are left unchanged. Then, we can glue together the two adjacent black and white edges belonging to defects on the left on the one hand, and those on the right on the other, to get an alternating boundary.

To get the lower bounds, we proceed similarly to transform injectively a triangulation A with an alternating boundary of length $2(p+q+1)$ into a triangulation with defects, with boundary parameters (p,q), and satisfying either the non-chaining or chaining boundary conditions.

We also start from a simple oriented leftmost path, this time from, say, the end of the root edge to the boundary vertex that sits $2p$ edges further, anticlockwise. Then, like before, we cut along this path and rotate the right part(s) by one edge clockwise, which will create the desired defects (see Figure 8.4.2). More precisely, the obtained Eulerian triangulations has an alternating boundary with defects non-chaining boundary conditions, with upper

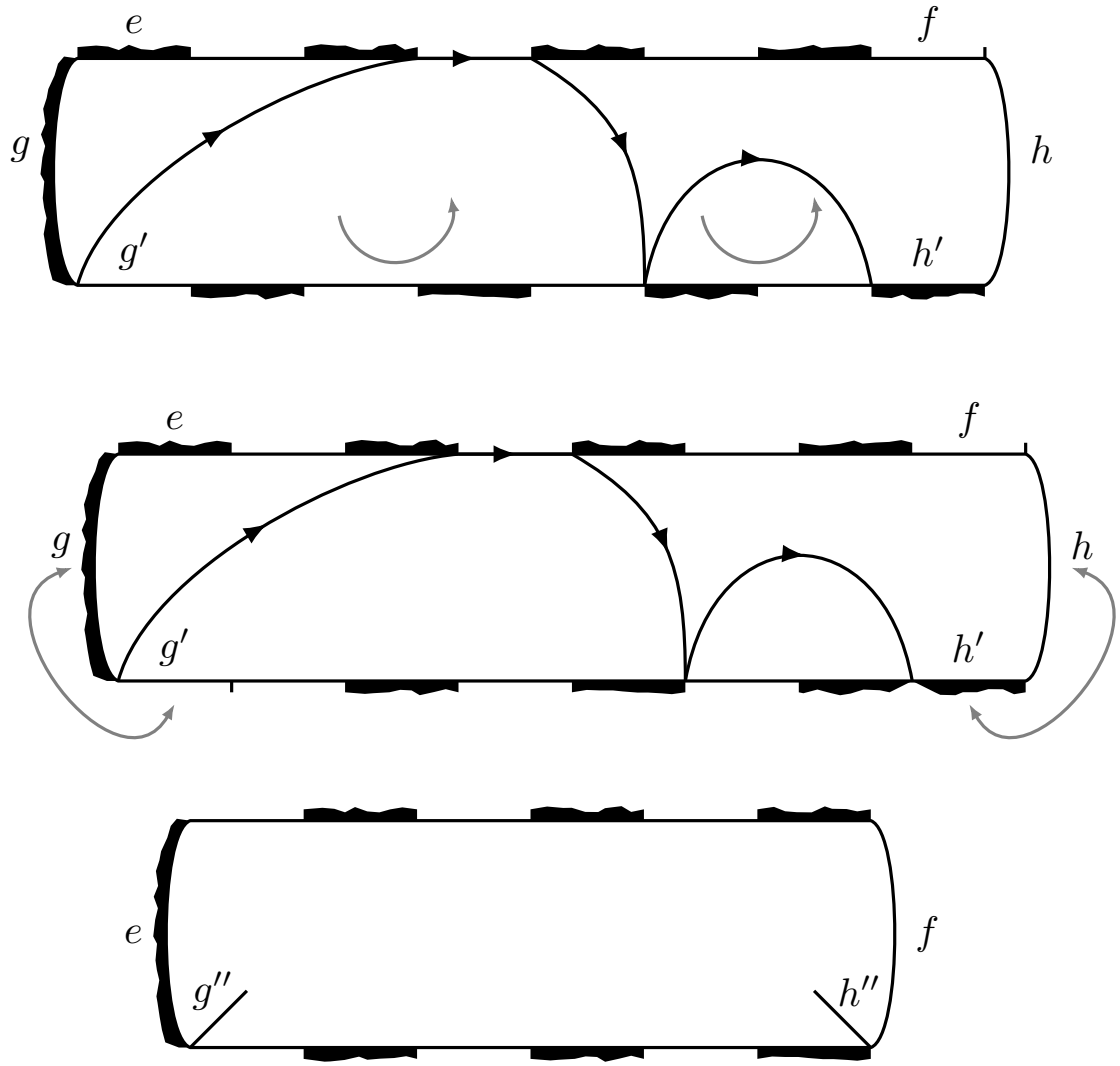

Figure 8.4.1 – We transform a triangulation wih defects into a completely alternating one, by rotating parts of it (top), then gluing together boundary edges (middle), to become inner edges (bottom).

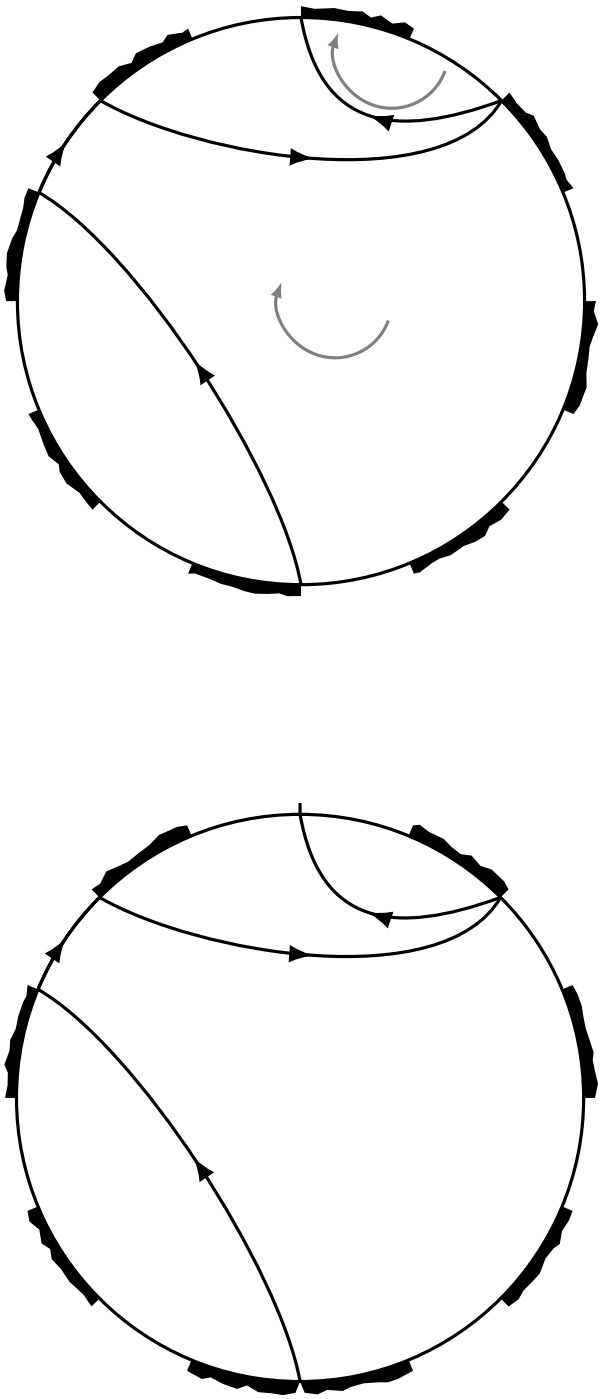

Figure 8.4.2 – We transform a triangulation with an alternating boundary (top) into one with defects (bottom), by rotating parts of it.

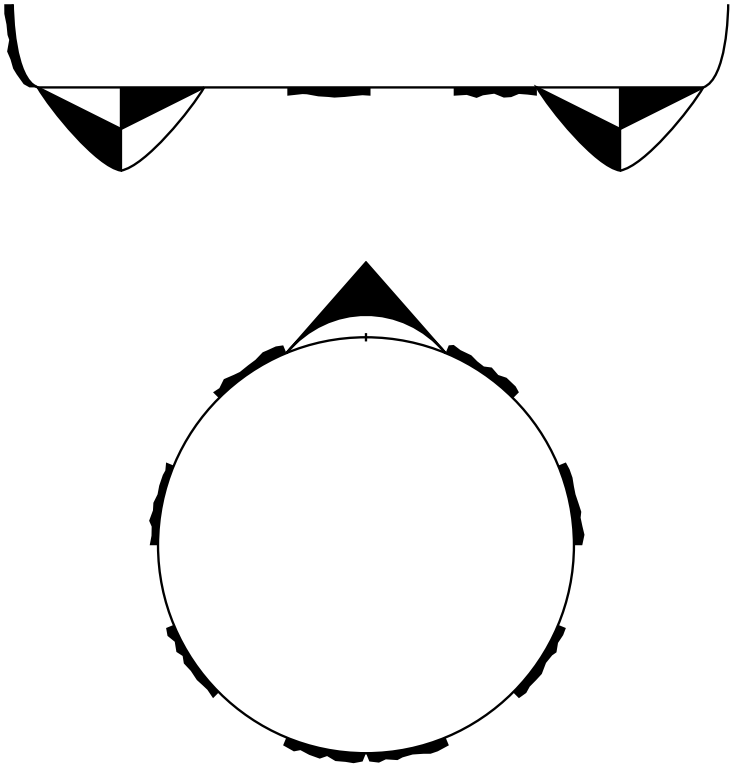

Figure 8.4.3 – Additional triangles needed, respectively before the transformation from chaining to alternating (top), and after the transformation from alternating to chaining (bottom).

boundary length $2p$ (on the left in the second drawing of Figure 8.4.2), and lower boundary length $2q$.

To transform an Eulerian triangulation with an alternating boundary into one with *chaining* boundary conditions, we want to proceed similarly. However, the triangulation with defects created by the above operation may have the vertex at the center of its "white-white" defect as a pinch point, which is not allowed in chaining boundary conditions. Therefore, to be sure to get the appropriate simplicity conditions, we add systematically a pair of triangles to A on the top two edges (see Figure 8.4.3), hence the additional constant in the bound. □

8.5 Ball events

Let us introduce a bit of notation, before stating the main result of this chapter. We want to study the spherical layer $\mathcal{B}^\bullet_{r+1}(\mathcal{U}) \setminus \mathcal{B}^\bullet_r(\mathcal{U})$, conditionally on $\mathcal{B}^\bullet_r(\mathcal{U})$. If A is an Eulerian triangulation with a boundary, such that $\mathbb{P}\big(\mathcal{B}^\bullet_{r+1}(\mathcal{U}) \setminus \mathcal{B}^\bullet_r(\mathcal{U}) = A\big) > 0$, then, from Section 8.3, A either has alternating semi-simple, alternating with defects and non-chaining, or alternating with defects and chaining, boundary conditions. If A is purely alternating, we suppose it comes with two distinguished vertices on its boundary other than the root; if A has defects, it comes naturally with two distinguished vertices, the ones where the defects are located.

We write $\tilde{\partial} A$ for the part of the boundary of A that goes from a distinguished vertex to another, and contains the root. Now, for two triangulations A, A' that are both of one of the above types, we write $A \sqsubset A'$ if A can be obtained as a subtriangulation of A' with roots coinciding, such that $\tilde{\partial} A$ is part of $\tilde{\partial} A'$, and no other edge of A is on $\partial A'$. Let Q be

the number of modules adjacent to $\partial\mathcal{B}^\bullet_{r+1}(\mathcal{U}) \setminus \tilde{\partial}\mathcal{B}^\bullet_{r+1}(\mathcal{U})$ (not counting the two extreme half-modules in the case $r \equiv 1 \pmod 3$): we consider them to be ordered clockwise. Let R' (resp. L') be the largest non-negative integer j such that the vertex $(j, 0)$ (resp. $(-j+1, 0)$) belongs to $\partial\mathcal{B}^\bullet_r(\mathcal{U}) \cap \partial\mathcal{U}$. We define similarly R'' and L'', replacing $\mathcal{B}^\bullet_r(\mathcal{U})$ by $\mathcal{B}^\bullet_{r+1}(\mathcal{U})$ (see Figure 8.5.1). Note that R' is thus the index of rightmost ghost module to have at least a vertex at distance at most r from the origin, and so on for the other integers L', R'', L''. We also denote by $\mathbf{P}_r$ the number of modules on the "upper boundary" $\partial\mathcal{B}^\bullet_r(\mathcal{U}) \setminus \tilde{\partial}\mathcal{B}^\bullet_r(\mathcal{U})$.

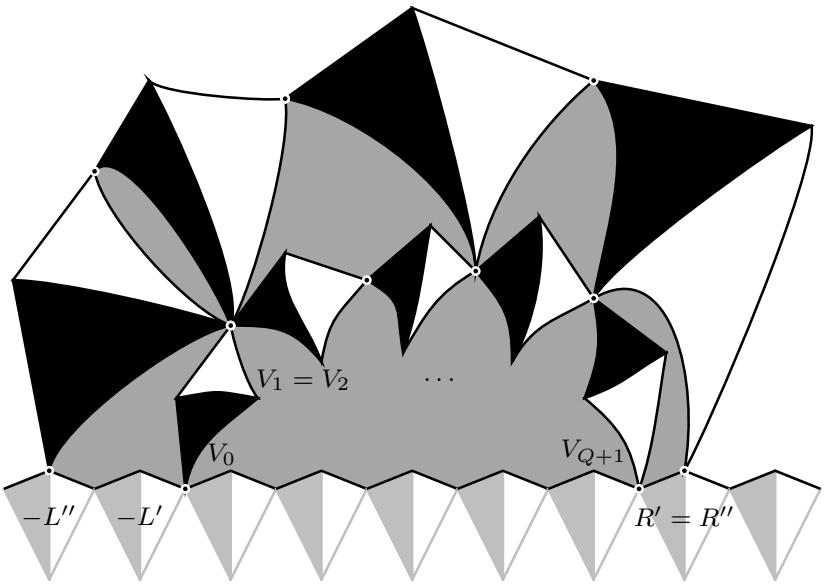

Figure 8.5.1 – Conventions for the parameters describing the spherical layer between $\mathcal{B}^\bullet_r(\mathcal{U})$ and $\mathcal{B}^\bullet_{r+1}(\mathcal{U})$, depicted here in a case where $r \equiv 0 \pmod 3$.

For $1 \le i \le Q$, we write V_i for the type-r vertex of the i-th module adjacent to $\partial\mathcal{B}^\bullet_{r+1}(\mathcal{U}) \setminus \tilde{\partial}\mathcal{B}^\bullet_{r+1}(\mathcal{U})$, and, for $1 \le j \le Q+1$, we write S_j for the number of modules on $\partial\mathcal{B}^\bullet_r(\mathcal{U})$ between V_{j-1} and V_j. Here, by convention, V_0 is set to be the vertex $(-L', 0)$, and V_{Q+1}, the vertex $(R', 0)$, and, if $r \equiv 2 \pmod 3$, we don't count the two extreme half-modules.

Let us note that a particular phenomenon can occur, due to the non-simplicity of $\partial\mathcal{U}$: the hull $\mathcal{B}^\bullet_r(\mathcal{U})$ can be "swallowed" by this boundary (see Figure 8.5.2). In that case, the "half-circumference" Q is zero, and we get slightly different expressions for the probabilities of the different possible configurations for the spherical layer between $\mathcal{B}^\bullet_{r-1}(\mathcal{U})$ and $\mathcal{B}^\bullet_r(\mathcal{U})$.

We have the following result:

Theorem 8.5.1. *For every $r \ge 0$, for any $q \ge 1$ and any $s_1, \dots, s_q, k_1, k_2 \ge 0$, we have*

$$\begin{aligned}&\mathbb{P}\big(Q = q, S_1 = s_1, \dots, S_{q+1} = s_{q+1}, L'' - L' = k_1, R'' - R' = k_2 | \mathcal{B}^\bullet_r(\mathcal{U})\big)\\ &\quad = \mathbb{1}_{\{s_1+s_2+\cdots+s_{q+1}=\mathbf{P}'_r\}} \cdot c_{m(r)} E_{m(r)}(q) F_{m(r)}(\mathbf{P}_r) \theta_{m(r)}(k_1, s_1) \theta_{m(r)}(k_2, s_2) \prod_{2\le i\le q} \theta(s_i),\end{aligned}$$

where $m(r) \in \{0, 1, 2\}$ is the random variable, determined by $\mathcal{U}$, such that $m(0) = 0$ and $m(r+1) \equiv m(r) + 1 \pmod 3$, except when $\mathcal{B}^\bullet_{r+1}(\mathcal{U})$ is swallowed up by $\partial\mathcal{U}$ and $m(r) = 0$, in which case $m(r+1) = 0$. The quantities depending on the value of $m(r)$ are:

- $\mathbf{P}'_r = \mathbf{P}_r$ *if* $m(r) = 0, 1$ *and* $\mathbf{P}'_r = \mathbf{P}_r - 1$ *if* $m(r) = 2$
- $c_0 = \frac{\rho}{\alpha^2}$, $E_0(q) = \frac{E(q)}{c\alpha^q}$, $F_0 = 1$, $\theta_0(k, s) = \theta(k + s)$,

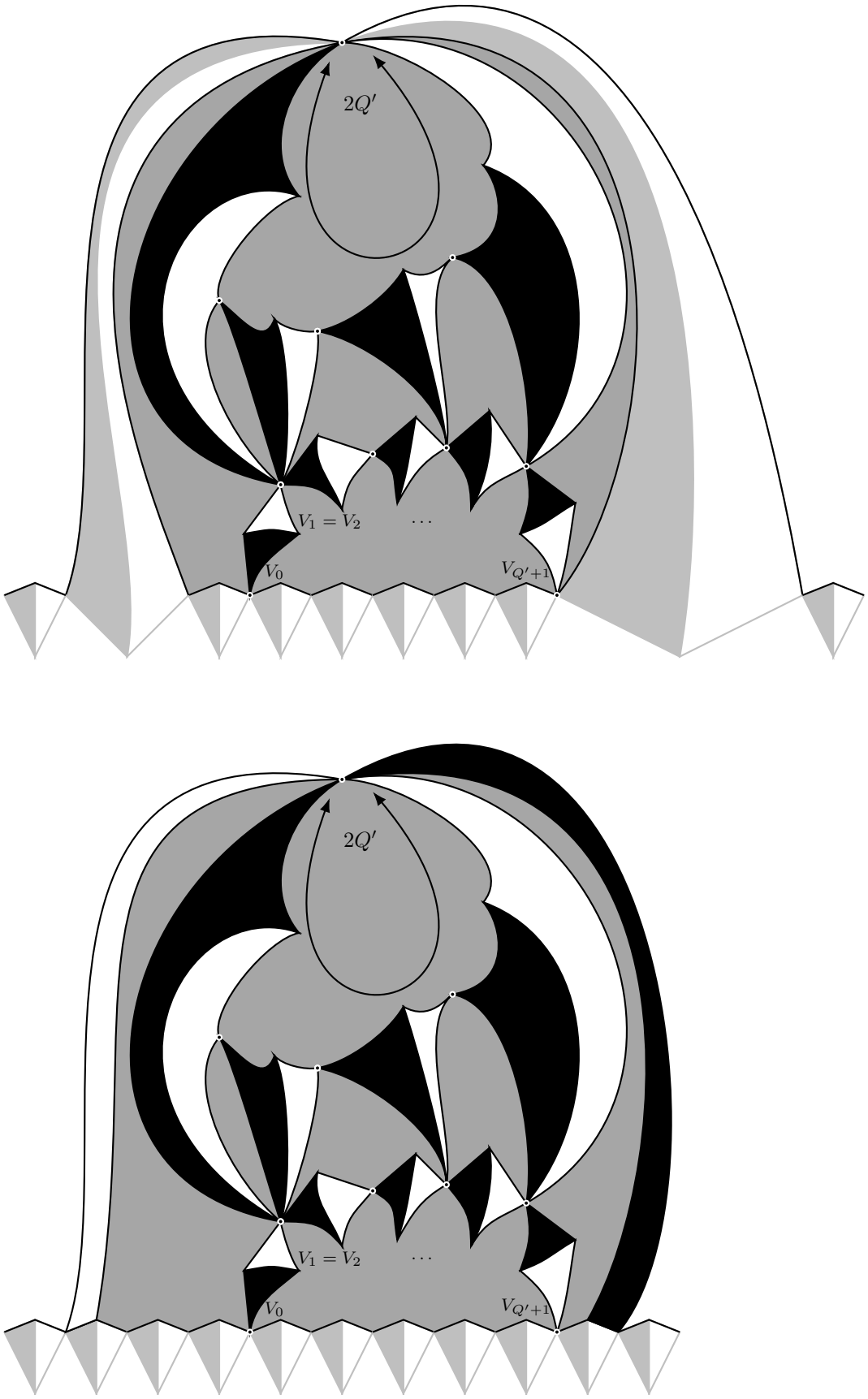

Figure 8.5.2 – Layout of the spherical layer between $\mathcal{B}^\bullet_r(\mathcal{U})$ and $\mathcal{B}^\bullet_{r+1}(\mathcal{U})$, when $r \equiv 0 \pmod 3$ (top) or $r \equiv 1 \pmod 3$ (bottom), and $Q = 0$, with the conventions of Figure 8.5.1. The event $Q = 0$ is not possible when $r \equiv 2 \pmod 3$.

- $c_1 = \frac{\alpha^2}{c'^2}$, $E_1(q) = \frac{E_c(q+1)}{c\alpha^{q+1}}$, $F_1(p) = \frac{c\alpha^p}{E(p)}$, $\theta_1 = \widetilde{\theta}$,
- $c_2 = \frac{\alpha^2\rho}{c'^2}$, $E_2 = 1$, $F_2(p) = \frac{c\alpha^p}{E_c(p)}$, $F_2 = 1$, $\theta_2 = \widetilde{\theta}_c$.

Similarly, for $Q = 0$, we have

$$\mathbb{P}\big(Q = 0, Q' = q' S_1 = s_1, \dots, S_{q'+1} = s_{q'+1}, L'' - L' = k_1, R'' - R' = k_2 | \mathcal{B}_r^\bullet(\mathcal{U})\big)$$
$$= \mathbb{1}_{\{s_1+s_2+\cdots+s_{q'+1}=\mathbf{P}'_r\}} \cdot c'_{m(r)} F_{m(r)}(\mathbf{P}_r)\theta_{m(r)}(k_1, s_1)\theta_{m(r)}(k_2, s_2)\theta(q') \prod_{2\le i\le q} \theta(s_i),$$

with $m(r)$ having now only 0 or 1 as possible values, and $c'_0 = \frac{\rho^2}{\alpha^3}$, $c'_1 = \frac{\rho^2}{\alpha}$.

Note that this gives an interpretation for the structure of the spherical hulls $\mathcal{B}_r^\bullet(\mathcal{U})$ in terms of a branching process with immigration and emigration, the offspring distribution being θ, and the immigration/emigration distribution θ, $\tilde{\theta}$ or $\tilde{\theta}_c$, depending on the value of r modulo 3. This gives the layout of the skeleton modules of the hull, which is then completed as usual with Boltzmann Eulerian triangulations with the appropriate boundary conditions.

This theorem also implies the following bounds:

Corollary 8.5.2. *There exists constants $0 < C_1 \le C_2$ such that, for every $r \ge 1$ and for every $k \ge 1$,*

$$C_1 k^{-3/2} \le \mathbb{P}\big(R'' - R' = k | \mathcal{B}_r^\bullet(\mathcal{U})\big) \le C_2 k^{-3/2}. \tag{8.5.1}$$

Proof of Theorem 8.5.1 and its corollary. To simplify notation, we will first work conditionally to the "good" event G_r, that none of the hulls up to $\mathcal{B}_r^\bullet(\mathcal{U})$ have been swallowed up by $\partial\mathcal{U}$, then see how incorporating the events in G_r^c yield the global statement of Theorem 8.5.1.

To prove Theorem 8.5.1, let us thus first start to work conditionally on G_r. We first derive expressions for the probability laws of $\mathcal{B}_r^\bullet(\mathcal{U})$, depending on the value of $m(r)$. We proceed with the same steps for each case: they will yield the different expressions that make up the cases of Theorem 8.5.1.

Suppose that $\mathbb{P}(\mathcal{B}_r^\bullet(\mathcal{U}) = A | G_r) > 0$. If $r \equiv 0 \pmod 3$, let m be the number of ghost modules adjacent to $\tilde{\partial}A$, q the number of modules on $\partial A \setminus \tilde{\partial}A$, and N the number of black triangles in A. Then, for $p > m$, the property $A \sqsubset \mathcal{T}_n^{(p)}$ will hold if and only if $\mathcal{T}_n^{(p)}$ can be obtained by gluing an Eulerian triangulation with an alternating semi-simple boundary of length $2(q + p - m)$ to A, so that a part of length $2q$ of this boundary is identified to $\partial A \setminus \tilde{\partial}A$. Thus, for n large enough,

$$\mathbb{P}\Big(A \sqsubset \mathcal{T}_n^{(p)} | G_r\Big) = \frac{B_{n-N,p+q-m}}{B_{n,p}}.$$

The asymptotics of $B_{n,p}$ (see (7.4.3) in Chapter 7) yield:

$$\mathbb{P}\Big(A \sqsubset \mathcal{T}_\infty^{(p)} | G_r\Big) = \frac{C(p+q-m)}{C(p)}\rho^{-N},$$

and then

$$\mathbb{P}(\mathcal{B}_r^\bullet(\mathcal{U}) = A | G_r) = \alpha^{(q-m)}\rho^{-N}. \tag{8.5.2}$$

If $r \equiv 1 \pmod 3$, let m be the number of ghost modules adjacent to $\tilde{\partial}A$ (including the two extremes ones that are only half adjacent to $\tilde{\partial}A$), q the number of modules on $\partial A \setminus \tilde{\partial}A$, and N the number of black triangles in A.

Then, similarly, for p and n large enough,

$$\mathbb{P}\Big(A \sqsubset \mathcal{T}_n^{(p)} | G_r\Big) = \frac{B^{(1)}_{n-N,q,p-m}}{B_{n,p}},$$

so that

$$\mathbb{P}(\mathcal{B}_r^\bullet(\mathcal{U}) = A | G_r) = \frac{2\pi}{\sqrt{3}} E(q) \alpha^{-m} \rho^{-N}. \tag{8.5.3}$$

If $r \equiv 2 \pmod 3$, let m be the number of ghost modules adjacent to $\tilde{\partial} A$ (including the two extremes ones that are adjacent to the additional "half-modules" ending the chain delimiting A), q the number of modules on $\partial A \setminus \tilde{\partial} A$ (counting a total of 1 for the two extreme half-modules), and N the number of black triangles in A.

Then, for p and n large enough,

$$\mathbb{P}\Big(A \sqsubset \mathcal{T}_n^{(p)} | G_r\Big) = \frac{B^{(1,c)}_{n-N,q,p-m}}{B_{n,p}},$$

which yields similarly:

$$\mathbb{P}(\mathcal{B}_r^\bullet(\mathcal{U}) = A | G_r) = \frac{2\pi}{\sqrt{3}} E_c(q) \alpha^{-m} \rho^{-N}. \tag{8.5.4}$$

Having established expressions for the probabilities concerning the balls of $\mathcal{U}$, we first want to obtain an expression (depending on the value of r mod 3) for

$$\mathbb{P}\big(Q = q, S_1 = s_1, \dots, S_{q+1} = s_{q+1}, L'' - L' = k_1, R'' - R' = k_2 | \mathcal{B}_r^\bullet(\mathcal{U}), G_r\big).$$

To do so, let us compute, for A such that $\mathbb{P}(\mathcal{B}_r^\bullet(\mathcal{U}) = A | G_r) > 0$,

$$\mathbb{P}\big(Q = q, S_1 = s_1, \dots, S_{q+1} = s_{q+1}, L'' - L' = k_1, R'' - R' = k_2 | \mathcal{B}_r^\bullet(\mathcal{U}) = A, G_r\big).$$

This is equal to

$$\sum_{A'} \mathbb{P}\big(\mathcal{B}_{r+1}^\bullet(\mathcal{U}) = A' | \mathcal{B}_r^\bullet(\mathcal{U}) = A, G_r\big)$$

with the sum running over triangulations A' such that $A \sqsubset A'$, and the configuration of A' is consistent with the parameters q, s_1, etc. Then, for such a triangulation A',

$$\mathbb{P}\big(\mathcal{B}_{r+1}^\bullet(\mathcal{U}) = A' | \mathcal{B}_r^\bullet(\mathcal{U}) = A, G_r\big) = \frac{\mathbb{P}\big(\mathcal{B}_{r+1}^\bullet(\mathcal{U}) = A' | G_r\big)}{\mathbb{P}(\mathcal{B}_r^\bullet(\mathcal{U}) = A | G_r)},$$

which gives a different expression depending on the value of r mod 3, that we study now.

If $r \equiv 0 \pmod 3$,

$$\frac{\mathbb{P}\big(\mathcal{B}_{r+1}^\bullet(\mathcal{U}) = A' | G_r\big)}{\mathbb{P}(\mathcal{B}_r^\bullet(\mathcal{U}) = A | G_r)} = \frac{2\pi}{\sqrt{3}} E(q) \alpha^{-(k_1+k_2+1+p)} \rho^{-N}$$

where N is the number of black triangles of A' that are not in A, and p is the number of modules adjacent to $\partial A \setminus \tilde{\partial} A$. This yields, when summing over A':

$$\begin{aligned}
&\mathbb{P}\big(Q = q, S_1 = s_1, \dots, S_{q+1} = s_{q+1}, L'' - L' = k_1, R'' - R' = k_2 | \mathcal{B}_r^\bullet(\mathcal{U}) = A, G_r\big) \\
&= \frac{E(q)}{c\alpha^q} \frac{\rho}{\alpha^2} \cdot \theta(s_1 + k_1)\theta(s_2)\theta(s_3) \cdots \theta(s_q)\theta(s_{q+1} + k_2)
\end{aligned}$$

where $c = \sqrt{3}/2\pi$, and θ is defined as in Chapter 7. Now, summing over A (after multiplying by $\mathbb{1}_{\{\mathcal{B}_r^\bullet(\mathcal{U})=A\}}$), this gives

$$\begin{aligned}&\mathbb{P}\big(Q=q, S_1=s_1,\dots,S_{q+1}=s_{q+1}, L''-L'=k_1+1, R''-R'=k_2+1|\mathcal{B}_r^\bullet(\mathcal{U}), G_r\big)\\&=\frac{E(q)}{c\alpha^q}\frac{\rho}{\alpha^2}\cdot\mathbb{1}_{\{s_1+s_2+\cdots+s_{q+1}=\mathbf{P}_r\}}\cdot\theta(s_1+k_1)\theta(s_2)\theta(s_3)\cdots\theta(s_q)\theta(s_{q+1}+k_2)\end{aligned}\tag{8.5.5}$$

where $\mathbf{P}_r$ is the number of modules on the "upper boundary" $\partial\mathcal{B}_r^\bullet(\mathcal{U})\setminus\tilde{\partial}\mathcal{B}_r^\bullet(\mathcal{U})$.

Similarly, if $r\equiv 1 \pmod 3$,

$$\frac{\mathbb{P}\big(\mathcal{B}_{r+1}^\bullet(\mathcal{U})=A'|G_r\big)}{\mathbb{P}(\mathcal{B}_r^\bullet(\mathcal{U})=A|G_r)}=\frac{E_c(q+1)}{E(p)}\alpha^{-(k_1+k_2)+1}\rho^{-N}$$

which yields

$$\begin{aligned}&\mathbb{P}\big(Q=q, S_1=s_1,\dots,S_{q+1}=s_{q+1}, L''-L'=k_1, R''-R'=k_2|\mathcal{B}_r^\bullet(\mathcal{U})=A, G_r\big)\\&=\frac{E_c(q+1)}{\alpha^{q+1}}\frac{\alpha^p}{E(p)}\frac{\alpha^2}{c'^2}\tilde{\theta}(k_1,s_1)\tilde{\theta}(k_2,s_{q+1})\prod_{2\le i\le q}\theta(s_i),\end{aligned}$$

where

$$\tilde{\theta}(k,s)=c'\frac{1}{\rho}\alpha^{-(s+k)+1}\widetilde{Z}(k,s),$$

with $c'=\frac{16}{27}$ (from our results on $\widetilde{Z}$, this implies that $\tilde{\theta}$ is a probability distribution on $\mathbb{Z}_+\times\mathbb{Z}_+$). This gives:

$$\begin{aligned}&\mathbb{P}\big(Q=q, S_1=s_1,\dots,S_{q+1}=s_{q+1}, L''-L'=k_1, R''-R'=k_2|\mathcal{B}_r^\bullet(\mathcal{U}), G_r\big)\\&=\frac{E_c(q+1)}{\alpha^{q+1}}\frac{\alpha^{\mathbf{P}_r}}{E(\mathbf{P}_r)}\frac{\alpha^2}{c'^2}\cdot\mathbb{1}_{\{s_1+s_2+\cdots+s_{q+1}=\mathbf{P}_r\}}\cdot\tilde{\theta}(k_1,s_1)\theta(s_2)\theta(s_3)\cdots\theta(s_q)\tilde{\theta}(k_2,s_{q+1}).\end{aligned}\tag{8.5.6}$$

If $r\equiv 2 \pmod 3$, taking into account the two extreme half-modules for p, we have

$$\frac{\mathbb{P}\big(\mathcal{B}_{r+1}^\bullet(\mathcal{U})=A'|G_r\big)}{\mathbb{P}(\mathcal{B}_r^\bullet(\mathcal{U})=A|G_r)}=\frac{\sqrt{3}}{2\pi}\frac{\alpha^q}{E_c(p)}\alpha^{-(k_1+k_2)}\rho^{-N},$$

which yields

$$\begin{aligned}&\mathbb{P}\big(Q=q, S_1=s_1,\dots,S_{q+1}=s_{q+1}, L''-L'=k_1, R''-R'=k_2|\mathcal{B}_r^\bullet(\mathcal{U})=A, G_r\big)\\&=c\frac{\alpha^p}{E_c(p)}\frac{\alpha^2\rho}{c'^2}\tilde{\theta}_c(k_1,s_1)\tilde{\theta}_c(k_2,s_{q+1})\prod_{2\le i\le q}\theta(s_i),\end{aligned}$$

where $\tilde{\theta}_c$, defined similarly to $\tilde{\theta}$, is also a probability distribution on $\mathbb{Z}_+\times\mathbb{Z}_+$. Thus

$$\begin{aligned}&\mathbb{P}\big(Q=q, S_1=s_1,\dots,S_{q+1}=s_{q+1}, L''-L'=k_1, R''-R'=k_2|\mathcal{B}_r^\bullet(\mathcal{U}), G_r\big)\\&=c\frac{\alpha^{\mathbf{P}_r}}{E_c(\mathbf{P}_r)}\frac{\alpha^2\rho}{c'^2}\cdot\mathbb{1}_{\{s_1+s_2+\cdots+s_{q+1}=\mathbf{P}_r-1\}}\cdot\tilde{\theta}_c(k_1,s_1)\theta(s_2)\theta(s_3)\cdots\theta(s_q)\tilde{\theta}_c(k_2,s_{q+1}).\end{aligned}\tag{8.5.7}$$

Note that, with similar arguments, we also obtain for the first hull $\mathcal{B}_1^\bullet(\mathcal{U})$:

$$\mathbb{P}(Q=q, L=k_1+1, R=k_2+1)=\frac{E(q)}{c\alpha^q}\frac{\rho}{\alpha^3}\theta(0)^{q-1}\theta(k_1)\theta(k_2).\tag{8.5.8}$$

We now want to obtain, from the preceding results, lower and upper bounds on

$$\mathbb{P}\big(S_{Q+1} = s, R'' - R' = k+1 | \mathcal{B}_r^\bullet(\mathcal{U}), G_r\big),$$

once again separating the different cases for the value of r mod 3.

If $r \equiv 0 \pmod 3$, we have

$$\begin{aligned}
&\mathbb{P}\big(S_{Q+1} = s, R'' - R' = k+1 | \mathcal{B}_r^\bullet(\mathcal{U}), G_r\big) \\
&= \mathbb{1}_{\{s \le \mathbf{P}_r\}} \sum_{q=1}^{+\infty} \sum_{k_1, s_1 + \cdots + s_q = \mathbf{P}_r - s} \\
&\mathbb{P}\big(Q = q, S_1 = s_1, \dots, S_q = s_q, S_{q+1} = s, L'' - L' = k_1 + 1, R'' - R' = k+1 | \mathcal{B}_r^\bullet(\mathcal{U}), G_r\big) \\
&= \mathbb{1}_{\{s \le \mathbf{P}_r\}} \sum_{q=1}^{\infty} \frac{E(q)}{c\alpha^q} \frac{\rho}{\alpha^3} \left(\sum_{s_1 + \cdots + s_q = \mathbf{P}_r - s} \theta([s_1, \infty)) \theta(s_2) \theta(s_3) \cdots \theta(s_q) \right) \theta(s+k).
\end{aligned}$$

Now, as $E(q) \underset{q \to \infty}{\sim} \frac{27\sqrt{6}}{32\pi} 4^q$, there exists some constants $0 < C_3 < C_4$ such that $C_3 \le \frac{E(q)}{c\alpha^q} \frac{\rho}{\alpha^3} \le C_4$ for all $q \ge 1$, thus

$$\begin{aligned}
&C_3 \mathbb{1}_{\{s \le \mathbf{P}_r\}} \sum_{q=1}^{\infty} \left(\sum_{s_1 + \cdots + s_q = \mathbf{P}_r - s} \left(\theta(s_1) + \theta((s_1, \infty)) \right) \theta(s_2) \theta(s_3) \cdots \theta(s_q) \right) \theta(s+k) \\
\le &\mathbb{P}\big(S_{Q+1} = s, R'' - R' = k+1 | \mathcal{B}_r^\bullet(\mathcal{U}), G_r\big) \\
\le &C_4 \mathbb{1}_{\{s \le \mathbf{P}_r\}} \sum_{q=1}^{\infty} \left(\sum_{s_1 + \cdots + s_q = \mathbf{P}_r - s} \left(\theta(s_1) + \theta((s_1, \infty)) \right) \theta(s_2) \theta(s_3) \cdots \theta(s_q) \right) \theta(s+k).
\end{aligned}$$

Note that, for any integer $p \ge 0$,

$$\sum_{q=1}^{\infty} \left(\sum_{s_1 + \cdots + s_q = p} \theta((s_1, \infty)) \theta(s_2) \theta(s_3) \cdots \theta(s_q) \right) = 1.$$

Indeed, if $X_1, X_2, \dots$ is a sequence of i.i.d. random variables with distribution θ, and if $H_p = \min\{q \ge 1 | X_1 + \cdots + X_q > p\}$, then the above expression is just $\sum_{q \ge 1} \mathbb{P}(H_p = q)$, which is 1. We are thus left with bounding

$$\sum_{q=1}^{\infty} \left(\sum_{s_1 + \cdots + s_q = \mathbf{P}_r - s} \theta(s_1) \theta(s_2) \theta(s_3) \cdots \theta(s_q) \right),$$

and, by the renewal theorem, as θ has a positive mean (equal to 1), this can be bounded by constants that depend neither on s nor on $\mathbf{P}_r$.

Therefore,

$$C_3 \mathbb{1}_{\{s \le \mathbf{P}_r\}} \theta(s+k) \le \mathbb{P}\big(S_{Q+1} = s, R'' - R' = k+1 | \mathcal{B}_r^\bullet(\mathcal{U}), G_r\big) \le C_4 \mathbb{1}_{\{s \le \mathbf{P}_r\}} \theta(s+k), \tag{8.5.9}$$

for some new constants $0 < C_3 < C_4$, independent of s, k and $\mathbf{P}_r$.

If $r \equiv 1 \pmod 3$, then we obtain similarly

$$\begin{aligned}
&\mathbb{P}\big(S_{Q+1} = s, R'' - R' = k | \mathcal{B}_r^\bullet(\mathcal{U}), G_r\big) \\
&= \mathbb{1}_{\{s \le \mathbf{P}_r\}} \sum_{q=1}^{+\infty} \sum_{k_1, s_1 + \cdots + s_q = \mathbf{P}_r - s} \\
&\mathbb{P}\big(Q = q, S_1 = s_1, \dots, S_q = s_q, S_{q+1} = s, L'' - L' = k_1, R'' - R' = k | \mathcal{B}_r^\bullet(\mathcal{U}), G_r\big) \\
&= \mathbb{1}_{\{s \le \mathbf{P}_r\}} \sum_{q=1}^{\infty} \frac{E(q)}{c\alpha^q} \frac{\alpha^2}{c'^2} \left(\sum_{s_1 + \cdots + s_q = \mathbf{P}_r - s} \hat{\theta}(s_1)\theta(s_2)\theta(s_3)\cdots\theta(s_q) \right) \tilde{\theta}(k, s)
\end{aligned}$$

where $\hat{\theta}(s) = \sum_{k=0}^{\infty} \tilde{\theta}(k, s)$. Using a variant of the renewal theorem for delayed renewal processes (see [Bla53]), we obtain that, for some constants $0 < C_3 < C_4$ that are once again independent of k, s and $\mathbf{P}_r$,

$$C_3 \mathbb{1}_{\{s \le \mathbf{P}_r\}} \tilde{\theta}(k, s) \le \mathbb{P}\big(S_{Q+1} = s, R'' - R' = k | \mathcal{B}_r^\bullet(\mathcal{U}), G_r\big) \le C_4 \mathbb{1}_{\{s \le \mathbf{P}_r\}} \tilde{\theta}(k, s). \quad (8.5.10)$$

Finally, for $r \equiv 2 \pmod 3$, we have

$$\begin{aligned}
&\mathbb{P}\big(S_{Q+1} = s, R'' - R' = k | \mathcal{B}_r^\bullet(\mathcal{U}), G_r\big) \\
&= \mathbb{1}_{\{s \le \mathbf{P}_r - 1\}} \sum_{q=1}^{+\infty} \sum_{k_1, s_1 + \cdots + s_q = \mathbf{P}_r - s} \\
&\mathbb{P}\big(Q = q, S_1 = s_1, \dots, S_q = s_q, S_{q+1} = s, L'' - L' = k_1, R'' - R' = k | \mathcal{B}_r^\bullet(\mathcal{U}), G_r\big) \\
&= \mathbb{1}_{\{s \le \mathbf{P}_r - 1\}} \sum_{q=1}^{\infty} c \frac{\alpha^{\mathbf{P}_r}}{E_c(\mathbf{P}_r)} \frac{\alpha^2 \rho}{c'^2} \left(\sum_{s_1 + \cdots + s_q = \mathbf{P}_r - s - 1} \hat{\theta}_c(s_1)\theta(s_2)\theta(s_3)\cdots\theta(s_q) \right) \tilde{\theta}_c(k, s)
\end{aligned}$$

(where $\hat{\theta}_c$ is defined like $\hat{\theta}$), which yields a similar result.

Thus, using the bounds from Proposition 8.4.1, there exist some constants $0 < C_3 < C_4$, independent of k, s and $\mathbf{P}_r$ such that, for every $r \ge 1$, if $r \equiv 0, 1 \pmod 3$,

$$C_3 \mathbb{1}_{\{s \le \mathbf{P}_r\}} \theta(k+s) \le \mathbb{P}\big(S_{Q+1} = s, R'' - R' = k | \mathcal{B}_r^\bullet(\mathcal{U}), G_r\big) \le C_4 \mathbb{1}_{\{s \le \mathbf{P}_r\}} \theta(k+s), \quad (8.5.11)$$

and, if $r \equiv 2 \pmod 3$,

$$C_3 \mathbb{1}_{\{s \le \mathbf{P}_r - 1\}} \theta(k+s) \le \mathbb{P}\big(S_{Q+1} = s, R'' - R' = k | \mathcal{B}_r^\bullet(\mathcal{U}), G_r\big) \le C_4 \mathbb{1}_{\{s \le \mathbf{P}_r - 1\}} \theta(k+s). \quad (8.5.12)$$

From the asymptotics of θ, this implies that there exist constants $0 < C_1 < C_2$ such that, for any r,

$$C_1 k^{-3/2} \le \mathbb{P}\big(R'' - R' = k | \mathcal{B}_r^\bullet(\mathcal{U}), G_r\big) \le C_4 k^{-3/2}. \quad (8.5.13)$$

As announced before, we will now treat the possible "swallowing up" of $\mathcal{B}_r^\bullet(\mathcal{U})$ by the boundary of $\mathcal{U}$, that was excluded in G_r. First, it cannot occur for all values of r: indeed, while it is possible for $r \equiv 1$ or $2 \pmod 3$ (see Figure 8.5.2), it cannot happen for $r \equiv 0 \pmod 3$, as in that case the leftmost and rightmost vertices of $\partial\mathcal{U} \cap \partial\mathcal{B}_r^\bullet(\mathcal{U})$ cannot be separating vertices of $\partial\mathcal{U}$.

Before getting into the calculations, we need a bit of additional notation. Suppose the hull $\mathcal{B}^\bullet_{r+1}(\mathcal{U})$ (with $r \equiv 0$ or $1 \pmod 3$) is swallowed by $\partial\mathcal{U}$. As, by our conventions, the half-circumference Q of $\mathcal{B}^\bullet_{r+1}(\mathcal{U})$ is zero, we need to introduce a new quantity Q', which counts the number of modules of type $(r, r+1, r+2)$ that form a loop touching the unique vertex of $\partial\mathcal{B}^\bullet_{r+1}(\mathcal{U})$ that is at distance $r+1$ from the root (see Figure 8.5.2). Similarly as before, we then denote by V'_i, for $1 \le i \le Q'$, the type-r vertex of the i-th module of this looping chain, and, for $1 \le j \le Q'+1$, we write S'_j for the number of modules on $\partial\mathcal{B}^\bullet_r(\mathcal{U})$ between V'_{j-1} and V'_j. R', R'', L' and L'' can be defined as before.

We are thus interested in determining the probability of a similar event as before, for the first r for which $\mathcal{B}^\bullet_{r+1}$ is swallowed by $\partial\mathcal{U}$:

$$\mathbb{P}\big(Q = 0, R'' - R' = k+1, S'_{Q'+1} = s | \mathcal{B}^\bullet_r(\mathcal{U}), G_r\big).$$

Having treated this first occurence, we will see that the probabilities concerning the following hulls just fall back to case that we have already treated before, and see how we can work, in general, from the last "swallowing up" event.

We will once again treat separately the cases $r \equiv 0 \pmod 3$ and $r \equiv 1 \pmod 3$.

If $r \equiv 0 \pmod 3$, we obtain, similarly as before,

$$\begin{aligned}&\mathbb{P}\big(Q = 0, R'' - R' = k+1, S'_{Q'+1} = s | \mathcal{B}^\bullet_r(\mathcal{U}), G_r\big)\\ &= \frac{\rho^2}{\alpha^3}\left(\sum_{q'\ge 1}\theta(q')\left(\sum_{s_1+\cdots+s_{q'}=\mathbf{P}_r - s}\theta([s_1,\infty))\cdots\theta(s_{q'})\right)\right)\theta(s+k),\end{aligned} \tag{8.5.14}$$

the factor $\theta(q')$ accounting for the fact that we have an additional slot bounded by the looping chain of modules.

Roughly bounding this factor by 1 for any q', we can apply the same arguments as before, that ensure the existence of a constant $C > 0$, independent of s and $\mathbf{P}_r$, such that

$$\mathbb{P}\big(Q = 0, R'' - R' = k+1, S'_{Q'+1} = s | \mathcal{B}^\bullet_r(\mathcal{U}), G_r\big) \le C\mathbb{1}_{\{s\le\mathbf{P}_r\}}\theta(s+k).$$

As for the case $r \equiv 1 \pmod 3$, we have

$$\begin{aligned}&\mathbb{P}\big(Q = 0, R'' - R' = k+1, S'_{Q'+1} = s | \mathcal{B}^\bullet_r(\mathcal{U}), G_r\big)\\ &= \frac{c\alpha^{\mathbf{P}_r}}{E(\mathbf{P}_r)}\frac{\rho^2}{\alpha}\left(\sum_{q'\ge 1}\theta(q')\left(\sum_{s_1+\cdots+s_{q'}=\mathbf{P}_r - s}\hat\theta(s_1)\cdots\theta(s_{q'})\right)\right)\tilde\theta(k,s),\end{aligned} \tag{8.5.15}$$

so that, using a bigger constant C if necessary, we have

$$\mathbb{P}\big(Q = 0, R'' - R' = k+1, S'_{Q'+1} = s | \mathcal{B}^\bullet_r(\mathcal{U}), G_r\big) \le C\mathbb{1}_{\{s\le\mathbf{P}_r\}}\theta(s+k)$$

in that case as well.

This proves that this special case does not modify the global asymptotics given in (8.5.1) for the spherical layer $\mathcal{B}^\bullet_{r+1}(\mathcal{U}) \setminus \mathcal{B}^\bullet_r(\mathcal{U})$: indeed, the lower bound of (8.5.1) is still valid, and, from what precedes, the upper bound is undisturbed, up to a change of the constant C_2.

Let us now consider the consequences for the next spherical layers. As can be seen in Figure 8.5.2, if $r \equiv 0 \pmod 3$ and the hull $\mathcal{B}^\bullet_{r+1}(\mathcal{U})$ is swallowed up by $\partial\mathcal{U}$, this leads to what can be interpreted as a reinitialization of the value of the radius $\pmod 3$: indeed, the whole boundary $\partial\mathcal{B}^\bullet_{r+1}(\mathcal{U})$ is contained in $\partial\mathcal{U}$, so that we can see v, the only vertex

on $\partial\mathcal{B}_{r+1}(\mathcal{U})$ at distance $r+1$ from the origin, as a new "starting point" for the next spherical layer, which will have the same law as $\mathcal{B}_1^\bullet(\mathcal{U})$. As, from (8.5.1), we have the same bounds for the asymptotics of $\mathbb{P}(R''-R'=k|\mathcal{B}_t^\bullet(\mathcal{U}))$ for all values of $t \pmod 3$, this reinitialization thankfully does not modify this asymptotic behavior.

When the hull $\mathcal{B}_{r+1}^\bullet(\mathcal{U})$ is swallowed up but $r \equiv 1 \pmod 3$, we see from Figure 8.5.2 that the possible configurations for the layer between $\mathcal{B}_{r+1}^\bullet(\mathcal{U})$ and $\mathcal{B}_{r+2}^\bullet(\mathcal{U})$ are just a special case of those already considered before.

Thus, when studying the spherical layer between $\mathcal{B}_r^\bullet(\mathcal{U})$ and $\mathcal{B}_{r+1}^\bullet(\mathcal{U})$, in the general case, where possibly several "swallowing up" events have occured before, we get one of the expressions (8.5.5), (8.5.6), (8.5.7), (8.5.8), (8.5.14), (8.5.15). The case to consider is not determined by the value of r mod 3, but by some counter $m(r,\mathcal{U}) \in \{0,1,2\}$, such that $m(r+1,\mathcal{U}) \equiv m(r,\mathcal{U})+1 \pmod 3$, except when $\mathcal{B}_{r+1}^\bullet(\mathcal{U})$ is swallowed up by $\partial\mathcal{U}$ and $m(r,\mathcal{U})=0$, in which case $m(r+1,\mathcal{U})=0$. □

8.6 Distances along the boundary

Similarly to section 4 of [CLG19], we will now show lower bounds on the (oriented) distances along the boundary of $\mathcal{U}$, that will carry over to $\mathcal{L}$ thanks to an absolute continuity property of Corollary 8.6.4.

Let us start with $\mathcal{U}$. We denote by $(-L_r^{\mathcal{U}},0)$ (resp. $(R_r^{\mathcal{U}},0)$) the left-most (resp. right-most) vertex in $\partial\mathcal{B}_r^\bullet(\mathcal{U})\cap\partial\mathcal{U}$, and set by convention $R_0^{\mathcal{U}}=L_0^{\mathcal{U}}=0$, and consider $\mathcal{B}_0^\bullet(\mathcal{U})$ to be the trivial edge-triangulation.

We show the following proposition:

Proposition 8.6.1. *The sequences $((r^{-2}L_r^{\mathcal{U}},0))_{r\geq 1}$ and $((r^{-2}R_r^{\mathcal{U}},0))_{r\geq 1}$ are bounded in probability: for every $\varepsilon>0$, there exists a constant K such that*

$$\sup_{r\geq 1}\mathbb{P}\big(L_r^{\mathcal{U}}\geq Kr^2\big)\leq\varepsilon \text{ and } \sup_{r\geq 1}\mathbb{P}\big(R_r^{\mathcal{U}}\geq Kr^2\big)\leq\varepsilon.$$

Consequently, for every $r\geq 1$,

$$\mathbb{P}\Big(\min_{|j|\geq Kr^2}\overrightarrow{d}_{\mathcal{U}}((0,0),(j,0))>r\Big)\geq 1-2\varepsilon. \tag{8.6.1}$$

Furthermore, if, for $m\geq 1$, $T_m=\min\{r\geq 1\,\big|\,R_r^{\mathcal{U}}>m\}$, then there exists a constant K' such that, for every $m\geq 1$ and every $j\geq 1$,

$$\mathbb{P}\big(R_{T_m}^{\mathcal{U}}-m>j\big)\leq K'\sqrt{\frac{m}{m+j}}.$$

Proof. The first statement follows from (8.5.1). The second one is an immediate consequence, considering that, if $j>R_r^{\mathcal{U}}$, then, by definition, $\overrightarrow{d}_{\mathcal{U}}((0,0),(j,0))>r$.

The proof of the third statement is very similar to the proof of the equivalent statement in Proposition 13 of [CLG19], but the calculations are slightly more involved, as we do not have explicit expressions for the probabilities of the ball events, or for the distribution θ. We therefore give the full detail of these calculations.

Like in [CLG19], it suffices to show the existence of a constant K', that does not depend on m, such that, for every $k\geq 0$, for every $l\in\{0,1,\dots,m\}$, and for every $j\geq 0$,

$$\mathbb{P}\big(R_{k+1}^{\mathcal{U}}-R_k^{\mathcal{U}}>l+j|\mathcal{B}_k^\bullet(\mathcal{U})\big)\leq K'\sqrt{\frac{m}{m+j}}\,\mathbb{P}\big(R_{k+1}^{\mathcal{U}}-R_k^{\mathcal{U}}>l|\mathcal{B}_k^\bullet(\mathcal{U})\big). \tag{8.6.2}$$

Indeed, we have that, for every $j \geq 0$,

$$\begin{aligned}\mathbb{P}\big(R^{\mathcal{U}}_{T_m} - m > j\big) &= \sum_{k=0}^{\infty} \mathbb{P}\big(R^{\mathcal{U}}_k \leq m, R^{\mathcal{U}}_{k+1} - R^{\mathcal{U}}_k > m + j - R^{\mathcal{U}}_k\big) \\ &= \sum_{k=0}^{\infty} \mathbb{E}\Big[\mathbb{1}_{\{R^{\mathcal{U}}_k \leq m\}}\, \mathbb{P}\big(R^{\mathcal{U}}_{k+1} - R^{\mathcal{U}}_k > m + j - R^{\mathcal{U}}_k | \mathcal{B}^{\bullet}_k(\mathcal{U})\big)\Big]\end{aligned}$$

which yields, with (8.6.2),

$$\begin{aligned}\mathbb{P}\big(R^{\mathcal{U}}_{T_m} - m > j\big) &\leq K' \sqrt{\frac{m}{m+j}} \sum_{k=0}^{\infty} \mathbb{E}\Big[\mathbb{1}_{\{R^{\mathcal{U}}_k \leq m\}}\, \mathbb{P}\big(R^{\mathcal{U}}_{k+1} - R^{\mathcal{U}}_k > m - R^{\mathcal{U}}_k | \mathcal{B}^{\bullet}_k(\mathcal{U})\big)\Big] \\ &= K' \sqrt{\frac{m}{m+j}}.\end{aligned}$$

Let us now prove (8.6.2). The case $k = 0$ follows from (8.5.8). For $k \geq 1$, (8.5.11) yields, for every $j \geq 0$,

$$C_1 \sum_{i=0}^{\infty} \sum_{s=0}^{\mathbf{P}'_k} \theta(s + l + j + i) \leq \mathbb{P}\big(R^{\mathcal{U}}_{k+1} - R^{\mathcal{U}}_k > l + j | \mathcal{B}^{\bullet}_k(\mathcal{U})\big) \leq C_2 \sum_{i=0}^{\infty} \sum_{s=0}^{\mathbf{P}'_k} \theta(s + l + j + i),$$

where $\mathbf{P}'_k = \mathbf{P}_k$ for $m(k,\mathcal{U}) = 0$ or 1, and $\mathbf{P}'_k = \mathbf{P}_k - 1$ in the case $m(k,\mathcal{U}) = 2$.

Thus, it suffices to show that there exists a constant K'' such that, for every $p \geq 1$, for every $l \in \{0, 1, \ldots, m\}$ and every $j \geq 0$,

$$\sum_{i=0}^{\infty} \sum_{s=0}^{p} \theta(s + l + j + i) \leq K'' \sqrt{\frac{m}{m+j}} \sum_{i=0}^{\infty} \sum_{s=0}^{p} \theta(s + l + i). \tag{8.6.3}$$

Now, from the asymptotics of θ (and the fact that $\theta(n)$ is positive for any n), we have the existence of two constants $0 < c < C$ such that, for every n, $cn^{-5/2} \leq \theta(n) \leq Cn^{-5/2}$. This implies that, for any $l \in \{0, 1, \ldots, m\}$, for any $i \geq 0$ and $p \geq 1$,

$$\sum_{s=0}^{p} \theta(l + i + s) \geq c \sum_{s=0}^{p} (l + i + s)^{-5/2} = c' \left((l+i)^{-3/2} - (l + i + p)^{-3/2} \right),$$

which gives, when summing over i,

$$\sum_{i=0}^{\infty} \sum_{s=0}^{p} \theta(l + i + s) \geq c'' \left(l^{-1/2} - (l+p)^{-1/2} \right) = c'' l^{-1/2} \left(1 - \sqrt{\frac{l}{l+p}} \right).$$

Similarly, we show that, for any $l \in \{0, 1, \ldots, m\}$, for any $j \geq 0$ and $p \geq 1$,

$$\sum_{i=0}^{\infty} \sum_{s=0}^{p} \theta(l + j + i + s) \leq C'(l+j)^{-1/2} \left(1 - \sqrt{\frac{l+j}{l+j+p}} \right) \leq C'(l+j)^{-1/2} \left(1 - \sqrt{\frac{l}{l+p}} \right),$$

the last inequality coming from the fact that $x \mapsto \frac{x}{x+p}$ is increasing on $\mathbb{R}_+$.

Gathering the preceding bounds, we get, for any $l \in \{0, 1, \ldots, m\}$, for any $j \geq 0$ and $p \geq 1$,

$$\sum_{i=0}^{\infty} \sum_{s=0}^{p} \theta(l + j + i + s) \leq K'' \sqrt{\frac{l}{l+j}} \sum_{i=0}^{\infty} \sum_{s=0}^{p} \theta(l + i + s).$$

To obtain (8.6.3), note that, for any $l \in \{0, 1, \ldots, m\}$, for any $j \geq 0$, $\sqrt{l/(l+j)} \leq \sqrt{m/(m+j)}$.

□

To carry these estimates over to $\mathcal{L}$, we need an additional property, slightly stronger than (8.6.1).

Proposition 8.6.2. *Let $\varepsilon > 0$. For every integer $A > 0$, there exists $K > 0$ sufficiently large such that, for every $r \geq 1$,*

$$\mathbb{P}\Big(\min_{0\leq i\leq Ar^2,\, j\geq Kr^2} \overrightarrow{d}_{\mathcal{U}}((i,0),(j,0)) \leq r\Big) \leq \varepsilon.$$

Proof. The proof of this result is very similar to the proof of Proposition 14 in [CLG19]. As it is very short, we give it here as well.

Fix $A > 0$. Then, using the last result of the previous proposition, we can choose an integer $A' > A$ large enough so that, for every $r \geq 1$,

$$\mathbb{P}\Big(R^{\mathcal{U}}_{T_{Ar^2}} \geq A'r^2\Big) < \frac{\varepsilon}{2}.$$

Fix $r \geq 1$ and define, for every $j \geq 0$,

$$\widetilde{R}^{\mathcal{U}}_j := R^{\mathcal{U}}_{T_{Ar^2}+j} - R^{\mathcal{U}}_{T_{Ar^2}}.$$

Since T_{Ar^2} is a stopping time for the process $(R^{\mathcal{U}}_j)_{j\geq 0}$, we get from the tail asymptotics of $(R^{\mathcal{U}}_j)$ that the sequence $(j^{-2}\widetilde{R}^{\mathcal{U}}_j)_{j\geq 0}$ is also bounded in probability, uniformly in r. Therefore, we can choose an integer $K > A'$, that does not depend on the choice of r, such that

$$\mathbb{P}\Big(\widetilde{R}^{\mathcal{U}}_r \geq (K-A')r^2\Big) < \frac{\varepsilon}{2}.$$

Finally, note that any vertex $(i,0)$ with $0 \leq i \leq Ar^2$ belongs to the hull of radius T_{Ar^2}. And, on the event $\{R^{\mathcal{U}}_{T_{Ar^2}} < A'r^2\} \cap \{\widetilde{R}^{\mathcal{U}}_r < (K-A')r^2\}$, we have $R^{\mathcal{U}}_{T_{Ar^2}+r} < Kr^2$, so that vertices $(j,0)$ with $j \geq Kr^2$ do not belong to the hull of radius $T_{Ar^2} + r$. Thus, on this event we have $\overrightarrow{d}_{\mathcal{U}}((i,0),(j,0)) > r$ for any $0 \leq i \leq Ar^2$ and $j \geq Kr^2$. □

We will now establish a link between the layers in $\mathcal{L}$ and in $\mathcal{U}$. For this purpose we will need a bit of additional notation. For every integer $r \geq 1$, $\mathcal{U}_{[0,r]}$ will stand for the infinite rooted planar map comprised of the first r layers of $\mathcal{U}$, that is, the strip between the boundary of $\mathcal{U}$ and the skeleton modules at level $r-1$ (included). Similarly, let $\mathcal{L}_{[0,r]}$ be the rooted planar map obtained by keeping only the first r layers of $\mathcal{L}$ (having the skeleton modules at level r as ghost modules).

Let us fix $r \geq 1$, recall that $\Gamma_{(i,r)}$ stands for the subtree of descendants of $(\frac{1}{2}+i, r)$ in the infinite tree associated to $\mathcal{U}$. For every $i \in \mathbb{Z}$, let $\Gamma_{(i,r)}(r)$ be the set of vertices of $\Gamma_{(i,r)}$ at height r. Let also $K_r \geq 1$ be the first integer $i \geq 1$ such that $\Gamma_{(i,r)}(r) \neq \varnothing$.

We also define $i_r < 0$ as the largest integer $i < 0$ such that $\mathscr{T}_i$ has height at least r, and, as before, $\mathscr{T}_{i_r}(r)$ will be the set of vertices at height r in $\mathscr{T}_{i_r}$.

Proposition 8.6.3. *Let $\widetilde{\mathcal{U}}_{[0,r]}$ be the infinite rooted planar map obtained by re-rooting $\mathcal{U}_{[0,r]}$ at the edge from (J_r, r) to $(\frac{1}{2}+J_r, r+\varepsilon)$, where, given K_r, J_r is chosen uniformly at random in $\{1,\dots,K_r\}$. Then, for any nonnegative measurable function f,*

$$\mathbb{E}\Big[K_r \cdot f\left(\widetilde{\mathcal{U}}_{[0,r]}\right)\Big] = \mathbb{E}\big[\#\mathscr{T}_{i_r}(r) \cdot f\left(\mathcal{L}_{[0,r]}\right)\big].$$

Proof. Let us sketch an idea of the proof, which can be adapted verbatim from the one of Proposition 8 of [CLG19].

It suffices to show that the distribution of the configuration of the skeleton modules is the same for $\widetilde{\mathcal{U}}_{[0,r]}$, under the measure having density K_r with respect to $\mathbb{P}$, and for $\mathcal{L}_{[0,r]}$, under the measure having density $\#\mathscr{T}_{i_r}(r)$ with respect to $\mathbb{P}$. In both cases, this configuration is encoded by a doubly infinite sequence of trees, therefore it is enough to verify that these two sequences have the same distribution, which is quite straightforward. □

Corollary 8.6.4. *For every $\varepsilon > 0$, we can choose $\delta > 0$ small enough, so that for every $r \geq 1$, for every measurable set A, the property $\mathbb{P}\Big(\widetilde{\mathcal{U}}_{[0,r]} \in A\Big) \leq \delta$ implies $\mathbb{P}\big(\mathcal{L}_{[0,r]} \in A\big) \leq \varepsilon$.*

Proof. Let us give an idea of the proof, which is very similar to the proof of Corollary 9 in [CLG19] (up to the differences in the explicit expressions).

Let $\delta \in (0,1)$, and consider an event A such that $\mathbb{P}\Big(\widetilde{\mathcal{U}}_{[0,r]} \in A\Big) \leq 9\delta^2/2$. By Proposition 8.6.3, for every $r \geq 1$,

$$\mathbb{E}\Big[K_r \cdot \mathbf{1}_A\left(\widetilde{\mathcal{U}}_{[0,r]}\right)\Big] = \mathbb{E}\big[\#\mathscr{T}_{i_r}(r) \cdot \mathbf{1}_A\left(\mathcal{L}_{[0,r]}\right)\big], \tag{8.6.4}$$

and, from (7.5.18) in Chapter 7, the distribution of K_r is given by

$$\mathbb{P}(K_r \geq j) = \left(1 - \frac{3}{(r+2)^2 - 1}\right)^{j-1} \qquad \forall j \geq 1,$$

which implies that $\mathbb{E}\big[(K_r)^2\big] \leq 2/9((r+2)^2-1)^2$.

Then, by the Cauchy-Schwarz inequality, the left-hand side of (8.6.4) is bounded above by

$$\mathbb{E}\big[K_r^2\big]^{1/2}\,\mathbb{P}\Big(\widetilde{\mathcal{U}}_{[0,r]} \in A\Big)^{1/2} \leq \delta((r+2)^2-1).$$

Now, for any $M > 0$, the right-hand side of (8.6.4) is bounded below by

$$M((r+2)^2-1)\,\mathbb{P}\big(\{\mathcal{L}_{[0,r]} \in A\} \cap \{\#\mathscr{T}_{i_r}(r) \geq M((r+2)^2-1)\}\big).$$

By combining the two bounds, we get that

$$\mathbb{P}\big(\{\mathcal{L}_{[0,r]} \in A\} \cap \{\#\mathscr{T}_{i_r}(r) \geq M\}\big) \leq \frac{\delta}{M},$$

so that it suffices to obtain an upper bound on $\mathbb{P}\big(\#\mathscr{T}_{i_r}(r) < M((r+2)^2-1)\big)$, to finally have an upper bound on $\mathbb{P}\big(\mathcal{L}_{[0,r]} \in A\big)$.

To bound $\mathbb{P}\big(\#\mathscr{T}_{i_r}(r) < M((r+2)^2-1)\big)$, observe that $\mathscr{T}_{i_r}$ is a Galton-Watson tree with offspring distribution θ conditioned on non-extinction at generation r, so that the generating function of $\#\mathscr{T}_{i_r}(r)$ is

$$\mathbb{E}\Big[x^{\#\mathscr{T}_{i_r}(r)}\Big] = \frac{\mathbb{E}_1\left[x^{Y_r}\right] - \mathcal{P}_1\left(Y_r = 0\right)}{1 - \mathcal{P}_1\left(Y_r = 0\right)} = 1 - \frac{(r+2)^2 - 1}{\left(r + \sqrt{\frac{4-x}{1-x}}\right)^2 - 1} \qquad \forall x \in [0,1),$$

using (7.5.7) and (7.5.18) in Chapter 7.

From this, it is straightforward to obtain that $((r+2)^2-1)^{-1}\#\mathscr{T}_{i_r}(r)$ converges in distribution to a random variable U with Laplace transform $\mathbb{E}\big[e^{-\lambda U}\big] = 1 - (1+\sqrt{3/\lambda})^{-2}$. As $U > 0$ a.s., we can find $M > 0$ such that $\mathbb{P}\big(\#\mathscr{T}_{i_r}(r) < M((r+2)^2-1)\big) \leq \varepsilon/2$ for every $r \geq 1$. If we choose δ small enough, we will also have $M \geq 2\delta/\varepsilon$, so that

$$\mathbb{P}\big(\mathcal{L}_{[0,r]} \in A\big) \leq \varepsilon.$$

□

We can now derive lower bounds for the distances along the boundary of $\mathcal{L}$. Recall the leftmost mirror geodesics defined in Chapter 7 for finite cylinder triangulations and for $\mathcal{L}$. We also define for $\mathcal{U}$, in a similar way, the leftmost mirror geodesic from (i,r) to $\partial\mathcal{U}$: at each step $n \geq 0$, it visits a vertex $\omega(n)$ in $\mathcal{U}_{r-n}$, and chooses at step $n+1$ the leftmost edge between $\omega(n)$ and $\mathcal{U}_{r-n-1}$. We also have that, for $1 \leq i < j$, the leftmost mirror geodesics from (i,r) and (j,r) to $\partial\mathcal{U}$ coalesce before hitting $\partial\mathcal{U}$, if and only if all the trees $\Gamma_{(i,r)}, \Gamma_{(i+1,r)}, \ldots, \Gamma_{(j-1,r)}$ have height strictly smaller than r.

Proposition 8.6.5. *For every $\varepsilon > 0$, there exists an integer $K > 0$ such that, for every $r \geq 1$,*

$$\mathbb{P}\Big(\min_{|j|\geq Kr^2} \overrightarrow{d}_{\mathcal{L}}((0,0),(j,0)) \geq r\Big) \geq 1-\varepsilon.$$

Consequently, for $K' = 4K$, we also have, for every $r \geq 1$,

$$\mathbb{P}\Big(\min_{|j|\geq 2K'r^2} \quad \min_{-K'r^2\leq i\leq K'r^2} \overrightarrow{d}_{\mathcal{L}}((i,0),(j,0)) \geq r\Big) \geq 1-2\varepsilon.$$

Proof. Let us give an idea of the proof, which is very similar to the proof of Proposition 15 in [CLG19].

Let us start with the first assertion. By symmetry, we can focus on the event "there is a path in $\mathcal{L}_{[0,r]}$ of (oriented) length strictly smaller than r, going from $(0,0)$ to $(j,0)$, for some $j \geq Kr^2$", that we denote by $A_r(K)$. Using the absolute continuity of Corollary 8.6.4, it suffices to show that, for K large enough, for every $r \geq 1$,

$$\mathbb{P}\Big(\widetilde{U}_{[0,r]} \in A_r(K)\Big) < \varepsilon.$$

Recalling the notation of Proposition 8.6.3, we have

$$\{\widetilde{U}_{[0,r]} \in A_r(K)\} \subset \{\min_{i\geq Kr^2} \overrightarrow{d}_{\mathcal{U}}((J_r,r),(J_r+i,r))\}.$$

Hence, we are left to bound the probability of the right-hand side event. Let $(I_r,0)$ be the endpoint of the leftmost mirror geodesic from $(1,r)$ to $\partial\mathcal{U}$ in $\mathcal{U}$. As $1 \leq J_r \leq K_r$, we get that the leftmost mirror geodesic from (J_r,r) to $\partial\mathcal{U}$ coalesces with the one from $(1,r)$ before hitting $\partial\mathcal{U}$ (possibly only at $\partial\mathcal{U}$). Therefore, we have

$$\overrightarrow{d}_{\mathcal{U}}((I_r,0),(J_r,r)) = r.$$

Let now $(I'_r(K),0)$ be the endpoint of the leftmost mirror geodesic from (Kr^2,r) to $\partial\mathcal{U}$ in $\mathcal{U}$. Suppose that both $J_r < Kr^2$, and $\overrightarrow{d}_{\mathcal{U}}((J_r,r),(J_r+i,r)) < r$, for some $i \geq Kr^2$. Then the endpoint of the leftmost mirror geodesic from (J_r+i,r) to $\partial\mathcal{U}$ is $(j,0)$, for some $j \geq I'_r(K)$, as $J_r+i \geq Kr^2$. Then, using the triangle inequality and the fact that reversing an oriented distance at most doubles it, we get

$$\overrightarrow{d}_{\mathcal{U}}((I_r,0),(j,0)) \leq \overrightarrow{d}_{\mathcal{U}}((I_r,0),(J_r,r)) + \overrightarrow{d}_{\mathcal{U}}((J_r,r),(J_r+i,r)) + \overrightarrow{d}_{\mathcal{U}}((J_r+i,r),(j,0)) < 4r.$$

We have thus obtained that

$$\mathbb{P}\Big(\widetilde{U}_{[0,r]} \in A_r(K)\Big) \leq \mathbb{P}\big(J_r \geq Kr^2\big) + \mathbb{P}\Big(\min_{j\geq I'_r(K)} \overrightarrow{d}_{\mathcal{U}}((I_r,0),(j,0)) < 4r\Big). \tag{8.6.5}$$

As noted in the proof of Proposition 8.6.3, we have $\mathbb{E}\big[J_r^2\big] \leq 2/9((r+2)^2-1)^2$, so, by Markov's inequality, there exists K_0 such that $\mathbb{P}\big(J_r \geq Kr^2\big) \leq \varepsilon/4$ for $K \geq K_0$.

We now tackle the second term in the right-hand side of (8.6.5): it suffices to have bounds of the form

$$\mathbb{P}\big(I_r \geq Br^2\big) \leq \varepsilon/4 \tag{8.6.6}$$

$$\mathbb{P}\big(I'_r(K) < B'r^2\big) \leq \varepsilon/4, \tag{8.6.7}$$

for some constants $B' > B > 0$. Indeed, Proposition 8.6.2 will then give us a bound on

$$\mathbb{P}\Big(\min_{j \geq I'_r(K)} \overrightarrow{d}_{\mathcal{U}}((I_r, 0), (j, 0)) < 4r\Big).$$

To prove the bound (8.6.6), note that I_r is bounded above by the size N_r of the generation r of the tree $\Gamma_{(0,r)}$. From (7.5.7) in Chapter 7, we obtain that $r^{-2}N_r$ converges in distribution, yielding (8.6.6).

It remains to show (8.6.7). From the construction of $\mathcal{U}$, $I'_r(K)$ is bounded below by

$$M_r(K) := \sum_{l=1}^{Kr^2-1} \#\Gamma_{(l,r)}(r),$$

and, using (7.5.7) once again, we obtain that $r^{-2}M_r(K)$ converges in distribution to a random variable U_K with Laplace transform $\mathbb{E}\big[e^{-\lambda U_K}\big] = \exp(-3K/(\sqrt{3/\lambda}+1)^2)$. Thus, U_K/K converges in probability to 3 as $K \to \infty$, so that, taking K large enough, for all r sufficiently large, (8.6.7) holds, for $B' = K/3$, which is larger than B for K large enough. Then, for smaller values of r, we can take K even larger to get the same bound (using here the law of large numbers). This completes the proof of the first assertion.

The details of the calculations involved to get (8.6.6) and (8.6.7) can be adapted verbatim from the proof of Proposition 15 in [CLG19] (up to differences in the explicit expressions for generating functions).

The second assertion follows from the first one, as detailed in Chapter 7. □

CHAPITRE 9

Énumération de triangulations eulériennes à bord alternant

Ce chapitre est une version préliminaire d'un travail en cours avec Jérémie Bouttier.

Contents

9.1 Introduction

9.1.1 Framework and motivation

Let A be a rooted planar Eulerian triangulation, that is, a triangulation whose vertices all have even degree. The orientation of the root edge of A fixes a **canonical orientation** of all its edges, by requiring that orientations alternate around each vertex. By construction, edges around a given face are necessarily oriented either all clockwise, or all anti-clockwise. This induces a natural bicoloration of the faces of A, by setting for instance that clockwise faces are black, and anti-clockwise faces, white.

The **oriented geodesic distance** of any vertex of A from the origin (that is, the root vertex ρ) is the minimal length of a path from the origin to that vertex, respecting the orientation. Bouttier, Di Francesco and Guitter [BDFG04] have established a bijection between rooted Eulerian triangulations and a particular class of labeled trees, using this oriented pseudo-distance. As this result suggests, the oriented distance is central in the structure of planar Eulerian triangulations.

In Chapter 7, building upon this bijective result, we prove that uniform planar Eulerian triangulations, equipped with either the usual graph distance or the oriented pseudo-distance, converge to the ubiquitous Brownian map. To do so, a deep analysis of the structure of planar Eulerian triangulations equipped with the oriented distance is needed, including new enumeration results, that are derived in this present chapter.

For this chapter to be self-contained, we give a shortened version of the discussion of Chapter 7 that justifies which types of maps we will focus on here.

Let us consider a rooted Eulerian triangulation A, equipped with its canonical orientation and oriented geodesic distance $\vec{d}$.

Definition 9.1.1. In a rooted Eulerian triangulation A, a **vertex of type n** is a vertex whose canonical labeling by the oriented geodesic distance is n. An **edge of type $n \to m$** is an oriented edge that starts at a vertex of type n and ends at a vertex of type m. A **triangle of type n** is a triangle adjacent to one vertex of type $n-1$, one of type n and one of type $n+1$.

For each type-n black face f of A, there is exactly one white face f' that shares its $n+1 \to n-1$ edge. We call the union of f and f' a **type-n module**.

We define the **ball $\mathcal{B}_n(A)$** as the submap of A obtained by keeping only the faces and edges of A incident to at least a vertex at distance $n-1$ or less from the origin, and cutting along the edges of type $n \to n+1$ (see Figure 9.1.1).

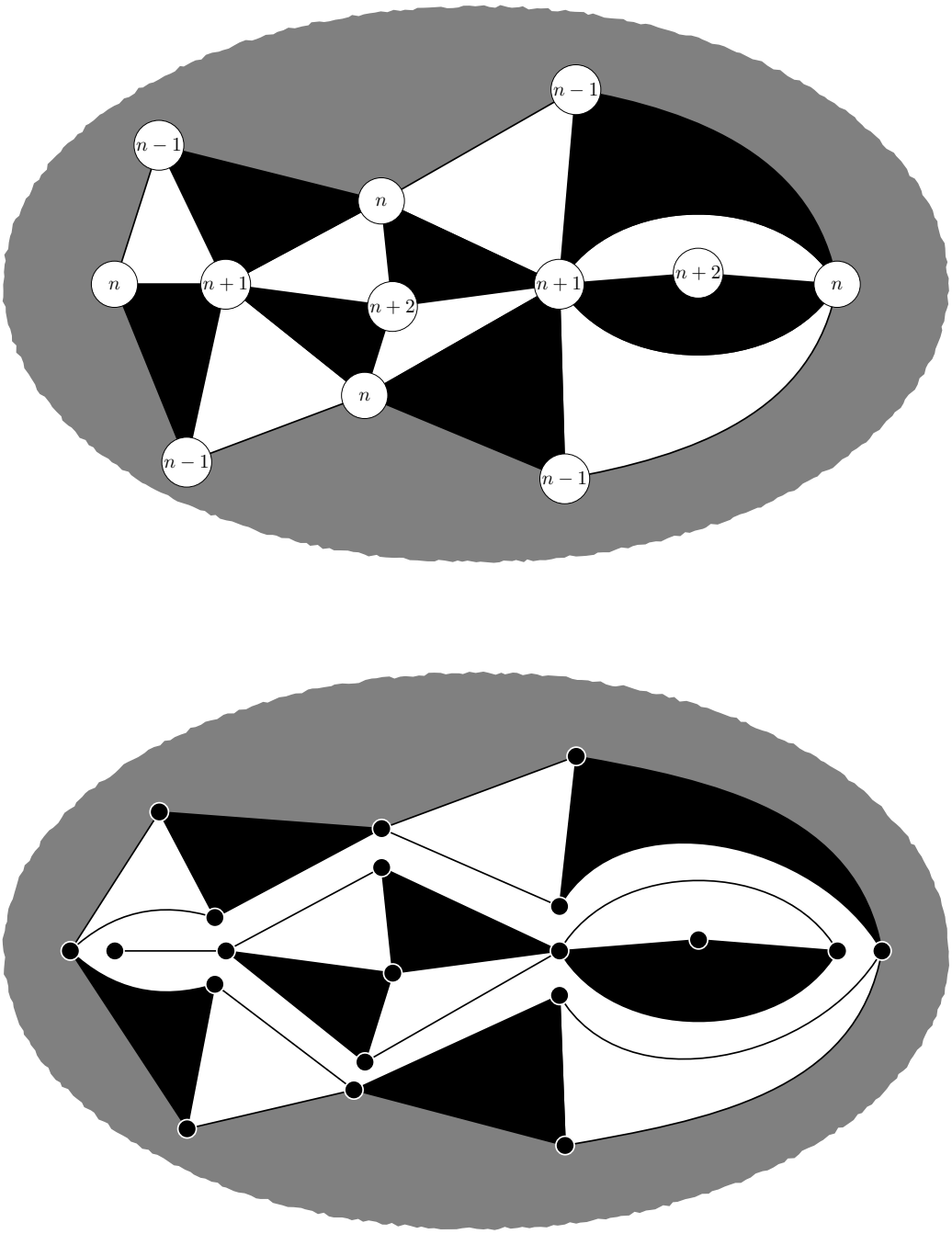

Figure 9.1.1 – In an Eulerian triangulation (top), we cut along the edges of type $n \to n+1$ to separate the ball of radius n from the components of its complement (bottom). This possibly induces the duplication of edges and vertices in the ball.

Let us be more precise: denote by $A \setminus \mathcal{B}_n(A)$, the subcomplex of A (seen as a 2-cell complex), obtained by removing the faces and edges of A that are incident to at least a vertex at distance n or less from the origin: the connected components of $A \setminus \mathcal{B}_n(A)$ are

Eulerian triangulations with a boundary. In $\mathcal{B}_n(A)$, we replace each map in $A \setminus \mathcal{B}_n(A)$ by a single, simple face. In particular, if two faces of A of type n that share a type-$(n \to n+1)$ edge, in $\mathcal{B}_n(A)$ their respective type-$(n \to n+1)$ edges are not identified, so that their common type-$(n+1)$ vertex gives rise to two vertices in $\mathcal{B}_n(A)$ (see Figure 9.1.2). Two type-n faces f, f' may also share a type-$(n+1)$ vertex v but no edge: in that case, it means that v is also shared by faces of types $n+1$, so that we would need to add these faces and the type $n \to n+1$ edges they share with f and/or f', in order to identify the type-$(n+1)$ vertices of f and f' into v. Note that as $\mathcal{B}_n(A)$ contains all the type-$(n-1 \to n)$ edges of A, type-n vertices of A are never duplicated in $\mathcal{B}_n(A)$.

Thus, $\mathcal{B}_n(A)$ is an Eulerian triangulation with simple boundaries, and the faces adjacent of $\mathcal{B}_n(A)$ to these boundaries compose the type-n modules of A, so that each part of $\partial\mathcal{B}_n(A)$ is **alternating**, that is, the adjacent edges alternating between edges incident to black faces, and edges alternating between edges incident to white faces.

Let us now consider a connected component m of $A \setminus \mathcal{B}_n(A)$. It is a planar Eulerian triangulation with a boundary, which has the same length as the corresponding one of $\mathcal{B}_n(A)$, and is also alternating. However, the boundary of m is not necessarily simple. More precisely, a type-$(n+1)$ vertex v of A that sits on the boundary of m is attached to the type-$(n \to n+1)$ edges and type-$(n+1)$ faces that are adjacent to v in A, as they were excluded from $\mathcal{B}_n(A)$, so that v may be a separating vertex in the external face of m. This is not the case for type-n vertices, as $\mathcal{B}_n(A)$ contains all the type-$(n-1 \to n)$ edges and type-n faces of A. Thus, the boundary of m can have separating vertices, but only on boundary vertices that have a white triangle before them and a black one after (as it corresponds to the type-$(n+1)$ vertices of A). We call such boundary conditions **semi-simple**.

Let v be a distinguished vertex of A at oriented distance at least $n+1$ from the root. We can now define the **hull $\mathcal{B}_n^\bullet(A)$** of $\mathcal{B}_n(A)$, as the union of $\mathcal{B}_n(A)$ and all the connected components of its complement that do not contain v. In a more picturial way, for each component m of $A \setminus \mathcal{B}_n(A)$ that does not contain v, we glue the boundary of m to the corresponding boundary of $\mathcal{B}_n(A)$. This is well-defined, because the latter is simple, and they both have the same length. The resulting map $\mathcal{B}_n^\bullet(A)$ has only one boundary, which is alternating and simple, and its complement in A has one boundary, which is alternating and semi-simple.

As is to be expected, these families of Eulerian triangulations with a boundary play an important role in the description of the structure of large uniform random planar Eulerian triangulations. More precisely, this structure involves **Boltzmann** triangulations sampled in those families, that is, random maps with a fixed boundary length, but not a fixed volume. We thus derive asymptotic enumeration results for these families of maps in Section 9.3.

Consider now a rooted infinite Eulerian triangulation of the **half-plane** A, with an infinite alternating and semi-simple boundary, as is the case of the Upper-Half Plane Eulerian Triangulation considered in Chapter 8. Then, the boundary of its balls and hulls will no longer be strictly alternating.

Indeed, the faces adjacent to the boundary of $\mathcal{B}_n^\bullet(A)$ still form a chain of type-n modules, but we must pay attention to what happens at the intersection between this chain and the half-plane boundary of A. For reasons that are detailed in Chapter 8, the different possibilities at this intersection are those depicted in Figure 9.1.3. We see that, in the first two cases, the alternation of black and white fails at this intersection: we say that the boundary of the hull has **defects**. Here as well, the boundary of the complement of a hull

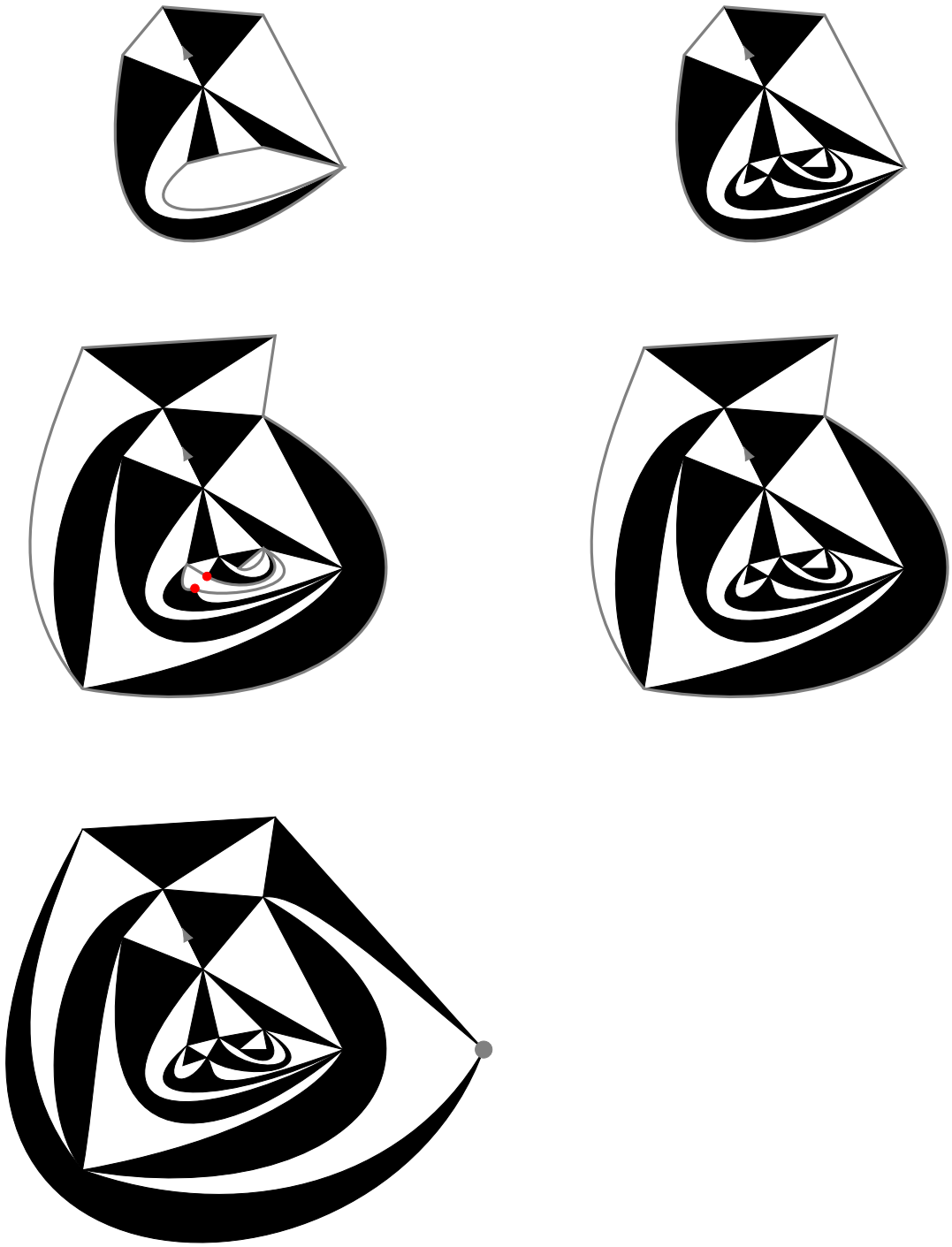

Figure 9.1.2 – A rooted, pointed planar Eulerian triangulation (bottom left) and its balls (left) and corresponding hulls (right) (the ball of radius 3 can be identified with its hull, as it contains the marked vertex). The boundaries are lined in thick gray. We can see an example of duplication of vertices in the ball of radius 2, marked in red.

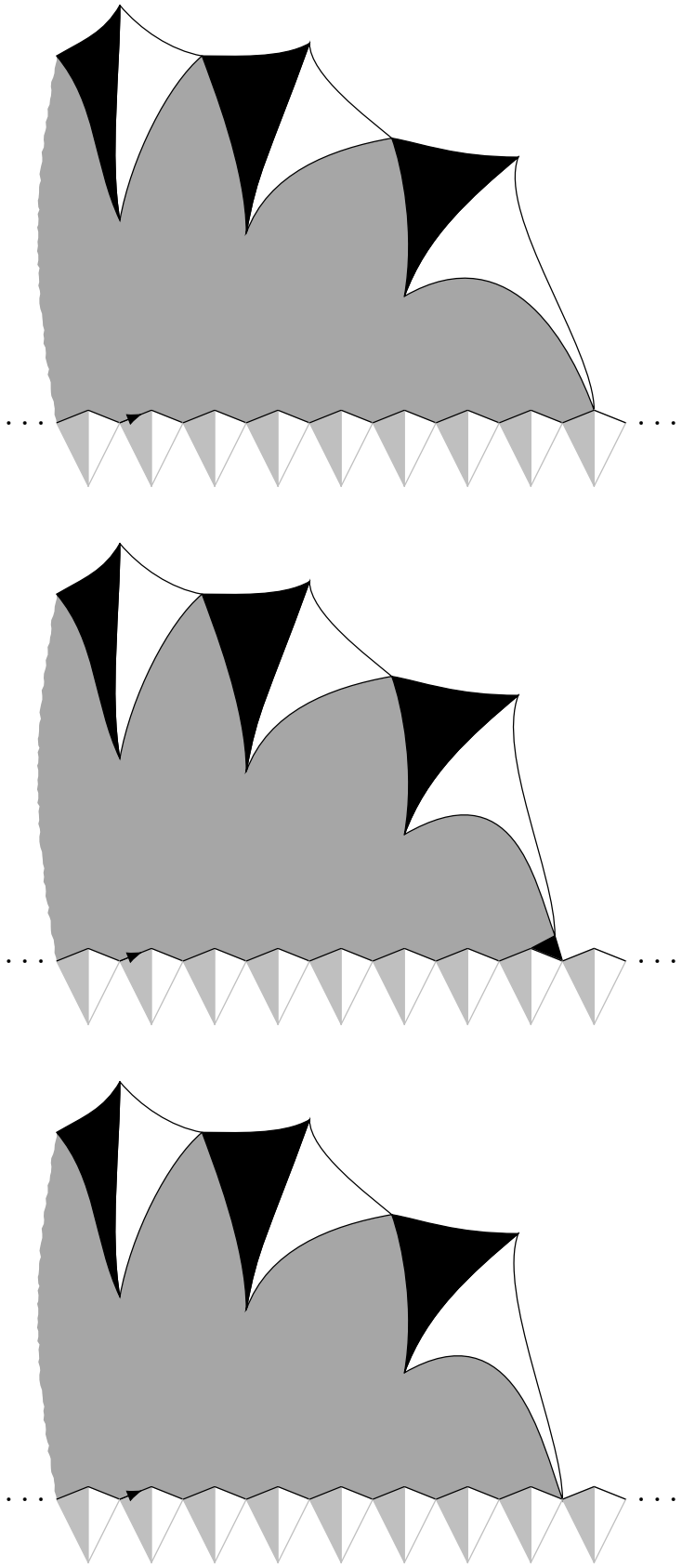

Figure 9.1.3 – The possible configurations for the chain of boundary modules of the hulls of a rooted half-planar Eulerian triangulation: only the right part is shown, as the left part has symmetric conditions. The modules in pale grey represent the semi-simple, alternating conditions on the half-plane boundary.

will have the same color conditions, but specific simplicity conditions, that we do not want to justify here. We will however give a precise definition of these boundary conditions in Section 9.5, in which we similarly derive asymptotic enumeration results for this second type of maps, which are crucial for Chapter 8.

Note that, in either case, the present work establishes parametrizations of the generating functions for these families of maps by explicit, rational functions, which contain much more information than the necessary asymptotics. These rational parametrizations can be seen as particular instances of the general framework of **topological recursion**, as we will explain later.

All computations are available in the Maple companion file [Map].

9.1.2 Related works

The first enumeration results for planar Eulerian triangulations were established by Tutte, using recursion [Tut62]. These results were later revisited in a bijective approach by Bouttier, Di Francesco and Guitter [BDFG04].

Eulerian triangulations with a monochromatic boundary, whose generating function will be an essential tool in this present work, have been enumerated in several more general works on constellations. The first one expressed in terms of maps was by Bousquet-Mélou and Schaeffer, where they also use a bijection with a family of trees [BMS00]. Later, Albenque and Bouttier recovered the same results with techniques relating them to continued fractions [AB12].

Eulerian triangulations with a boundary can also be seen as a particular case of bicolored triangulations with a boundary. On that front, there was recent progress for triangulations endowed with Ising models [AMS; CT]. While Eulerian triangulations have a much less complicated structure than the Ising model, they do share with it a richness in possible boundary conditions that is not present in usual triangulations. It would be interesting to explore this aspect more in further works, by studying boundary conditions that are more general than the specific ones studied here.

Finally, as we will explain later, the recursions we establish can be seen as particular instances of the very general framework of topological recursion, see [Eyn16].

9.2 Monochromatic boundary

We start by recalling known results about the generating function of Eulerian triangulations with a (general) monochromatic boundary, as it is an essential ingredient to enumerate the families we will focus on later.

Let us denote by $F_p = F_p(t)$ this generating function, with p the boundary length and t the weight per vertex. By convention, we set $F_0 = t$ to account for the vertex map.

As a particular case of the works of Bousquet-Mélou and Schaeffer [BMS00] or Albenque and Bouttier [AB12] on planar constellations, we get the following explicit expression for the coefficients of F_{3n} (F_p vanishes when p is not a multiple of 3):

$$\begin{aligned}[t^m]F_{3n} &= \frac{3n}{m-n-1}2^{m-2n-1}\binom{2m-2n-2}{m-2n-1}\binom{3n-1}{n-1} \\ &= \frac{2^{m-2n-2}}{3n+1}\left(2\binom{2n+1}{m}\binom{3n+1}{2n+1}\binom{2m-2n-2}{m-2n-1} - \binom{2n+2}{m}\binom{3n+1}{2n}\binom{2m-2n-3}{m-2n-2}\right).\end{aligned} \tag{9.2.1}$$

We define the Laurent series

$$Y(x) := x^2 + \sum_{p\geq 0} \frac{F_p}{x^{p+1}}. \tag{9.2.2}$$

From (9.2.1), Y has the following Laurent expansion in x:

$$\begin{aligned} Y(x) &= x^2 + \sum_{n\geq 0} \frac{1}{3n+1} \left(\binom{3n+1}{2n+1} V^{2n+1} - \binom{3n+1}{2n} V^{2n+2} \right) x^{-3n+1} \\ &= x^2 + \frac{V - 2V^2}{x} + \frac{V^3 - 3V^4}{x^4} + \frac{3V^5 - 10V^6}{x^7} + \dots \end{aligned} \tag{9.2.3}$$

where $V = V(t)$ is the series determined by $t = V - 2V^2$.

The observant reader might notice that V is the generating function of trees endowed with a weight 2 per edge and weight t per vertex. This is to be expected, as the proof of Bousquet-Mélou and Schaeffer's work relies on a bijection between planar constellations and a specific type of decorated plane trees.

This implies the following proposition:

Proposition 9.2.1. *Set*

$$x(\zeta) := V\zeta + \zeta^{-2}, \quad y(\zeta) := V^2\zeta^2 + \zeta^{-1}. \tag{9.2.4}$$

Then we have

$$Y(x(\zeta)) = y(\zeta). \tag{9.2.5}$$

Note that this result is a particular case of Theorem 8.3.1 in [Eyn16]. We give here an independent proof that relies on (9.2.1).

Proof. Locally around $\zeta = \infty$, $x(\zeta)$ admits a unique inverse $\zeta(x)$, whose Laurent series expansion can be determined by Lagrange inversion:

$$\begin{aligned} \zeta(x) &= \frac{x}{V} - \sum_{n\geq 0} \frac{1}{3n+2} \binom{3n+2}{2n+1} V^{2n+1} x^{-3n+2} \\ &= \frac{x}{V} - \frac{V}{x^2} - 2\frac{V^3}{x^5} - 7\frac{V^5}{x^8} - \dots \end{aligned}$$

By plugging this expansion into $y(\zeta)$, we recover the equation (9.2.3) on Y. □

9.3 Alternating boundary

We are interested in enumerating Eulerian triangulations with an **alternating** and **semi-simple** boundary. We thus want to determine the generating series

$$B(t, z) = \sum_{n,p\geq 0} B_{n,p} t^n z^p$$

where $B_{n,p}$ is the number of Eulerian triangulations with a semi-simple alternating boundary of length $2p$ and with n black triangles.

While the above convention is more natural and convenient for applications, the previous section shows that enumerating by vertices and having inverse weights for the perimeter variable yields simpler expressions. We will thus use the latter conventions for most of the calculations, then go back to the former to compute asymptotic results. For similar reasons, we will stick to general boundaries (instead of semi-simple) until computing asymptotics.

We will give more details about the conversions between these different conventions and families when they arise.

9.3.1 Recursion

We want to compute the generating function for Eulerian triangulations with a (general) alternating boundary. In order to write down a Tutte equation, we need to consider a more general class of boundaries, namely of the form $\bullet^p \circ^q (\bullet\circ)^r$ (in other words, a black part of length p, a white part of length q, and an alternating part of length $2r$ starting with black. We denote by $F_{p,q,r}(t)$ the corresponding generating function (with a weight t per vertex).

Proposition 9.3.1. *For $q \geq 0$ we have*

$$F_{p,q+1,r} = F_{p+2,q,r} + \sum_{p'=0}^{p-1} F_{p'} F_{p-p'-1,q,r} + \sum_{r'=0}^{r-1} F_{p,1,r'} F_{0,q,r-r'-1}. \tag{9.3.1}$$

This equation fully determines $F_{p,q,r}$ when supplemented with the boundary conditions

$$F_{p,0,0} = F_p, \quad F_{p,0,r} = F_{p+1,1,r-1} \quad (r \geq 1). \tag{9.3.2}$$

Proof. We prove this equation with the usual method of "peeling" a boundary edge, here the leftmost white one: it can either be adjacent to an inner black triangle (accounting for the $F_{p+2,q,r}$ term), or it can be identified with a black boundary edge of the black part (accounting for the $F_{p'}F_{p-p'-1,q,r}$ part), or it can be identified with a black boundary edge of the alternating part (accounting for the third term).

Note that the boundary conditions simply express that the two generating functions enumerate the same maps. □

We introduce the generating functions

$$W_q(x,w) = \sum_{p\geq 0}\sum_{q\geq 0} \frac{F_{p,q,r}}{x^{p+1}w^{r+1}}, \quad A_q(w) = \sum_{r\geq 0} \frac{F_{0,q,r}}{w^{r+1}}, \quad B_q(w) = \sum_{r\geq 0} \frac{F_{1,q,r}}{w^{r+1}}. \tag{9.3.3}$$

We are chiefly interested in the series A_0, which corresponds to a purely alternating boundary. Note that we have $A_q = 0$ (resp. $B_q = 0$) unless q (resp. $q-1$) is a multiple of 3. The Tutte equation (9.3.1) amounts to

$$W_{q+1}(x,w) = Y(x)W_q(x,w) - xA_q(w) - B_q(w) + W_1(x,w)A_q(w), \tag{9.3.4}$$

while the boundary conditions (9.3.2) imply

$$wW_0(x,w) - Y(x) + x^2 = xW_1(x,w). \tag{9.3.5}$$

The fact that one gets the coefficients of the generating function W_{q+1} from coefficents of W_q with lower indices, along with some boundary terms, and that this recursive process is driven by $Y(x)$, which corresponds to the "zero case" of the recursion, is an example of the general framework of topological recursion. Indeed, in this framework, topological objects (maps, manifolds, moduli spaces ...) in some family (triangulations with simple boundaries, Riemann surfaces with marked points ...), with a specific topological complexity (a given genus, number of boundaries or marked points ...) can be enumerated recursively from objects in the same family with a lower topological complexity, this recursion being driven by the **spectral curve**, a parametrized complex manifold than can be interpreted as the case of zero complexity in the family. Here, the functions $(x(\zeta), y(\zeta))$ can thus be seen as defining such a spectral curve.

In particular, observe that we have a closed system for the values $q = 0, 1$. Indeed, by eliminating W_0, we get the equation

$$K(x,w)W_1(x,w) = R(x,w) \tag{9.3.6}$$

where

$$K(x,w) = w - wA_0(w) - xY(x), \quad R(x,w) = Y(x)^2 - x^2Y(x) - xwA_0(w). \tag{9.3.7}$$

We recognize a functional equation with one catalytic variable (x), which is amenable to the kernel method.

Before proceeding, it is convenient to use the spectral curve presented in the previous section, by performing a change of variables $x \to \zeta$. By a slight abuse of notation we write $W_1(\zeta, w)$ instead of $W_1(x(\zeta), w)$, and similarly for K and R:

$$K(\zeta,w) = w - wA_0(w) - x(\zeta)y(\zeta), \quad R(\zeta,w) = y(\zeta)^2 - x(\zeta)^2y(\zeta) - x(\zeta)wA_0(w). \tag{9.3.8}$$

Let us assume that there exists a Laurent series $\omega(\zeta)$ such that the substitution $w \to \omega(\zeta)$ is well-defined in the series A_0 and W_1, and such that $K(\zeta, \omega(\zeta)) = 0$. Then, it follows from (9.3.6) that $R(\zeta, \omega(\zeta)) = 0$. By (9.3.8), we deduce a system of equations for $\omega(\zeta)$ and $A_0(\omega(\zeta))$, which is immediately solved with the result

$$\omega(\zeta) = \frac{y(\zeta)^2}{x(\zeta)} = \frac{V^2(\zeta^3+1)^2}{V\zeta^3+1}, \quad A_0(\omega(\zeta)) = 1 - \frac{x(\zeta)^2}{y(\zeta)} = 1 - \frac{(V\zeta^3+1)^2}{\zeta^3(V^2\zeta^3+1)}. \tag{9.3.9}$$

Note that $\omega(\zeta) = V\zeta^3 + o(1)$ for $\zeta \to \infty$, which shows that the substitution $w \to \omega(\zeta)$ is indeed well-defined. We recognize a rational parametrization for the series A_0. We also see that we can simplify expressions by working with the parameter $s = \zeta^3$, which yields:

Theorem 9.3.2. *The generating function $A_0(w)$ for Eulerian triangulations with an alternating boundary admits the rational parametrization $A_0(w(s)) = a_0(s)$, where*

$$w(s) = \frac{(V^2s+1)^2}{Vs+1}, \quad a_0(s) = \frac{(1-2V)s-1}{s(V^2s+1)}. \tag{9.3.10}$$

As was the case for $x(\zeta)$, $w(s)$ admits locally around $s = \infty$ a unique inverse $s(w)$, which has the Laurent series expansion

$$s(w) = \frac{w}{V^3} + \frac{V-2}{V^2} - \frac{(V-1)^2}{Vw} + \dots \tag{9.3.11}$$

This yields

$$A_0(w) = \frac{V-2V^2}{w} + \frac{V^2(1-3V+V^2)}{w^2} + \frac{V^3(2-8V+7V^2-2V^3)}{w^3} + \dots \tag{9.3.12}$$

Note that the leading term is equal to t/w, as it should be. The next term yields $F_{0,0,1} = F_{1,1,0} = V^2(1-3V+V^2) = F_3 + t^2$, which is consistent.

Remark. Traditionally, in the kernel method, one attempts to solve the equation $K(z,w) = 0$ for the catalytic variable (here ζ) in terms of the other variable (w). Here, it works more directly by solving in the other way since K and R are just affine functions of w and $wA_0(w)$.

9.3.2 Conversions in the parametrization

Let $A(u,z)$ be the generating function of planar Eulerian triangulations with a **general** alternating boundary, with a weight u per **vertex** and a weight z per pair of edges on

the boundary. From the preceding results, we get immediately the following rational parametrization of A:

$$\begin{cases} u = V - 2V^2 \\ A = \frac{V(1+W)(1-2V-V^2W)}{1+VW} \\ z = \frac{W(1+VW)}{V(1+W)^2}. \end{cases}$$

(Here we have made the additional change of variables $W = 1/sV^2$.)

Let $F(t, z)$ be the generating function for Eulerian triangulations with a general alternating boundary, but with t counting the number of black triangles. We can get a system of equations between the number of vertices v, the number of black triangles b and the boundary length $2p$, by combining Euler's formula and a double counting of the total number of edges e:

$$\begin{cases} v - e + 2b + 1 = 2 \\ 2e = 6b + 2p, \end{cases}$$

which yields:

$$v = b + p + 1.$$

Therefore, if the function $T(t, z)$ enumerates the same triangulations, but with now a weight t per **black triangle**, we have

$$T(t, z) = \frac{A(t, z/t)}{t},$$

so that T satisfies the new system:

$$\begin{cases} t = V - 2V^2 \\ T = \frac{V(1+W)(1-2V-V^2W)}{1+VW} \cdot \left(V - 2V^2\right)^{-1} = \frac{(1+W)(1-2V-V^2W)}{(1+VW)(1-2V)} \\ z = \frac{W(1+VW)}{V(1+W)^2} \cdot \left(V - 2V^2\right)^{-1} = \frac{W(1-2V-V^2W)^2}{(1+VW)(1-2V)}. \end{cases}$$

Let us finally get to $B(t, z)$, the generating function of planar Eulerian triangulations with a **semi-simple** boundary.

Considering that a triangulation with a general boundary can be decomposed into a semi-simple "core" (which is the semi-simple component containing the root) and general components attached to every other vertex on the boundary, we have the following relation between T and B:

$$T(t, z) = B(t, zT(t, z)).$$

This implies that B admits the parametrization:

$$\begin{cases} t = V - 2V^2 \\ B = \frac{(1+W)(1-2V-V^2W)}{(1+VW)(1-2V)} \\ z = \frac{W(1-2V-V^2W)}{1+W}. \end{cases} \tag{9.3.13}$$

9.3.3 Asymptotics

The parametrization obtained in the preceding subsection yields the following asymptotics:

Theorem 9.3.3. *We have*

$$[t^n]B(t, z) = \sum_{p \geq 0} B_{n,p} z^p \underset{n \to \infty}{\sim} 32 \frac{z}{\sqrt{\pi(z-1)(4z-1)^3}} 8^n n^{-5/2} \quad \forall\, z \in [0, \frac{1}{4}). \tag{9.3.14}$$

This implies the following results:

$$B_{n,p} \underset{n\to\infty}{\sim} C(p)8^n n^{-5/2} \quad \forall\, p, \tag{9.3.15}$$

with

$$C(p) \underset{p\to\infty}{\sim} \frac{\sqrt{3}}{2\pi} 4^p \sqrt{p}. \tag{9.3.16}$$

Proof. From (9.3.13), we obtain that B must satisfy:

$$\begin{aligned} &16t^3(z-1)^2B^4 - 32t^2(z-1)^2(t+z)B^3 \\ &+ t(z-1)(24t^2z + 32tz^2 + 16z^3 - 16t^2 - 52tz - 16z^2 - z)B^2 \\ &- z(z-1)(8t^2 - 20t - 1)(t+z)B + z^2(t+1)^3 = 0. \end{aligned}$$

This equation on B has 4 solutions, among which three have some negative coefficients, so that we identify the last one as B. By definition, it is algebraic in t. Moreover, the relation $t = V - 2V^2$ is easily inverted into $V = (1 - \sqrt{1-8t})/4$, so that B has a unique singularity in t, at $t = 1/8$.

We then use the transfer theorem (see Theorem VI.3 in [FS09]) to obtain (9.3.14), which immediately yields (9.3.15).

Then, as the function of z appearing in (9.3.14) is algebraic and has a unique dominant singularity at $z = 1/4$, we can apply the transfer theorem once again to get (9.3.16).

All these computations are available in the companion Maple file. □

In particular, for any $p \geq 1$, the sum $Z(p) = \sum_n B_{n,p} 8^{-n}$ is finite, which makes it possible to define the **Boltzmann distribution** on Eulerian triangulations of the p-gon (with a semi-simple alternating boundary), that assigns a weight $8^{-n}/Z(p)$ to each such triangulation having n black triangles. For application purposes, we also derive exact and asymptotic results on the Boltzmann partition function Z:

Proposition 9.3.4. *The partition function Z of Boltzmann Eulerian triangulations with a semi-simple alternating boundary has the following behavior:*

$$\sum_{p\geq 0} Z(p) z^p = \frac{1}{2} \frac{1 + 7z - 8z^2 + \sqrt{(z-1)(4z-1)^3}}{1-z}, \qquad \forall\, z \in [0, \frac{1}{4}) \tag{9.3.17}$$

$$Z(p) \underset{p\to\infty}{\sim} \frac{1}{4}\sqrt{\frac{3}{\pi}} 4^p p^{-5/2} \text{ and } Z(0) = 1. \tag{9.3.18}$$

9.4 Monochromatic then alternating boundaries

The Tutte equation of the previous section also allows us to compute the bivariate generating function of Eulerian triangulations with a "monochromatic then alternating" boundary, namely a boundary of the form $\bullet^p(\bullet\circ)^r$ for some p and r. If we take only positive values of r, then it is given by $W_1(x, w)$, while, if we also include the "trivial" contribution from the case $r = 0$, it is given by $W_0(x, w)$, from the convention of (9.3.2).

By (9.3.6) we readily find

$$W_1(x, w) = \frac{R(x, w)}{K(x, w)}. \tag{9.4.1}$$

Using the rational parametrizations $x(\zeta)$ and $w(s)$, we get

$$W_1(\zeta, s) = \frac{(V - 3V^2 + V^3)s\zeta^3 - V(s + \zeta^3) - 1}{\zeta^2(Vs+1)(V^3 s\zeta^3 - 1)} \tag{9.4.2}$$

and, by (9.3.5),

$$W_0(\zeta, s) = \frac{(V^2 - 2V^2)s\zeta^3 - V^2(s + \zeta^3) - 1}{\zeta(V^2 s + 1)(V^3 s\zeta^3 - 1)}. \tag{9.4.3}$$

For later use, we also compute the series W_2 corresponding to boundaries of the form $\bullet^p \circ^2 (\bullet\circ)^r$. We simply use (9.3.4) and the expression

$$B_1(s) = \lim_{\zeta\to\infty} W_1(\zeta, s)x(\zeta)^2 = \frac{(1 - 3V + V^2)s - 1}{s(Vs + 1)} \tag{9.4.4}$$

(which is consistent with the relation $A_0 = (t + B_1)/w$) to get

$$W_2(\zeta, s) = y(\zeta)W_1(\zeta, s) - B_1(s) = \frac{(1 - 3V)s\zeta^3 - s - \zeta^3}{s\zeta^4(V^3 s\zeta^3 - 1)}. \tag{9.4.5}$$

9.5 Alternating boundary with defects

9.5.1 Recursion

We are now interested in enumerating planar Eulerian triangulations with an **alternating boundary with defects of size 1**, that is, a boundary on which the colors alternate save for two instances. As was the case for the strictly alternating case, in order to obtain a recursion equation, we need to to consider a broader family of maps: namely, planar Eulerian triangulations with a (general) boundary of the form $\bullet^{p+1}(\circ\bullet)^{r_1} \circ^{q+1} (\bullet\circ)^{r_2}$. We claim that the corresponding generating function $G_{p,r_1,q,r_2} = G_{p,r_1,q,r_2}(t)$ (with a weight t per vertex) is symmetric in p and q as well as in r_1 and r_2. Indeed, the counting problem does not change if we perform a cyclic rotation, a reflection or a color switch on the boundary type. Permuting r_1 and r_2 is simply done by a reflection, and permuting p and q by a reflection and a color switch.

We then define the series

$$P_q(x, w_1, w_2) := \sum_{p,r_1,r_2\geq 0} \frac{G_{p,r_1,q,r_2}}{x^{p+1} w_1^{r_1+1} w_2^{r_2+1}}$$

and

$$E_{p,q}(w_1, w_2) := \sum_{r_1,r_2\geq 0} \frac{G_{p,r_1,q,r_2}}{w_1^{r_1+1} w_2^{r_2+1}}.$$

As explained above, these functions should be symmetric in w_1 and w_2, and furthermore $E_{p,q} = E_{q,p}$ vanishes unless $p \equiv q \pmod 3$. Our purpose is to compute $E_{1,1}$ (note that $E_{0,0}$ corresponds to pure alternating boundaries with two markings).

We have $G_{p,0,q,r_2} = F_{p+1,q+1,r_2}$, hence the coefficient of $1/w_1$ in P_q reads

$$\begin{aligned}\lim_{w_1\to\infty} w_1 P_q(x, w_1, w_2) &= \sum_{r_2\geq 0} \left(\sum_{p\geq 0} \left(\frac{F_{p,q+1,r_2}}{x^p w_2^{r_2+1}} \right) - \frac{F_{0,q+1,r_2}}{x^0 w_2^{r_2+1}} \right) \\ &= xW_{q+1}(x, w_2) - A_{q+1}(w_2).\end{aligned}$$

For $r_1 \geq 1$ and q not a multiple of 3, if we perform a peeling on the leftmost white edge, we get

$$G_{p,r_1,q,r_2} = G_{p+3,r_1-1,q,r_2} + \sum_{p'=0}^{p} F_{p'} G_{p-p',r_1-1,q,r_2} + \sum_{r'=0}^{r_1-1} F_{0,0,r'} G_{p,r_1-1-r',q,r_2}.$$

Here, the first term corresponds to the case where we discover a new triangle, the second term (the sum over p') to the case where the white edge is matched with one of the $p+1$ black edges on its left, and the third term (the sum over r') to the case where the white edge is matched with one of the black edges on its right, which is necessarily in the first alternating block (it cannot be in the second block by parity constraints - this would be possible for q a multiple of 3).

We deduce that, if $q' = 1, 2$ is the remainder of the Euclidean division of q by 3,

$$\begin{aligned} &P_q(x, w_1, w_2) - \frac{xW_{q+1}(x, w_2) - A_{q+1}(w_2)}{w_1} \\ &= \frac{xY(x)}{w_1} P_q(x, w_1, w_2) - \frac{x^{2-q'}}{w_1} E_{q',q}(w_1, w_2) + A_0(w_1) P_q(x, w_1, w_2). \end{aligned}$$

Note that we once again have a recursion driven by the spectral curve Y.

We can rewrite this equation as

$$K(x, w_1) P_q(x, w_1, w_2) = R_q(x, w_1, w_2) \tag{9.5.1}$$

where K is the same kernel as in (9.3.8), and

$$R_q(x, w_1, w_2) = xW_{q+1}(x, w_2) - A_{q+1}(w_2) - x^{2-q'} E_{q',q}(w_1, w_2).$$

We now go to the rational parametrizaton $x = x(\zeta), w_1 = w(s_1), w_2 = w(s_2)$, with $w(s)$ as in Theorem 9.3.2. As in Section 9.3, if we take $s_1 = \zeta^3$, then $K(\zeta, s_1)$ vanishes, so we deduce from (9.5.1) that $R_q(\zeta, \zeta^3, s_2)$ vanishes as well. Noting that A_{q+1} vanishes if $q' = 1$, we hence get

$$E_{q',q}(\zeta^3, s_2) = W_{q+1}(\zeta, s_2) \quad \text{if } q' = 1.$$

For $q = q' = 1$, we thus obtain the expression

$$E_{1,1}(s_1, s_2) = \frac{(1 - 3V)s_1 s_2 - s_1 - s_2}{s_1 s_2 (V^3 s_1 s_2 - 1)}.$$

Note that this expression is symmetric in s_1 and s_2, as it should be.

9.5.2 Simplicity conditions

While having a very symmetric definition of the parameters describing an alternating boundary with defects was convenient for deriving equations on generating functions, for our applications in Chapter 8, it is more convenient to switch to a different convention, with "upper" and "lower" parts in the boundary, that do not play exactly the same role, as depicted in Figure 9.5.1.

For our applications, we consider two different types of simplicity conditions: either **semi-simple non-chaining**, or **semi-simple chaining**. Each of these can be defined by the allowed identifications of boundary vertices, starting from the layout given in Figure 9.5.1: those allowed identifications are given in Figure 9.5.2 and Figure 9.5.3 respectively. They both have semi-simple conditions on their upper and lower boundary parts separately (up to a switch between black and white), but identifications between top and bottom boundary vertices are only allowed in the chaining case, so that an Eulerian triangulation with chaining boundary conditions are a "chain" of Eulerian triangulations with defects, hence the name.

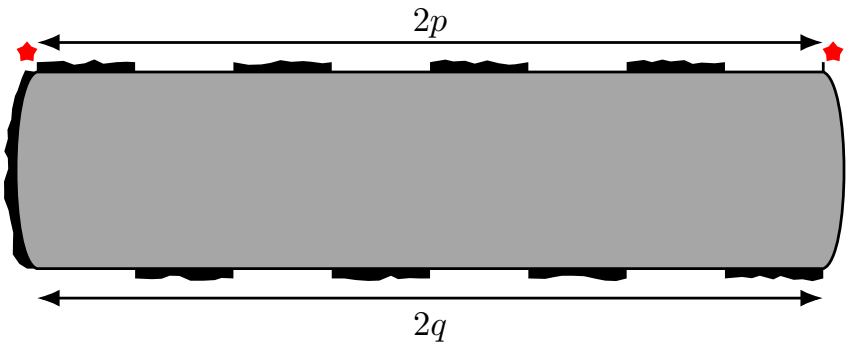

Figure 9.5.1 – General layout of a boundary with two defects of size 1, marked by red stars.

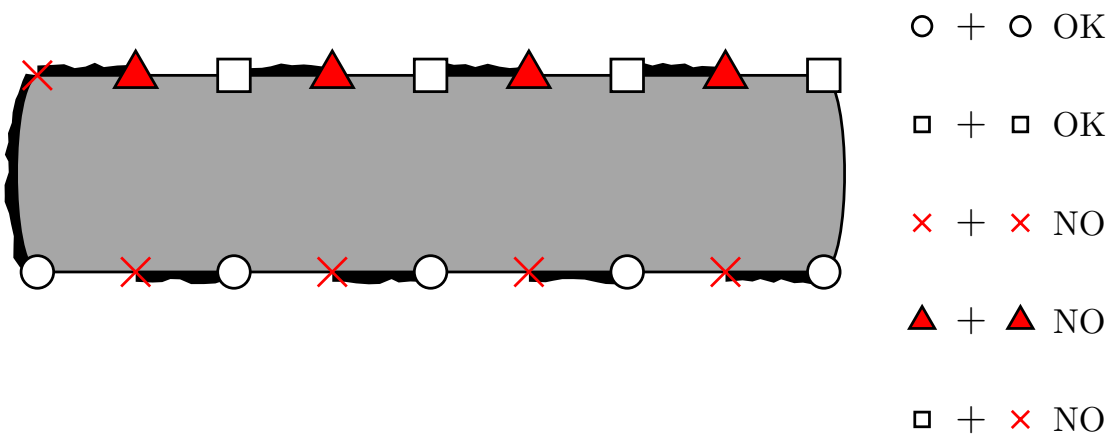

Figure 9.5.2 – Semi-simple non-chaining boundary conditions. The prohibition of the "square-cross" identifications means that we have no chaining configurations here.

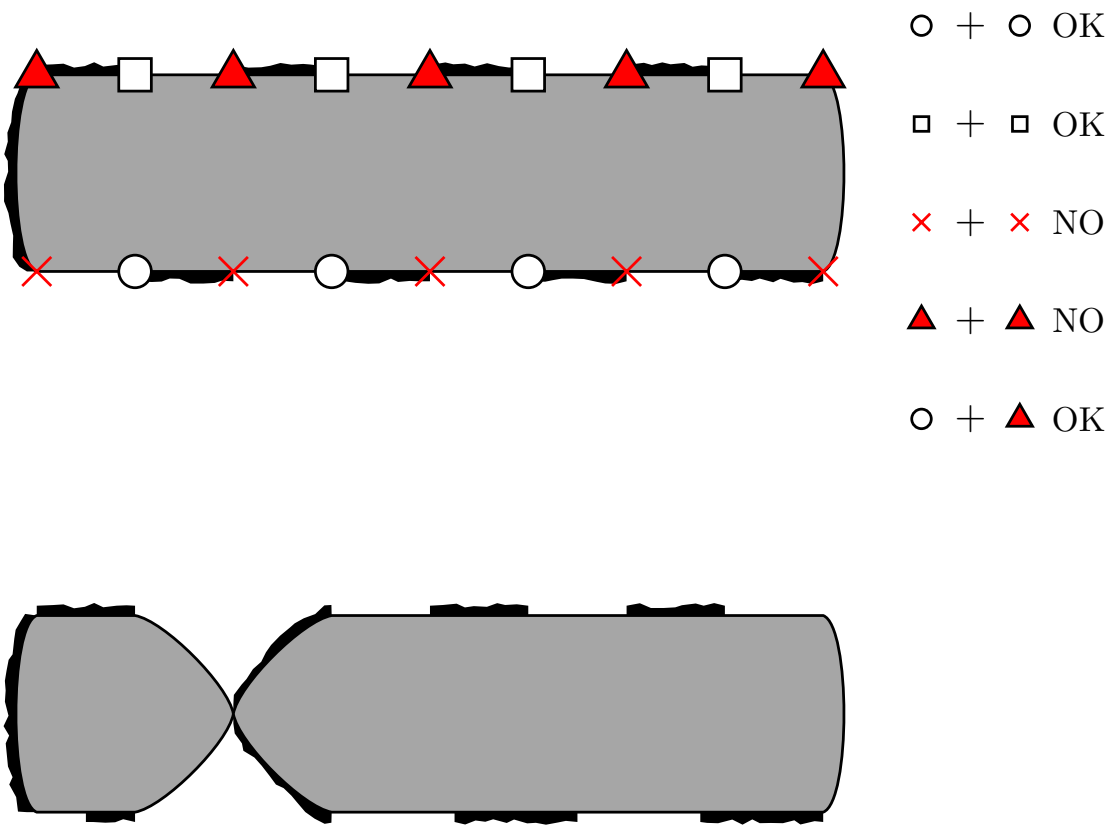

Figure 9.5.3 – Semi-simple chaining boundary conditions, and an example of a chaining configuration, corresponding to a “circle-triangle” identification.

Let us introduce a bit of notation: the generating functions for these non-chaining and chaining Eulerian triangulations are respectively

$$B^{(1)}(t,y,z) = \sum_{n,p,q\geq 0} B^{(1)}_{n,p,q} t^n y^p z^q$$

and

$$B^{(1,c)}(t,y,z) = \sum_{n,p,q\geq 0} B^{(1,c)}_{n,p,q} t^n y^p z^q$$

where t enumerates the number of black triangles, y the half-length of the upper boundary, and z the half-length of the lower boundary.

9.5.3 Conversions in the parametrization

We have now obtained a rational parametrization of $A^{(1)}(u,y,z)$, the generating series of planar Eulerian triangulations with a **general** alternating boundary with defects of size 1, with u counting the number of **vertices**:

$$\begin{cases} u = V - 2V^2 \\ A^{(1)} = \frac{(V^2 s_2+1)^2}{V s_2+1}\left[\frac{(1-3V)s_1 s_2 - s_1 - s_2}{s_1 s_2 (V^3 s_1 s_2 - 1)} + \frac{(V^2 s_2+1)^2}{V s_2+1}\cdot\frac{(1-2V)s_2 - 1}{s_2(V^2 s_2+1)} - (V-2V^2)\right] \\ y = \frac{V s_1+1}{(V^2 s_1+1)^2} \\ z = \frac{V s_2+1}{(V^2 s_2+1)^2}. \end{cases}$$

Now, by replacing s_i with the variable $W_i = 1/(s_i V^2)$, we obtain:

$$\begin{cases} u = V - 2V^2 \\ A^{(1)} = \frac{(1+W_2)^2 V^2 (V^3 W_2 W_1 + (W_1+W_2-1)V^2 + 3V - 1)(1+W_1)}{(VW_2+1)^2 (VW_1W_2 - 1)} \\ y = \frac{W_1(1+VW_1)}{V(1+W_1)^2} \\ z = \frac{W(1+VW_2)}{V(1+W_2)^2}. \end{cases}$$

We will not write down the parametrizations for the other generating functions, as they get quite cumbersome; they can be found in the companion Maple file. We will just detail here the relations between the different generating functions, that yield their successive parametrizations.

As before, if $F^{(1)}(t,y,z)$ counts the same maps as $A^{(1)}$, but with t accounting for the black faces, then:

$$F^{(1)}_{n,p,q} = A^{(1)}_{n+p+q+2,p,q}$$

or in other words:

$$F^{(1)}(t,y,z) = \frac{A^{(1)}(t, y/t, z/t)}{t^2}.$$

Then, $F^{(1)}$ can be expressed in terms of $B^{(1)}$ by the following relation:

$$F^{(1)}(t,y,z) = B^{(1)}(t, yF(t,y), zF(t,z)).$$

As for $B^{(1,c)}$, note that a chaining Eulerian triangulation with defects is precisely made of a chain of non-chaining triangulations with defects, so that:

$$B^{(1,c)}(t,y,z) = \frac{B^{(1)}(t,y,z)/B(t,z)}{1 - zB^{(1)}(t,y,z)/B(t,z)}.$$

9.5.4 Asymptotics

We are interested in the asymptotic behavior of $B^{(1)}_{n,p,q}$ and $B^{(1,c)}_{n,p,q}$ as $n \to \infty$, then $q \to \infty$. As the systems that characterize them are more complicated than the one for B, we confine ourselves to local results around the singularities in t, y and z:

Theorem 9.5.1. *The coefficients of the generating function $B^{(1)}$ have the following asymptotic behavior:*

$$B^{(1)}_{n,p,q} \underset{n\to\infty}{\sim} D(p,q)8^n n^{-5/2} \quad \forall\, p, q, \tag{9.5.2}$$

with

$$D(p,q) \underset{q\to\infty}{\sim} E(p)4^q\sqrt{q} \quad \forall\, p \tag{9.5.3}$$

and

$$E(p) \underset{p\to\infty}{\sim} \frac{9\sqrt{6}}{4\pi}4^p. \tag{9.5.4}$$

Similarly, for $B^{(1,c)}$,

$$B^{(1,c)}_{n,p,q} \underset{n\to\infty}{\sim} D_c(p,q)8^n n^{-5/2} \quad \forall\, p, q \tag{9.5.5}$$

with

$$D_c(p,q) \underset{q\to\infty}{\sim} E_c(p)4^q\sqrt{q} \quad \forall\, p \tag{9.5.6}$$

$$E_c(p) \underset{p\to\infty}{\sim} \frac{144\sqrt{6}}{49\pi}4^p. \tag{9.5.7}$$

Proof. To simplify notation, we only explain the steps of the calculations concerning $B^{(1)}$, as those for $B^{(1,c)}$ are very similar. All these calculations can be found in the companion Maple file.

As, once again, $B^{(1)}$ has a unique singularity in t, at $t = t_c = 1/8$, we start by applying the transfer theorem for the variable t (keeping y, z fixed, and not W_1, W_2), which yields (9.5.2). We then check that, near t_c, $B^{(1)}$ has a unique dominant singularity in z, which corresponds to its unique dominant singularity in W_2. We can then apply the transfer theorem for z, which yields (9.5.3), and then proceed similarly for y. □

Note that these asymptotics are very similar to the strictly alternating case, which means that we can see the introduction of these defects as a "small perturbation" for enumerative properties, when both parts of the boundary are large.

Like in the strictly alternating case, the asymptotic in n implies that we can define "Boltzmann" coefficients

$$\widetilde{Z}(p,q) = \sum_n \frac{1}{8^n} B^{(1)}_{n,p,q} \quad \text{and} \quad \widetilde{Z}_c(p,q) = \sum_n \frac{1}{8^n} B^{(1,c)}_{n,p,q}.$$

Note that these coefficients are now bivariate.

We also investigate some asymptotic behavior of these new Boltzmann coefficients, which are also useful in the study of large planar Eulerian triangulations:

Proposition 9.5.2. *The coefficients $\widetilde{Z}$ have the following properties:*

$$\frac{1}{4^p}\sum_q \widetilde{Z}(p,q)\left(\frac{1}{4}\right)^q \underset{p\to\infty}{\sim} \frac{9\sqrt{3}}{8\sqrt{\pi}p^{3/2}} \tag{9.5.8}$$

$$\frac{1}{4^q}\sum_p \widetilde{Z}(p,q)\left(\frac{1}{4}\right)^p \underset{q\to\infty}{\sim} \frac{9\sqrt{3}}{8\sqrt{\pi}q^{3/2}} \tag{9.5.9}$$

$$\sum_{p,q} \widetilde{Z}(p,q)\left(\frac{1}{4}\right)^p\left(\frac{1}{4}\right)^q = \frac{27}{8}. \tag{9.5.10}$$

The same results (down to the multiplicative constants) hold for the coefficients $\widetilde{Z}_c$.

Bibliography

[AB12] M. Albenque and J. Bouttier. "Constellations and multicontinued fractions: application to Eulerian triangulations". In: *24th International Conference on Formal Power Series and Algebraic Combinatorics (FPSAC 2012)*. Discrete Math. Theor. Comput. Sci. Proc., AR. Assoc. Discrete Math. Theor. Comput. Sci., Nancy, 2012, pp. 805–816.

[AB16] J. Ambjørn and T. Budd. "Multi-point functions of weighted cubic maps". In: *Ann. Inst. H. Poincaré D* 3.1 (2016), pp. 1–44.

[ABA] L. Addario-Berry and M. Albenque. *Convergence of odd-angulations via symmetrization of labeled trees*. arXiv: `1904.04786 [math.PR]`.

[ABA17] L. Addario-Berry and M. Albenque. "The scaling limit of random simple triangulations and random simple quadrangulations". In: *Ann. Probab.* 45.5 (2017), pp. 2767–2825.

[ABACFG] L. Addario-Berry, O. Angel, G. Chapuy, Éric Fusy, and C. Goldschmidt. "Voronoi tessellations in the CRT and continuum random maps of finite excess". In: *Proceedings of the Twenty-Ninth Annual ACM-SIAM Symposium on Discrete Algorithms*, pp. 933–946.

[Abr16] C. Abraham. "Rescaled bipartite planar maps converge to the Brownian map". In: *Ann. Inst. Henri Poincaré Probab. Stat.* 52.2 (2016), pp. 575–595.

[ABT03] R. Arratia, A. D. Barbour, and S. Tavaré. *Logarithmic Combinatorial Structures: A Probabilistic Approach*. EMS Monographs in Mathematics. European Mathematical Society, 2003.

[ACCR13] O. Angel, G. Chapuy, N. Curien, and G. Ray. "The local limit of unicellular maps in high genus". In: *Electron. Commun. Probab.* 18.86 (2013).

[AGJL14] J. Ambjørn, A. Görlich, J. Jurkiewicz, and R. Loll. "Quantum gravity via causal dynamical triangulations". In: *Springer handbook of spacetime*. Springer, Dordrecht, 2014, pp. 723–741.

[AMS] M. Albenque, L. Ménard, and G. Schaeffer. *Local convergence of large random triangulations coupled with an Ising model*. arXiv: `1812.03140 [math.CO]`.

[Ang03] O. Angel. "Growth and percolation on the uniform infinite planar triangulation". In: *Geom. Funct. Anal.* 13 (2003), 935–974.

[BBS07] K. Becker, M. Becker, and J. Schwarz. *String Theory and M-theory: A Modern Introduction*. Cambridge University Press, 2007.

[BCP] T. Budzinski, N. Curien, and B. Petri. *Universality for random surfaces in unconstrained genus*. arXiv: 1902.01308 [math.PR].

[BDFG03] J. Bouttier, P. Di Francesco, and E. Guitter. "Statistics of planar graphs viewed from a vertex: a study via labeled trees". In: *Nuclear Physics B* 675.3 (2003), pp. 631 –660.

[BDFG04] J. Bouttier, P. Di Francesco, and E. Guitter. "Planar Maps as Labeled Mobiles". In: *Electr. J. Combin.* 11.1 (2004).

[BDR15] V. Bonzom, T. Delepouve, and V. Rivasseau. "Enhancing non-melonic triangulations: A tensor model mixing melonic and planar maps". In: *Nuclear Phys. B* 895 (2015), pp. 161–191.

[BGH] D. Benedetti, R. Gurau, and S. Harribey. *Line of fixed points in a bosonic tensor model*. arXiv: 1903.03578 [hep-th].

[BGR12] V. Bonzom, R. Gurau, and V. Rivasseau. "Random tensor models in the large N limit: Uncoloring the colored tensor models". In: *Phys Rev D* 85 (2012), p. 084037.

[BGRR11] V. Bonzom, R. Gurau, A. Riello, and V. Rivasseau. "Critical behavior of colored tensor models in the large N limit". In: *Nuclear Physics B* 853 (2011), 174–195.

[BHS] O. Bernardi, N. Holden, and X. Sun. *Percolation on triangulations: a bijective path to Liouville quantum gravity*. arXiv: 1807.01684 [math.PR].

[Bil99] P. Billingsley. *Convergence of probability measures*. Second. Wiley Series in Probability and Statistics: Probability and Statistics. John Wiley & Sons, Inc., New York, 1999.

[BJM14] J. Bettinelli, E. Jacob, and G. Miermont. "The scaling limit of uniform random plane maps, *via* the Ambjørn-Budd bijection". In: *Electron. J. Probab.* 19 (2014), no. 74, 16.

[BL17] V. Bonzom and L. Lionni. "Counting Gluings of Octahedra". In: *Elec. J. Combin.* 24.3 (2017), p. 3.36.

[Bla53] D. Blackwell. "Extension of a renewal theorem". In: *Pacific J. Math.* 3 (1953), pp. 315–320.

[BM17] J. Bettinelli and G. Miermont. "Compact Brownian surfaces I: Brownian disks". In: *Probab. Theory Related Fields* 167.3-4 (2017), pp. 555–614.

[BMS00] M. Bousquet-Mélou and G. Schaeffer. "Enumeration of planar constellations". In: *Adv. in Appl. Math.* 24.4 (2000), pp. 337–368.

[Bon] V. Bonzom. *Maximizing the number of edges in three-dimensional colored triangulations whose building blocks are balls*. arXiv: 1802.06419 [math.CO].

[Bud16] T. Budd. "The peeling process of infinite Boltzmann planar maps". In: *Electron. J. Combin.* 23.1 (2016), Paper 1.28, 37.

[Bud18] T. Budzinski. "The hyperbolic Brownian plane". In: *Probab. Theory Related Fields* 171.1-2 (2018), pp. 503–541.

[Car19] A. Carrance. "Uniform random colored complexes". In: *Random Structures & Algorithms* 55.3 (2019), pp. 615–648.

[CC15] M. Casali and P. Cristofori. "Cataloguing PL 4-manifolds by gem-complexity". In: *Electron. J. Combin.* 22.4 (2015).

[CF04] C. Cooper and A. Frieze. "The size of the largest strongly connected component of a random digraph with a given degree sequence". In: *Combin. Probab. Comput.* 13 (2004), 319–337.

[CF16] A. Costa and M. Farber. "Random Simplicial Complexes". In: *Configuration Spaces: Geometry, Topology and Representation Theory*. Ed. by F. Callegaro, F. Cohen, C. De Concini, E. M. Feichtner, G. Gaiffi, and M. Salvetti. Springer International Publishing, 2016, pp. 129–153.

[CGP80] A. Cavicchioli, L. Grasseli, and M. Pezzana. "Su una decomposizione normale per le n-varietá chiuse". In: *Boll. Un. Mat. Ital.* 17-B (1980), pp. 1146–1165.

[CHN] N. Curien, T. Hutchcroft, and A. Nachmias. *Geometric and spectral properties of causal maps*. arXiv: `1710.03137 [math.PR]`.

[CLG14] N. Curien and J.-F. Le Gall. "The Brownian plane". In: *J. Theoret. Probab.* 27.4 (2014), pp. 1249–1291.

[CLG17] N. Curien and J.-F. Le Gall. "Scaling limits for the peeling process on random maps". In: *Ann. Inst. Henri Poincaré Probab. Stat.* 53.1 (2017), pp. 322–357.

[CLG19] N. Curien and J.-F. Le Gall. "First-passage percolation and local modifications of distances in random triangulations". In: *Ann. Sci. ENS* , in press (2019).

[CM15] P. Cristofori and M. Mulazzani. "Compact 3-manifolds via 4-colored graphs". In: *RACSAM* (2015), pp. 1–22.

[CP16] S. Chmutov and B. Pittel. "On a surface formed by randomly gluing together polygonal discs". In: *Advances in Applied Mathematics* 73 (2016), pp. 23–42.

[CS04] P. Chassaing and G. Schaeffer. "Random planar lattices and integrated superBrownian excursion". In: *Probab. Theory Related Fields* 128.2 (2004), pp. 161–212.

[CT] L. Chen and J. Turunen. *Critical Ising model on random triangulations of the disk: enumeration and local limits*. arXiv: `1806.06668 [math.PR]`.

[CV81] R. Cori and B. Vauquelin. "Planar maps are well labeled trees". In: *Canad. J. Math.* 33 (1981), pp. 1023–1042.

[Des00] S. Deser. "Infinities in quantum gravities". In: *Ann. Phys.* 9.3-5 (2000), pp. 299–306.

[DGR13] S. Dartois, R. Gurau, and V. Rivasseau. "Double Scaling in Tensor Models with a Quartic Interaction". In: *J. High Energ. Phys.* 2013.88 (Aug. 22, 2013).

[DGR14] T. Delepouve, R. Gurau, and V. Rivasseau. "Universality and Borel Summability of Arbitrary Quartic Tensor Models". In: *Ann. Inst. H. Poincaré Probab. Statist.* 52.2 (Mar. 2014), pp. 821–848.

[DKRV] F. David, A. Kupiainen, R. Rhodes, and V. Vargas. *Liouville Quantum Gravity on the Riemann sphere*. arXiv: `1410.7318 [math.PR]`.

[DR] N. Delporte and V. Rivasseau. *The Tensor Track V: Holographic Tensors*. arXiv: `1804.11101 [hep-th]`.

[DR16] T. Delepouve and V. Rivasseau. "Constructive Tensor Field Theory: the T^4_3 Model". In: *Communications in Mathematical Physics* 345.2 (2016), pp. 477–506.

[DS] B. Duplantier and S. Sheffield. *Liouville Quantum Gravity and KPZ*. arXiv: `0808.1560 [math.PR]`.

[Eyn16] B. Eynard. *Counting surfaces*. Vol. 70. Progress in Mathematical Physics. CRM Aisenstadt chair lectures. Birkhäuser/Springer, [Cham], 2016.

[FG82] M. Ferri and C. Gagliardi. "The Only Genus Zero n-Manifold is S^n". In: *Proc. AMS* 85 (1982), pp. 638–642.

[FGG86] M. Ferri, C. Gagliardi, and L. Grasselli. "A graph-theoretical representation of PL-manifolds—a survey on crystallizations." In: *Aequationes Math.* 31 (1986), 121–141.

[FGZJ95] P. Francesco, P. Ginsparg, and J. Zinn-Justin. "2D gravity and random matrices". In: *Physics Reports* 254.1 (1995), pp. 1 –133.

[FH17] L. Federico and R. van der Hofstad. "Critical window for connectivity in the configuration model." In: *Combin. Probab. Comput.* 26.5 (2017), pp. 660–680.

[FS09] P. Flajolet and R. Sedgewick. *Analytic combinatorics*. Cambridge University Press, Cambridge, 2009.

[Gag79] C. Gagliardi. "Extending the concept of genus to dimension N". In: *Proc. AMS* 81.3 (1979), pp. 473–481.

[Gag81] C. Gagliardi. "Regular imbeddings of edge-coloured graphs". In: *Geometriae Dedicata* 11 (1981), pp. 397–414.

[Gam06] A. Gamburd. "Poisson-Dirichlet Distribution for random Belyi surfaces". In: *The Ann. Probability* 34 (2006), 1827–1848.

[GHPR] E. Gwynne, N. Holden, J. Pfeffer, and G. Remy. *Liouville quantum gravity with central charge in (1,25): a probabilistic approach*. arXiv: `1903.09111 [math.PR]`.

[GHS] C. Garban, N. Holden, and X. Sepulveda A. Sun. *Liouville dynamical percolation*. arXiv: `1905.06940 [math.PR]`.

[GKMW18] E. Gwynne, A. Kassel, J. Miller, and D. Wilson. "Active Spanning Trees with Bending Energy on Planar Maps and SLE-Decorated Liouville Quantum Gravity for $\kappa > 8$". In: *Communications in Mathematical Physics* 358.3 (2018), pp. 1065–1115.

[GKT17] S. Giombi, I. Klebanov, and G. Tarnopolsky. "Bosonic tensor models at large N and small ϵ". In: *Phys. Rev. D* 96 (10 2017), p. 106014.

[GR11] R. Gurau and V. Rivasseau. "The 1/N expansion of colored tensor models in arbitrary dimension". In: *EPL* 95 (2011), p. 50004.

[GR12] R. Gurau and J. Ryan. "Colored Tensor Models - a Review". In: *SIGMA* 8 (2012), p. 020.

[GR14] R. Gurau and J. Ryan. "Melons are branched polymers". In: *Ann. Henri Poincar'e* 15.11 (2014), 2085–2131.

[GR15] R. Gurau and V. Rivasseau. "The multiscale loop vertex expansion". In: *Ann. Henri Poincaré* 16.8 (2015), pp. 1869–1897.

[GRV] C. Guillarmou, R. Rhodes, and V. Vargas. *Polyakov's formulation of 2d bosonic string theory*. arXiv: `1607.08467 [math-ph]`.

[GS16] R. Gurau and G. Schaeffer. "Regular colored graphs of positive degree". In: *Annales de l'IHP D* 3 (2016), pp. 257–320.

[Gur10] R. Gurau. "Lost in translation: topological singularities in group field theory." In: *Class. Quant. Grav.* 47 (2010), p. 235023.

[Gur11a] R. Gurau. "Colored Group Field Theory". In: *Communications in Mathematical Physics* 304.1 (2011), pp. 69 –93.

[Gur11b] R. Gurau. "The 1/N Expansion of Colored Tensor Models". In: *Annales Henri Poincaré* 12.5 (2011), p. 829.

[Gur12] R. Gurau. "The Complete 1/N Expansion of Colored Tensor Models in Arbitrary Dimension". In: *Annales Henri Poincaré* 13.3 (2012), pp. 399–423.

[Gur16] R. Gurau. "Invitation to random tensors". In: *SIGMA* 12 (2016), Paper No. 094.

[Hof16] R. van der Hofstad. *Random graphs and complex networks, volume 1*. Cambridge Series in Statistical and Probabilistic Mathematics. Cambridge University Press, 2016.

[JM05] S. Janson and J.-F. Marckert. "Convergence of discrete snakes". In: *J. Theoret. Probab.* 18.3 (2005), pp. 615–647.

[Kah14] M. Kahle. "Topology of random simplicial complexes: a survey". In: *Algebraic topology: applications and new directions*. Vol. 620. Contemp. Math. Amer. Math. Soc., 2014, pp. 201–221.

[Koz08] D. Kozlov. *Combinatorial Algebraic Topology*. Springer, 2008.

[Kri] K. Krikun. *Local structure of random quadrangulations*. arXiv: `0512304 [math.PR]`.

[Kri05] M. Krikun. "Uniform Infinite Planar Triangulation and Related Time-Reversed Critical Branching Process". In: *Journal of Mathematical Sciences* 131.2 (2005), pp. 5520–5537.

[KRS] T. Krajewski, V. Rivasseau, and V. Sazonov. *Constructive Matrix Theory for Higher Order Interaction*. arXiv: `1712.05670 [hep-th]`.

[Leh] T. Lehéricy. *First-passage percolation in random planar maps and Tutte's bijection*. arXiv: `1906.10079 [math.PR]`.

[LG13] J.-F. Le Gall. "Uniqueness and universality of the Brownian map". In: *Ann. Probab.* 41 (2013), pp. 2880–2960.

[LGL] J.-F. Le Gall and T. Lehéricy. *Separating cycles and isoperimetric inequalities in the uniform infinite planar quadrangulation*. arXiv: `1710 . 02990 [math.PR]`.

[LGP08] J.-F. Le Gall and F. Paulin. "Scaling limits of bipartite planar maps are homeomorphic to the 2-sphere". In: *Geom. Funct. Anal.* 18.3 (2008), 893–918.

[LGW06] J.-F. Le Gall and M. Weill. "Conditioned Brownian trees". In: *Ann. Inst. H. Poincaré Probab. Statist* 42.4 (2006), 455–489.

[Lig85] T. Liggett. "An improved subadditive ergodic theorem". In: *Ann. Probab.* 13 (1985), pp. 1279–1285.

[Lio] L. Lionni. "Topology and distances in large random colored triangulations of positive degree". In preparation.

[LS08] M. Larsen and A. Shalev. "Characters of symmetric groups: sharp bounds and applications". In: *Invent. Math.* 174 (2008), pp. 23–42.

[LZ04] S. Lando and A. Zvonkin. *Graphs on surfaces and their applications*. Vol. 141. Encyclopaedia of Mathematical Sciences. With an appendix by Don B. Zagier, Low-Dimensional Topology, II. Springer-Verlag, Berlin, 2004.

[Map] Maple companion file, avalaible on the author's website.

[McD05] D. McDonald. "The local limit theorem: A historical perspective." In: *JIRSS* 4 (2005), pp. 73–96.

[Mie13] G. Miermont. "The Brownian map is the scaling limit of uniform random plane quadrangulations". In: *Acta Math.* 210 (2013), pp. 319–401.

[MM41] J. Mayer and E. Montroll. "Molecular distributions". In: *J. Chem. Phys* 9 (1941), 2–16.

[MS] J. Miller and S. Sheffield. *Liouville quantum gravity and the Brownian map I: The QLE(8/3,0) metric*. arXiv: `1507.00719 [math.PR]`.

[MT01] B. Mohar and C. Thomassen. *Graphs on surfaces*. Johns Hopkins Studies in the Mathematical Sciences. Johns Hopkins University Press, 2001.

[Ori09] D. Oriti. "The group field theory approach to quantum gravity". In: *Approaches to Quantum Gravity: Toward a New Understanding of Space, Time and Matter*. Ed. by D. Oriti. Cambridge University Press, 2009, pp. 310–331.

[OSVT13] D. Ousmane Samary and F. Vignes-Tourneret. "Just Renormalizable TGFT's on $U(1)^d$ with Gauge Invariance". In: *Commun. Math. Phys.* 329.2 (Oct. 26, 2013), pp. 545 –578.

[Pap68] F. Papangelou. "A lemma on the Galton-Watson process and some of its consequences". In: *Proc. Amer. Math. Soc.* 19 (1968), pp. 1469–1479.

[Pez74] M. Pezzana. "Sulla struttura topologica delle varieta compatte". In: *Atti Sem. Mat. Fis. Univ. Modena* 23 (1974), 269–277.

[Pez75] M. Pezzana. "Diagrammi di Heegaard e triangolazione contratta". In: *Boll. Un. Mat. Ital.* 12 (1975), 98–105.

[Pol81] A Polyakov. "Quantum geometry of bosonic strings". In: *Phys. Lett. B* 103.3 (1981), pp. 207–210.

[PS06] N. Pippenger and K. Schleich. "Topological Characteristics of Random Triangulated Surfaces". In: *Random Structures And Algorithms* 28 (2006), 247–288.

[Reg61] T. Regge. "General relativity without coordinates". In: *Nuovo Cim.* 19 (1961), p. 558.

[Rej16] K. Rejzner. *Perturbative algebraic quantum field theory*. Mathematical Physics Studies. Springer, Cham, 2016.

[Rib] S. Ribault. *Conformal field theory on the plane*. arXiv: `1406.4290 [hep-th]`.

[Rov11] C. Rovelli. "Loop quantum gravity: the first 25 years". In: *Class Quant Grav* 28.15 (2011), p. 153002.

[RVT19] V. Rivasseau and F. Vignes-Tourneret. "Constructive Tensor Field Theory: The T_4^4 Model". In: *Comm. Math. Phys.* 366.2 (2019), pp. 567–646.

[Sch98] G. Schaeffer. "Conjugaison d'arbres et cartes combinatoires aléatoires". PhD thesis. Université Bordeaux I, 1998.

[Sti93] J. Stillwell. *Classical Topology and Combinatorial Group Theory*. Springer, 1993.

[Tho99] G. Thorleifsson. "Lattice gravity and random surfaces". In: *Nuclear Physics B - Proceedings Supplements* 73.1 (1999), pp. 133 –145.

[Tut62] W. T. Tutte. "A census of slicings". In: *Canadian J. Math.* 14 (1962), pp. 708–722.

[Tut63] W. Tutte. "A census of planar maps". In: *Canad. J. Math.* 15 (1963), 249–271.

[Wat95] Y. Watabiki. “Construction of non-critical string field theory by transfer matrix formalism in dynamical triangulation”. In: *Nuclear Phys. B* 441.1-2 (1995), pp. 119–163.

[Wit] E. Witten. *An SYK-like Model Without Disorder*. arXiv: 1610.09758 [hep-th].

[Wor99] N. C. Wormald. “Models of random regular graphs”. In: *Surveys in combinatorics, 1999 (Canterbury)*. Vol. 267. London Math. Soc. Lecture Note Ser. Cambridge Univ. Press, Cambridge, 1999, pp. 239–298.

Triangulations colorées aléatoires

Résumé. L'unification de la mécanique quantique et de la relativité générale est un des grands problèmes ouverts en physique théorique. Une des approches possibles est de définir des espaces géométriques aléatoires avec des bonnes propriétés, qui peuvent être interprétés comme des espaces-temps quantiques. Cette thèse aborde des aspects mathématiques des modèles de tenseurs colorés, un type de modèle de physique théorique qui s'inscrit dans cette approche. Ces modèles décrivent des espaces linéaires par morceaux appelés trisps colorés, en toute dimension.

Au cours de cette thèse, nous avons tout d'abord étudié des modèles aléatoires uniformes sur les trisps colorés, en toute dimension. Nous prouvons que ces modèles ont une limite singulière, ce qui a aussi donné lieu à un théorème central limite sur le genre d'une grande carte aléatoire uniforme.

Nous avons ensuite étudié le cas particulier de la dimension 2, où les trisps colorés sont un type particulier de cartes, les triangulations eulériennes. Nous montrons que les triangulations eulériennes planaires convergent vers la carte brownienne, qui est un objet aléatoire continu universel en dimension 2. Ce résultat est particulièrement remarquable étant donnée la complexité de la structure des triangulations eulériennes, en comparaison avec les autres familles de cartes qui convergent vers la carte brownienne.

Mots-clés : cartes aléatoires, graphes aléatoires, permutations aléatoires, modèles de tenseurs colorés, trisps colorés, triangulations eulériennes, gravité quantique, combinatoire analytique.

Random colored triangulations

Abstract. The unification of quantum mechanics and general relativity is one of the big open problems in theoretical physics. One of the possible approaches is to define random geometric spaces with the right properties, that can be interpreted as quantum spacetimes. This thesis touches on mathematical aspects of colored tensor models, a type of theoretical-physical model that belongs to this approach. These models describe piecewise-linear spaces called colored trisps, in any dimension.

Over the course of this thesis, we first studied uniform random models of colored trisps, in any dimension. We prove that these models have a singular limit, which also lead to a Central Limit Theorem for the genus of a large uniform random map.

We then studied the special case of dimension 2, in which colored trisps are a particular type of maps, Eulerian triangulations. We show that planar Eulerian triangulations converge to the Brownian map, which is a universal continuum random object in dimension 2. This result is particularly remarkable, given the complexity of the structure of Eulerian triangulations, compared to other families of maps that are known to converge to the Brownian map.

Keywords: random maps, random graphs, random permutations, colored tensor models, colored trisps, Eulerian triangulations, quantum gravity, analytic combinatorics.

Image de couverture : Une triangulation eulérienne du cylindre, munie de sa décomposition en couches.

ED 512
INFOMATHS
Ecole doctorale

UNIVERSITÉ DE LYON